FINAL REPORT

Separation of Colloidal Particles from Groundwater by Cross-Flow Electro-Filtration Process for Improving Analysis of Lead: Year II

C. P. Huang: Principal Investigator
Y. T. Lin: Graduate Research Assistant
Department of Civil and Environmental Engineering
University of Delaware
Newark, Delaware19716

March 1, 2003

Project Officer: Paul F. Sanders
Division of Science & Research
Department of Environmental Protection
Trenton, New Jersey

Table of Content

LIST OF TABLES

LIST OF FIGURES

LIST OF TABLE (APPENDIX)

LIST OF FIGURE (APPENDIX)

1.0 Introduction

Groundwater monitoring is essential to data collection during environmental site investigation. Past practice depends on existing water supply wells for water sample collection. However, the function and characteristics of supply wells are different from those of a monitoring well. A water supply well does not always satisfy the special requirements of environmental monitoring. Water supply wells harvest water from the best available aquifer; whereas, environmental monitoring wells are always located at critically impacted geological formations.

Chemical constituents in water are conveniently divided into soluble (or dissolved) and insoluble (or particulate) fractions. This is generally done by filtering the water sample through a filter membrane of specific cut-off pore size (currently 0.45 μm pore size). Due to small size, colloids tend to clog the filter, form filter cake and render filtration difficult. Furthermore, deposition of colloids on the filter will tend to increase the chemical concentration, e.g. lead, in the particulate fraction.

Numerous studies have demonstrated that the presence of colloidal material in groundwater may facilitate the transport of organic and inorganic contaminants (Sheppard, Campbell et al. 1979; Means and Wijayaratne 1982; Takayanagi and Wong 1983; Chiou, Malcolm et al. 1986). Colloidal material having a diameter in the range of 0.01 to 10 μm my originate from macromolecular components of dissolved organic carbons, such as humic acids, biological materials, and micro-emulsions of non aqueous phase liquids (NAPL) and weathering products. The effect of colloidal material on contaminants in the saturated zone depends on the nature of relative interactions between the contaminants and the colloids, the groundwater, and the soil matrix. As a general rule, metals tend to attach onto negatively charged colloids.

Conventional groundwater sampling procedures stress speedy pumping and rely on filtration to compensate for turbidity. The validity of the resulting samples is therefore questionable (Kearl, Korte et al. 1992). Vigorous bailing of groundwater samples may increase oxygen concentrations and disturb particles and colloids in the influence zone of the well. Agitation of the monitoring well may generate additional colloids or particulate with adsorbed organic and inorganic chemicals of concern. It is generally accepted that the water in the well casing may not be representative of the formation water, so it needs to be purged

prior to collecting the water samples. Traditional sampling methods rely on purging and sampling with bailers or high speed pumps to remove 3-5 well casing volumes. This can lead to excessive drawdown, accelerated groundwater flow, aeration of water in the well, stirring up sediments in the well, and abrasion of the well casing. Following well purging, there is a cursory evaluation of water quality stability, usually pH, temperature, and specific conductivity (Puls and Barcelona 1996). This sampling practice tends to disturb colloidal material and bring it into water samples of interest. The water is generally filtered, especially for metal analysis, then analyzed for dissolved constituents such as lead. Current technique uses 0.45-μm filters to divide the dissolved from the insoluble particulate chemical constituents. This will include colloidal material between a size of 0.01 to 0.45 μm and exclude those from the 0.45 to 10-μm portion of colloids in the determination of dissolved lead. Moreover, due to small size, it is difficult to filter groundwater of high solid concentration (or turbidity).

Low-flow sampling was developed to allow for collection of samples while causing as little disturbance in the well and the surrounding formation as possible, and to base the collection of the water samples on continuous observations of stability parameters during purging. In this manners, representative unfiltered samples can be collected. The major feature of the low-flow purge method is the velocity with which water enters the pump intake and that is imparted to the formation pore water in the immediate vicinity of the well screen (Puls and Barcelona 1996). Although low-flow- purge technique can minimize the introduction of particulate into groundwater samples, it is slow and thereby expensive.

Soil contamination by lead can cause potential groundwater pollution problems. Lead in solid-water systems is mostly associated with solids, i.e. colloidal or particulate state. During site investigation water samples are taken from monitoring wells for chemical analysis, i.e. lead. The size of particulate matter in water can range from 1 to 5,000 μm and colloidal matter from 0.01 to 10 μm. There is an overlap of particles in the range of 1 to10 μm that is rejected during conventional filtration. This complicates the process of segregating dissolved and particulate matters. An improvement of the separation of overlapped pore size may result in the development of a protocol that would allow the use of filtered samples in site investigations. It is proposed that lead contaminated groundwater samples from wells containing high levels of particulates be subjected to separation with a

series of filter sizes from 0.45 to 10 μm. This data should be compared to conventional bailer samples and low-flow-purged samples. An acceptable filtering procedure would be one that eliminates the presence of artificially introduced particulate matter while still allowing naturally occurring colloid matter to be determined.

Traditional methods depend on speed pumping and bailers. This sampling practice tends to disturb colloidal matter and bring it into water samples. The water is generally filtered, especially for metal analysis, then analyzed for dissolved constituents such as lead. Current technique uses 0.45-μm filters to divide dissolved from particulate chemical constituents. This will include colloidal material between 0.01- 0.45 μm and exclude the 0.45 to 10-μm portion of colloids in the determination of dissolved lead. Moreover, due to the small size, it is difficult to filter groundwater of high solid concentration (or turbidity). Although low flow purge technique can minimize the introduction of particulate into groundwater samples, but it is also slow and expensive.

In order to determine the lead speciation in groundwater, it is necessary to separate the colloids into various size fractions then analyze the lead content in each individual fraction separately. Specifically, it is necessary to separate the colloidal matter over the size range of 0.01 to 10 μm without difficulty.

2.0 Literature Review

2.1 Groundwater Sampling

2.1.1 Background

Environmental groundwater monitoring is relatively new. The earliest work borrowed information and methods from the water supply well. However, the water quality monitoring goals for a water supply wells are much different from those of monitoring wells. With time, it becomes apparent that water well practices do not always satisfy the special requirements of environmental monitoring. One of the greatest disparities is in the water-bearing units. Water supply wells will tap the best available aquifer. Environmental monitoring wells must produce from the critically impacted geologic unit, usually irrespective of its actual ability to produce water.

One of the issues of sampling impaired formations is the role of colloids with respect to contaminant transport. Low-flow sampling was developed for collecting samples that are as undisturbed and representative as possible without filtration, thereby giving true and accurate information regarding water quality, including the colloidal content.

The goal of groundwater sampling is to collect samples that are as representative of the groundwater as possible. The contribution to sample turbidity made by conventional well purging and water sampling techniques has generated much interest recently. Vigorous removal of groundwater in a typical monitoring well will likely mobilize otherwise stable particulates and may create artificial colloids also due to changes in dissolved gases or the breakup of larger colloids.

The traditional bailer sampling or pumping may increase the concentration of colloid-adsorbed metals and hydrophobic organic compounds in groundwater samples. Alternative approaches to sampling suggest a procedure to minimize the introduction of otherwise immobile colloids into wells by slow, prolonged pumping.

2.1.2 Hydrogeological Effects on Samples

While traditional sampling techniques can adversely affect the quality of collected samples because of artificially generated turbidity, hydrogeological effects also can confound our understanding of the true distribution and concentration of contaminants.

Mixing of contaminated water with uncontominated water in both the subsurface and a monitoring well can occur when purging and sampling are improperly performed. This

problem increases with longer well screens, higher pump rates, bailing and when variable stratigraphy exists across the screened interval. Long well screens tend to average the contaminant concentration over the vertical screen dimension; i.e., over the screen length. This is because traditional sampling techniques simultaneously pull water from all zones that the screen intersects, both contaminated and uncontaminated. This may be satisfactory if the desired result is a concentration integrated over a fairly large volume of the aquifer. It yields little information, however, about plume thickness or contaminant concentration gradients within the actual plume.

The problem can be worsened by stratigraphic variations that result in zones of high natural groundwater flow layered with less permeable zone across the screened interval. In this situation, the water is transferred preferentially into the well casing from the higher permeability flow zones, whether or not these are the zones of maximum contaminant.

2.1.3 Colloidal Transport

Numerous studies have demonstrated that the presence of colloidal matter in groundwater may facilitate the transport of organic and inorganic contaminants (Sheppard et al., 1979; Means and Wijayaratne, 1982; Takayanagi and Wong, 1984; Chiou et al., 1986; Sandhu and Mills, 1987; Puls et al., 1991). Colloidal matter with diameter in the range of 1 nm to 10 μm may originate from macromolecular components of dissolved orgain carbon, such as humic substances, biologic matters, and microemulsions of nonaqueous phase liquids, or from inorganic mineral precipitates and weathering materials. For example, Dioxin, which is extremely hydrophobic, trends to sorb to nonionic colloids.

Conventional groundwater sampling procedure stress speed in purging and sampling and rely on filtering to compensate for turbidity. The representativeness of the resulting samples is questionable. Vigorous bailing of groundwater samples to develop and sample wells may increase oxygen concentrations and redox potentials as well as physically disturb particles and colloids in the well's zone of influence. This agitation of a monitoring well during bailing (in conjunction with other physical/chemical effects) may generate additional colloids or particulate with adsorbed organic and inorganic chemicals of concern.

2.1.4 Traditional Methods

It is generally accepted that the water in the well casing may not be representative of the formation water, so it needs to be purged prior to sample collection. Traditional materials

and methods stress speed and maintaining the status quo. Traditional sampling methods rely on purging and sampling using bailers or high-speed pumps to removal 3 to 5 well casing volumes. This can lead to excessive drawdown, accelerated groundwater flow, aeration of water in the well, stirring up of sediments in the well, and abrasion of the well casing. Following this purge, there is a cursory evaluation of water quality stability – usually pH, temperature, and specific conductance – which have been shown to be poor indicators of the actual variation between "stagnant" well water and "fresh" formation water.

Finally, the water samples are collected; these samples need to be filtered to compensate for the excess turbidity. Usually, only samples for analysis are filtered. Filtering is done using a default pore filter size (typically 0.45 μm) that is the middle of the size range for colloids. This default method does not take into account site-specific factors, which might include contaminant transport by colloids larger than 0.45 μm or the presence of organic contaminants on colloids.

2.1.5 Low-flow Sampling

Low-flow sampling was developed to allow for collection of samples while causing as little disturbance in the well and the surrounding formation as possible, to base the collection of the water samples on continuous observations of stability parameters during purging. In this manner, representative unfiltered samples can be collected.

Low-flow is somewhat of a misnomer, because the important factor is the velocity with which water enters the pump intake and that is imparted to the formation. It does not necessarily relate to the rate with which water is discharged from the pump. Water level drawdown in the well during purging and sampling provides the best indication of the stress imparted by the sampling process, and so the change in water level is a stabilization parameter.

The pumping rate should be stable and specific to the well being sampled. The pump discharge should be set at a rate that minimizes drawdown. Typically, flow rate is 0.5 to 5 L/min, but coarser formations may allow higher flow rates as long as little or no drawdown is created. Low-flow purging should be done with the pump intake located in the middle or slightly above the middle of the screened interval. These methods often bring about groundwater stabilization with the removal of one to three well volumes. In high-hydraulic-conductivity formations with dedicated equipment, well may stabilize as soon as the water in

the pump is purged, because natural groundwater flow is constantly purging the water in the well and the low-flow method creates little or no mixing with the water above the screen.

Water quality stabilization is determined by observing the trends of a number of parameters that are measured and evaluated in the field during purging. Water quality stabilization is achieved when the values of the parameters remain at ± 5% over successive readings. It is not necessary to have or even consider "purging" and" stabilization" as separate step. Measurements of the field parameters can begin as soon as the pumping rate is stabilized. Stabilization parameters include pH, specific conductance, redox potential, dissolved oxygen, temperature, and turbidity. Of these, pH and temperature have the lowest degree of indicativeness, and turbidity is the last parameter to stabilize. Many regulators use 10 nephelometric turbidity units (NTU) as criteria, even though natural turbidity in groundwater at a site may be higher.

Low-flow sampling can be performed using either dedicated or portable equipment. The advantages of dedicated equipment include fewer disturbances in the well (which is an overall goal of the method), less purge water, less decontamination, and less setup time. However, dedicated equipment requires a high initial investment. Low-flow sampling data may be comparable to historical data collected by traditional methods from a site. Although the sample collection method should be linked to the data, the data from the two methods can probably be correlated, and the necessity for using low-flow method should be re-examined. However, if the data collected by low-flow methods are different from historical data collected by traditional methods, then the two types of data cannot be correlated, and the old data should be noted as questionable.

Low-flow sampling is not simple, nor is it inexpensive. It is likely that sampling will take more field time, more equipment, and more documentation.

2.2 Low-Flow Sampling Protocols

2.2.1 Sampling Recommendations

Water samples should not be taken immediately following well development. Sufficient time should be allowed for the groundwater flow regime in the vicinity of the monitoring well to stabilize and to approach chemical equilibrium with the well construction materials. The lag time will depend on site conditions and methods of installation but often exceeds one week.

Well purging is nearly always necessary to obtain samples of water flowing through the geologic formations in the screened interval. Rather than using a general but arbitrary guideline of purging three casing volumes prior to sampling, it is recommended that an in-line water quality measurement device (e.g., flow-through cell) be used to establish the stabilization time for several parameters (e.g., pH, specific conductance, redox, dissolved oxygen, and turbidity) on a well specific basis. Data on pumping rate, drawdown, and volume required for parameter stabilization can be used as a guide for conducting subsequent sampling activities.

The following are recommendations for consideration, before, during and after sampling (Puls, Powell et al. 1991):

1. Use low-flow rates (< 0.5 L/min), during both purging and sampling to maintain minimal drawdown in the well;
2. Maximize tubing wall thickness, minimize tubing length;
3. Place the sampling device intake at the desired sampling point;
4. Minimize disturbances of the stagnant water column above the screened interval during water level measurement and sampling device insertion;
5. Make proper adjustments to stabilize the flow rate as soon as possible;
6. Monitor water quality indicators during purging;
7. Collect unfiltered samples to estimate contaminant loading and transport potential in the subsurface system.

2.2.2 Equipment Calibration

Prior to sampling, all sampling devices and monitoring equipment should be calibrated according to manufacture's recommendations.

Calibration of pH is performed with at least two buffers that bracket the expected range. Dissolved oxygen calibration is corrected for local barometric readings and elevation.

2.2.3 Water Level Measurement and Monitoring

It is recommended that a device be used which will least disturb the water surface in the casing. Well depth should be obtained from the well logs. Measuring to the bottom of the well casing will only cause resuspension of settled solids from the formation and require longer purging times for turbidity equilibration. Measure well depth after sampling is

completed. The water level measurement should be taken from a permanent reference point which is surveyed relative to ground elevation.

2.2.4 Pump Type

The use of low flow (e.g., 0.1 - 0.5 L/min) pumps is suggested for purging and sampling all types of analyses. All pumps have some limitations and these should be investigated with respect to application at a particular site. Bailers are inappropriate devices for low flow sampling.

1. General considerations

There are no unusual requirements for groundwater sampling devices when using low flow, minimal drawdown techniques. The major concern is that the device gives consistent results and minimal disturbance of the sample across a range of low flow rates (i.e., < 0.5 L/min). Clearly, pumping rates that cause minimal to no drawdown in one well could easily cause significant drawdown in another well finished in a less transmissive formation. In this sense, the pump should not cause under pressure or temperature changes or physical disturbance on the water sample over a reasonable sampling range. Consistency in operation is critical to meet accuracy and precision goals.

2. Advantages and disadvantages of sampling devices

A variety of sampling devices are available for low flow (minimal drawdown) purging and sampling. These include peristaltic pumps, bladder pumps, electrical submersible pumps, and gas-driven pumps. Devices which lend themselves to both dedication and consistent operation at definable low flow rates are preferred. It is desirable that the pump be easily adjustable and operates reliably at lower flow rates. The peristaltic pump is limited to shallow applications and can cause degassing resulting in alteration of pH, alkalinity, and some volatile loss. Gas-driven pumps should be of the type that does not allow the gas to be in direct contact with the sampled fluid.

Clearly, bailers and other grab type samplers are ill-suited for low flow sampling since they will cause repeated disturbance and mixing of stagnant water in the casing and dynamic water in the screened interval. Similarly, the use of inertial lift foot-valve type samplers may cause much disturbance at the point of sampling. Use of these devices also tends to introduce uncontrolled and unacceptable operator variability.

2.2.5 Pump Installation

Any portable sampling device should be slowly and carefully lowered to the middle of the screened interval or slightly above the middle (e.g., 1-1.5 m below the top of a 3-m screen). This is to minimize excessive mixing of the stagnant water in the casing above the screen with the screened interval zone water, and to minimize resuspension of solids which will have collected at the bottom of the well. These two disturbance effects have been shown to directly affect the time required for purging. There also appears to be a direct correlation between size of portable sampling devices relative to the well bore and resulting purge volumes and times. The key is to minimize disturbance of water and solids in the well casing.

2.2.6 Filtration

Although filtration may be appropriate, filtration of a sample may cause a number of unintentended changes to occur (e.g., oxidation, aeration) possibly leading to filtration-induced artifacts during sample analysis and uncertainty in the results. In this study, we skip this step.

2.2.7 Monitoring of Water Level and Water Quality Indicator Parameter

Check water level periodically to monitor drawdown in the well as a guide to flow rate adjustment. The goal is to maintain a minimal drawdown (<0.1 m) during purging. This goal may be difficult to achieve under some circumstance due to geologic heterogeneities within the screened interval, and may require adjustment based on site-specific conditions and personal experience. The water quality indicator parameters monitored can include pH, redox potential, conductivity, dissolved oxygen (DO) and turbidity. The last three parameters are often the most sensitive. Pumping rate, drawdown, and the time or volume refer sensitive representative stabilization of parameter readings can be used as guide to purge the well. Measurements should be taken every three to five minutes if the above-well purging rates are used. Stabilization is achieved after all parameters have stabilized for three successive readings. In lieu of measuring all five parameters, a minimum subset would include pH, conductivity, and turbidity or DO. Three successive readings should be within ± 0.1 for pH, ± 3 % for conductivity, ± 10 mv for redox potential, and ± 10% for turbidity and DO. Stabilized purge indicator parameter trends are generally obvious and follow either an exponential or asymptotic change to stable values during purging. Dissolved oxygen and

turbidity usually require the longest time for stabilization. The above stabilization guidelines are provided for estimates based on experience.

2.2.8 Sampling, Sample Containers and Preservation

Upon achieving parameter stabilization, sampling can be initiated. Sampling flow rate may remain at established purge rate or may be adjusted slightly to minimize aeration, bubble formation, turbulent filling of sample bottles, or loss of volatiles due to extended residence time in tubing. Typically, flow rates less than 0.5 L/min are appropriate. The device used for sampling was the same as used for purging. Sampling should take place from the least to the most contaminated wells. Generally parameters such as Fe^{2+}, CH_4, H_2S/HS and alkalinity should be sampled first. The sequence in sampling for most inorganic parameters is immaterial unless filtered (dissolved) samples are desired.

The appropriate sample container will be prepared in advance during actual sample collection for analyses of interest and include sample preservative where necessary. Water samples are collected directly into this container from the pump tubing. Immediately after a sample bottle has been filled, it must be preserved as specified in the site. Sample preservation requirements are based on the analyses being performed. It may be advisable to add preservatives to sample bottles in a controlled setting prior to entering the field in order to reduce the chances of improperly preserving sample bottles or introducing field contaminants into a sample bottle while adding the preservatives.

After a sample container has been filled with groundwater, A cap is screwed on tightly to prevent the container from leaking. A sample label is filled out. The samples should be stored inverted at 4^oC.

2.2.9 Blanks

The following blanks should be collected:

1. Field blank: One field blank should be collected from each source water (distilled/deionized water) used for sampling equipment decontamination or for assisting well development procedures.
2. Equipment blank: One equipment blank should be taken prior to the commcncement of field work, from each set of sampling equipment to be used for that day.

3. Trip blank: A trip blank is required to accompany each volatile sample shipment. These blanks are prepared in the laboratory by filling a 40-mL volatile organic analysis (VOA) bottle with distilled/deionized water.

2.3 Crossflow Electrofiltration

2.3.1 Filtration

Filtration is pressure-driven filtration process. The task of separating solids from liquids is important in nearly every field of industrial production: waste water treatment and environmental protection, mineral processing industry, coal and ore, basic chemicals and synthetic fertilizer, colour and pigment chemistry, biotechnology, biomedicine, food industry, and drinking water treatment, just to name a few (Iritani, Ohashi et al. 1992; Weber and Stahl 2002).

Filtration is an accepted technique for separation of solid-liquid system. However, one of the major bottlenecks in the application of the filtration process is the flux decline due to membrane fouling. Such flux decline is mainly to the formation of highly resistant filter cake caused by accumulation of the colloidal or the proteinanceous solutes on the membrane surface (Iritani, Nakatsuka et al. 1991; Iritani, Mukai et al. 2000). The formation of these layers reduces the permeate flux and can make the process uneconomic to operate due to either low permeate fluxes or the need to replace membranes too frequently. In order to maintain a high filtration rate for extended period of time, therefore, it would be necessary to prevent a continuous buildup of solutes on the filtering surface. Various techniques have been developed to reduce or prevent polarization and fouling. Indeed, various ingenious techniques have been developed for reducing the amount of cake forming; including crossflow filtration (Iritani, Sumi et al. 1991), dynamic filtration with rotating cylindrical membrane (Murase, Iritani et al. 1989), upward and inclined filtration (Iritani, Watanabe et al. 1991; Iritani, Watanabe et al. 1992; Iritani, Mukai et al. 2000). Among them, crossflow filtration is a management techniques developed to minimize accumulation of the dispersed phase on the membrane.

2.3.2 Crossflow Filtration

Crossflow membrane filtration was originally conceived to reduce concentration polarization by utilizing hydrodynamic forces to hinder solute deposition at the membrane surface. This technique was developed by Zhevnovatyi (Turkson, Mikhlin et al. 1989/90).

In 1970 Bechhold found by experiments that at the filtration of colloidal and very fine suspensions a flow parallel to the filter medium increases the filtrate volume before the filter medium is blocked due to a compact layer formation. Bechhold used a stirred filtration cell to create the shear flow across the filter media (Altmann and Ripperger 1997). The cross-flow filtration technique involves the feed stream being pumped at a relatively high velocity parallel to a membrane surface. This is helps to reduce the concentration polarization by thinning the boundary thickness and by assisting in sweeping away the filter cake or gel layer film (filter cake refer to colloidal particles and gel layer to macromolecules). Today the crossflow filtration is a standard operation in many medical and technical applications. A flow parallels to the filter medium reduces the formation of the layer and keeps it at a low level. So it is possible to get a quasi-stationary filtrate flow for a long time (Altmann and Ripperger 1997).

The crossflow filtration is influenced by complex effects of a great number of parameters, e.g. crossflow velocity, transmembrane pressure, membrane resistance, layer resistance, size distribution of the suspended particles, particle form, agglomeration behavior and surface effect of the particles etc (Altmann and Ripperger 1997).

Crossflow filtration was conceived as a means of removing liquid from a suspension rapidly by preventing cake formation at the filter surface. Cake formation was intended to be prevented by using adequate crossflow velocities to induce high shear rates across the filter septum; crossflow velocities of 3 m/s were quite usual in the earlier days of crossflow filtration, but the failure of the shear generated by these velocities to increase permeate (filtrate) rates has led industry to use increasingly higher crossflow velocities until today when 4 to 7 m/s is quite usual (Wakeman and Tasleton 1991).

In the crossflow filtration, the suspension flows parallel over the membrane, and the permeate flows normally through the membrane because of the transmembrane pressure. Particles flow into the direction of the membrane, too, where are retained and form the filter cake. Particle deposition on the layer is mostly an irreversible process (Altmann and Ripperger 1997). Adhesive and friction forces are dominating on a deposited particle. The effect can be concluded from the experiments: The build-up of the layer is a continual process, while the removal of the layer only take place by removing large agglomerates or large layer fragment (Altmann and Ripperger 1997). Only large particles, agglomerate and

layer fragments can be detached from the layer (Altmann and Ripperger 1997). The filter cake increases the flow resistance and considerably reduce the specific permeate rate. It could be shown that fine particles are deposited at the membrane even for high crossflow velocities (Altmann and Ripperger 1997). Fine particles increase the resistance, which in tern decreases the permeate rate further.

Because the flow resistance increases with decreasing particle size, the mechanical filtration of fine particle suspensions is time-consuming. The formation rate of these layers reducing the permeate flux dramatically increase and can make the process uneconomic to operate due to either low permeate fluxes or the need to replace membranes too frequently. In many, if not a majority, of instance these high shear rates do not prevent contamination of the surface and can actually further decrease permeation rates (Wakeman and Tasleton 1991; Altmann and Ripperger 1997). However, because of the limitations of obtaining sufficiently high crossflow velocities and the inevitability of membrane/solute interactions, concentration polarization still take place.

Various other techniques, including the use of abrasives and filter aids, backwashing and backpulsing, flow reversal and pulsed crossflows have been devised to reduce the effects of the fouling layers. These techniques generally lead to reduced membrane lifetimes or to complexities in the filter operating cycle, both of which are undesirable (Wakeman and Tasleton 1991).

The other techniques to reduce these foulants (Radovich and Sparks 1980) including using turbulence promoters, chemically modifying the membrane surface, or employing additional force field (e.g. electric field or acoustic) inside the filter. Coupling of two or more force fields can give synergy to enhance permeate flux. Rotating membranes (Rushton and Zhang 1988; Park, Choi et al. 1994), crossflow electro- (Henry, Lawler et al. 1977; Wakeman and Tarleton 1987; Bowen, Kingdon et al. 1989; Bowen 1992; Bowen and Sabuni 1994; Wakeman and Sabri 1995; Akay and Wakeman 1996) or acoustic (Muralidhara, Ensminger et al. 1985; Muralidhara and Senapati 1986) and cross flow electro-acoustic (Belfort 1987; Wakeman and Tasleton 1991; Tarleton and Wakeman 1995) filtrations represent important applications of external force field superimposed orthogonally on the main hydrodynamic field in order to enhance permeate flux. Pulsatile flows represent an axial superimposition of two flow fields (Belfort, Davis et al. 1994). Pulsatile flows, on the

other hand, can be considered to be the axial superimposition of two flow field (Burgmayer and Murray 1982; Misra and Varanasi 1991). The effect of superimposed sonic fields in enhancing permeate flux is not solute selective but that of the electric field can be solute selective (Wakeman 1998).

When particle size becomes small, the ratio of particle surface area to volume increases. It becomes advantage to use surface properties, like surface charge, for solid-liquid separation processes. Therefore, charge characteristics of particles are known to play an important role in solid- liquid separation processes (Lo, Gidaspow et al. 1983).

Due to the selectivity of an electric field based on particle or solutes charge sign and density, the concentration of various solutes or particles in permeate will depend on the charge structure of the solute or particles. The effect of enhancing permeate flux by an electric field can be solute or particle selective and is best suited to the filtration of charged solutes (Wakeman 1998).

Electrofiltration of aqueous dispersions, i.e., filtration through porous materials (granules, fibers, mesh) placed in an electric field, can bee used in chemical technology for separation of aqueous dispersions (e.g. for purification of wastewater), in the food industry for separating food dispersions, and in microbiology, medicine and radioactive industry for purifying solution (Veselov 1983; Il'in and Kolesnikov 2001). Electrofiltration equipment is much more efficient than settlers, which makes it possible to reduce the treatment time by a factor of 10-20 and decrease the area occupied by the equipment by a factor of 3-5 (Il'in and Kolesnikov 2001). There have been numerous literature reports where electrochemical techniques have been developed to assist membrane processes: in a preventative role by stopping membranes from becoming fouled, in a restorative role by assisting in cleaning of membranes that are already fouled, or by enabling the selective separation of species based on charge and size (Henry, Lawler et al. 1977; Huotari, Tragardh et al. 1999; Webster, Chilukuri et al. 2000; Zhang, Tan et al. 2000).

An applied electric field is established between the electrodes of appropriate polarity (usually so that the membrane is proximity to a negative field since most particles of interest in aqueous solution are negative charged, particularly for colloidal solution). Crossflow membrane filtration enhanced by a D.C. (direct current) electric field, call electrofiltration has been investigated from the seventies (Henry, Lawler et al. 1977). The industrial take-up

of crossflow filtration in the 1980's as a means of slurry dewatering has focused more recent interest of using the electrophoretic effects to reduce fouling of the filter surface (Henry, Lawler et al. 1977; Lee, Gidaspow et al. 1980; Yukawa, Shimura et al. 1983; Verdegan 1986; Wakeman and Tarleton 1987).

In electrofiltration, the accumulation of the solutes on the membrane surface is limited by the imposed electrophoretic force. Fouling can be reduced progressively by increasing the electric field strength to induce an electrophosetic velocity to the particles in the feed stream in a direction away from the filter surface. The extent of the increase in permeates rates as a result of imposing the electric field is ultimately dependent on the particle size and the charge density around its surface. In addition, the filtration rate through the filter cake is dramatically enhanced due to electroosmosis as a secondary electrokinetic phenomenon. This method is best suited to the separation of nano-sized colloid since its surface charge changes according the solution pH.

2.3.3 Crossflow Electrofiltration

Crossflow electrofilitation is a hybrid separation process which combines the features of crossflow filtration and electrophoretic separation devices. Several investigators subsequently reported combination of crossflow filtration and electrofiltration (Bier 1959; Yukawa, Shimura et al. 1983; Radovich, Behnam et al. 1985; Wakeman and Tarleton 1987). In crossflow filtration, a filter cake is formed on the membrane in the course of filtration. This cake acts as an additional resistance and significantly decreases the high initial permeate flow rate and thus the efficiency of the process. Like a conventional crossflow filter, the influent flow of contaminated fluid is directed parallel to the filter media surface. In this case, as particles in suspensions carry an electric charge, it is possible by means of a suitable superposition of the crossflow filtration with an electric field to prevent or reduce cake formation, and to considerably increase the stationary permeate rate. In crossflow electrofilitation a D.C. electric field is applied normal to this surface. If the field is of sufficient strength and proper polarity, charged particles will migrate away from the media surface by electrophoresis, given rise to a clear boundary layer. Particle-free fluid can then be withdrawn through the media.

In the theory, the behavior of a crossflow electrofiltratio toward charged particles should approximate that of the mythical ideal filter. Nearly complete separation should be

obtained for particles of all sizes without a corresponding increase in pressure drop. From the standpoint of electrophoretic separation, it is immaterial whether the contaminant is an ion or a grain of sand, as long as it has sufficient charge. Since the contaminant does not come in direct contact with the media, no increase in pressure drop should be observed: hence, crossflow electrofiltration should be characterized by extremely long service intervals. Crossflow electrofiltration offers great promise in reducing the fouling problems associated with charged particles and colloids (Wakeman and Tasleton 1991).

The cross-flow filtration process has been investigated extensively. Manegold was the first to study the process of combining conventional pressure filtration and electrophoresis (Manegold 1937). It was not until 1977 when Henry provided a fundamental analysis of the cross-flow electrofiltration process (Henry, Lawler et al. 1977). Moulik (1976) applied an electrostatic field to microfilters and reported excellent removal of colloidal particles such as bentonite and algal cells (Moulik 1976).

Archer et al (1993) designed an electrode capable of generating non-uniform electric fields over a large surface area to separate yeast cells from water (Archer, Render et al. 1993). They reported that a linear relationship between dielectrophoretic collection and pulse length over the range 0 to 100 second. Lo et al. (1993) separated Al_2O_3 colloids from non-aqueous solution using cross-flow electrofiltration process. The effect of feed rate, diving pressure, and electrical field strength on the filtration rate and total solid deposition rate on the collection electrode was evaluated. Results indicate that extent of filter fouling is greatly decreased.

Majmudar and Manohar (1994) reported the separation of TiO_2 from aqueous solution by electrophoretic filtration (Majmudar and Manohar 1994). Experiments were carried out at different voltages and flow rates. It was observed that voltage lower than 10 V and higher than 50 V was largely inefficient in solid separation. The optimal conditions were 15 V and 200-mL/h flow rate. It was further observed that 96% separation was the maximum obtainable.

Wakeman and Sabri (1995) reported that direct current electric fields reduce cake formation in cross-flow membrane filtration (Wakeman and Sabri 1995). Operating parameters such as filtration pressure, cross-flow velocity, electric field gradient, pH and feed concentration can affect filter performance. Verdegan (1986)studied the separation of

fine particles (<10 μm) from nonpolar liquids by crossflow electrofiltration process (Verdegan 1986). He reported that crossflow electrofiltration has many distinct advantages over conventional separation processes: high removal for all particle sizes, long life, and minimal power requirement. Akay and Wakeman (1996) reported enhanced removal of a double chain cationic surfactant (diocatadecyldimethlammonium chloride) in water using the crossflow electrofiltration process (Akay and Wakeman 1996). Wakeman reported electrophoretically assisted cross-flow microfiltration of bovine serum albumin (BSA), ovalbumin and denatured lactalbmin (Wakeman 1998). It is shown that steady state flux is higher when an electric field is applied than it is with conventional crossflow microfiltration. The flux is an almost independent of the membrane pore size. Finer pore sizes enable steady state flux and rejection conditions to be reached sooner. von Zumbusch et al. (1998) reported that the alternating electric field diminished membrane fouling and hence yields a higher specific filtrate flux. The effect of the electric field depends on frequency (0.5-50 Hz), field strength (0-80 $V\text{-}cm^{-1}$), conductivity (1-10 mS^{-1}), and protein concentration (0.1-5 w%) (Zumbusch, Kulcke et al. 1998). Low frequency and high field strength yield the best result for electroultrafiltration with alternating fields. The effectiveness of the electric field increases with rising conductivity p to the point where a limiting electrolytic current is reached. Increasing protein concentration diminishes the effect of the electric field.

Houtain et al. (1999) reported that applying an electrostatic field across crossflow filtration could greatly increase the flux rate (Huotari, Tragardh et al. 1999). Weigert et al. (1999) conducted the first pilot plant study on microfiltration of mineral and biological slurries with cross-flow filtration, coupled with constant and pulsed fields and reported that the specific permeate rate markedly increases compared to the value without an electrostatic field. For mineral slurry, the increase in flux rate was more than 10 fold. An estimation of the specific energy input demonstrates the cost-saving potential of this technique.

2.4 Lead

2.4.1 Lead in the Environment

Lead has been an important metal in human society for many thousand years. Unique physical characteristics such as low melting point, good workability and durability made lead a popular construction material in our early society. The use of lead pipe for water

transmission of the Roman Empire is a significant example. Lead has also been used over the year as a glaze on pottery, in cosmetics and as a wine sweetener.

The use of lead, however, has increased dramatically since the early days of industrial revolution. Annual lead production has stabilized at the annual rate of 2.5 million tons pre annum. As many as 40 counties worldwide have workable lead deposits, with Russia, USA, Australia and Canada (ca. 60% of the total) being the four major lead producing countries. Mining, smelting and refining of lead, as well as the production and use of lead-based products give rise to the release of lead into the environment. This takes the form primarily of either lead-rich aqueous effluent streams, or emission of fume and dust into air. A large part of the lead discharged into surface waters in rapidly incorporated into suspended and bottom sediments and most of this lead will ultimately be found in the marine sediments. Of greater concern, however, is the emission of lead into the atmosphere. The finer aerosol particles may be transported long distance from their source before deposition onto land or sea. Although the magnitude of the resulting pollution is very small at large distances, significant concentrations in soils and vegetation can occur close to a major source of lead, such as a smelter or busy highway. Most of this lead will ultimately be found in marine sediments. When incorporated in the soil, lead is of very low mobility. Hence once contaminated, a soil is liable to remain polluted with lead.

Soils contamination by lead can cause potential groundwater pollution problems. Stumm and Bilinski divided the lead species into three group: "soluble" (< 0.001 μm), "colloidal" (0.001 μ m- 1 μm) and " particulate" (>1 μm) (Stumm and Bilinski 1972) (Table 1). Soluble lead species are free lead ion, ion pairs or organic complexes. Colloidal lead species are those bound to high molecular weight organic ligands and those adsorbed on colloids such as hydrous oxides of Mn or Fe. Particulate lead species are those incorporated with organic particles, remains of microorganisms, and lead precipitates. The current method for the determination of dissolved lead (or heavy metals) uses 0.45-μm filters. This is in the mid size range of colloids.

2.4.2 Aqueous Chemistry of Lead

Lead is a heavy metal with an atomic weight of 207.2, in its neutral state it contains 82 neutrons, protons and electrons. In aquatic systems Pb usually loses two of the 6p electrons giving it a net charge of +2. The remaining $6s^2$ electrons are the outer shell

electrons that exist as a lone pair. This lone pair has significant influence on the reactivity and coordination of Pb^{2+} ions. Lead can also lose both 6s electrons under severe oxidizing conditions giving it a net positive charge of +4. Lead (IV) is not very stable in most environments, thus, the divalent form usually controls the fate of Pb in aqueous geochemical conditions. Since Pb is a strongly sorbed atom, and its solubility is low at relevant pH values, most natural waters have low concentrations of aqueous Pb. In fact, a significant amount of Pb in waterways may exist in an undissolved state, and is being transported as colloidal particles (Hem 1976).

The solution concentration of Pb in natural waters with pH nears neutral is normally less than 10 μg/L (Hem 1976). The common species of aqueous Pb in acid soils are Pb^{2+}, organic-Pb, $PbSO_4^0$ and $PbHCO^{3+}$, and for alkaline soils $PbHCO_3^0$, $PbHCO^{3+}$, organic-Pb, $Pb(CO_3)_2^{2-}$, and $PbOH^+$ (Sposito 1989). The behavior of Pb in solution is largely governed by the size (ionic radius = 1.2 Å), valence and electronegativity of the ion. These characteristics contribute to the strength and number of water molecules surrounding the Pb atom (the hydration number for Pb is between 5 to 8) (Burgess 1978). Lead is considered a type B ion, or a soft sphere ion, which means that the electron sheath is easily deformed by external charges making it more polarizable than type A ions. Another classification scheme (Sparks 1995) considers Pb a soft acid, which corresponds to most type B ions. The hard and soft acid classification scheme predicts that a particular acid will have a strong affinity for its respective hard or soft base. This means that Pb will have a strong affinity to form covalent bonds with soft base. Soft bases are atoms and molecules that have a low electronegativity, are Lewis bases, easily polarized, and easily oxidized.

Many experiments conducted have shown that soils form strong complexes with Pb (Zimdahl and Skogerboe 1977). This strong sorption is a result of Pb forming specific bonds with functional groups on oxides, edges of clay minerals, and organic matter. In addition Pb may form precipitates with inorganic C, Cl, P, and S anions.

Groundwater monitoring is an important part of site remediation and environmental risk assessment. However, very little is understood of the aqueous chemistry of lead. Using 0.45 μm filters as the criteria, lead in groundwater can be divided into "dissolved" and "particulate" fractions. As mentioned above, the "dissolved" lead includes mainly free Pb(II) and its hydrolysis species, ion-pairs, and organo-lead complexes. "Particulate" lead is

collection of all lead species that are associated with greater than 0.45-μm particulate. Chemically, "particulate" lead can be further fractionated into the following forms: (1) adsorbed at particles surface, (2) present as discrete carbonate minerals or co-precipitated with major carbonate phases, (3) occluded in iron and/or manganese oxyhydroxide, (4) bound with organic matter, in either living or detritus form, (5) bound with amorphous authigenic sulfides or in more crystalline forms, or (6) bound in lattice positions in aluminosilicates, in resistant oxides or in resistant sulfides.

Lead has a strong tendency to form ion pairs, principally $PbHCO_3^+$ and $PbCO_3^0$ at the pH of the most waters. The formation of lead ion pairs increased the concentration of total dissolved lead in water. Lead can also form strong complexes with organic matter such as the ill-defined humic acid and fulvic acid, and increase the concentration of lead in water.

As indicated in Figure 1, pH plays an important role on the adsorption of lead onto hydrous ferric and manganese oxides (Gadde and Laitinen 1974). This is an important linkage in the hydrogeochemical cycle of lead. Hydrous ferric and manganese oxides are readily reduced and hence become soluble under anaerobic conditions; consequently, lead will become mobilized. However, there may be concomitant formation of metal sulfides which are even less soluble than hydrous oxides of ferric and manganese. Typically three lead compounds govern the solubility of lead in water, via the following equilibrium:

$$Pb(OH)_{2(S)} \Leftrightarrow Pb^{2+} + 2OH^-; K_{so} = 10^{-15.5} @ 25^o C \quad (2.1)$$

$$PbCO_{3(S)} \Leftrightarrow Pb^{2+} + CO_3^{2-}; K_{so} = 10^{-13.2} @ 25^o C \quad (2.2)$$

$$Pb_3(OH)_2(CO_3)_{2(S)} \Leftrightarrow Pb^{2+} + 2OH^- + 2CO_3^{2-}; K_{so} = 10^{-46.8} @ 25^o C \quad (2.3)$$

Conceptually, the solid material can be partitioned into specific fraction (cf. (1) to (6) above); sequential extractions with appropriate reagents can then be devised to leach successive fractions "selectively" from the particulate sample. Various chemical reagents have been proposed to determine the metal species in particulate(Engler, Brannon et al. 1977; Gibbs 1977; Tessier, Campbell et al. 1979; Forstner and Patchineelam 1980). Regardless of the specific chemicals used, these chemicals can be divided into classes of similar chemical behavior, for example:

- Concentrated insert electrolytes (desorption of electrostatically adsorbed metals);
- Weak acids (dissolution of carbonate phases; desorption of specifically adsorbed metals);
- Complexing agents (competition for metal complexes with organic functional groups; dissolution of precipitates);
- Oxidizing agent (oxidation of organic mater andsulfides);
- Strong mineral acids (dissolution of resistant oxides, sulfides and aluminonsolicates).

Table 2 gives a list of sequential extraction procedures(Chao and Theobald 1976; Engler, Brannon et al. 1977; Tessier, Campbell et al. 1979; Rapin and Forstner 1983).

3.0 Methods and Materials

3.1 Crossflow Electrofiltration

This research is to develop a cross-flow eletrofiltration technology for improving the analysis of lead in particular in groundwater samples. During this project period, we have designed and constructed a prototype cross-flow electro-filtration system. As indicated in Figure 2 the main filter unit consists of an external tube (insulated), an inner electrically charged cathodic filter membrane, and a co-centric anodic rod. The external tube has a diameter of 8.9 cm, the inner filter has a diameter of 3.0 cm and the co-centric rod is a 0.5-cm stainless wire. The total module is 22.5 cm long. This module has a total filtration surface area of 212 cm^2. The cathode and the anode are connected to an A.C. power supply (Figure 3). The CFEF filter unit is feed from a Milipore cross flow module, model ProFlux M12 (Figure 4). A computer with necessary software is used to control the filtration rate and flow direction (Figure 5). Figure 6 shows the total CFEF system. Figure 7 illustrates the schematic presentation of flow direction and sampling points.

3.2 Laboratory Experiments

Laboratory experiments will be conducted first to evaluate the performance of the CFEF unit. The following operational conditions will be tested: (1) clogging, (2) flux production, (3) rejection rate, (4) quality of flux, namely, lead concentration and turbidity, and (5) backwash frequency. The degree of filter clogging can be measured in terms of several properties including pressure drop and water quality of the filtrate, i.e. turbidity. During the course of filtration, the pressure of the system will be continuously monitored. Flux production is expressed in terms of mass (or volume) of water produced per time per unit area of the filter, i.e. cm^3/cm^2-min. Rejection rate is the mass of concentrate stream produced per nit area filter per time, e.g. g/cm^2-min. The concentration of lead and turbidity of the filtrate will also be measured during filtration. The frequency of filter backwash will be evaluated. The volume of backwash water and the backwash time and interval will be studied.

Laboratory experiments will be run for the following condition: (1) filtration rate, (2) water quality (turbidity, particle size and surface characteristics of particles) and (3)

electrostatic field. The filtration rate will be from 1.2 to 8 cm^3/cm^2-min. The field strength applied will be in the range from 0 to 194 V/cm.

Groundwater samples to be collected from wells will be characterized for lead. The solid in the groundwater will be characterized for particle size and distribution, and surface charge. Data collected in laboratory will be analyzed and expressed as a function of operation parameters.

3.2. Field Experiments

3.2.1 Field Sampling

On January 15 and May 31, 2002, we made two trips to the Denzer-Schaefer site, Toms River, Bayvile, Ocean County, New Jersey, for field sampling (Figure A1and A2). Water samples were taken from #10 and #5S wells. Bailing, low flow purging and high flow purging technique were used. The flow rate of low flow and high flow purging were 0.1 and 5 L/min, respectively. At well #10, the depth to static water level was approximately 25 feet. The final drawdown water levels were approximately 25 to 31 feet for low flow purging and bailing technique, respectively. At well #5S, the depth to static water level was approximately 24 feet. The final drawdown water levels were 24, 27 and 27 feet for low flow purging, bailer and high flow purging technique, respectively. Table 1 shows the description of well water samples.

3.2.2 Sampling materials and devices

A Grundfos Redi-Flo2® electric submersible pump (Figures A3 and A4) was used to sample the wells using low-flow purging technique. The pump was set with the pump intake at ~ 0.6 m above the bottom of the wells and 0.6 m below the top of the wells in the 3-m long screens, and 0.6 m below the top of the screen in the 1.2-m long screen. A PE bailer (Figure A5) with 1-L capacity was used to sample the same wells.

3.2.3 Sampling Procedure

The low-flow sampling procedures were generally followed when using the Grundfos Redi-Flo2® electric submersible pump to collect samples. Water levels were measured and recorded prior to purging and were monitored continuously during purging to evaluate drawdown in the wells, flow rates were adjusted from 0.1 to 0.3 L/min to minimize drawdown to < 0.1 m. Dissolved oxygen, pH, temperature, specific conductance, turbidity were measured about every 2-5 minute. All instruments were precalibrated daily according

to manufacturer's recommendations. Equipment of water quality parameters (WQP's) was defined as three successive readings within ± 10 % for dissolved oxygen (DO) and turbidity, ± 3 % for specific conductance, and ± 0.1 for pH. Temperature was recorded but not used for stabilization assessment. Samples were collected after turbidity equilibrated during purging.

When the bailer was used, three well volumes (volume of water standing in the casing and screened interval) were used as standard purge volume criterion. The same WQP's were measured, but only after each well volume was collected, and these values were not used for evaluation of well purging sufficiency. These samples had substantially greater turbidity than those collected using low-flow purging and sampling techniques.

3.3 Chemical Analysis

3.3.1 Particle Size

Particles are ubiquitous in natural waters and in water and wastewater treatment streams. Particle size distribution analysis can help to determine the makeup of natural waters, treatment plant influent, process water, and finished water. Similarly, it can aid in designing treatment processes, making decisions about changes in operations, and/or determining processes efficiency. Methods for measuring particle size distribution included herein depend on electronic measurement devices because manual methods are likely to be too slow for routine analysis. However, when particle size analysis is to include size distribution of large (>500 μm) aggregate, use direct microscopic counting and sizing. Three instrument types are included: electrical sensing zone instruments, light-blockage instrument, and light-scattering instrument.

Light-scattering instruments may be either flow or static devices. In flow instruments, the direct path of the light beam through the flow cell is blocked by a particle as it flow through the measurement zone with the fluid, and light scattered over a fixed range of angles is collected and measured. Particle size is determined from the angle and intensity of scattering based on the principles of Fraunhofer diffraction and/or Mie scattering. In the static instruments, the particles remain quiescent and a laser light beam scans part of the suspension. Scattered light is collected by a photovoltaic cell and the resulting response from the all particles scanned is mathematically deconvoluted to generate the size distribution. The average particle size was determined by a light-scattering size analyzer using the

ZETASIZER 3000HSA particle measurement (Malvern Instrument Ltd., Malvern, Worcs, United Kingdom) in this research.

3.3.2 The Electrophoretic Mobility of Particles

The electrophoretic mobility of particles in the well water samples was determined by the ZETASIZER 3000HSA zeta potential meter (Malvern Instrument Ltd., Malvern, Worcs, United Kingdom). The sample solution at different ionic strengths of 10^{-3}, 10^{-2}, 10^{-1} M $NaClO_4$ was stirred with a stir bar. The initial pH was measured while the suspension was being stirred. Then the pH was adjusted in the range from 2.0 to 11.0 by 0.1N NaOH and 0.1 N $HClO_4$. About 20 mL of the sample was injected into the electrophoresis chamber. The purpose of electrophoresis experiment is to determine the surface charge of the colloid particles, the identification of the potential determining ion (PDI), and the stability of suspensions.

3.3.3 The Total Solid Content

Analytical procedures for total solid content are followed (2540.B) the Standards Methods for the Examination of Water and Wastewater (1995). A well-mixed sample is evaporated in a weighed dish and dried to constant weight in an oven at 103 to 105^{o}C. The increase in weight over that of the empty dish represents the total solid. Briefly the following describe the procedures.

1. Heat clean dish to 103 -105^{o}C for 1 h.
2. Store and cool dish in desiccators until needed. Weigh immediately before use.
3. Choose a sample volume that will yield a residue between 10 to 200 mg. Pipet a measured of well mixed sample to a preweighed dish and evaporate to dryness in a drying oven. Stir sample with a magnetic stirrer during transfer.
4. Dry evaporated sample for at least 1 h in an oven at 103-105^{o}C.
5. Cool dish in desiccators to ambient temperature, and weigh. Repeat cycle of drying, cooling, desiccating, and weighing until a constant weigh is obtained, or until weigh change is less than 4% of previous weight or 0.5 mg, whichever is less.
6. Calculate solid concentration: mg total solids/L=(A-B)*1000/(sample volume, mL)
   A = weight of dried residue + dish, mg, and
   B = weight of dish, mg

3.3.4 The Soluble and Total Lead

Analytical procedures for total lead analysis followed EPA (3020A) SW-846 method. Briefly the following describe the procedures.

1. Transfer a 100-mL representative aliquot of the well-mixed sample to 150 mL Griffin beaker and add 3-mL of concentrated HNO_3.
2. Cover the beaker with a ribbed watch glass.
3. Place the beaker on a hot plate and cautiously evaporate to a small volume (5 mL), making certain that the sample does not boil and that no portion of the bottom of the beaker is allowed to go dry.
4. Cool the beaker and add another 3 mL portion of concentrated HNO_3. Cover the beaker with a non-ribbed watch glass and return the beaker to the hot plate. Increase the heating temperature so that a gentle reflux action occurs.
5. Continue heating, adding additional acid as necessary, until the digestion is complete (generally indicated when the digestate is light in color or does not change in appearance with continued refluxing).
6. When the digestion is complete, evaporate to a low volume (3-mL); use a ribbed watch glass, not allowing any portion of the bottom of beaker to go dry. Remove the beaker and add approximately 10-mL of water, mix, and continue warming the beaker for 10 to 15 minutes to allow additional solubilization of any residue to occur.
7. Remove the beaker from the hot plate and wash down the beaker walls. Centrifuge at relative centrifugal force (RCF) 10,621g (10,000 rpm) for 60 minute and (when necessary) filter through a 0.45 μm Millipore membrane the sample to remove insoluble material that may interfere with injecting the sample into the graphite furnace atomic absorption spectrophotometer (GFAA). Adjust to the final volume of 100-mL with water.

To prepare water sample for soluble lead analysis, after centrifugation at a relative centrifugal force (RCF) of 10,621 g (10,000 rpm) for 60 minutes, the supernatant was filtrated through a 0.45 μm Millipore membrane. The filtrate was collected for lead analysis with GFAA. The particles collected were analyzed for various lead fractions according to the sequential extraction procedures(Tessier, Campbell et al. 1979).

Lead concentration was analyzed with an atomic absorption spectrophotometer (PerKinElmer Aanalyst-800, überlingen, Germany). Before analysis, allow the lamp to warm up for a minimum of 15 minutes. During this period, align the position of the autosampler. Subsequently, light the flame and regulate the fuel and oxidant flows. Run a series of standards during sample analysis. Construct a calibration curve by plotting the concentration of standards against absorbance. Standards were run each time as a series of samples was run. A standard were run for approximately every 10 sample runs.

3.3.5 Lead Speciation

The samples were stored at 4 ^{o}C. Experiments were conducted to characterize the performance of cross-flow electro-filtration module under various conditions, specifically, pH, and applied electrostatic field. The solids collected from filtrate water and concentrated water were further separated by centrifuging at 10,000 rpm (about 12,000 g) for 30 minute and then dried at 105 ^{o}C in a drying oven.

The sequential methodology chosen was that of Tessier et al., 1979. The sequential digestion identifies five metal fractions:

1. Exchangeable or adsorbed trace metals:

   These are loosely bound to the substrate and would change in concentration with changes in ionic composition of the overlying water. This fraction is exchanged using magnesium chloride solution at pH 7.0 (1 M $MgCl_2$, pH 7.0).

2. Metals bound to detrital carbonates:

   Changes in environmental pH would affect the binding of metals to carbonates. It is extracted with sodium acetate at pH 5.0 (1 M NaOAc adjusted to pH 5 with 0.5 M HOAc)

3. Metal coprecipitated with Fe and Mn oxides as coatings on particles:

   These are extracted using hydroxylamine hydrogen chloride (0.04 M $NH_2OH{\cdot}HCl$ in 25% (v/v) HOAc).

4. Metals associated with organic matter:

   Metals can either be incorporated into the tissues of living organisms, deposited as detritus, or can be found as a coating covering grains. Metals associated with organic matter would be released into the environment under oxidizing conditions. The

organic fraction was extracted using nitric acid, hydrogen peroxide and ammonium acetate (0.02 M HNO_3, 30% H_2O_2, 3.2 M NH_4OAc).

5. The residual fraction of heavy metals:

   The residual fraction of heavy metals is that trapped in the crystal lattices of primary and secondary minerals. Only released to environment upon complete destruction of the crystal in which they are found. The residual fraction was extracted using a mixture of concentrated hydrofluoric and perchloric acids (HF-$HClO_4$).]

The selective extraction was conducted in centrifuge tubes (Teflon, 50 mL) to minimize losses of solid material. Between each successive extraction, solids were separated by centrifuging (Labnet, model Z383K), at (RCF) 10,621 g (or 10,000 rpm) for 30 minutes. The supernatant was removed with a pipet and analyzed for heavy metals; whereas the residue was washed with 8-mL of deionized water. After centrifugation for 30 minutes, this second supernatant was discarded. The volume of rinse water used was kept to minimum as to avoid excessive solubilization of solid material, particularly organic matter. For residual trace metal analysis, the solid was digested with 5:1 mixture of hydrofluoric and perchloric acids. The sample was first digested in a centrifuge tube (Teflon) with a solution of concentrated $HClO_4$ (2mL) and HF (10 mL) to near dryness; subsequently a second addition of $HClO_4$ (1 mL) and HF (10 mL) was made and again the mixture was evaporated to near dryness. Finally, $HClO_4$ (1 mL) alone was added and the sample was evaporated until white fumes appears. The residue was dissolved in 12 N HCl (5 mL) and diluted to 25 mL. Table 2 shows the detailed procedures of the Tessier method for the sequential extraction of lead.

Lead concentration was analyzed with an atomic absorption spectrophotometer PerKinElmer Aanalyst-800 (überlingen, Germany). Before analysis, allow the lamp to warm up for a minimum of 15 minutes. During this period, align the position of autosampler. Subsequently, light the flame and regulate the flow of fuel and oxidant. Run a series of standards during sample analysis. Construct a calibration curve by plotting the concentration of standards against absorbance. Standards were run each time as a series of samples was run. A standard was run for approximately every 10 sample runs. Deionized water used in preparing stock solution and each leaching step was obtained from CORNING MEGA-PURE system MP-290 (New York, USA). All glassware, polypropylene, or Teflon containers, including sample bottles, flasks and pipets, should be washed in the following

sequence: detergent, tap water, 1:1 nitric acid, tap water, 1:1 hydrochloric acid, tap water, and reagent water. All acids used in the digestion and sequential extraction procedures were of trace metal grade and all other reagents used were of analytical grade or better.

4.0 Results and Discussion

4.1 Groundwater Sampling

It must be noted that the solid content was high in these well waters and the pump screen was clogged quickly during low flow purging last year. We had to lift the pump screen head from the well for cleaning frequently during water sampling. As a result, it is possible that the water samples collected may be disturbed. This year, we follow the standard low flow purging procedures (2.2 and 2.3) closely. The pump screen was not clogged anymore during low flow purging. And consequently we did not have to lift the pump screen head for cleaning during water sampling.

4.1.1 Particle Size

The results show that the particles appear to be monodispersed in the well #10 and #5S. The average particle diameter of water sample in the well #10 is in the range of 297 to 495 nm. The average particle diameter of water sample in well #5S is in the range of 522 to 1,007 nm. The above results show that the size of particles in the well #5 is larger than those from well #10. Another observation is that the size of particles in well #10 and #5S by bailing sampling method are larger than that from well #10 and #5S by low flow purging method. In the well #5S, the particle size of water sample collected by low flow purging sampling, high flow purging sample, and bailing sampling method are 522 ± 16, 817 ± 77, and 1007 ± 72 nm, respectively. In the well #10, the particle size of water samples collected by low flow purging sampling and bailing sampling method are 315 ± 4 and 495 ± 19 nm. Results also indicate that water-sampling methods appear to strongly impose effect on the particle size distribution. These results are different from last yeas. The mean particle size of water samples in the well #10 collected by the bailing sampling method is 490 ± 14 nm at last year, which is same as this year. The mean particle size of water samples in the well #5S collected by the bailing sampling method is 727 ± 59 nm at last year, which is almost same as sample collected by low flow purging sampling method obtained this year. But the mean particle size of water sample in well #10 and #5S collected by low flow purging method is 476 ± 19 and 774 ± 30 nm at last year, which is greater than those at this year. Because the pump screen was clogged during low flow purging at last year, we had lifted the pump screen head from the well for cleaning frequently during water sampling. As a result, it is possible

that the water samples collected may be disturbed. The is why the mean particle size of water sample in well #10 and #5S collected by the bailing sampling method is same as water sample collected by the low flow purging sampling method as reported last year. Table 3 lists the average particle size of the water samples for well #10 and #5S water sample.

4.1.2 The Electrophoretic Mobility of Particle

Figures 1 to 7 show the zeta potential (surface charge) as a function of ionic strength of these colloidal particles in well #10 and #5S water samples. In the well #10 water samples, the zeta potential of particle are around -12 mV at pH 2. In the well #5S water sample, the zeta potential of particle is similar as well #10 water samples. Results show that the pH_{zpc} of all water samples collected by low flow purging sampling, high flow purging sampling, and bailing sampling method is approximately 1 and that the colloidal particle is negatively charged at the pH values greater than 2. The results also indicate that water-sampling methods appear to impose no effect on the pH_{zpc} and surface charge of colloidal particles as expected.

4.1.3 The Total Solid Content

Table 4 shows the concentration of total solid in the well #10 and #5S water samples for bailer, low flow purge and high flow purging technique. In the well #10 water samples, the total solid content is in the range of 0.94 to 1.74 g/L. The total solid concentration is in the range of 2.94 to 12.22 g/L for well water #5S. The results show that the total solid concentration of water samples in well #5S is greater than those in the well #10. Results indicate that the total solid concentrations of well #5S are 2.94 ± 0.01, 11.98 ± 0.02 and 12.22 ± 0.03 g/L, respectively, for water samples obtained by low flow purging, high flow purging and bailing methods. The total solid content of water samples in well #5S collected by low flow purging sampling method is less than those by high flow purging sampling and bailing method. For the well #10, the results of water samples are similar as well #5S. The total solid content of water samples collected by low flow purging sampling is less than bailing sampling technique. Apparently the disturbance caused by bailer and high flow purging technique brings about high total solid concentration in the water samples.

4.1.4 The Total and Soluble Lead

Table 5 gives the total lead and soluble lead in well #10 and #5S waters. The range of the average total lead concentration was 164, 377 and 401 μg/L, respectively, in water

sample collected by low flow purging, high flow purging and bailing sampling method in well #5S. The range of the soluble lead concentration in well #5S was 4, 3 and 4 μg/L for the low flow purging, high flow purging and the bailer technique. For well #10, the total lead concentration of water collected by low flow purging and bailing sampling method was 11 and 28 μg/L. The soluble lead concentration in well #10 was 1 μg/L and close to the detection limit (ND<1 μg/L) for the bailer and the low flow purging technique, respectively. Based on above results, the lead concentration of well #5S water samples was greater than those in well #10. Results show that the lead was almost adsorbed on the colloid matter. Another observation is that the total lead concentrations in water samples collected by bailing and high flow purging sampling method were generally greater than these in water samples collected by low flow purging sampling method. According to the total solid content and lead concentration of water samples data, the more total solid content the water samples contain, the more lead concentration the water samples have.

4.1.5 The Lead Speciation

Although the total and soluble concentration of heavy metals in contaminated groundwater is of general relevance to the assessment of potential toxicity, a key point is to determine how much of heavy metal is mobile or plant-available under natural environmental conditions. Heavy metal mobility and availability in contaminated materials depends, to a large extent, upon the different chemical and mineralogical forms that present. Toxic trace elements released into aquatic systems are generally bound to particulate matter. However, some of colloid-bound metals may remobilize and be released back to waters with changes of environmental conditions, and impose adverse effects on living organisms. Besides the physical, chemical and biological characteristics of the interstitial water and colloid, the chemical partitioning of trace metals is very important in determining the bio-availability of trace metals (Luoma 1983). The major mechanism of metal accumulation in particulate can be grouped in five major metal geochemical forms (Tessier, Campbell et al. 1979; Salomons and Forstner 1980): (1) exchangeable; (2) bound to carbonate phase; (3) bound to iron-manganese oxides; (4) bound to organic matter; and (5) residual metal phase. These metal fractions have different mobility, biological availability and chemical behaviors. Thus, it is necessary to identify and quantify the metal forms in order to assess the environmental impacts of contaminated groundwater. Many previous studies have attempted to define these

forms. Most previous studies frequently used selective extraction analysis (Sims and Patrick 1978; Miller, McFee et al. 1983; Hickey and Kittrick 1984; Miller, Martens et al. 1986; Xian 1989; Xian and Shokohifard 1989; Clevenger 1990; Dudka and Chlopecka 1990; Chlopecka 1993; Ramos, Hernandez et al. 1994; Chen, Tan et al. 1996; Chlopecka, Bacon et al. 1996; Gee, Ramsey et al. 1997; Morera, Echeverria et al. 2001; Svete, Milacic et al. 2001; Zhang, Wang et al. 2002). The method of Tessier et al. (1979) is one of the most thoroughly researched and widely used to evaluate the possible chemical associations of metals.

Figures 8 and 9 show the distribution of the lead species, namely, exchangeable, bound to carbonates, bound to Fe/Mn oxide, bound to organic matter and residual in sequential extraction from well 10 and #5S water sample. The corresponding raw data are shown in Table 6. Detailed lead distribution in various geochemical forms is listed in Figures A6 – A12.

Exchangeable metal ions are a measurement of trace metals that are released most readily into environment. With respect to the total lead content, the exchangeable fraction is a minor component (generally less than detection limit) and varies slightly with sampling technique in all water samples. For well #5S water sample by the bailing sampling method, lead was mostly concentrated in the residual fraction. The percentage of lead associated with various fractions followed the order: residual (69%) > organic matter (16%) ≈ Fe-Mn oxide (15%). For well #5S water sample by the low flow purging sampling method, lead was mostly concentrated in the residual fractions. The percentage of lead associated with various fractions followed the order: residual (87%) > organic matter (8%) ≈ Fe-Mn oxide (5%). For well #5S water sample by the high flow purging sampling method, lead was mostly concentrated in the residual fractions. The percentage of lead associated with various fractions followed the order: residual (84%) > organic matter (9%) ≈ Fe-Mn oxide (7%). For well #10 water sample by the bailing method, lead was mostly concentrated in the residual fraction. The percentage of lead associated with various fractions followed the order: residual (93%-94%) > Fe-Mn oxide (3%-5%) ≈ organic matter (1%-4%). For well #10 water sample by the low flow purging method, lead was mostly concentrated in the residual fractions. The percentage of lead associated with various fractions followed the order: residual (85%-87%) > Fe-Mn oxide (10%-12%) > organic matter (3%). The results show

that lead was concentrated in the residual fraction in all well water samples. And the sampling methods did not affect the distribution of lead speciation.

The bio-availability of lead in particulate is thought to decrease approximately in the order of the extraction sequence, from readily available to unavailable, because the strength of extraction reagents used increases in the sequence. Hence, the exchangeable fraction may indicate the form of the metal that are most available for plant uptake. The second step extracts metals bound to carbonate and specifically adsorbed phases, which can easily become mobile and available under lower pH condition. The remaining three fractions (Fe-Mn oxide, organic matter and residual) are generally strongly held within the particulate and normally unavailable to plants. Based on the results, it can be seen that the fraction exchangeable/bound to carbonate is minor. This is indicative of strong bounding of lead to oxides, organic matters and silicates. This chemical bounding is strong enough to accumulate metal in the particulate and, under natural environmental conditions, the release of lead is not significant.

4.2 Operation and Performance of CFEF Module Using Groundwater Samples

4.2.1 Operation of CFEF Module

Since the solid concentration of water sample exceeds the detection limit of 1,000 nephelometer turbidity units (NTU) and the total volume of each water sample available was about 20 liters, the water samples were diluted with distilled water. Laboratory experiments were conducted to evaluate the performance of the cross-flow electro-filtration unit. The following operational conditions were tested: (1) clogging, (2) flux production, (3) quality of flux, and (4) backwash frequency. The degree of filter clogging can be measured in terms of several properties including pressure drop and water quality of the filtrate, i.e. turbidity. During the course of the filtration, the pressure of the system was monitored continuously. Flux production is expressed in terms of mass (or volume) of water produced per time per unit area of the filter, i.e. cm^3/cm^2-min. The turbidity of the filtrate was measured during filtration. The frequency of filter backwash was evaluated.

It is hypothesized that the naturally occurring particles can be separated according to particle size and surface charge. Furthermore, it is expected that pH and applied field control the particle size and surface charge of naturally occurring particulate, laboratory experiments were run under the following conditions: filtration rate constant at 1.1 cm^3/cm^2-min,

electrostatic field strength applied at 0, 32.3 (100), 60.3 (187), 64.5 (200), 71.3 (221), 96.8 (300), 112.6 (349), 119.7 (371), 123.9 (384), 129.0 (400), 137.1 (425), 138.7 (430), 142.6 (442) and 152.9 V/cm (474 V).

4.2.2 Clogging

The degree of filter clogging was measured in terms of several properties including pressure drop and water quality of the filtrate i.e. turbidity. During the course of filtration, the pressures of the system were monitored continuously. The initial pressure of inlet and outlet were controlled at 1 and 2 psi, respectively. At the end of experiments, the pressure of inlet and outlet always remained unchanged. This means that the pressure drop is minimal and that the filter is not clogged.

4.2.3 Quality of Flux

Suspended and colloidal matter such as clay, silt, finely divided organic and inorganic matter cause the turbidity in water. The turbidity (in NTU unit) of the filtrate was measured against a calibration curve using dilute water sample solutions. Figures A13 – A19 show the calibration curves of water samples for turbidity measurements of well #10 and #5S water samples. A linear relationship exits between turbidity and the solid concentration of water samples was observed. The turbidity (NTU) is related to the water sample concentration, C (g/L), by the following expressions:

Sample	Empirical Equation	Corr. Coef.
10IIB01	NTU = 3.2 + 347.53C	$R^2 = 0.9996$
10IIB02	NTU = -4.2 + 818.96C	$R^2 = 0.9999$
10IIL01	NTU = 3.6 + 207.11C	$R^2 = 0.9989$
10IIL02	NTU = 4.0 + 174.18C	$R^2 = 0.9971$
5SIIIL03	NTU = -12.2 + 1018.2C	$R^2 = 0.9990$
5SIIIB03	NTU = -5.8 + 1456.9C	$R^2 = 0.9993$
5SIIIH03	NTU = -15.7 + 1654.4C	$R^2 = 0.9988$

The results show that all water samples have a high refractive index, which contribute turbidity to the water even at very low total solid concentrations.

4.2.4 Backwash Frequency

The filter shows no clogging after operation for 2 hours. Therefore, it is not necessary to backwash the filter.

4.2.5 Effect of Electrostatic Field Applied

Figure 10 shows the visual appearance of well #5S for low flow purging samples under various electrostatic fields. Figure 10 indicates that filtrate is clearer than the raw water sample in the presence of electrostatic field. Figures 11 - 22 show the effect of electrostatic field on the removal of particles collected from well #10 and #5S. Figure A20, A22, A24, A26, A28, A30, A32, A34 and A36 give the residual turbidity of the filtrate, and Figure A21, A23, A25, A27, A29, A31, A33, A35 and A37 represent the removal efficiency as a function of time at various electrostatic field values. The corresponding raw data are show in Tables 7 and A1-A20. The removal efficiency of colloidal particle is expressed by:

$$R_i = \frac{T_o - T_i}{T_o} x100(\%) \qquad (1)$$

Where:

R_i : Removal efficiency at the ith minute

T_0 : The turbidity of suspension at 0 minute

T_i : The turbidity of suspension at the ith minute

Results indicate that the removal rate is fast for all water samples during the first 4 minutes. The final removal efficiency was 6, 31, 54, and 64%, respectively, at the electrostatic field of 0, 32.3, 64.5, and 71.3 V/cm (0, 100, 200, and 221V) for well #10 water sample collected by the bailing sampling (Figure 11). For well #10 water sample collected by low flow purging sampling, the final removal efficiency was 2, 39, and 64%, respectively, at electrostatic field of 0, 32.3, and 60.3 V/cm (0, 100, and 187V), respectively (Figure 13). Based on the results for well #10 water samples, it is clear that high electrostatic field will benefit the removal efficiency. For the well #5S, the final removal efficiency was 7, 40, 54, 69, 78 and 75%, respectively, at the electrostatic field of 0, 32.3, 64.5, 96.8, 119.7 and 123.9

V/cm (0, 100, 200, 300,371 and 384 V) for water sample collected by the low flow purging sampling (Figure 14). For water samples collected by bailing sampling, the final removal efficiency was 6, 34, 48, 64, 80 and 82%, respectively, at electrostatic field of 0, 32.3, 64.5, 96.8, 129.0 and 138.7 V/cm (0, 100, 200, 300, 400 and 430 V), respectively (Figure 17). For water sample collected by high flow purging sampling, the final removal efficiency was 4, 30, 47, 60 and 70 %, respectively, at electrostatic field of 0, 32.3, 64.5, 96.8 and 117.7 V/cm (0, 100, 200, 300 and 365 V), respectively (Figure 20). According to the results, in the absence of an electrostatic field condition (i.e., 0 V), the final removal efficiency was about 2 to 6%. As expected, high electrostatic field will enhance the removal efficiency of particles.

In well #10 water sample by bailing sampling and well #5S water sample by high flow purging sampling, the electrostatic field strength applied was only at 71.3 (221 V) and 117.7 V/cm (365 V) (Figures 11 and 20). Higher field strength can not be achieved because of its high conductivity (120 and 80 μmhos). The conductivity of a solution is a measurement of the ability of a solution to conduct a current and is directly attributable to ions in solution. Electric current is transported through solution via the movement of ion, and conductivity increases as ion concentration increases. The resistivity is reversely related to conductivity:

$$\mathbf{R} = \rho \frac{\mathbf{1}}{\mathbf{A}} = \frac{1}{\mu} \frac{\mathbf{1}}{\mathbf{A}} \qquad (2)$$

Where R, ρ, and A are resistance, resistivity, and crosses-section area of conductor, respectively.

Based on the *Ohm's law*, we can determine the resistance of the CFEF unit between two points by applying a given potential difference, V, between them and measuring the current, I:

$$\mathbf{V} = \mathbf{IR} \qquad (3)$$

Where V is in volt, I is in ampere, and R is in ohm (Ω), respectively.

Equation (3) shows that there is a relationship between V and R at constant I. If the resistance decreases as conductivity increases, the potential difference will decrease under constant current condition. In other words, there is a reverse relationship between potential difference and the conductivity of the solution. The maximum current of power supply used in our experiment is only 1,000 mA. This is the main reason why we can not increase the

voltage to 60 0V (or electrostatic field) in well #10 and #5S water samples. To verify the above hypothesis, we dilute the sample (decreasing the conductivity of solution) and repeatedly run the well #10 and #5S water samples (Tables A3, A4, A19 and A20). The initial turbidity of well #10 and #5S water samples decreases from 207 and 720 NTU to 98 and 285 NTU, respectively. The initial conductivity decreased from 120 and 80 μmho to 50 and 49 μmho, respectively for well #10 and well #5S. The conductivity of the final concentrate was 50, 70, 135, and 190 μmho, respectively, at electrostatic potential of 100, 200, 300, and 349 V (or 32.3, 64.5, 96.8, and 112.6 V/cm) for well #10 water sample by the bailing sampling. The higher electrostatic field can be applied until 349 volt was applied. The removal efficiency was 4, 35, 52, 66, and 74%, respectively, at electrostatic field of 0, 32.3, 64.5, 96.8, and 112.6 V/cm (Figure 12). For well #5S water sample collected by the high flow purging sampling, the conductivity of final concentrate is 60, 76, 85, 100 and 116 μmho, respectively, at electrostatic potential of 100, 200, 300, 400 and 442 V (or 32.3, 64.5, 96.8, 129.0 and 142.6 V/cm). The higher electrostatic field can be applied until 442 V was applied. The removal efficiency was 6, 37, 56, 61, 75 and 80%, respectively, at electrostatic field of 0, 32.3, 64.5, 96.8, 129.0 and 142.6 V/cm (Figure 21). According to the above results, the total solid content can affect the conductivity of water sample and then change the performance of CFEF process. The question is that the removal efficiency will be the same under same electrostatic field applied and various total solid concentrations.

4.2.6 Effect of Total Solid Content

Figures 15, 18 and 21.show results on the effect of electrostatic field on the removal of total solid (total solid concentration: 0.18 ~ 0.68 g/L) for well #5S water samples. The corresponding raw data are shown in Table 7 and Tables A9-A20. The final removal efficiency error was 0.7, 1.9, 1.6 and 0.8 %, respectively, at the electrostatic field of 0, 32.3, 64.5 and 96.8 V/cm (or 0, 100, 200 and 300 V) for well #5S water sample collected by the low flow purging sampling at total solid concentration of 0.7 and 0.4 g/L. The final removal efficiency error was 3.4, 0.2, 0.1 and 0.2%, respectively, at the electrostatic field of 32.3, 64.5, 96.8 and 129.0 V/cm for well #5S water sample collected by the bailing sampling at total solid concentration of 0.52 and 0.27 g/L. For well #5S water sample collected by high purging sampling at total solid concentration of 0.44 and 0.18 g/L, the final removal efficiency error was 5.1, 4.1 and 0.5 % at the electrostatic field of 32.3, 64.5 and 96.8 V/cm,

respectively. The results show that there is no distinct difference in removal efficiency at various total solid concentrations within the concentration range tested.

4.2.7 The Particle Size Distribution of Filtrate and Concentrate

Figures 23-30 show the effect of electrostatic field on the particle size distribution of filtrates and concentrates. The corresponding raw data are show in Figures A38-78. The mean particle diameter is in the range of 441 and 286 nm for well #10 water samples collected by bailing and low flow purging sampling, respectively. For well #5S, the mean particle diameter of water samples collected by low flow purging, bailing and high flow purging sampling method is 522, 1007 and 817 nm, respectively (Table 3). The average particle size of filtrate for water sample collected by those in the low flow purging, bailing and high flow purging sample in well #10 and #5S is less than raw and concentrate. Figures 10 and 11 and show the effect of electrostatic field on the particle size distribution of filtrates and concentrates. According to the above results, the mean particle size of filtrate decrease as the applied electrostatic field increase.

4.2.8 The Total and Soluble Lead concentration of Filtrate and Concentrate

Table 9 shows the total lead and soluble lead concentration of filtrate and concentrate for well water samples #10 and #5S. The total and soluble lead concentration of filtrate were < 1 μg/L in well#10 water sample collected by the bailing. The total and soluble lead concentration of concentrate were also < 1 μg/L in well#10 water sample collected by bailing. The total lead concentration of the concentrate was in the range of 2 to 6 μg/L. Results show that the total lead concentration increases as the applied electrostatic field increases in the well #10 water sample collected by bailing sampling. In the well#10 water sample collected by the low flow purging sampling technique, the soluble lead concentration of filtrate was close to the detection limit (< 1 μg/L). The total lead concentration of filtrate was 6 μg/L. These results were different from the well #10 water sample collected by bailing. This could be contributed to the applied electrostatic field. The soluble lead concentration of concentrate was in the range of 12 to 13 μg/L and greater than that in the absence of electrostatic field (i.e. 0 V). From the results, we can attribute the high lead concentration to the high particle loading.

For well #5S water samples collected by the low flow purging, bailing and high flow purging sampling method, the soluble lead concentration of filtrate and concentrate were 1

and 2 μg/L, respectively. The total lead concentration in the filtrate was 20, 17, 13, 10, 8 and 9 μg/L, respectively, at the electrostatic field of 0, 32.3, 64.5, 96.8, 119.7 and 123.9 V/cm in well #5S water sample collected by the low flow purging sampling method (Figure 31). The total lead concentration in the filtrate was 27, 13, 12, 9, 7 and 5 μg/L, respectively, at the electrostatic field of 0, 32.3, 64.5, 96.8, 129.0 and 138.7 V/cm in well #5S water sample collected by the bailing sampling method (Figure 32). For well #5S water sample collected by the high flow purging sampling method, the total lead concentration in the filtrate was 23, 18, 16, 13 and 13 μg/L, respectively, at the electrostatic field of 0, 32.3, 64.5, 96.8 and 117.7 V/cm (Figure 33). The results show that the total lead concentration in the filtrate decreases with increasing the electrostatic field in well #5S water sample collected by the low flow purging method. The soluble lead concentration in the concentrate was also in the range of 1 and 2 μg/L in well #5S water sample collected by the low flow purging, bailing and high flow purging method. The total lead concentration of the concentrate was 20, 23, 26, 34, 28 and 29 μg/L, respectively, at the electrostatic field of 0, 32.3, 64.5, 96.8, 119.7 and 123.9 V/cm in well #5S water sample collected by the low flow purging method. The total lead concentration in the concentrate was 18, 26, 25, 32, 28 and 27 μg/L, respectively, at the electrostatic field of 0, 32.3, 64.5, 96.8, 129.0 and 138.7 V/cm in the well #5S sample collected by the bailing method. For the well #5S water sample collected by the high flow purging method, the total lead concentration in the concentrate was 23, 29, 30, 32 and 34 μg/L, respectively, at the electrostatic field of 0, 32.3, 64.5, 96.8 and 117.7 V/cm. Results showed the total lead concentration in the concentrate decreased as the applied electrostatic field increased in the well #5S water sample collected by the low flow purging, bailing and high flow purging method. The result was different from the total lead concentration in the filtrate. This could be attributed to the applied electrostatic field. From the results, we can attribute the high lead concentration to the high particle loading.

4.2.9 The Speciation of Lead

Figures 34-38 show the effect of electrostatic field on the distribution of the lead species, including exchangeable, bound to carbonates, bond to Fe/Mn oxide, bound to organic matter and residual in sequential extraction fraction for well #10 and #5S water samples. The corresponding raw data are shown in Tables 10 to 14. Detailed of lead distribution in various geochemical forms is listed in Figures A79 to A103.

Exchangeable metal ions are a measure of trace metals that are released most readily into environment. With respect to the total lead content, the exchangeable fraction was less than the detection limit. For well #10 water sample by the bailing sampling method, lead was mostly concentrated in the residual fraction and vary slightly with various electrostatic fields. The percentage of lead associated with various particulate fractions at electrostatic field of 32.3 V/cm (100 V) followed the order: residual (33%) ≈ Fe-Mn oxide (33%) > carbonate (29%) > organic matter (5%). The percentage of lead associated with various particulate fractions at electrostatic field of 64.5 V/cm (200 V) followed the order: residual (35%) > carbonate (31%) > Fe-Mn oxide (30%) > organic matter (4%). The percentage of lead associated with various particulate fractions at electrostatic field of 96.8 V/cm (300 voltage) followed the order: residual (49%) > carbonate (25%) > Fe-Mn oxide (20%) > organic matter (6%). The percentage of lead associated with various particulate fractions at electrostatic field of 112.6 V/cm (349 V) followed the order: residual (43%) > carbonate (29%) > Fe-Mn oxide (22%) > organic matter (6%) at electrostatic field of 112.6 V/cm (349 voltage). According the above results, the percentage of lead associated with organic matter fraction varied slightly with electrostatic field strength. The percentage of lead associated with the residual fraction increased as electrostatic field increased. The percentage of lead associated with the Fe-Mn oxide fraction decreased as electrostatic field increased.

For well #5S water samples, the exchangeable and carbonate fraction were minor components (generally less than 3%) and varied slightly with various electrostatic field. For water samples collected by the low flow purging method, lead was mostly concentrated in the residual fraction and varied slightly with electrostatic field. The percentage of lead associated with various particulate fractions at various electrostatic fields followed the order: residual (67 ~ 83%) > organic matter (8 ~ 14%) ≈ Fe-Mn oxide (7 ~ 16%) > carbonate (2 ~ 3%). The result shows that the percentage of lead associated with inorganic matter and Fe-Mn oxide fractions almost same at various electrostatic field.

For well #5S water sample collected by the bailing sampling method, lead was mostly concentrated in the residual fraction and the exchange fraction were minor components (generally less than detection limit). The percentage of lead associated with residual fractions was 39,59,80,78 and 81%, respectively, at electrostatic field of 32.3 (100), 64.5 (200), 96.8 (300), 129.0 (400) and 138.7 V/cm (or 430 V), respectively. The percent of lead

associated with Fe-Mn oxide fraction was 33, 21, 10, 10 and 8%, respectively, at electrostatic field of 32.3 (100), 64.5 (200), 96.8 (300), 129.0 (400) and 138.7 V/cm (or 430 voltage). The percentage of lead associated with organic matter fraction was 21, 17, 9, 10 and 9%, respectively, at electrostatic field of 32.3 (100), 64.5 (200), 96.8 (300), 129.0 (400) and 138.7 V/cm (or 430 voltage). The percentage of lead associated with carbonated fraction was 7, 3, 1, 2 and 2%, respectively, at electrostatic of 32.3 (100), 64.5 (200), 96.8 (300), 129.0 (400) and 138.7 V/cm (or 430 voltage). The result show the percentage of lead associate with residual fraction increased with increasing applied electrostatic field. The percentage of lead associated with Fe-Mn oxide, organic matter and carbonate fraction slightly decreasd with increasing the electrostatic field.

For well #5S water sample collected by the high flow purging sampling method, lead was mostly concentrated in the residual fraction and the exchange fraction were minor components (generally less than detection limit). The percentage of lead associated with residual fraction was 80, 77, 85 and 88%, respectively, at electrostatic field of 32.3 (100), 64.5 (200), 96.8 (300), 129.0 (400) and 138.7 V/cm (or 430 voltage). The percentage of lead associated with the other fractions at various electrostatic fields followed the order: organic matter (6 ~ 11%) ≈ Fe-Mn oxide (5 ~ 10%) > carbonate (1 ~ 2%). The results show that the percentage of lead associated with residual fraction slightly increased with applied electrostatic field increasing. The other observation is that the percentage of lead associated with inorganic matter and Fe-Mn oxide fractions almost same at various electrostatic field.

According to the above results, the percentage of lead associated with the organic matter fraction wais almost the same as the percentage of lead associated with Fe-Mn oxide and varies slightly with electrostatic field strength for all particulates collected from the well #5S water samples. For the particulate in well #5S water sample collected by the bailing sampling method, the percentage of lead associated with the residual fraction increased as electrostatic field increases.

4.3 Operation and performance of CFEF Module Using Surrogate Colloidal Particles

We selected colloidal silica (SiO_2) as the surrogate colloidal particles for studies. The surface charge of colloidal silica is negative, which is the same as naturally occurring particles collected from the groundwater. The particle size of colloidal silica is from 76 to 126 nm which is smaller than naturally occurring particle collected from groundwater (see

4.1). Laboratory experiments using colloidal silica were conducted to characterize the performance of the cross flow electro-filtration module under various conditions, namely, pH and applied voltage.

4.3.1 Particle and Characterization

The colloidal silica was obtained from the Nissan Chemical Industries, Ltd. (Chiba, Japan). Results show that the particles appear to be monodispersed. The mean particle diameter of Snowtex 20L and Snowtex ZL are 76 and 126 nm, respectively. Another observation is that the particle size of colloidal silica is larger than those in the groundwater studied (297 to 1,007 nm).

Figures 39 and 40 show the zeta potential (surface charge) as a function of ionic strength of the colloidal silica. Results show that the pH_{zpc} is approximately 1~2 and that the colloidal silica is negatively charged at the pH values greater than 2. The results also indicate that the pH_{zpc} and surface charge of colloidal silica is same as naturally occurring particles collected from groundwater studied.

4.3.2 Operation of CFEF Model

Since the concentration of the colloidal silica sample exceeded the detection limit of 1,000 NTU and the total volume of each water sample available was about 2 liters, the colloidal silica samples were diluted with distilled water. The initial pH values were measured while the suspension was being stirred. Then the pH was adjusted to the range from 5 to 9.0 with 5N $HClO_4$ and/or 5N NaOH. Laboratory experiments were conducted to evaluate the performance of the cross-flow electro-filtration unit. The operational conditions were same as section 4.2.1.

As mentioned above, it is hypothesized that the colloidal particles can be separated according to particle size and surface charge. Furthermore, it is expected that pH and applied field control the particle size and surface charge of colloidal particulate, laboratory experiments were run under the following conditions: (1) pH and (2) initial electrostatic field applied. The filtration rate was kept constant at 1.1 cm^3/cm^2-min. The pH value of solution was adjusted to the range between 5 and 9.0 with 5N $HClO_4$ and/or 5N NaOH. The electrostatic field strength applied was at 0, 32.3 (100), 64.5 (200), 96.8 (300), 129.0 (400) and 138.7 (or 430), 161.3 (500), 174.2 (540) and 187.7 V/cm (587 V).

4.3.3 Clogging

The degree of filter clogging was measured in terms of pressure drop and water quality of the filtrate i.e. turbidity. During the course of filtration, the pressures of the system were monitored continuously. The initial pressure of inlet and outlet were controlled at 1 and 2 psi, respectively. At the end of experiment, the pressure of inlet and outlet always remained unchanged. This means that the pressure drop is minimal and that the filter is not clogged.

4.3.4 Quality of Flux

Figures A104 and A105 show the calibration curve of colloidal silica for turbidity measurement. A linear relationship exits between turbidity and the solid concentration of colloidal silica was observed. The turbidity (NTU) is related to the water sample concentration, C (g/L), by the following expressions:

Sample	Empirical Equation	Corr. Coef.
SNOWTEX 20L	NTU= 3.0 + 48.09C	R^2=0.997
SNOWTEX ZL	NTU= 2.3 + 0.23C	R^2=0.999

The results show that all water samples have a high refractive index, which contribute turbidity to the water even at very low concentrations.

4.3.5 Backwash Frequency

The filter shows no clogging after operation for 3 hours. Therefore, it is not necessary to backwash the filter.

4.3.6 Effect of Electrostatic Field Applied

Figure 41 shows the visual appearance of colloidal silica Snowtex 20L under various electrostatic fields. Figure 41 indicates that filtrate is clearer than the raw water sample in the presence of electrostatic field. Figures 42-43 show the effect of electrostatic field on the removal of particles. The corresponding raw data are show in Tables 7 and A21-A24. The removal efficiency of colloidal particle is expressed as equation 1.

Results indicate that the removal rate is fast during the first 4 minutes. The final removal efficiency for Snowtex 20L was 2, 20, 45, 71, 94, 95, and 95.4%, respectively, at the electrostatic field of 0, 32.3, 64.5, 96.8, 129.0, 161.3, and 174.2 V/cm (0, 100, 200, 300, 400,

and 500, and 540V). For Snowtex ZL, the final removal efficiency was 3, 21, 60, 70, 93, 97, and 98%, respectively, at electrostatic field of 0, 32.3, 64.5, 96.8, 129.0, 161.3, and 187.7 V/cm (0, 100, 200, 300, 400, and 500, and 582V), respectively. As expected, high electrostatic field will enhance the removal efficiency of particles.

4.3.7 Effect of pH

Figures 44 and 45 show the effect of pH on the performance of the CFEF system. The corresponding raw data are shown in Tables 5, A110 to 113. The results show that the particle removal efficiency is slightly affected by pH. At pH value higher than pH_{zpc}, the particles are negatively charged. The zeta potential of colloidal silica present in the Snowtex 20L and ZL water samples is indistinguishable and is in the range of pH 5 to 7.

4.3.8 Effect of Salt Concentration

The sample solution were prepared with about 115 mg γ-Al_2O_3 /L in deionized-distilled water at different ionic strengths of 0, 10^{-3}, 10^{-2}, and 10^{-1}M NaCl. The initial pH values were measured while the suspension was being stirred. The electrostatic field strength applied was at 0, 96.8, and 161.3 V/cm for 0 M salt concentration water sample. The electrostatic field strength applied was at 0 and 52.6 V/cm for 10^{-3}M concentration salt water sample. Higher field strength can not be achieved because it's high conductivity (109 μ mhos). The result is the same as well #MW3 water sample (Third Quarter Report, 2001). So I repeatedly ran 0 M salt concentration water sample again at electrostatic field of 52.6 V/cm. Figures 46 and 47 show the effect of ionic strength on the removal of particles. Results indicate that the removal rate is fast during the first 4 minutes. The final removal efficiency was 10 and 42%, respectively, for 10^{-3} and 0 M salt concentration. It is indicated that high salt concentration will decline the removal efficiency of particle as expected. The results agree with last year report.

4.3.9 The Particle Size Distribution of Filtrate and Concentrate

Figures 48 and 49 show the effect of electrostatic field on the particle size distribution of filtrates and concentrates. The mean particle diameter is in the range of 78 to 102 nm for colloidal silica Snowtex 20L. The mean particle diameter is in the range of 123 to 149 nm for colloidal silica Snowtex ZL. The average particle size of filtrate is roughly the same as those of the concentrate. This is because the spread range of particle size distribution of colloidal silica is very narrow.

Figures 50 and 51 show the effect of pH on the particle size distribution of filtrate and concentrate. The mean particle diameter is in the range of 78 to 98 nm for colloidal silica Snowtex 20L. The mean particle diameter is in the range of 120 to 126 nm for colloidal silica Snowtex ZL. The average particle size of the filtrates is roughly the same as those of the concentrates. The effect of pH on the particle size distribution is the same as that of the electrostatic field. The major reason is that the range of particle size distribution of colloidal silica is very narrow.

4.4 Separation Various Particle Size Using CFEF Module

4.4.1 Bimodal of Particle Size Distribution

Because the spread range of particle sizes distribution of naturally occurring particles collected from groundwater samples are very narrow. We can not observe the separation effect of particle size using the CFEF technique. Therefore, we use naturally particle collected from groundwater samples and model colloidal silica (SiO_2) to prepare a bimodal of particle size distribution. Under the prevailing pH conditions of most groundwater, the surface charge of colloidal silica is negative. This is the same situation as naturally occurring particles collected from water sample. The mean particle sizes of colloidal silica and naturally occurring particle collected from water sample (10IIB02) are 76 and 441 nm, respectively. We prepare colloidal silica and naturally occurring particle at different concentration to determine the best proportion for bimodal distribution (Figure 52). Before any separation experiment, it is necessary to know of we can use turbidity instead of solid concentration to express the separation efficiency as both colloidal silica and naturally occurring particle are present simultaneously. Figures A31-A33 show the calibration curves for turbidity measurements. The results show that the predictive vales are in good agreement that the measured values

4.4.2 Effect of Electrostatic Field Applied

Figure 53 shows the effect of electrostatic field on the removal of particle in two different sizes. The corresponding raw data are shown in Figures A133 and A135. Results indicate that the removal rate is fast during the first 4 minutes. The final removal efficiency for 10IIB02 + Snowtex 20L was 7, 34, 48, 69, 78, and 80%, respectively, at the electrostatic field of 0, 32.3, 64.5, 96.8, 124.5, and 126.5 V/cm. As expected, high electrostatic fields will enhance the article removal efficiency.

4.4.3 The Particle Size Distribution of Filtrate

Figure 54 shows the effect of the electrostatic field on the particle size distribution of filtrates. According the Figure 54, the proportion of larger particle size (i.e. naturally occurring particle) decrease as the electrostatic field strength increases. On the other hand, the proportion of smaller particle (i.e. Snowtex 20L) increases as the electrostatic field of different strength increases. Base on the results, we can successfully separate particles of different size using the CFEF module. In this study, we used both 0.45 and 0.2 μm pore size filters to separate the above particles. During the filtration processes, the filter was easily hold up the fine particle, forming filter cake and rendering the filtration operation very difficult. Results show that both particles of different particle sizes were filtrated simultaneously.

5.0 Conclusion

1. Groundwater samples were collected from well #10 and #5S with bailers, high flow purging (HFP) and low flow purging techniques (LFP) at the Denzer-Schaefer site, Toms River, NJ. The pump screen was clogged quickly during low flow purging operation last year. We had to lift the pump screen head from the well for cleaning frequently during water sampling. As a result, it is possible that the water samples collected may be disturbed. This year, we follow closely the standard low flow purging procedure. The pump screen was not clogged anymore during low flow purging. The pump screen head did not need to be lifted for cleaning during water sampling.
2. The naturally occurring particles collected from well water appear to be monodispered. The pH_{zpc} of particulate collected from the well #10 and #5S is approximately 1.0. Results indicate that the naturally occurring particles are negatively charged at pH greater than 2. Results also indicate that water-sampling method appears to impose no effect on the pH_{zpc} and surface charge of colloidal particles as expected.
3. The mean particle size of naturally occurring particle collected from well #10 and #5S water samples is in the range from 297 to 1007 nm. Results show that the particle size in well #10 and #5S collected by high flow purging or bailing methods is larger than that of particles collected by low flow purging method. Results also indicate that water-sampling method appears to strongly affect the particle size distribution.
4. The total solid concentration of well #10 and #5S water collected by bailing method, high flow purging and the low flow purging techniques is in the range of 0.94 to 12.22 g/L. Results show that the total solid concentration of water samples in well #5S is greater than that in the well #10. Results also indicate that total solid concentration of all well water samples collected by bailer or high flow purging method is greater than that of well water samples collected by low flow purging technique.
5. The total lead concentration of well #5S water sample collected by the low flow purging, high flow purging and bailing method were 164, 377 and 401 μg/L, respectively. The range of soluble lead concentration was from 3 to 4 μg/L. For well #10, the total lead concentration of water samples collected by the low flow purging and bailing sampling method were 11 and 28 μg/L, respectively. The soluble lead concentration of water

samples collected by the low flow purging and bailing method were 1 μg/L. According to the results, the lead almost was adsorbed on the colloid. Another observation is that the total lead concentration in well water collected by bailing or high flow purging method was generally greater than that in water sample collected by low flow purging method. Apparently the disturbance caused by bailing and high flow purging brings about high total lead concentration in the water samples. This can be preliminarily attributed to the high solid content in the well water.

6. The colloidal silica (SiO_2) and naturally occurring colloid were selected for CFEF evaluation. The results show that the prototype CFEF unit functions properly. There is no clogging problem encountered. The final pressure at the inlet and outlet always remain identical and is equal to the final pressure. Therefore, it is not necessary to backwash the CFEF unit under the experimental conditions of this study.
7. A linear relationship exists between the turbidity and the total solid concentration of well water samples and surrogate colloidal particles. The linear correlation coefficient (R^2) is 0.99. It is possible to use turbidity measurements as an indication of water quality.
8. The removal rate of colloidal particle in water samples is faster during the first 1 to 4 minute and then remains constant.
9. The removal of naturally occurring particles collected from well #5S water sample is faster during the first 4 minutes. The final removal efficiency was 7, 40, 54, 69, 78 and 75%, respectively, at the electrostatic field of 0, 32.3, 64.5, 96.8, 119.7 and 123.9 V/cm (or 0, 100, 200, 300,371 and 384 V) for well #5S water sample collected by the low flow purging method. For well #5S water sample collected by bailing, the final removal efficiency was 6, 34, 48, 64, 80 and 82%, respectively, at electrostatic field of 0, 32.3, 64.5, 96.8, 129.0 and 138.7 V/cm (or 0, 100, 200, 300, 400 and 430 V), respectively. For well #5S water sample collected by high flow purging, the final removal efficiency was 4, 30, 47, 60 and 70 %, respectively, at electrostatic field of 0, 32.3, 64.5, 96.8 and 117.7 V/cm (0, 100, 200, 300 and 365 V), respectively. For well #10 or surrogate colloidal particle water samples, the results are similar to the well #5S. The removal efficiency increases with increasing the electrostatic field. As expected, high electrostatic field will enhance the removal efficiency of particles.

10. When the total solid concentration ranging between 0.18 to 0.68 g/L for well #5S water samples, there was no distinct difference in solid removal efficiency. For colloidal silica particle containing water samples, the effect of total solid content did not affect the removal rate of particle at the same electrostatic field strength. The results show that the removal efficiency of particle in water sample is independent under the experimental conditions.
11. The average size of particles in the filtrate for water sample collected by the low flow purging, bailing and high flow purging method in well #10 and #5S and surrogate water samples is less than those of the raw and concentrate water. According to results obtained the mean size of particles in the filtrate decreases as the applied electrostatic field increases.
12. Results show that the total lead concentration in the concentrate decreases as increasing applied electrostatic field. The other observations are that the total lead concentration in the filtrate decreases as applied electrostatic field increases. From the results, we can attribute the high lead concentration to the high particle loading.
13. For well #10 and #5S water sample collected by the low flow purging, bailing and high flow purging methods, lead was mostly concentrated in the residual fraction. With respect to the total lead content, the exchangeable fraction is a minor component. The percentage of lead associated with various particulate fractions at various electrostatic field followed the order: residual > Fe-Mn oxide > organic matter > carbonate. According to our results, the percentage of lead associated with organic matter fraction is almost the same as that associated with Fe-Mn oxide and varies slightly with electrostatic field strength in all particulates collected from the well water. For particulates collected from well #10 and #5S water by the bailing method, the percentage of lead associated with the residual fraction increases with electrostatic field.
14. The particle sizes distribution of naturally occurring particles collected from groundwater samples was wide-spreading. The surrogate colloidal particle (i.e., SiO_2) is narrowly distributed. The diameter of colloidal silica is smaller than naturally occurring colloidal particles. Therefore, both naturally occurring particles collected from groundwater samples and model colloidal silica (SiO_2) were selected to prepare a bimodal particle size distribution. Under the prevailing pH conditions of most groundwater, the surface charge

of colloidal silica is negative. The proportion of larger particle size (i.e., naturally occurring particle collected from groundwater) decrease as the electrostatic field strength increases. On the other hand, the proportion of smaller particle (i.e., colloidal silica) increases as the electrostatic field strength increases. Base on the results, it is clear that the CFEF technique can successfully separate particles of different size.

15. Results clearly indicate that the CFEF is able to separate the colloidal particles according to their size and surface charge. Most importantly, the distribution of lead in particles of different size and surface charge are different. Generally, the concentration of lead species increases with increasing field strength. That is, the smaller the particles the greater the metal concentration content at all fractions. The CFEF process can be an important technique for the speciation of various chemical species in natural water including groundwater. Moreover, CFEF is able to separate naturally colloidal particles with great ease; clogging, the most common operational problem is eliminated.

6.0 Literature Cited

Akay, G. and R. J. Wakeman (1996). "Electric field intensification of surfactant mediated separation processes." Chemical Engineering Research & Design: Transaction of the Institution of Chemical Engineers **74**(Part A): 517-525.

Altmann, J. and S. Ripperger (1997). "Particle deposition and layer formation at the crossflow microfiltration." Journal of Membrane Science **124**: 119-128.

Archer, G. P., M. C. Render, et al. (1993). "Dielectrophoretic concentration of micro-organisms using grid electrodes." Microbios **76**: 237-244.

Belfort, G. (1987). Advanced Biochemical Engineering. H. R. Bungay and G. Belfort. New York, Wiley. **Chapter 10**.

Belfort, G., R. H. Davis, et al. (1994). "The behavior of suspensions and macromolleculars in crossflow microfiltration." Journal of Membrane Science **96**(1-2): 1-58.

Bier, M. (1959). Electrophoresis. M. Bier. New York, Academic. **Chapter 15**.

Bowen, W. R. (1992). Design of electrically enhanced membrane separation processes. Colloid and surface Engineering. R. A. Williams. Oxford, Butterworth Heineman. **Chapter 7**.

Bowen, W. R., R. S. Kingdon, et al. (1989). "Electrically enhanced separation processes: The basis of in situ intermittent electrolytic membrane cleaning and in situ electrolytic membrane restoration." Journal of Membrane Science **40**(2): 219-229.

Bowen, W. R. and H. A. M. Sabuni (1994). "Electroosmotic membrane backwashing." Industrial & Engineering Chemistry Research **33**(5): 1245-1249.

Burgess, J. (1978). Metal ions in solution. Chinchester, England, John Wiley and Sons.

Burgmayer, P. and R. W. Murray (1982). "An ion gate membrane-electrochemical control of ion permeability through a membrane with an embedded electrode." Journal of the American Chemical Society **104**(22): 6139-6140.

Chao, T. T. and P. K. Theobald (1976). "The Singnificance of Secondary Iron and Manganese Oxides in Geochemical Exploration." Economic Geology **71**: 1560-1569.

Chen, W., S. K. Tan, et al. (1996). "Distribution, fractional composition and release of sediment-bound heavy metals in tropical reservoirs." Water, Air, and Soil Pollution **92**: 273-287.

Chiou, C. T., R. L. Malcolm, et al. (1986). "Water solubility enhancement of some organic pollutants and pesticides by dissolved humic and fulvic-acids." Environmental Science & Technology **20**(5): 502-508.

Chlopecka, A. (1993). "Form of trace metals from inorganic source in soils and amounts found in Spring Barley." Water, Air, and Soil Pollution **69**: 127-134.

Chlopecka, A., J. R. Bacon, et al. (1996). "Forms of cadmium, lead, zinc in contaminated soils from southwest Poland." Journal of Environmental Quality **25**: 69-79.

Clevenger, T. E. (1990). "Use of sequential extraction to evaluate the heavy metals in mining wastes." Water, Air, and Soil Pollution **50**: 241-254.

Dudka, S. and A. Chlopecka (1990). "Effect of soil-phase speciation on metal mobility and phytoavailability in sludge-amended soil." Water, Air, and Soil Pollution **51**: 153-160.

Engler, R. M., J. M. Brannon, et al. (1977). A practical selective extraction procedure for sediment characterization. Chemistry of Marine Sediments. T. F. Yen. Ann Arbort, MI, Ann Arbor Sci. Publ.**:** 163-180.

Forstner, U. and S. R. Patchineelam (1980). Chemical association of heavy metals in polluted water from lower Rhiner river. Water Effects, characterization, Fate and Removal. M. Kavenagh and O. J. Leckie. Washington DC, American Chemical Society**:** 177-193.

Gadde, R. R. and H. A. Laitinen (1974). "Studies of heavy metal adsorption by hydrous iron and manganese oxides." Analytical Chemistry **46**(13): 2022-2026.

Gee, C., M. H. Ramsey, et al. (1997). "Mineralogy and weathering processes in historical smelting slags-and their effect on the mobilisation of lead." Journal of Geochemical Exploration **58**(2-3): 249-257.

Gibbs, R. J. (1977). "Transport of teansition metals in the amazon and Yukon rivers." Geol. Soc. Am. Bull. **68**: 829-843.

Hem, J. D. (1976). Inorganic chemistry of Pb in water, U.S. Department of the interior, Washington.

Henry, J. D. J., L. F. Lawler, et al. (1977). "A solid/ liquid separation process based on cross flow and electrofiltration." AIChE Journal **23**(6): 851-859.

Hickey, M. G. and J. A. Kittrick (1984). "Chemical partitioning of cadmium, copper, nickel and zinc in soils and sediments containing high levels of hevay metals." Journal of Environmental Quality **13**: 372-376.

Huotari, H. M., G. Tragardh, et al. (1999). "Crossflow membrane filtration enhanced by an external DC electric field: A review." Chemical Engineering Research & Design **77**(A5): 461-468.

Il'in, V. I. and V. A. Kolesnikov (2001). "Electroflotation purification of radiocative waste waters." Atomic Energy **91**(1): 551-554.

Iritani, E., Y. Mukai, et al. (2000). "Effects of electric field on dynamic behaviors of dead-end inclined and downward ltrafiltration of protein solutions." Journal of Membrane Science **164**: 51-75.

Iritani, E., S. Nakatsuka, et al. (1991). "Effect of solution environment on unstirred dead-end ultrafiltration characteristics of proteinaceous solutions." Journal of Chemical Engineering of Japan **24**(2): 177-183.

Iritani, E., K. Ohashi, et al. (1992). "Analysis of filtration mechanism of dead-end electro-ultrafiltration for proteinaceous solution." Journal of Chemical Engineering of Japan **25**(4): 383-388.

Iritani, E., H. Sumi, et al. (1991). "Analysis of filtration mechanism of cross-flow upward and downward ultrafiltration." Journal of Chemical Engineering of Japan **24**(1): 39-44.

Iritani, E., T. Watanabe, et al. (1991). "Upward and inclined ultrafiltration under constant pressure by use of dead-end filter." Kagaku Kogaku Ronbunshu **17**(1): 206-209.

Iritani, E., T. Watanabe, et al. (1992). "Effects of pH and solvent density on dead-end upward ultrafiltration." Journal of Membrane Science **69**(1-2): 87-97.

Kearl, P. M., N. E. Korte, et al. (1992). "Suggested modifications to groundwater sampling procedures based on observations from the colloidal borescope." Groundwater Monitoring and Remedaition **12**(2): 155-161.

Lee, C. H., D. Gidaspow, et al. (1980). "Crossflow Electrofilter for non-aqueous slurries." Industrial & Engineering Chemistry Fundamentals **19**(2): 166-175.

Lo, Y. S., D. Gidaspow, et al. (1983). "Separation of colloidal particles from nonaqueous media by cross-flow electrofiltration." Separation Science and Technology **18**(12 & 13): 1323-1349.

Luoma, S. N. (1983). "Bioavailability of trace metals to aquatic organisms: a review." Science of the Total Environment **28**: 1-22.

Majmudar, A. A. and C. Manohar (1994). "Electrophoretic separation of dilute TiO_2 suspension." Separation Science and Technology **29**(7): 845-854.

Manegold, E. (1937). "The Effectiveness of filtration, dialysis, electrophoresis and their intercombination as purification processes." Transactions of the Faraday Society **33**: 1088-1094.

Means, J. C. and R. Wijayaratne (1982). "Role of natural colloids in the transport of hydrophobic pollutants." Science **215**(4535): 968-970.

Miller, W. P., D. C. Martens, et al. (1986). "Effect of Sequence in extraction of Trace Metals from Soils." SOIL SCI. SOC. AM. J. **50**: 598-601.

Miller, W. P., W. W. McFee, et al. (1983). "Mobility and retention of heavy metals in sandy soils." Journal of Environmental Quality **12**: 579-584.

Misra, S. and S. Varanasi (1991). "A model for the premeation characteristics of porous membranes with grafted polyelectrolyte brushes." Journal of Colloid Interface Science **146**(1): 251-275.

Morera, M. T., J. C. Echeverria, et al. (2001). "Isotherms and sequential extraction procedures for evaluating sorption and distribution of heavy metals in soils." Environmental Pollution **113**(2): 135-144.

Moulik, S. P. (1976). "Normal and reverse field induced flow behaviours in electrofiltration." Colloid and Polymer Science **254**: 39-44.

Muralidhara, H. S., D. Ensminger, et al. (1985). "Acoustic dewatering and drying (low and high frequency)." Drying Technology **3**(4): 529-566.

Muralidhara, H. S. and N. Senapati (1986). A novel electroacoustic separation process for fine particle suspensions. Advances in Solid/Liquid Separation. H. S. Muralidhara. Battelle, Ohio**:** 335.

Murase, T., E. Iritani, et al. (1989). "Periodic dynamic filtration by use of a creamic filter with rotating cylinder." Kagaku Kogaku Ronbunshu **15**(6): 1179-1186.

Park, J. Y., C. K. Choi, et al. (1994). "A study on dynamic separation of silica slurry using a rotating membrane-filter.1.Experiments and filtrate fluxes." Journal of Membrane Science **97**: 263-273.

Puls, R. W. and M. J. Barcelona (1996). "Low-flow (minimal drawdown) groundwater sampling procedures." U.S. Environmental Protection Agency, Groundwater Issue: EPA/540/S-95/504, April 1996.

Puls, R. W., R. M. Powell, et al. (1991). EPA/600/M-91/040. Washington, EPA.

Radovich, J. M., B. Behnam, et al. (1985). "Steady-state modeling of electroultrafiltration at constant concentration." Separation Science and Technology **20**(4): 315-329.

Radovich, J. M. and R. E. Sparks (1980). Electrophoretic techniques for controlling concentration polarization in ultrafiltration. Ultrafiltration Membranes and Application. A. R. Cooper. New York, Plenum Press**:** 249-268.

Ramos, L., L. M. Hernandez, et al. (1994). "Sequential fraction of copper, lead, cadmium and zinc in soils from or near Donana national park." Journal of Environmental Quality **23**: 50-57.

Rapin, F. and U. Forstner (1983). "Sequential leaching techniques for particulate metal speciation:The selectivity of various extractants." 4th International conference on heavy metals in the environment: 1074-1077.

Rushton, A. and G. S. Zhang (1988). "Rotary microporous filtration." Desalination **70**(1-3): 379-394.

Salomons, W. and U. Forstner (1980). "Trace metal analysis on polluted sediments Part II: evaluation of environmental impact." Environmental Technology Letters **1**: 506-517.

Sheppard, J. C., M. J. Campbell, et al. (1979). "Retention of neptunium, americim, and curium by diffusible soil particles." Environmental Science & Technology **13**(6): 680-684.

Sims, J. L. and W. H. Patrick, Jr (1978). "The distribution of micro-nutrient cations in soil under conditions of varying redox potential and pH." Soil Science Society of America Journal **42**: 258-262.

Sparks, D. L. (1995). Environmental Soil Chemistry. San Diego, CA, Academic Press.

Sposito, G. (1989). The Chemistry of Soils. New York, Oxford University Press.

Stumm, W. and H. Bilinski (1972). Trace meals in natural waters: Difficulties of interpretation arising form our ignorance of their speciation. Advances in Water Pollution Research, Proceeding, 6th International Conference, Jerusalem, Israel, Pergamon Press, Oxford.

Svete, P., R. Milacic, et al. (2001). "Partitioning of Zn, Pb and Cd in river sediments from a lead and zinc mining area using the BCR three-step sequential extraction procedure." Journal of Environmental Monitoring **3**(6): 586-590.

Takayanagi, K. and G. T. F. Wong (1983). "Organic and colloidal selenium in sothern chesapeake bay and adjacent waters." Marine Chemistry **14**(2): 141-148.

Tarleton, E. S. and R. J. Wakeman (1995). Crossflow electroacoustic separation. 1st International Conference on Science, Engineering and Technology of Intensive Processing, University of Nottingham, Nottingham.

Tessier, A., P. G. C. Campbell, et al. (1979). "Sequential Extraction Procedure for the Speciation of Particulate Trace Metals." Analytical chemistry **51**(7): 844-851.

Turkson, A. K., J. A. Mikhlin, et al. (1989/90). "Dynamic membranes. I. determination of optimum formation conditions and electrofiltration of bovine serum albumin with a rotating module." Separation Science and Technology **24**(15): 1261-1291.

Verdegan, B. M. (1986). "Cross flow electrofiltration of petroleum oils." Separation Science and Technology **21**(6-7): 603-623.

Veselov, Y. S. (1983). "Optimization of the parameters of the electrofiltration process by the method of steepest ascent." Journal of Applied Chemistry of the USSR **56**(3): 646-649.

Wakeman, R. J. (1998). "Electrically enhanced microfiltration of albumin suspensions." Food and Bioprodcts Processing **76**(C1): 53-59.

Wakeman, R. J. and M. N. Sabri (1995). "Utilizing pulsed electric fields in crossflow microfiltration of titania suspensions." Chemical Engineering Research & Design : Transactions of the Institution of Chemical Engineers. **73**(A4): 455-463.

Wakeman, R. J. and M. N. Sabri (1995). "Utilizing pulsed electric-fields in cross-flow microfiltration of titana suspension." Chemical Engineering Research & Design **73**(A4): 455-463.

Wakeman, R. J. and E. S. Tarleton (1987). "Membrane fouling prevention in crossflow microfiltration by hte use of electric-fields." Chemical Engineering Science **42**(4): 829-842.

Wakeman, R. J. and E. S. Tarleton (1987). "Membrane fouling prevention in crossflow microfiltration by the use of electric-fields." Chemical Engineering Science **42**(4): 829-842.

Wakeman, R. J. and E. S. Tasleton (1991). "An experimental study of electroacoustic crossflow microfiltration." Chemical Engineering Research and Design : Transactions of the Institution of Chemical Engineers. **69**(Part A): 386-397.

Weber, K. and W. Stahl (2002). "Improvement of filtration kinetics by pressure electrofiltration." Separation and Purification Technology **26**: 69-80.

Webster, R. D., S. V. V. Chilukuri, et al. (2000). "Electrochemical cleaning of microporous metallic filters fouled with bovine serum albumin and phosphate under low cross-flow velocities." Journal of Applied Electrochemistry **30**: 915-924.

Xian, X. (1989). "Effect of chemical forms of cadmium, zinc, and lead in polluted soils on their uptake by cabbage plants." Plant Soil **113**: 257-264.

Xian, X. and G. I. Shokohifard (1989). "Effect of pH on chemical forms and plan availability of cadmium, zinc, and lead in polluted soils." Water, Air, and Soil Pollution **45**: 265-273.

Yukawa, H., K. Shimura, et al. (1983). "Crossflow electroultrafiltration for colloidal solution of protein." Journal of Chemical Engineering of Japan **16**(4): 305-311.

Zhang, S., R. B. H. Tan, et al. (2000). Electrofiltration of aqueous suspensions. Journal of Colloid Interface Science. **228:** 393-404.

Zhang, S. Z., S. X. Wang, et al. (2002). "Distribution and speciation of heavy metals in surface sediments from Guanting Reservoir, Beijing." Jornal of Environmental Science and Health Part a-Toxic//Hazardous Substances & Environmental Engineering **37**(4): 465-478.

Zimdahl, R. L. and R. K. Skogerboe (1977). "Behavior of lead in the soil." Environmental Science & Technology **11**(13): 1202-1207.

Zumbusch, P. V., W. Kulcke, et al. (1998). "Use of alternating electrical fields as anti-fouling strategy in ultrafiltration of biological suspensions - Introduction of a new experimental procedure for crossflow filtration." Journal of Membrane Science **142**: 75-86.

Table 1. List of field samples

Well Name	Method[a]	Date	Size (L)	No. (#)	Field ID[b]	Laboratory ID	Weather
10	B	01/10/01	40	1	10-UD-004-01	10IB01	Snowy
	LFP	01/10/01	20	1	LFP-10-UD-009-01	10IL01	Snowy
	B	01/15/02	1	1	10-UD-026-01	10IIB01	Sunny
		01/15/02	20	2	10-UD-026-02	10IIB02	
	LFP	01/15/02	1	1	LFP-10-UD-025-01	10IIL01	
		01/15/02	20	2	LFP-10-UD-025-02	10IIL02	
5S	B	01/10/01	20	1	5S-UD-005-01	5SIB01	Snowy
	LFP	01/10/01	1	1	LFP-5S-UD-012-01	5SIL01	Snowy
				2	LFP-5S-UD-012-02	5SIL02	
				3	LFP-5S-UD-012-03	5SIL03	
				4	LFP-5S-UD-012-04	5SIL04	
				5	LFP-5S-UD-012-05	5SIL05	
				6	LFP-5S-UD-012-06	5SIL06	
				7	LFP-5S-UD-012-07	5SIL07	
				8	LFP-5S-UD-012-08	5SIL08	
				9	LFP-5S-UD-012-09	5SIL09	
				10	LFP-5S-UD-012-10	5SIL10	
	LFP	04/04/01	5	1	LFP-5S-UD-019-01	5SIIL01	Sunny
	LFP	04/04/01	20	2	LFP-5S-UD-019-02	5SIIL02	Sunny
				3	LFP-5S-UD-019-03	5SIIL03	
	B	04/04/01	20	1	5S-UD-021-01	5SIIB01	Sunny
				2	5S-UD-021-02	5SIIB02	
	B	04/04/01	5	3	5S-UD-021-03	5SIIB03	Sunny
	LFP	05/31/02	20	1	5S-UD-027-01	5SIIIL01	Sunny
				2	5S-UD-027-02	5SIIIL02	
	LFP	05/31/02	10	3	5S-UD-027-03	5SIIIL03	Sunny
	B	05/31/02	20	1	5S-UD-028-01	5SIIIB01	Sunny
				2	5S-UD-028-02	5SIIIB02	
	B	05/31/02	10	3	5S-UD-028-03	5SIIIB03	Sunny
	HFP	05/31/02	20	1	5S-UD-029-01	5SIIIH01	Sunny
				2	5S-UD-029-02	5SIIIH02	
	HFP	05/31/02	10	3	5S-UD-029-03	5SIIIH03	Sunny
	HFP	05/31/02	8	4	5S-UD-029-04	5SIIIH04	Sunny
MW3	B	04/04/01	20	1	MW3-UD-022-01	MW3IB01	Sunny
				2	MW3-UD-022-02	MW3IB02	
	B	04/04/01	8	3	MW3-UD-022-03	MW3IB03	Sunny
	LFP	04/04/01	8	1	LPF-MW3-UD-024-01	MW3IL01	Sunny
	LFP	04/04/01	20	2	LPF-MW3-UD-024-02	MW3IL02	Sunny
				3	LPF-MW3-UD-024-03	MW3IL03	

a: B: Bailer; LFP: Low flow purge; HFP: High flow purge

b: Well-analysis location-sample number; Well Name-Lab Name-Sample Series- Sample Number

Table 2. The Tessier sequential extraction procedures for lead speciation

Step	Form/association	Abbr.	Extraction agent	Time	Temperature
1	Exchangeable	EXC	8-mL of 1 M $MgCl_2$, pH 7.0	Shaking 1.0 h	25°C
2	Carbonate	CAB	8-mL of 1 M NaOAc – 0.5 M HOAc, pH 5.0	Soaking 5 h and shaking 3 h	25°C
3	Fe and Mn oxides	FMO	20-mL of 0.04M NH_2OH•HCl, 25% HOAC at 96±3°	Soaking 15 h and shaking 2 h in daylight	96°C
4	Organic matter	ORM	3-mL0.02 M HNO_3, 5-mL 30% H_2O_2, pH 2, mixture was heated at 85±2 °C for 2 h.	2 h	85°C
			A second 3-mL aliquot of 30% H_2O_2 (pH 2 with HNO_3) was added and heated at 85±2 °C for 3 h.	3 h	
			After cooling, 5-mL 3.2 M NH_4OAc in 20% (v/v) HNO_3 was added and diluted to 20-mL and shaking 30 min.	0.5 h	
5	Residual forms	RES	The residue was digested with HF-$HClO_4$ mixture.	-	-

1. The selective extractions were conducted in centrifuge tubes (Teflon, 50 mL) to minimize losses of solid material.
2. Between each successive extraction, separation was effected by centrifuging at (RCF 10,621 g (10,000 rpm) for 30 min.
3. The supernatant was removed with pipet and analyzed for trace metals; whereas the residue was washed with 8-mL of deionized water, after centrifugation for 30 min; this second supernatant was discarded.
4. The volume of rinse water used was kept to a minimum to avoid excessive solubilization of solid material, particularly organic matter.
5. For total or residual trace metal analysis, the solid was digested with a 5:1 mixture of hydrofluoric and perchloric acids. The sediment was first digested in a PTFE beaker with a solution of concentrated $HClO_4$ (2-mL) and HF (10-mL) to near dryness; subsequently a second addition of $HClO_4$ (1-mL) and HF (10-mL) was made and again the mixture was evaporated to near dryness. Finally, $HClO_4$ (1-mL) alone was added and the sample was evaporated until the appearance of white fumes. The residue was dissolved in 5-mL 12 N HCl and diluted to 25-mL.

Table 3. Diameter of naturally occurring particles in well water

Unit: nm

Laboratory Sample ID	10IIL01	10IIL02	10IIB01	10IIB02	5SIIIL03	5SIIIB03	5SIIIH03
Run 1	319.1	323.7	519.4	428.8	505.4	1079.3	892.3
Run 2	311.8	285.3	498.7	510.7	536.9	1004.6	737.8
Run 3	314.3	282.8	468.2	384.8	532.2	936.1	821.6
Average ± SD	315.1 ± 3.7	297.3 ± 22.9	495.4 ± 25.8	441.4 ± 63.8	521.8 ± 15.8	1006.7 ± 71.6	817.2 ± 77.3

Table 4. Total solids in well water

Unit: g/L

Laboratory Sample ID	Low flow purge		Bailer		Low flow purge	Bailer	High flow purge
	10IIL01	10IIL02	10IIB01	10IIB02	5SIIIL03	5SIIIB03	5SIIIH03
Run 1	0.935	0.953	1.112	1.753	***2.***93	12***.24***	11***.95***
Run 2	0.925	0.944	1.095	1.744	2.93	12.24	11.96
Run 3	0.938	0.949	1.102	1.740	2.94	12.26	11.98
Run 4	0.944	0.932	1.114	1.741	2.94	12.26	11.98
Run 5	0.935	0.928	1.101	1.728	2.94	12.18	11.98
Run 6	0.943	0.937	1.101	1.732	2.95	12.18	11.98
Run 7	0.940	0.940	1.119	1.766	2.95	12.21	12.01
Run 8	0.930	0.933	1.105	1.752	2.95	12.21	12.01
Run 9	0.937	0.941	1.107	1.743	-	-	-
Average ± SD	0.936 ± 0.006	0.940 ± 0.008	1.106 ± 0.007	1.744 ± 0.011	2.94 ± 0.01	12.22 ± 0.03	11.98 ± 0.02

Table 5. The total and soluble lead concentration in well water

Unit: μg/L

Sampling Method	Laboratory Sample ID	Total Lead	Soluble Lead
Low Flow Purging	10IIL01	11	1
	10IIL02	11	1
Bailer	10IIB01	13	1
	10IIB02	28	1
Low Flow Purging	5SIIIL01	245	3
	5SIIIL02	104	3
	5SIIIL03	144	5
	Average ± SD	164 ± 73	4 ± 1
Bailer	5SIIIB01	385	4
	5SIIIB02	426	4
	5SIIIB03	391	4
	Average + SD	401 ± 22	4 ± 0
High Flow Purge	5SIIIH01	288	2
	5SIIIH02	380	3
	5SIIIH03	463	5
	Average + SD	377 ± 88	3 ± 2

Table 6. Concentration of sequentially extracted lead in particles of well water

unit: pb-μg/particle-g

Laboratory Sample ID	10IIl01	10IIL02	10IIB01	10IIB02	5SIIIL01	5SIIIB02	5SIIIH02
pH	6.8	6.8	7.1	7.1	6.8	6.6	7.1
exchangeable	0.00	0.00	0.00	0.00	0.00	0.00	0.04
carbonate	0.00	0.00	0.00	0.00	0.02	0.00	0.00
Fe-Mn oxide	1.19	0.98	0.38	0.19	0.46	0.69	0.63
organic matter	0.27	0.32	0.10	0.28	0.64	0.73	0.79
Residual	8.50	8.83	7.82	6.65	7.30	3.11	7.04
Total	9.96	10.13	8.30	7.13	8.43	4.54	8.49

Table 7. The summary of performance of the cross-flow electrostatic-filtration module under various experimental conditions with water samples

Sample	Variation	Experimental Condition			Turbidity (NTU)		Removal (%)
		Electrostatic Field (V/cm)	Voltage	pH	Initial	Final	
10IIB02	Electrostatic Field	00.0	00	6.8	207	195	6
		32.3	100	6.8	207	142	31
		64.5	200	6.8	207	94	54
		71.3	221	6.8	207	74	64
		00.0	00	6.8	98	4	4
		32.3	100	6.8	98	65	35
		64.5	200	6.8	98	48	52
		96.8	300	6.8	98	33	66
		112.6	349	6.8	98	26	74
10IIL02	Electrostatic Field	00.0	00	7.1	31	31	2
		32.3	100	7.1	31	19	39
		60.3	187	7.1	31	11	64
Snowtex 20L	Electrostatic Field	00.0	00	6.2	35	35	2
		32.3	100	6.2	35	28	20
		64.5	200	6.2	35	19	45
		96.8	300	6.2	35	10	71
		129.0	400	6.2	35	2	94
		161.3	500	6.2	35	2	95
		174.2	540	6.2	35	2	96
	pH	96.8	300	9.0	35	11	69
		96.8	300	7.0	35	4	88
		96.8	300	6.2	35	10	71
Snowtex ZL	Electrostatic Field	00.0	00	5.0	58	56	3
		32.3	100	5.0	58	46	21
		64.5	200	5.0	58	23	60
		96.8	300	5.0	58	18	70
		129.0	400	5.0	58	4	93
		161.3	500	5.0	58	2	97
		187.7	582	5.0	58	1	98
	pH	96.8	300	9.0	58	24	58
		96.8	300	7.0	58	29	50
		96.8	300	5.0	58	18	70
10IIB02 + snowtex 20L	Electrostatic Field	00.0	00	8.2	72	67	7
		32.3	100	8.2	72	48	34
		64.5	200	8.2	72	37	48
		96.8	300	8.2	72	23	69
		124.5	386	8.2	72	16	78
		126.5	392	8.2	72	14	80

Table 7. The summary of performance of the cross-flow electrostatic-filtration module under various experimental conditions (continued)

Sample	Variation	Experimental Condition			Turbidity (NTU)		Removal (%)
		Electrostatic Field (V/cm)	Voltage	pH	Initial	Final	
5SIIIL01	Electrostatic Field	00.0	00	6.8	680	632	7.1
		32.3	100	6.8	680	411	39.6
		64.5	200	6.8	680	311	54.3
		96.8	300	6.8	680	213	68.7
		119.7	371	6.8	680	149	78.1
		123.9	384	6.8	680	169	75.1
		00.0	0	6.6	422	391	7.3
		32.3	100	6.6	422	267	36.7
		64.5	200	6.6	422	207	50.9
		96.8	300	6.6	422	141	66.6
		129.0	400	6.6	422	75	82.3
		137.1	425	6.6	422	69	83.6
5SIIIB02	Electrostatic Field	00.0	0	6.8	750	703	6.3
		32.3	100	6.8	750	495	34.0
		64.5	200	6.8	750	389	48.1
		96.8	300	6.8	750	272	63.7
		129.0	400	6.8	750	154	79.5
		138.7	430	6.8	750	139	81.5
		00.0	0	6.6	390	351	10.0
		32.3	100	6.6	390	274	29.7
		64.5	200	6.6	390	204	47.7
		96.8	300	6.6	390	142	63.6
		129.0	400	6.6	390	78	80.1
		152.9	474	6.6	390	50	87.1
5SIIIH02	Electrostatic Field	00.0	0	7.1	720	693	3.8
		32.3	100	7.1	720	506	29.7
		64.5	200	7.1	720	380	47.2
		96.8	300	7.1	720	291	59.6
		117.7	365	7.1	720	219	69.6
		00.0	0	6.8	285	269	6.3
		32.3	100	6.8	285	181	36.5
		64.5	200	6.8	285	126	55.8
		96.8	300	6.8	285	112	60.7
		129.0	400	6.8	285	72	74.8
		142.6	442	6.8	285	57	80.1

Table 8. The effect of total solid concentration under various electrostatic field strength

Sample	Electrostatic Field (V/cm)	Initial Total Solid Concentration (g/L)	Removal (%)	Error (%)
5SIIIL01	00.0	0.6798	7.1	0.69
		0.4264	7.3	
	32.3	0.6798	39.6	1.90
		0.4264	36.7	
	64.5	0.6798	54.3	1.62
		0.4264	50.9	
	96.8	0.6798	68.7	0.78
		0.4264	66.6	
	119.7	0.6798	78.1	-
	123.9	0.6798	75.1	-
	129.0	0.4264	82.3	-
	137.1	0.4264	83.6	-
5SIIIB02	00.0	0.5188	6.3	11.35
		0.2717	10.0	
	32.3	0.5188	34.0	3.38
		0.2717	29.7	
	64.5	0.5188	48.1	0.21
		0.2717	47.7	
	96.8	0.5188	63.7	0.04
		0.2717	63.6	
	129.0	0.5188	79.5	0.19
		0.2717	80.1	
	138.7	0.5188	81.5	-
	152.9	0.2717	87.1	-
5SIIIH02	00.0	0.4447	3.8	12.38
		0.1818	6.3	
	32.3	0.4447	29.7	5.14
		0.1818	36.5	
	64.5	0.4447	47.2	4.17
		0.1818	55.8	
	96.8	0.4447	59.6	0.46
		0.1818	60.7	
	117.7	0.4447	69.6	-
	129.0	0.1818	74.8	-
	142.6	0.1818	80.1	-

Table 9. The concentration of total and soluble lead in the filtrate and concentrate of CFEF operation

Unit: μg/L

Sample	Exper. Condition			Filtrate		Concentrate	
	Electrostatic Field (V/cm)	Voltage	pH	Soluble	Total	Soluble	Total
10IIB02	00.0	00	6.8	< 1	< 1	< 1	2
	32.3	100	6.8	< 1	< 1	< 1	6
	64.5	200	6.8	< 1	< 1	< 1	5
	71.3	221	6.8	< 1	< 1	< 1	6
	00.0	00	6.8	< 1	< 1	< 1	2
	32.3	100	6.8	< 1	< 1	< 1	4
	64.5	200	6.8	< 1	< 1	< 1	5
	96.8	300	6.8	< 1	< 1	< 1	6
	112.6	349	6.8	< 1	< 1	< 1	6
10IIL02	00.0	00	7.1	< 1	5	< 1	3
	32.3	100	7.1	1	6	2	13
	60.3	187	7.1	1	6	1	12
5SIIIL01	00.0	00	6.8	1	20	2	20
	32.3	100	6.8	1	17	2	23
	64.5	200	6.8	1	13	2	26
	96.8	300	6.8	1	10	1	34
	119.7	371	6.8	1	8	2	28
	123.9	384	6.8	1	9	2	29
5SIIIB02	00.0	0	6.8	1	27	1	18
	32.3	100	6.8	1	13	1	26
	64.5	200	6.8	1	12	1	25
	96.8	300	6.8	1	9	1	32
	129.0	400	6.8	1	7	1	28
	138.7	430	6.8	1	5	1	27
5SIIIH02	00.0	0	7.1	1	23	2	23
	32.3	100	7.1	1	18	1	29
	64.5	200	7.1	2	16	2	30
	96.8	300	7.1	1	13	2	32
	117.7	365	7.1	2	13	2	34

Table 10. Concentration of sequentially extracted and total lead as affected by electrostatic field strength in particles of well water sample 10IIB02

unit: pb-µg/soil-g

Field strength	E = 00 V/cm (V = 00)	E = 32.3 V/cm (V = 100)	E = 64.5 V/cm (V = 200)	E = 71.3 V/cm (V = 221)
pH	6.8	6.8	6.8	6.8
exchangeable	0.00	0.00	0.00	0.00
carbonate	0.00	14.05	12.52	8.97
Fe-Mn oxide	1.13	3.38	2.41	2.13
organic matter	13.30	2.44	1.92	1.99
Residual form	17.41	9.28	8.81	10.94
Total	31.84	29.14	25.65	24.04

Experimental conditions: initial total solid concentration = 0.26 g/L; pH = 6.8; sample: 10IIB02

Table 11. Concentration of sequentially extracted and total lead as affected by electrostatic field strength in particles of well water sample 10IIB02

unit: pb-µg/soil-g

Field strength	E = 32.3 V/cm (V = 100)	E = 64.5 V/cm (V = 200)	E = 96.8 V/cm (V = 300)	E = 112.6 V/cm (V = 349)
pH	6.8	6.8	6.8	6.8
exchangeable	0.00	0.00	0.00	0.00
carbonate	11.05	9.85	6.03	6.09
Fe-Mn oxide	12.80	9.59	4.75	4.62
organic matter	1.84	1.25	1.35	1.28
Residual form	12.87	11.26	11.87	9.33
Total	38.55	31.96	24.00	21.32

Experimental conditions: initial total solid concentration = 0.12 g/L; pH = 6.8; sample: 10IIB02

Table 12. Concentration of sequentially extracted lead as affected by electrostatic field strength in particles of well water sample 5SIIIL01

unit: pb-μg/soil-g

Field strength	E = 00 V/cm (V = 00)	E = 32.3 V/cm (V = 100)	E = 64.5 V/cm (V = 200)	E = 96.8 V/cm (V = 300)	E = 119.7 V/cm (V = 371)	E = 123.9 V/cm (V = 384)
pH	6.8	6.8	6.8	6.8	6.8	6.8
exchangeable	0.00	0.00	0.00	0.00	0.00	0.00
carbonate	0.00	0.24	0.28	0.21	0.22	0.24
Fe-Mn oxide	0.49	1.41	1.51	1.15	1.08	0.96
organic matter	0.73	1.41	1.38	1.19	1.12	1.01
Residual	6.51	7.44	6.46	5.98	5.49	10.69
Total	7.72	10.50	9.61	8.53	7.92	12.90

Experimental conditions: initial total solid concentration = 0.68 g/L; pH = 6.8; sample: 5SIIIL01

Table 13. Concentration of sequentially extracted lead as affected by electrostatic field strength in particles of well water sample 5SIIIB02

unit: pb-μg/soil-g

Field strength	E = 00 V/cm (V = 00)	E = 32.3 V/cm (V = 100)	E = 64.5 V/cm (V = 200)	E = 96.8 V/cm (V = 300)	E = 129.0 V/cm (V = 400)	E = 138.7 V/cm (V = 430)
pH	6.6	6.6	6.6	6.6	6.6	6.6
exchangeable	0.01	0.01	0.01	0.00	0.00	0.00
carbonate	0.00	0.40	0.20	0.15	0.14	0.14
Fe-Mn oxide	0.97	2.01	1.24	1.05	0.89	0.76
organic matter	0.89	1.29	1.03	1.03	0.94	0.85
Residual	2.22	2.35	3.53	8.69	7.04	7.70
Total	4.09	6.06	6.00	10.91	9.01	9.45

Experimental conditions: initial total solid concentration = 0.52 g/L; pH = 6.8; sample: 5SIIIB02

Table 14. Concentration of sequentially extracted lead as affected by electrostatic field strength in particles of well water sample 5SIIIH02

unit: pb-μg/soil-g

Field strength	E = 00 V/cm (V = 00)	E = 32.3 V/cm (V = 100)	E = 64.5 V/cm (V = 200)	E = 96.8 V/cm (V = 300)	E = 117.7 V/cm (V = 365)
pH	7.1	7.1	7.1	7.1	7.1
exchangeable	0.01	0.01	0.01	0.01	0.00
carbonate	0.00	0.20	0.14	0.13	0.11
Fe-Mn oxide	1.08	1.05	0.88	0.70	0.69
organic matter	0.83	1.05	0.97	0.78	0.81
Residual	7.38	9.81	6.86	8.81	11.60
Total	9.29	12.10	8.86	10.42	13.21

Experimental conditions: initial total solid concentration = 0.44 g/L; pH = 7.1; sample: 5SIIIH02

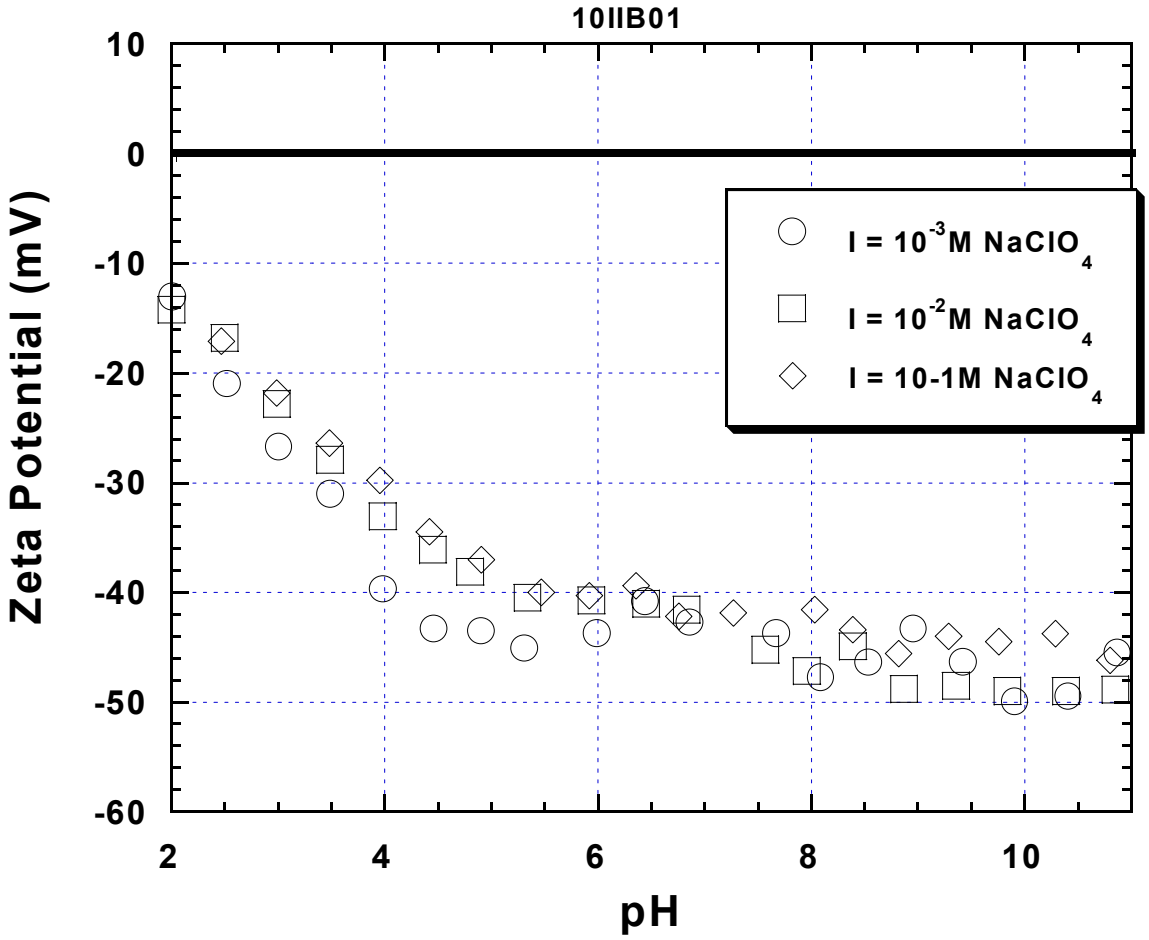

Figure 1. Zeta potential of naturally occurring particles as a function of pH (well #10, bailing sample, 10IIB01)

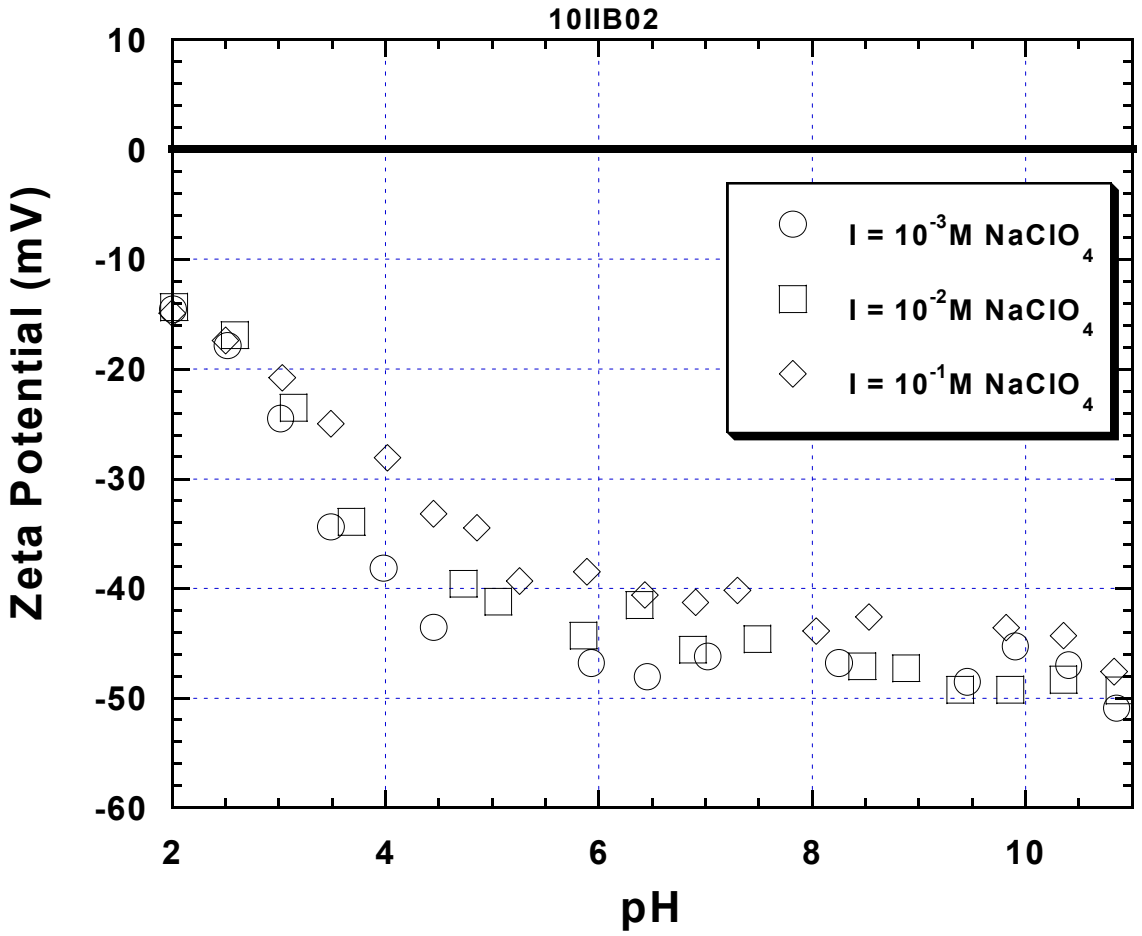

Figure 2. Zeta potential of naturally occurring particles as a function of pH (well #10, bailing sample, 10IIB02)

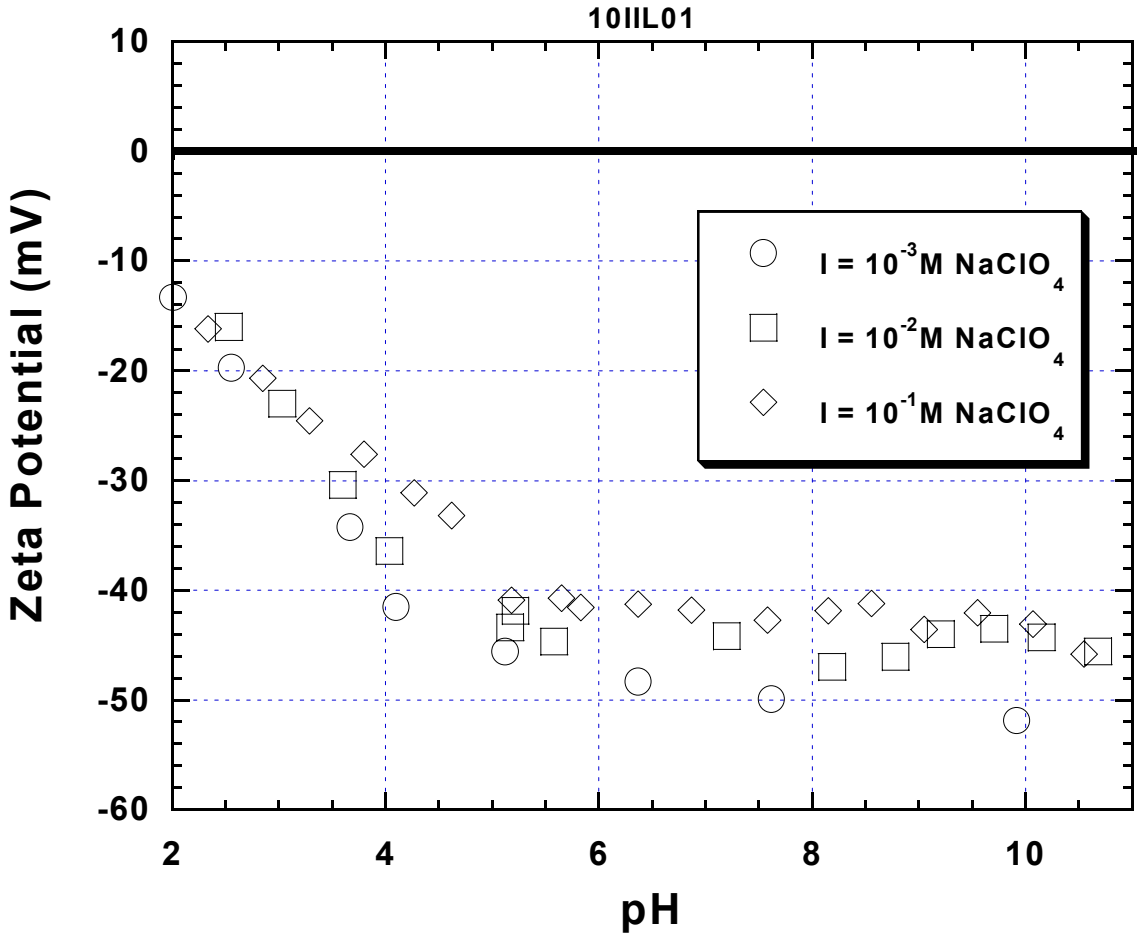

Figure 3. Zeta potential of naturally occurring particles as a function of pH (well #10, low flow purging sample, 10IIL01)

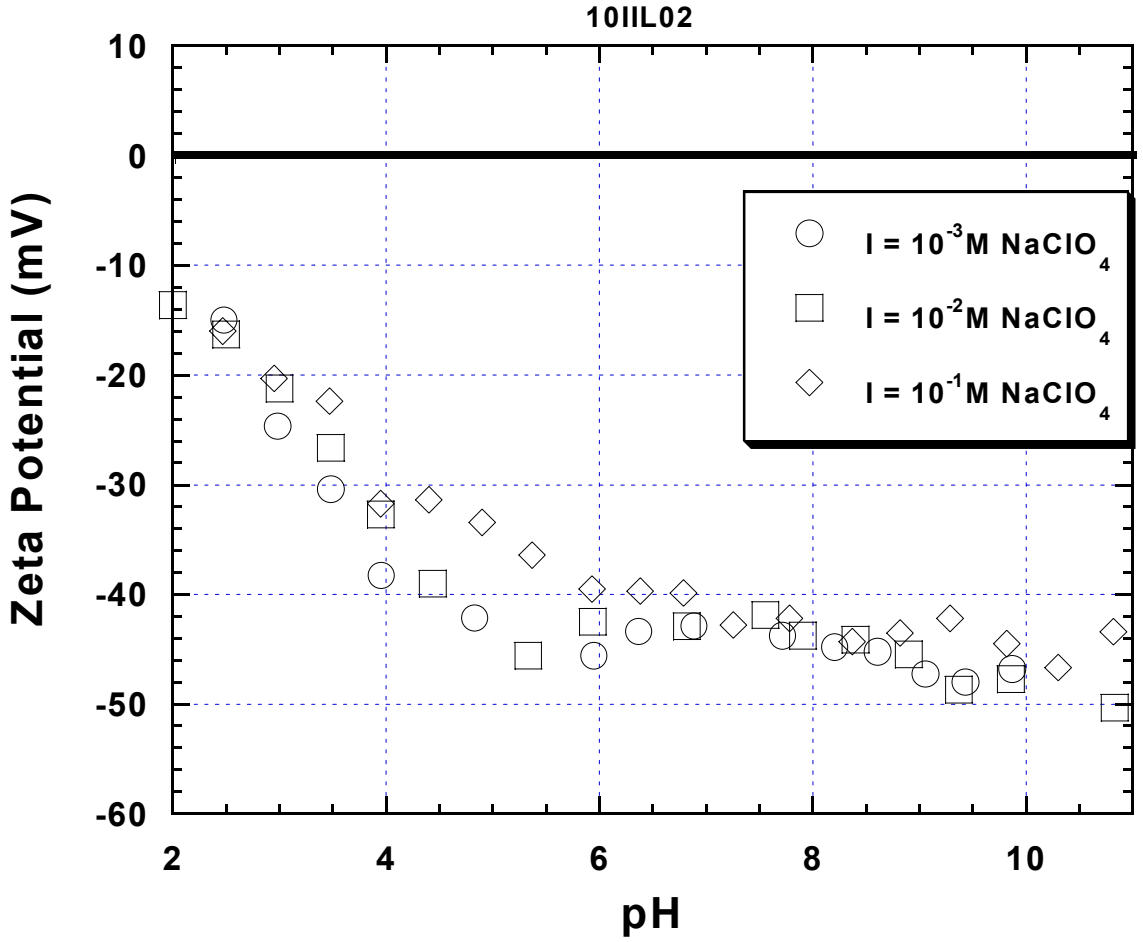

Figure 4. Zeta potential of naturally occurring particles as a function of pH (well #10, low flow purging sample, 10IIL02)

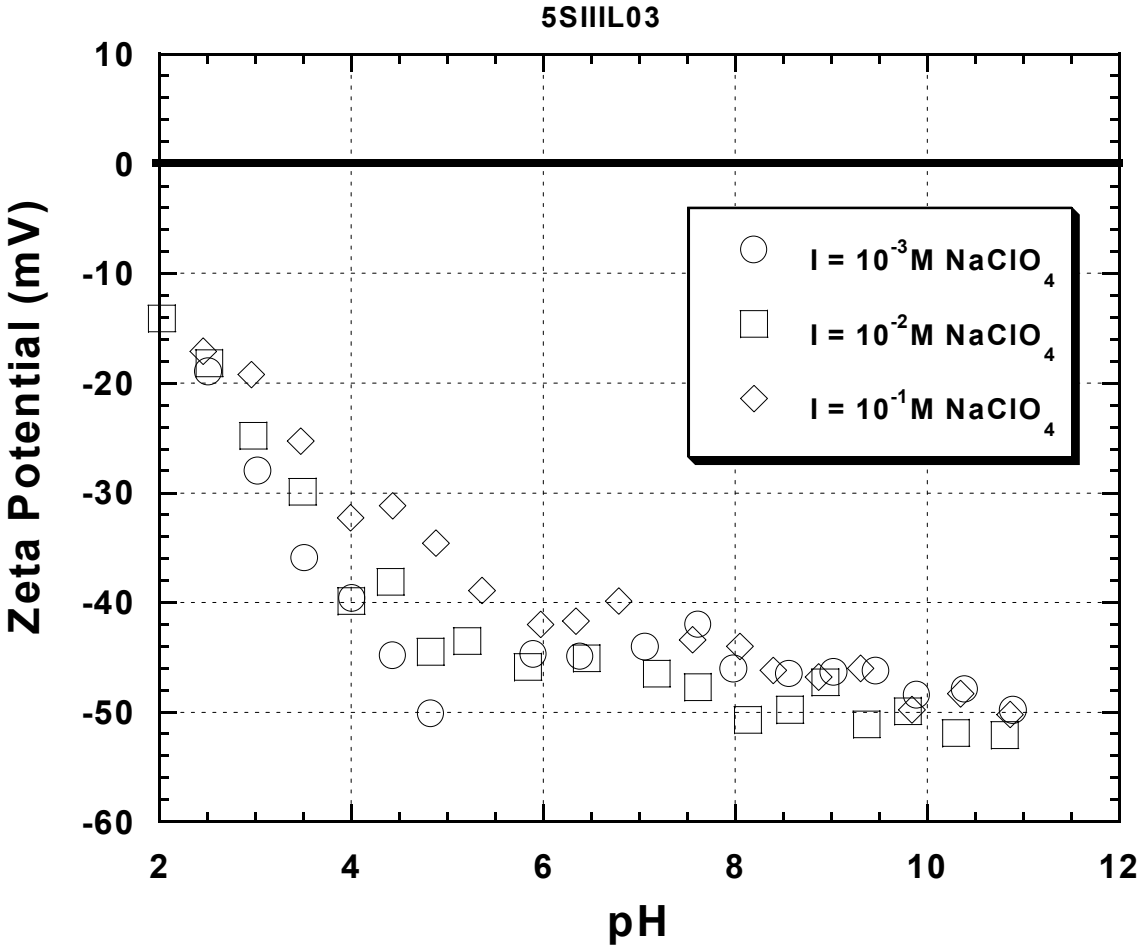

Figure 5. Zeta potential of naturally occurring particles as a function of pH (well #5S, low flow purging sample, 5SIIIL03)

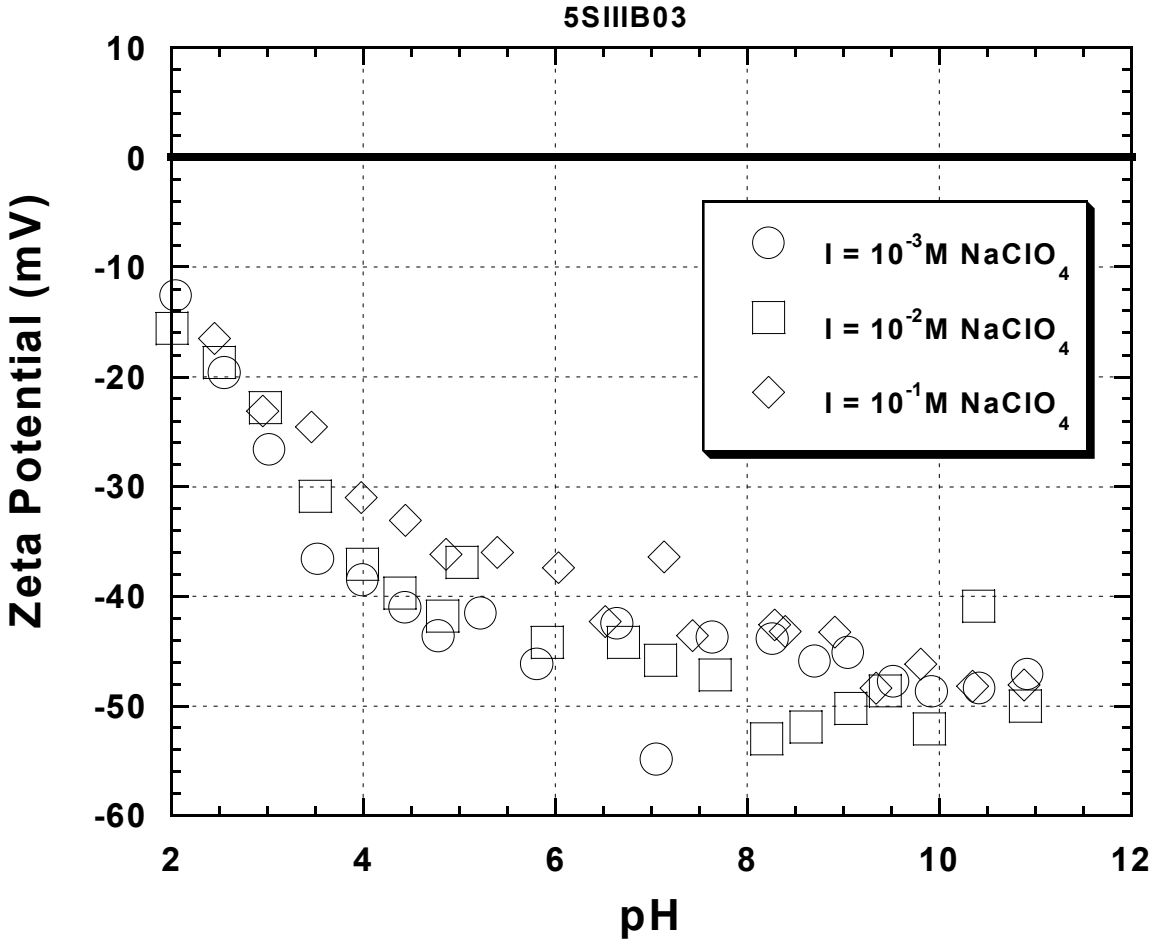

Figure 6. Zeta potential of naturally occurring particles as a function of pH (well #5S, bailing sample, 5SIIIB03)

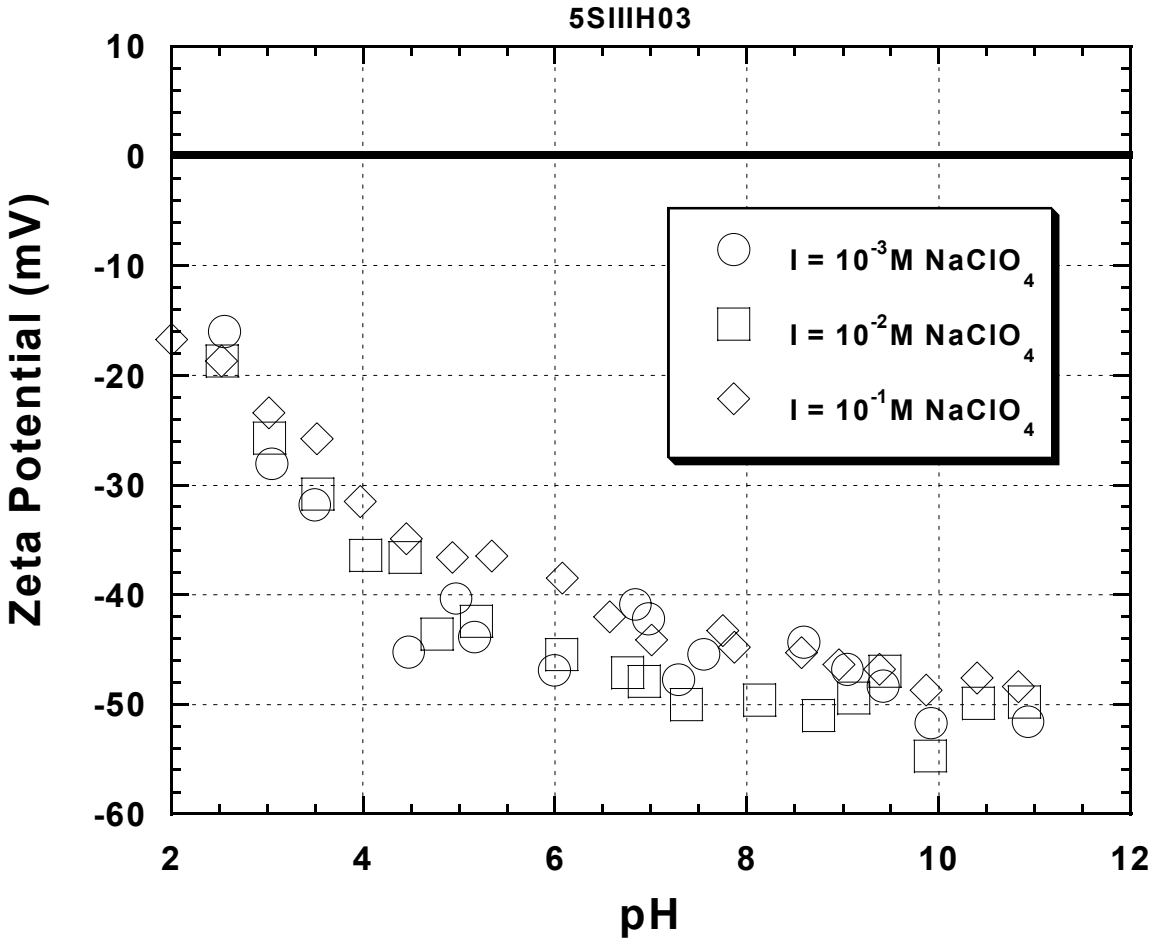

Figure 7. Zeta potential of naturally occurring particles as a function of pH (well #5S, high flow purging sample, 5SIIIH03)

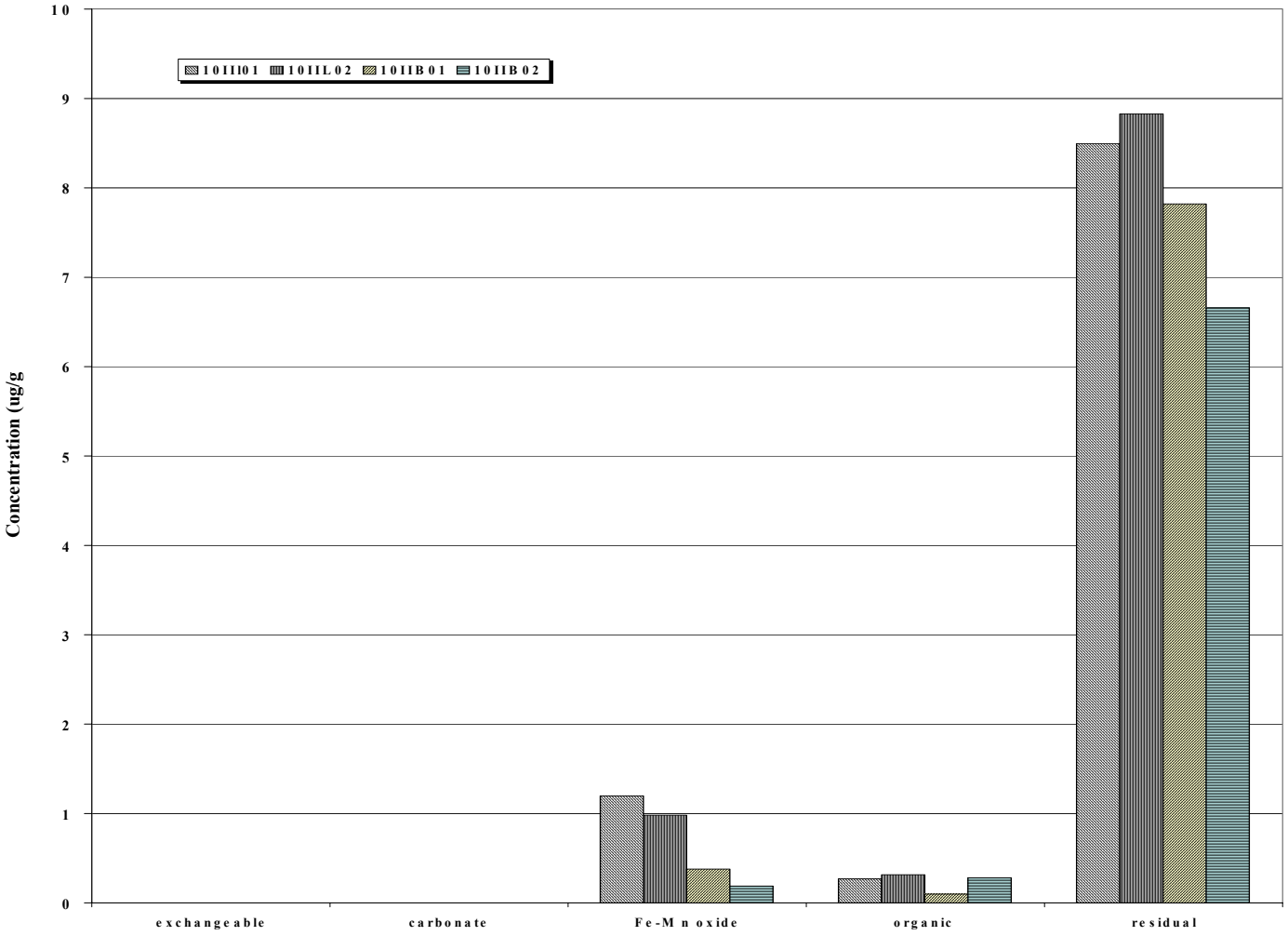

Figure 8. Distribution of lead species in particluate collected from well #10 water sample

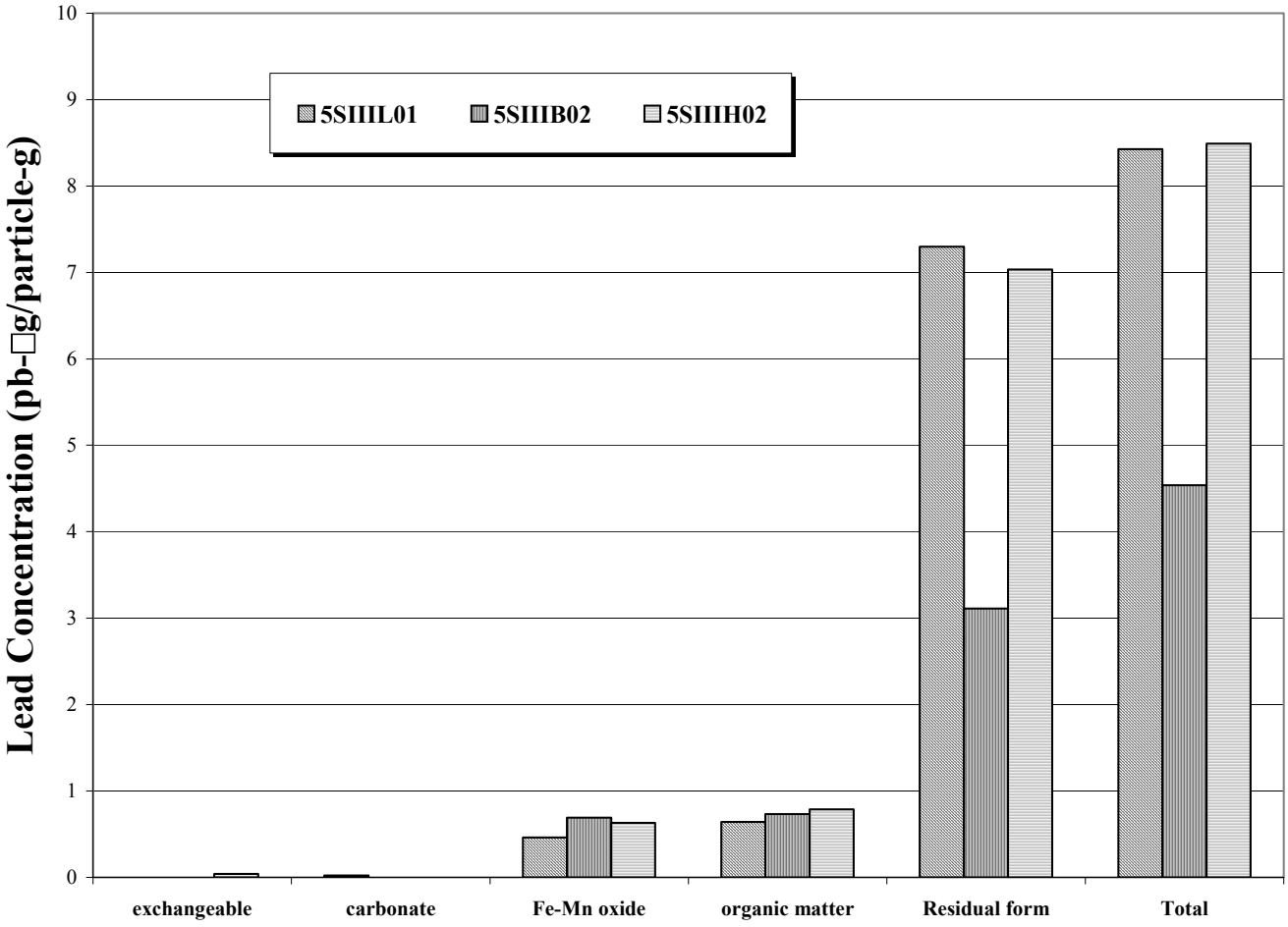

Figure 9. Distribution of lead species in particulates collected from well #5S water sample

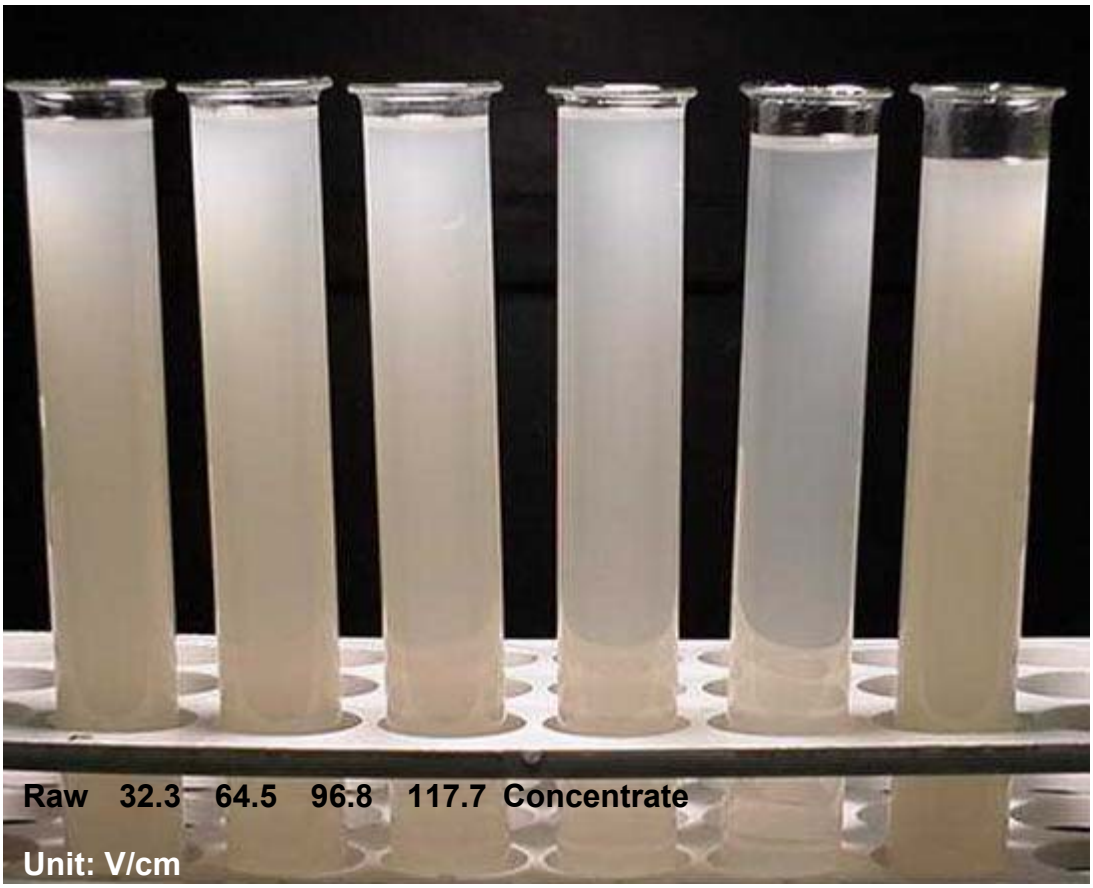

Figure 10. Visual comparison of water samples treated at various levels of electrostatic field (well #5S, high flow purging sample)

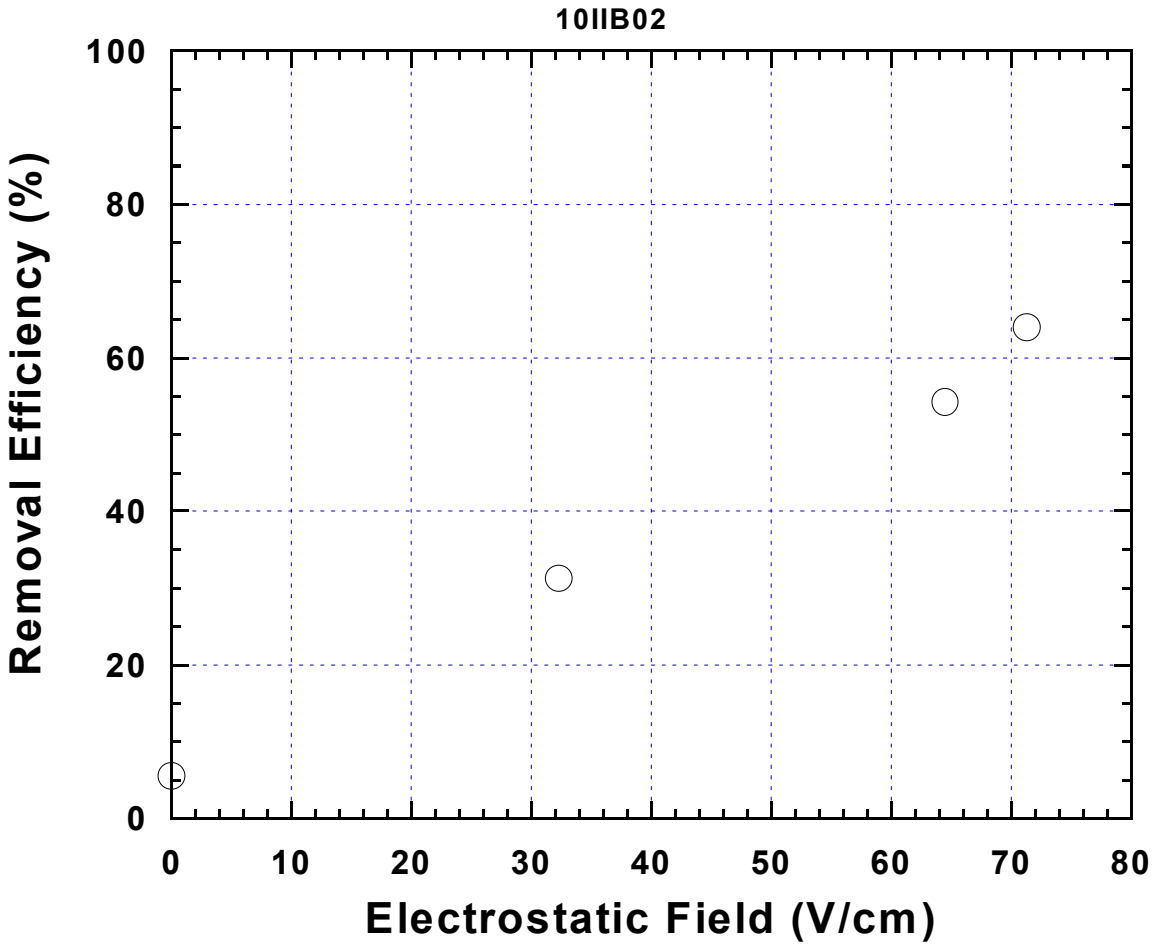

Figure 11. Removal efficiency as a function of time at various electrostatic field values (I). Experimental condition: pH = 6.8; Sample: 10IIB02

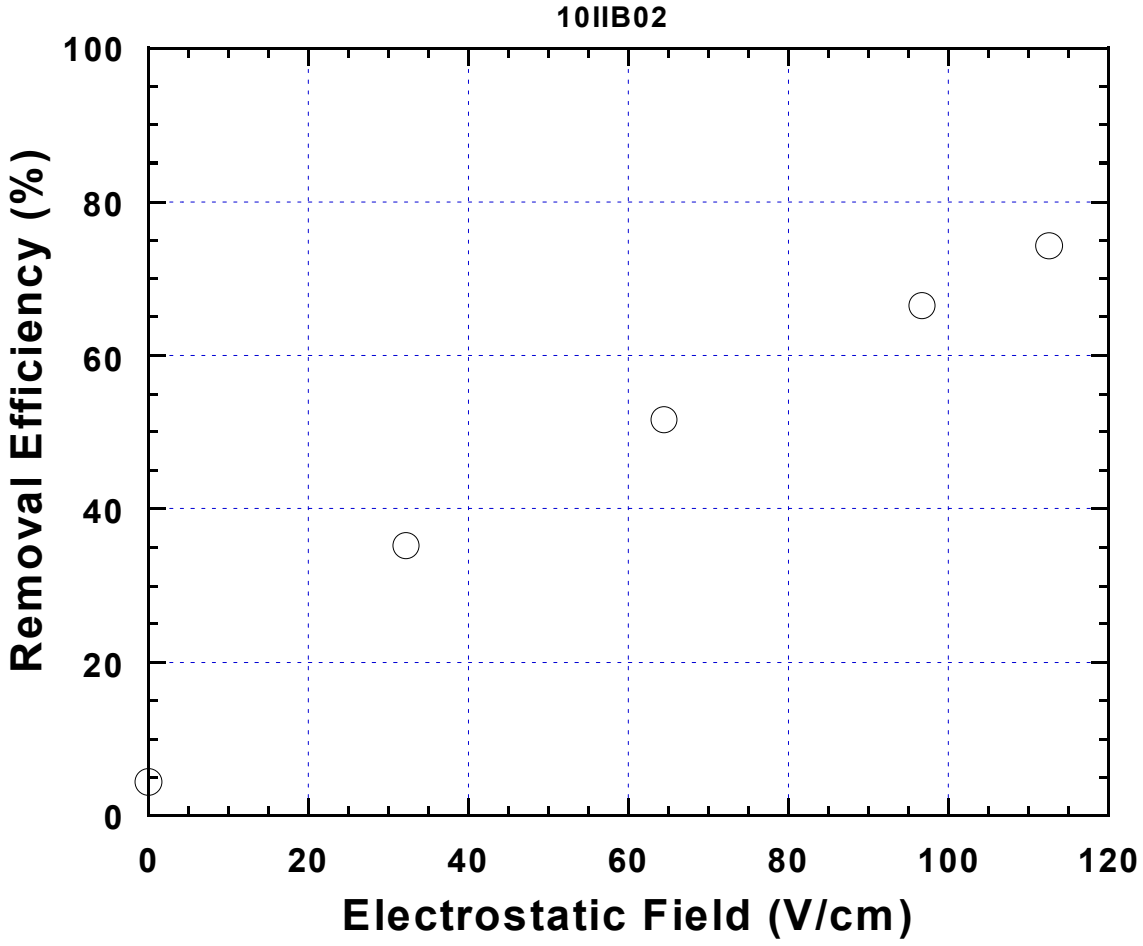

Figure 12. Removal efficiency as a function of time at various electrostatic field values (II). Experimental condition: pH = 6.8; Sample 10IIB02

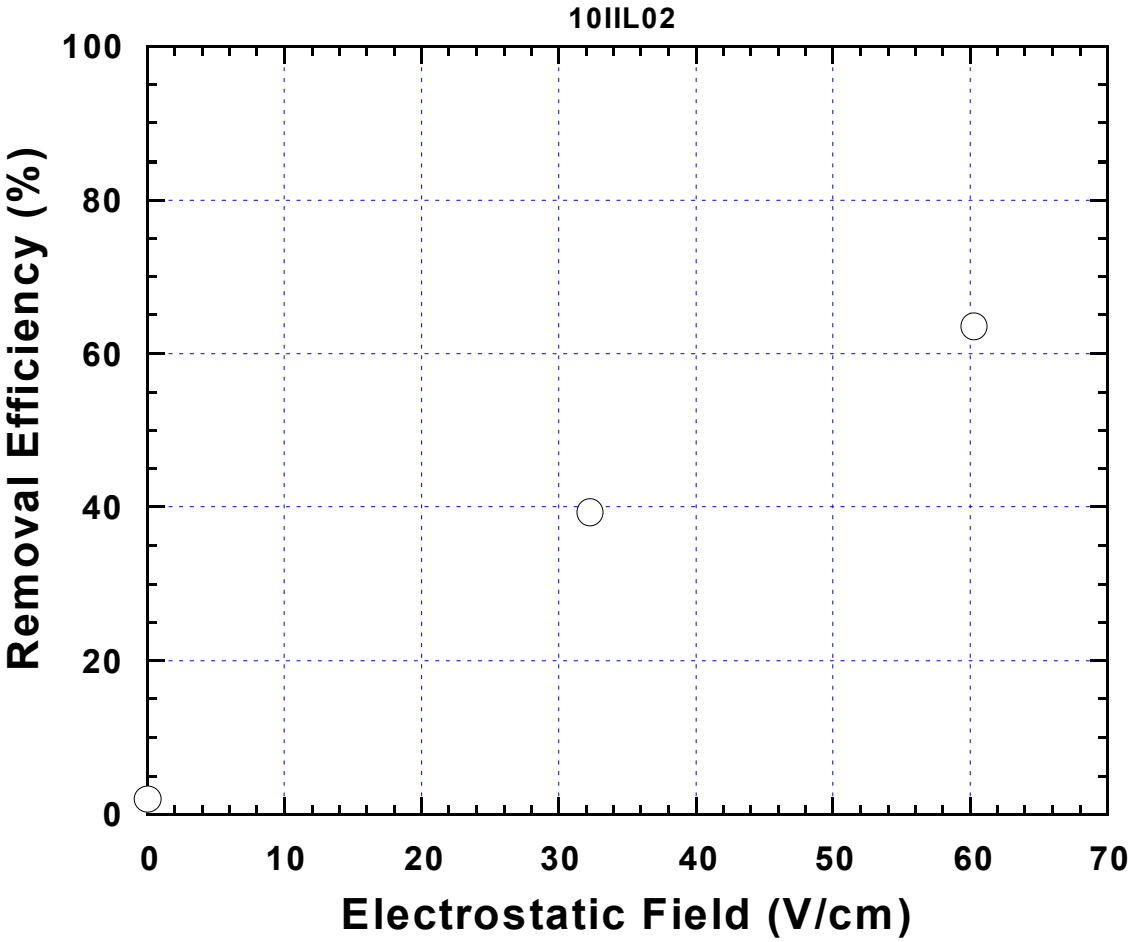

Figure 13. Removal efficiency as a function of time at various electrostatic field values. Experimental condition: pH = 7.1; Sample 10IIL02

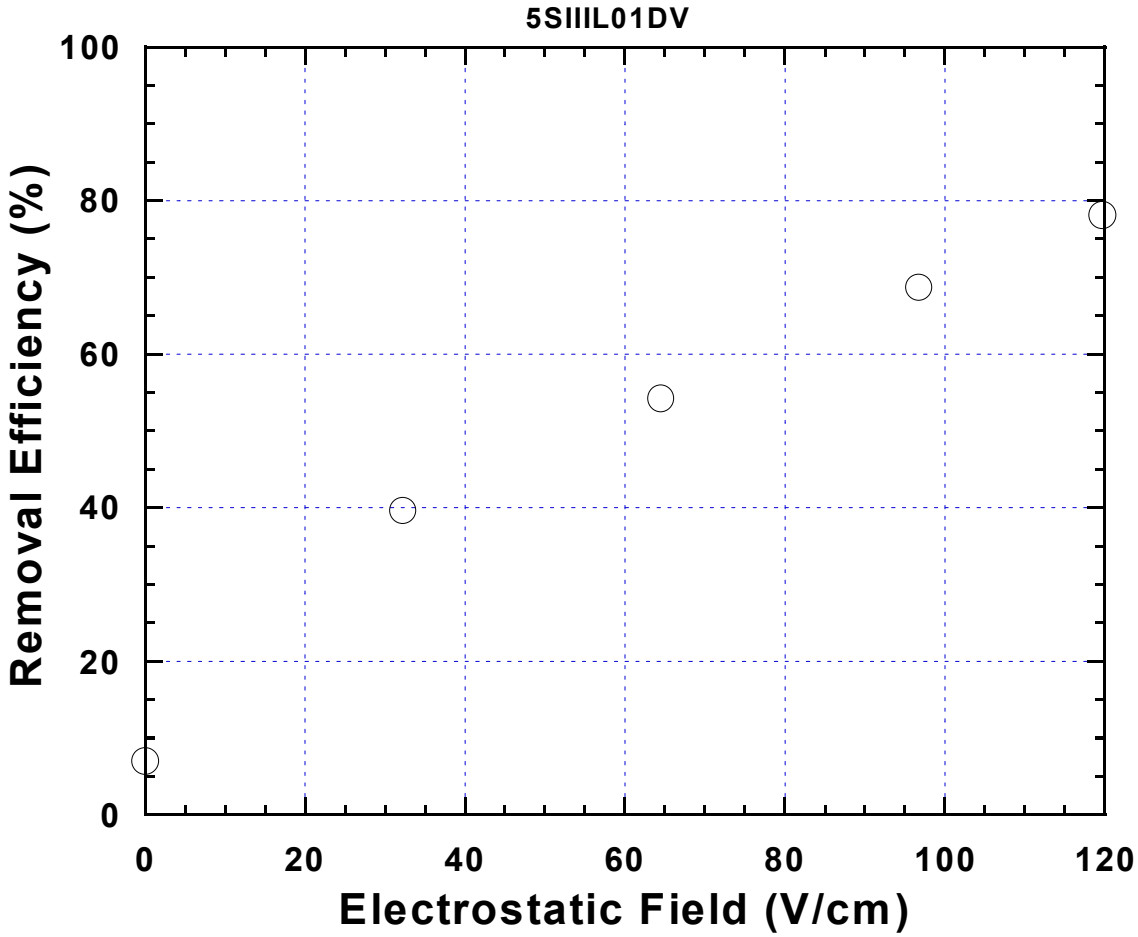

Figure 14. Removal efficiency as a function of time at various electrostatic field values (I). Experimental condition: pH = 6.8, initial turbidity = 680 NTU; Sample: 5SIIIL01

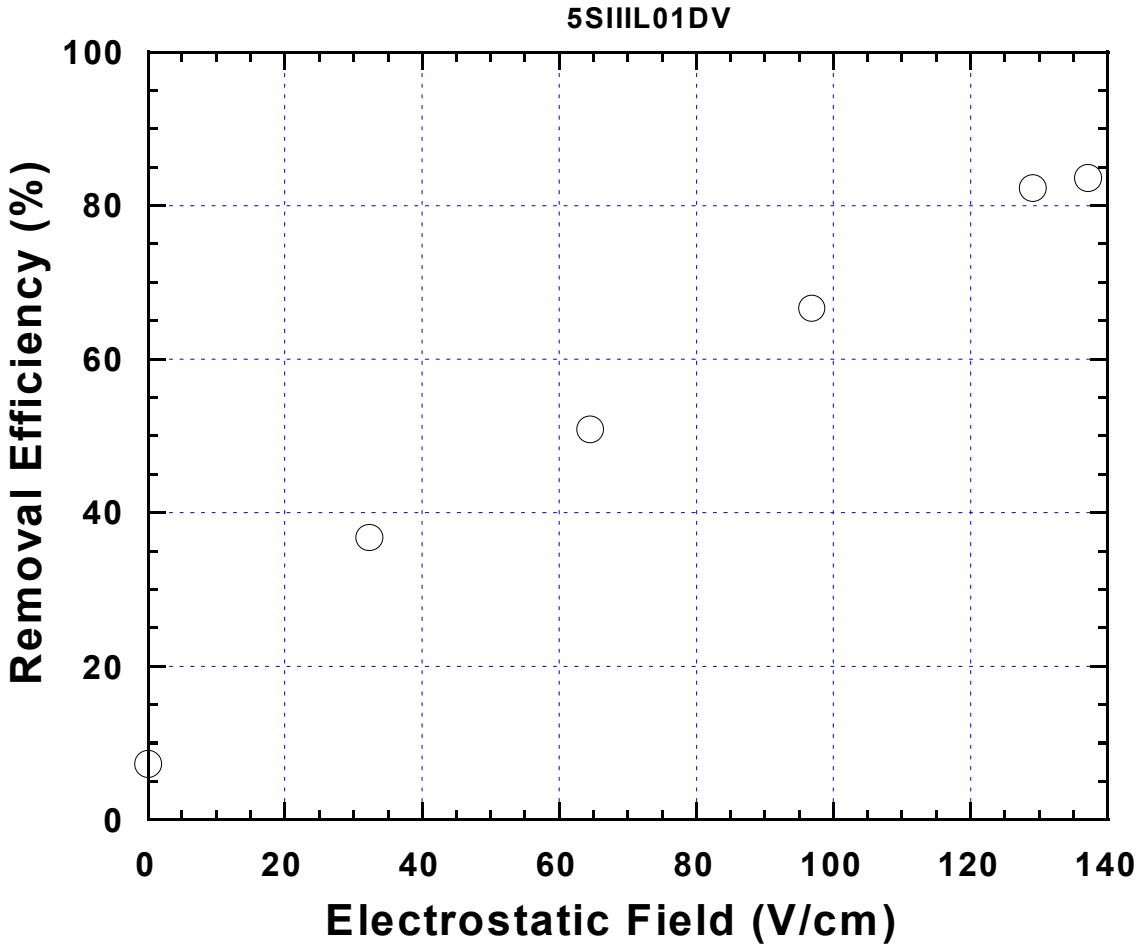

Figure 15. Removal efficiency as a function of time at various electrostatic field values (II). Experimental condition: pH = 6.6, initial turbidity = 422 NTU; Sample: 5SIIIL01

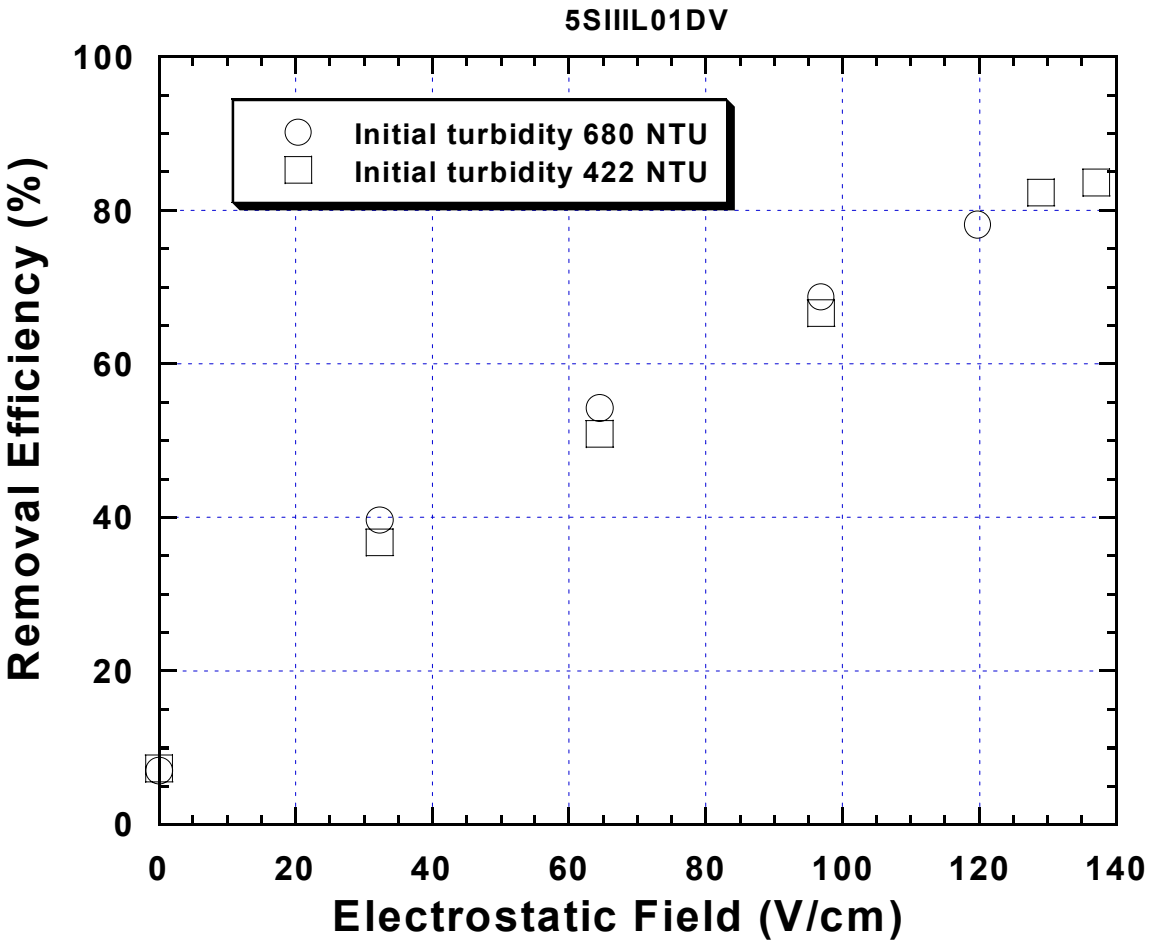

Figure 16. Removal efficiency as a function of time at various electrostatic field values (III). Sample: 5SIIIL01

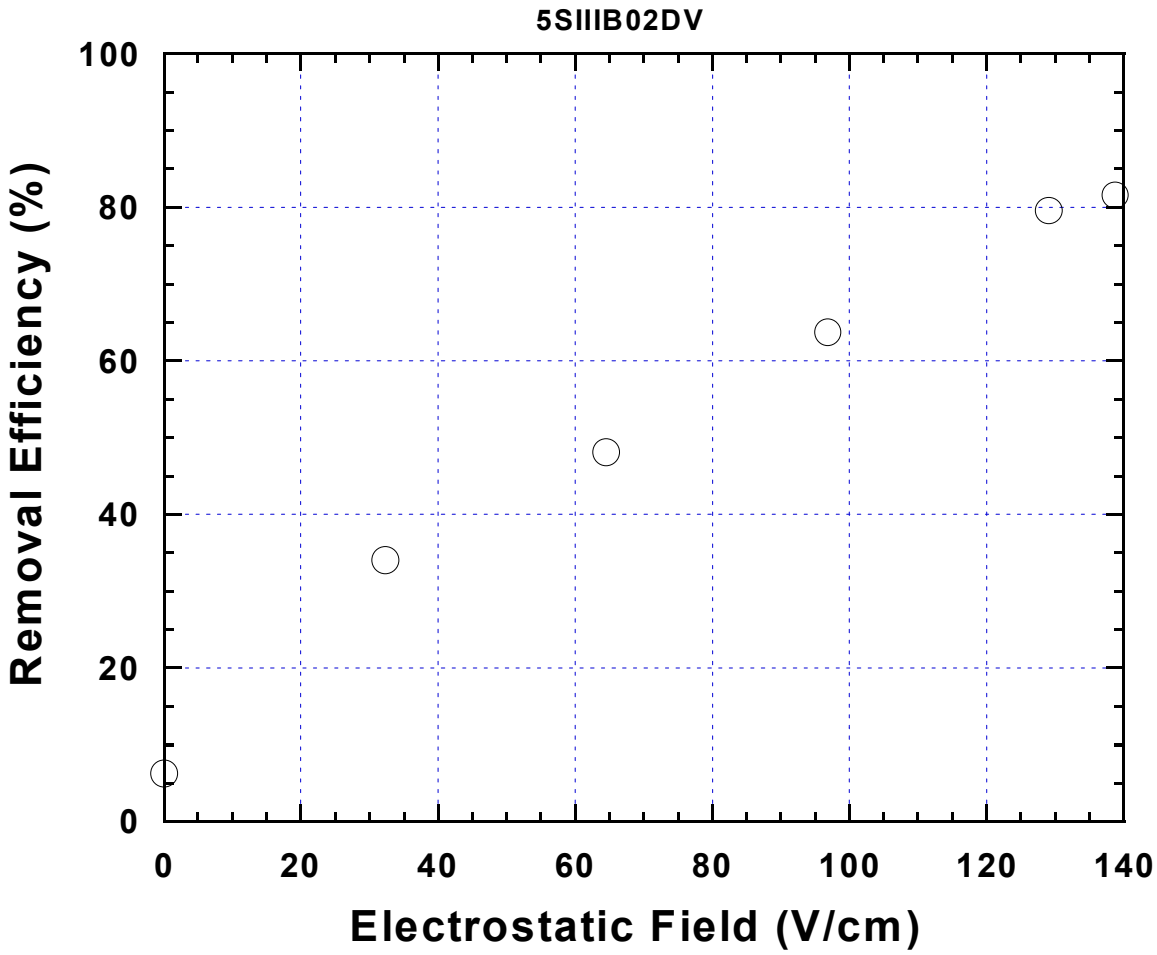

Figure 17. Removal efficiency as a function of time at various electrostatic field values (I). Experimental condition: pH = 6.8, initial turbidity = 750 NTU; Sample: 5SIIIB02

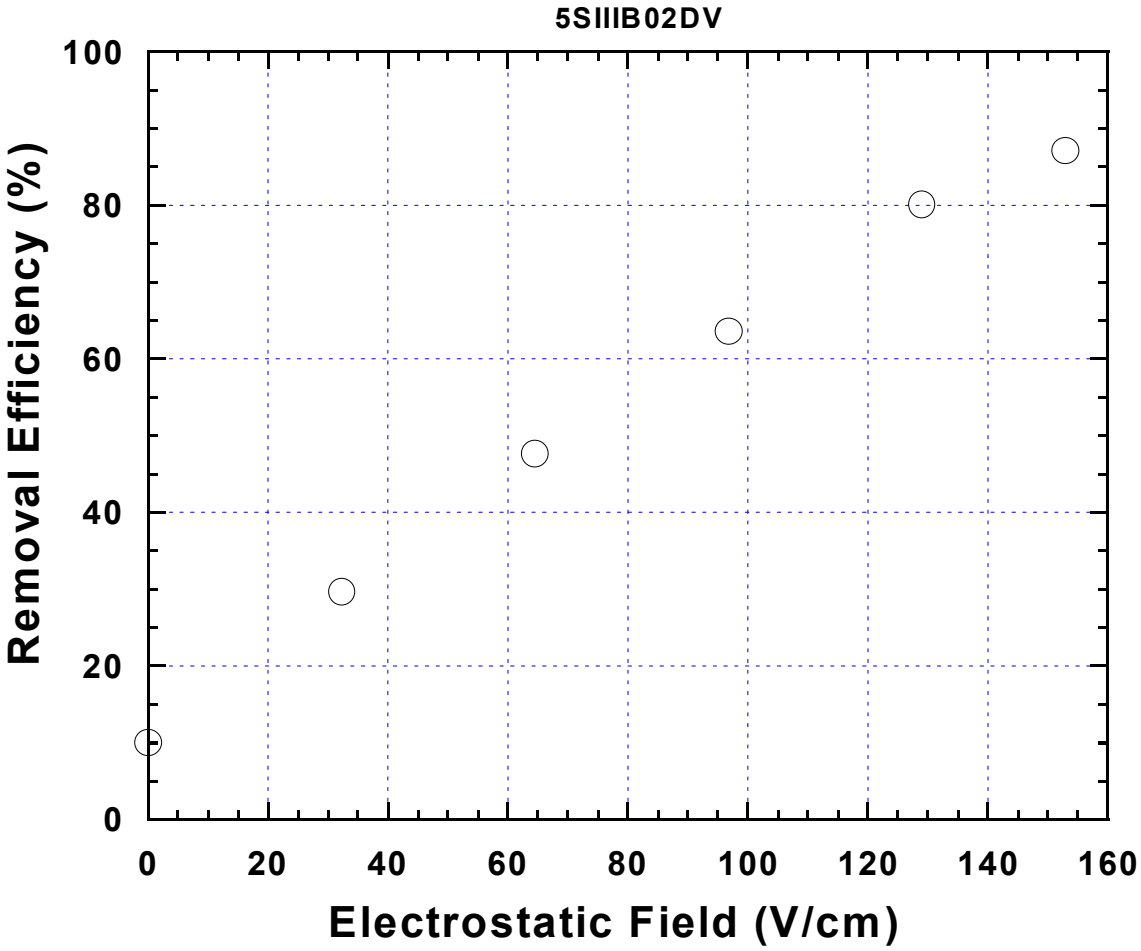

Figure 18. Removal efficiency as a function of time at various electrostatic field values (II). Experimental condition: pH = 6.6, initial turbidity = 390 NTU; Sample: 5SIIIB02

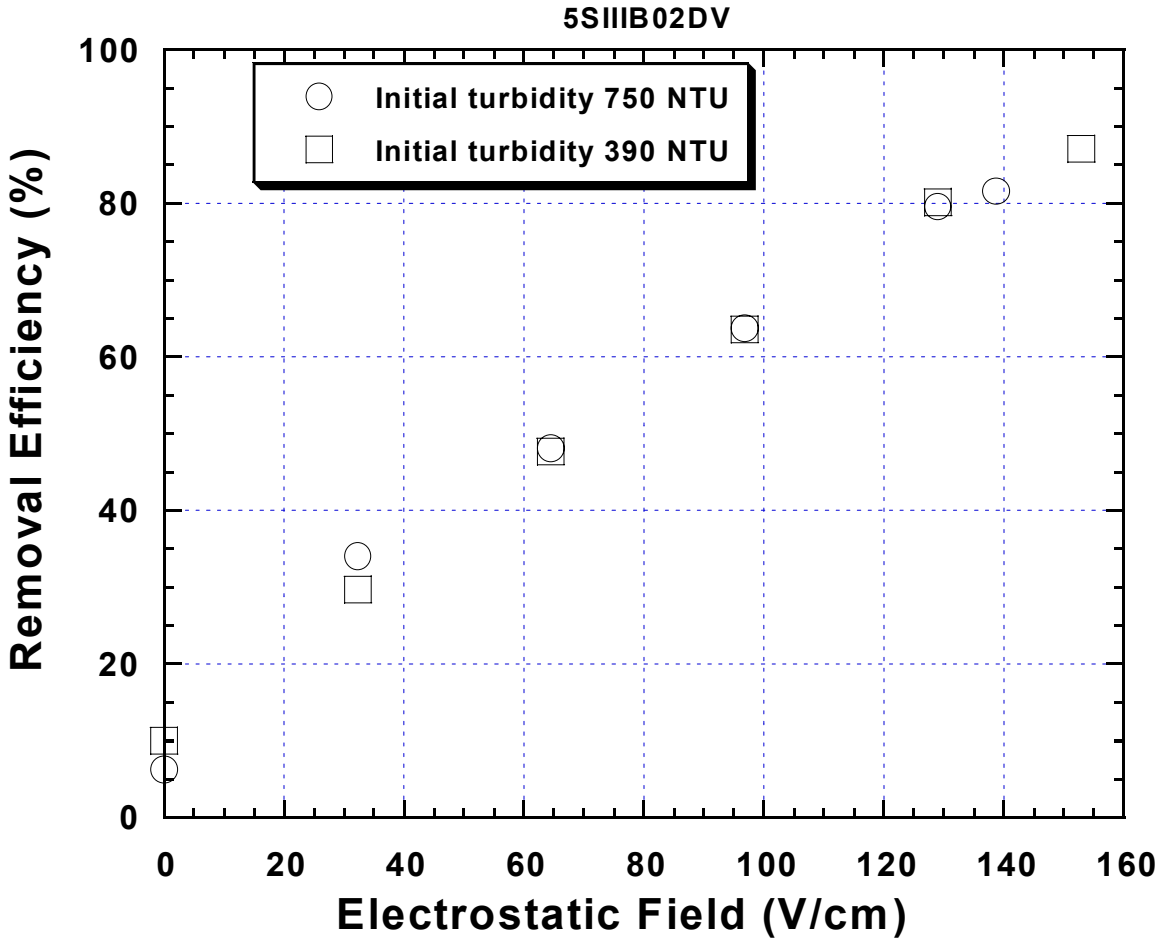

Figure 19. Removal efficiency as a function of time at various electrostatic field values (III). Experimental condition: pH = 6.6, initial turbidity = 390 NTU; Sample: 5SIIIB02

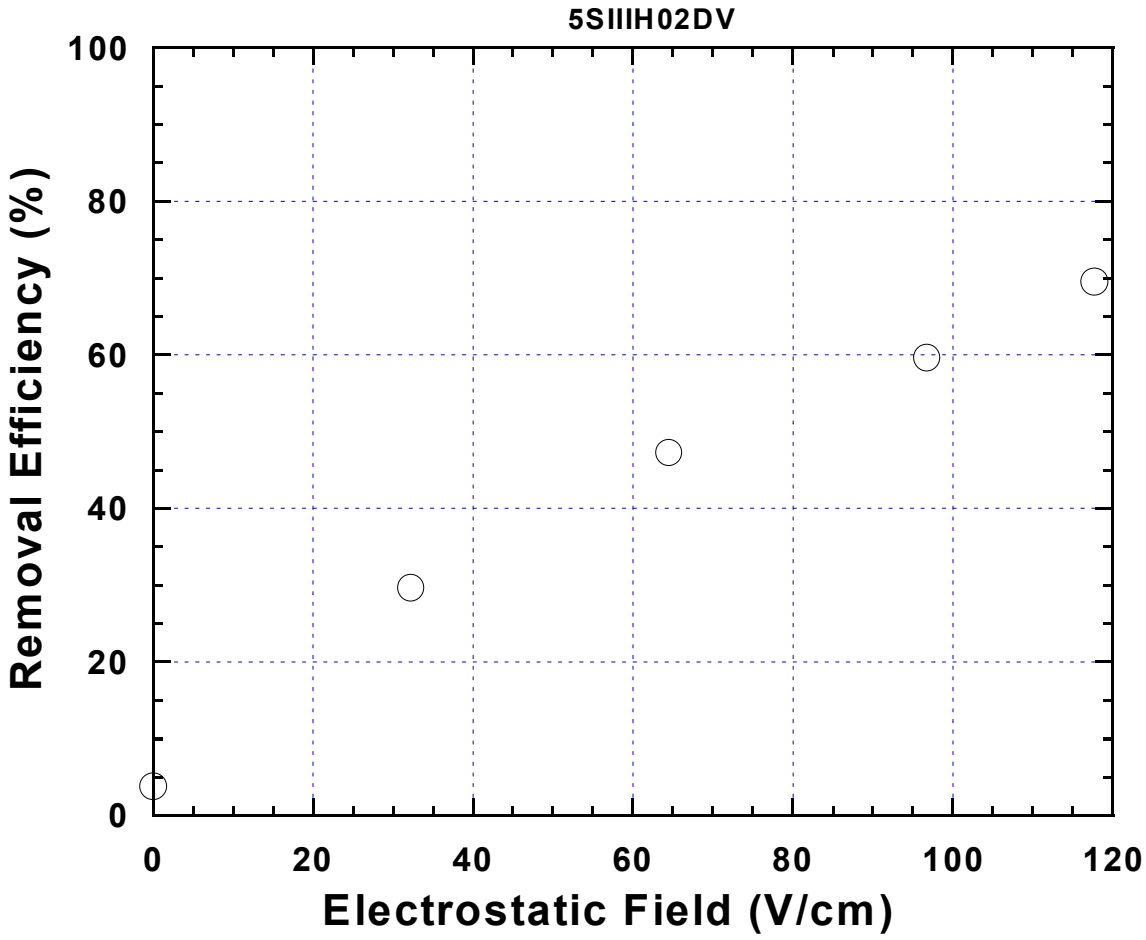

Figure 20. Removal efficiency as a function of time at various electrostatic field values (I). Experimental condition: pH = 7.1, initial turbidity = 720 NTU; Sample: 5SIIIH02

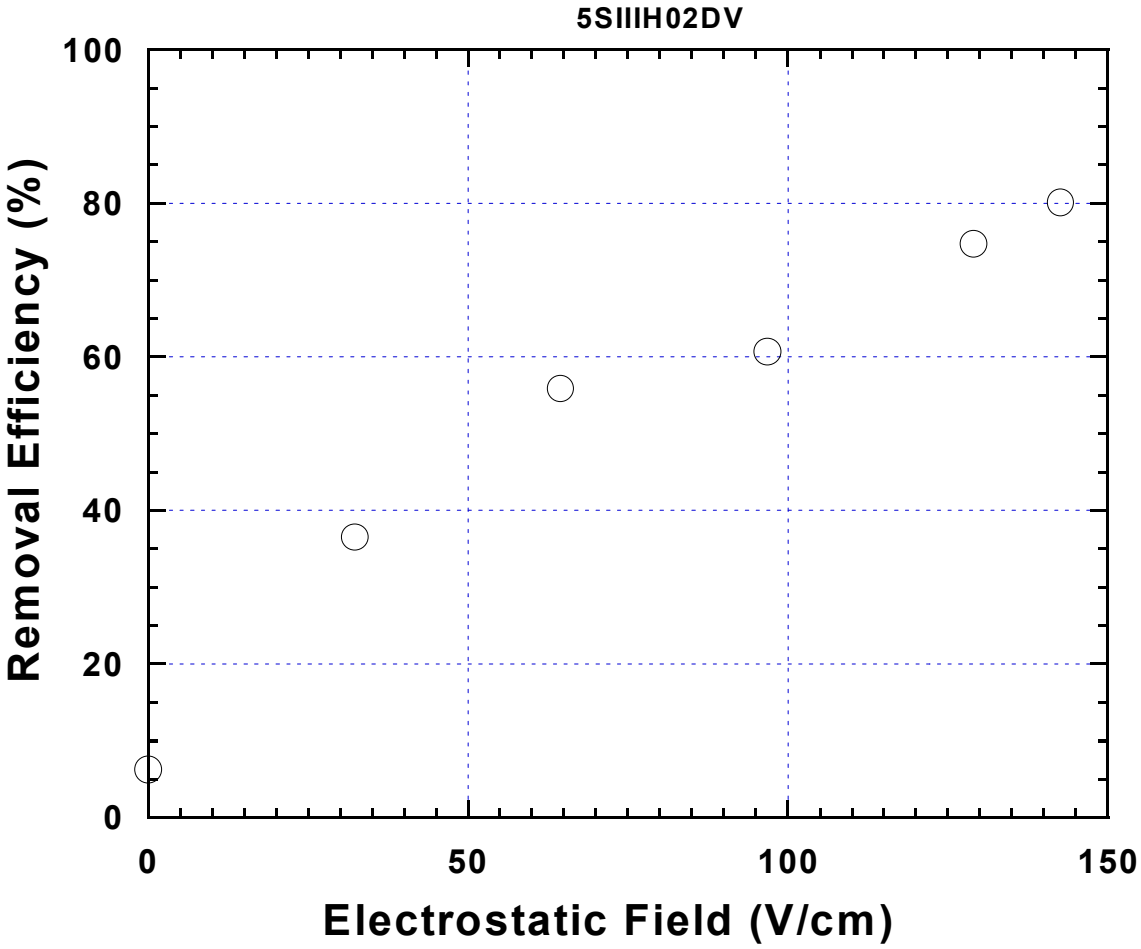

Figure 21. Removal efficiency as a function of time at various electrostatic field values (II). Experimental condition: pH = 6.8, initial turbidity = 285 NTU; Sample: 5SIIIH02

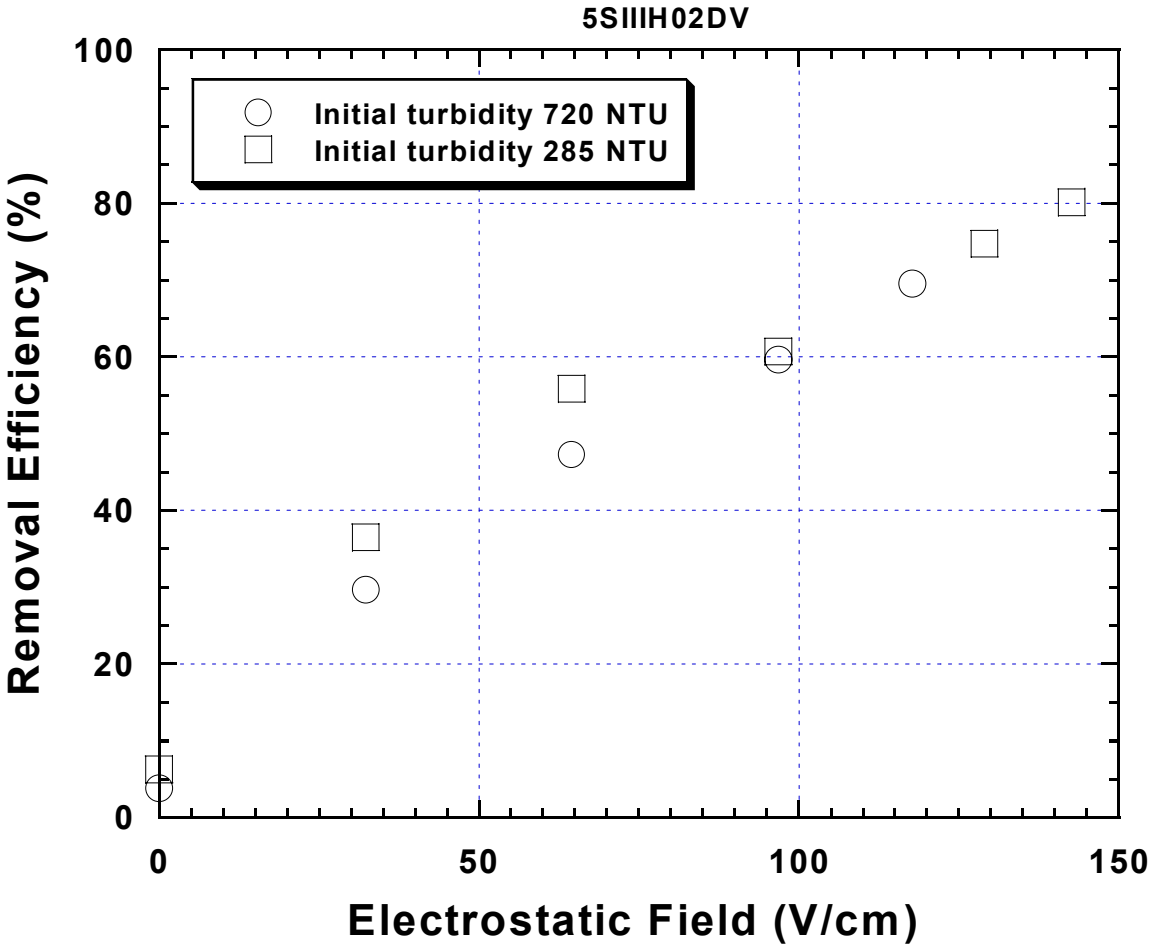

Figure 22. Removal efficiency as a function of time at various electrostatic field values (III). Sample: 5SIIIH02

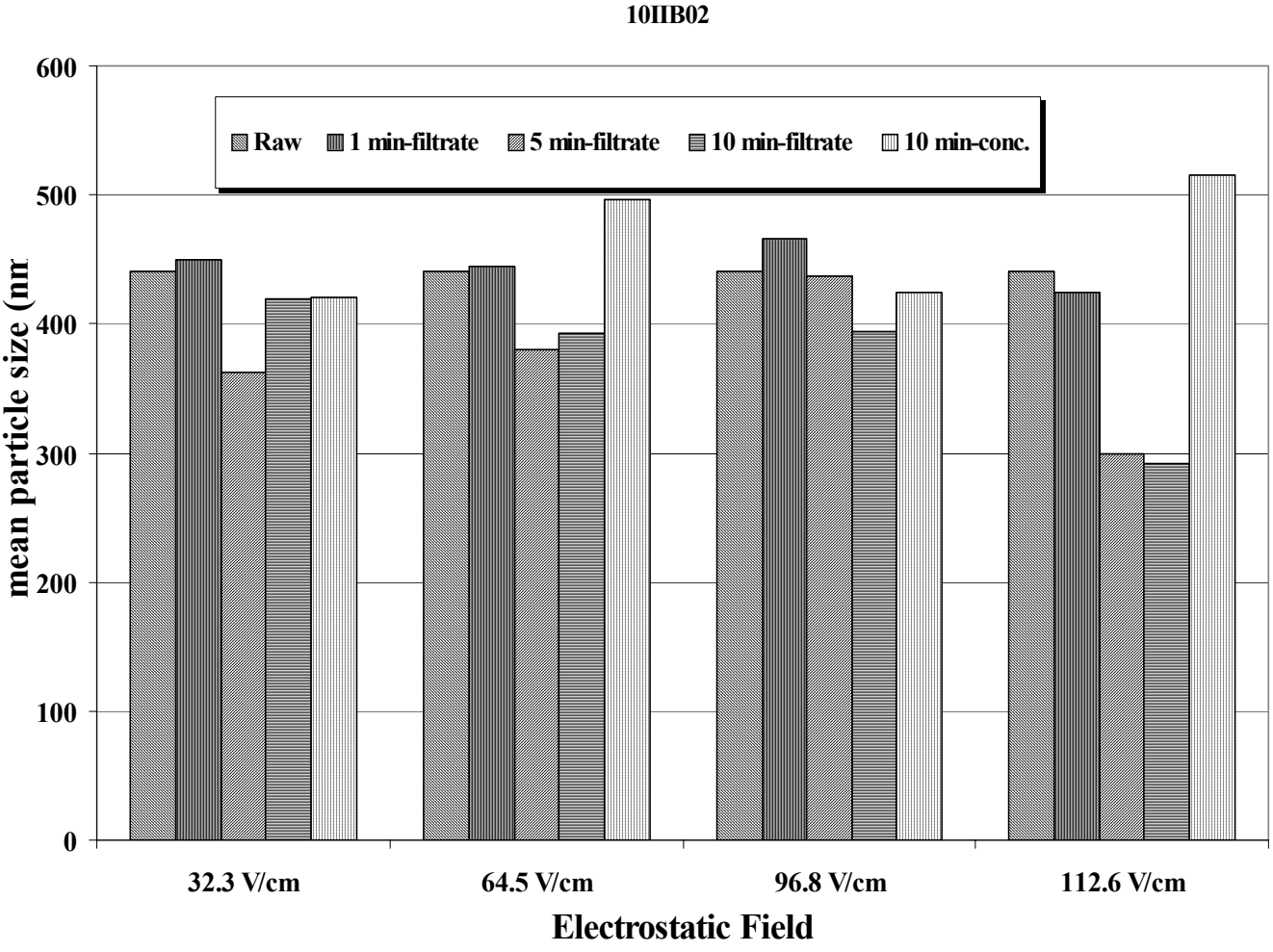

Figure 23. Distribution of particle size as affected by electrostatic field. Experimental condition: pH = 6.8; Sample: 10IIB02

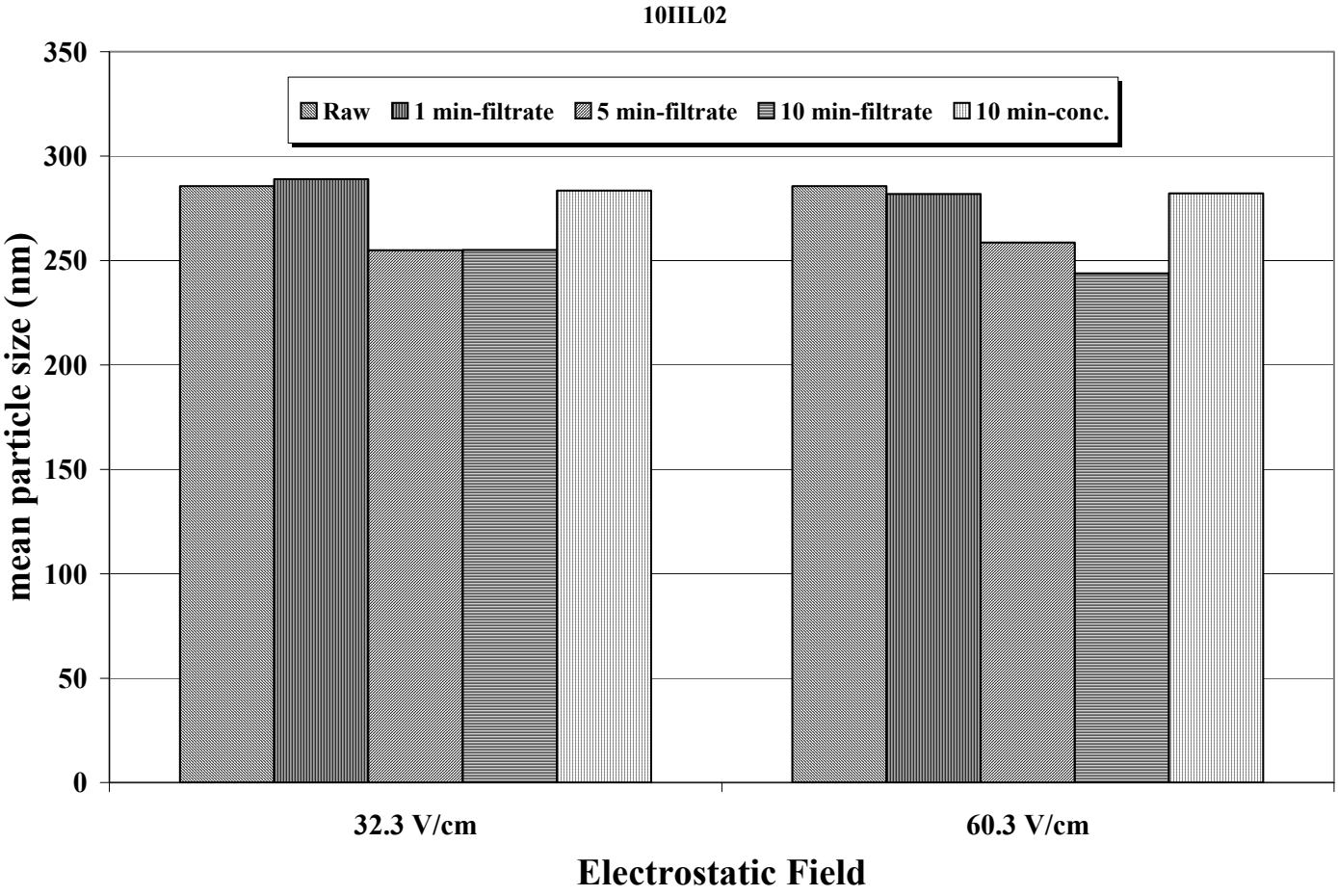

Figure 24. Distribution of particle size as affected by electrostatic field. Experimental condition: pH = 7.1; Sample: 10IIL02

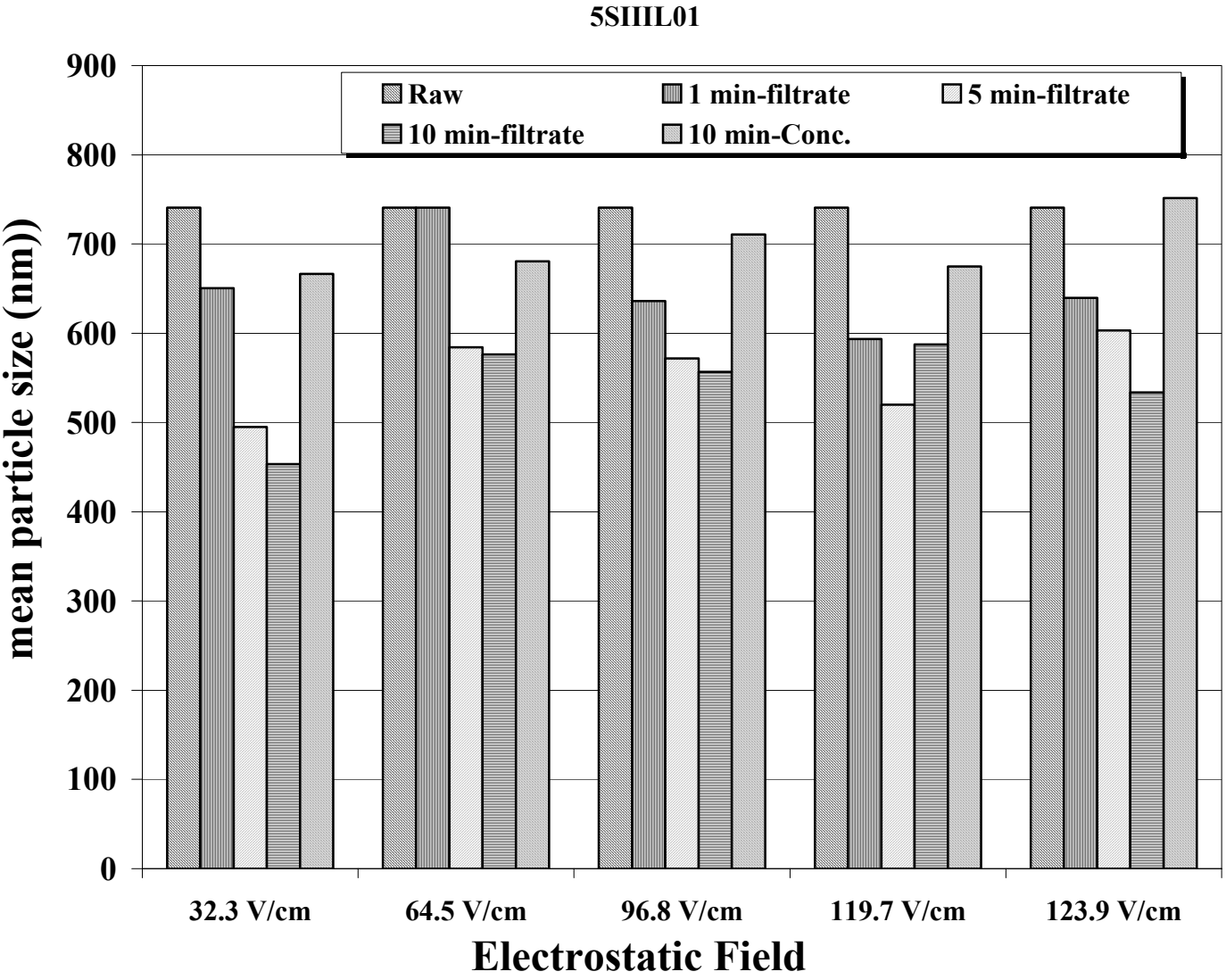

Figure 25. Distribution of particle size as affected by electrostatic field.
Experimental condition: pH = 6.8, initial turbidity = 680 NTU; Sample: 5SIIIL01

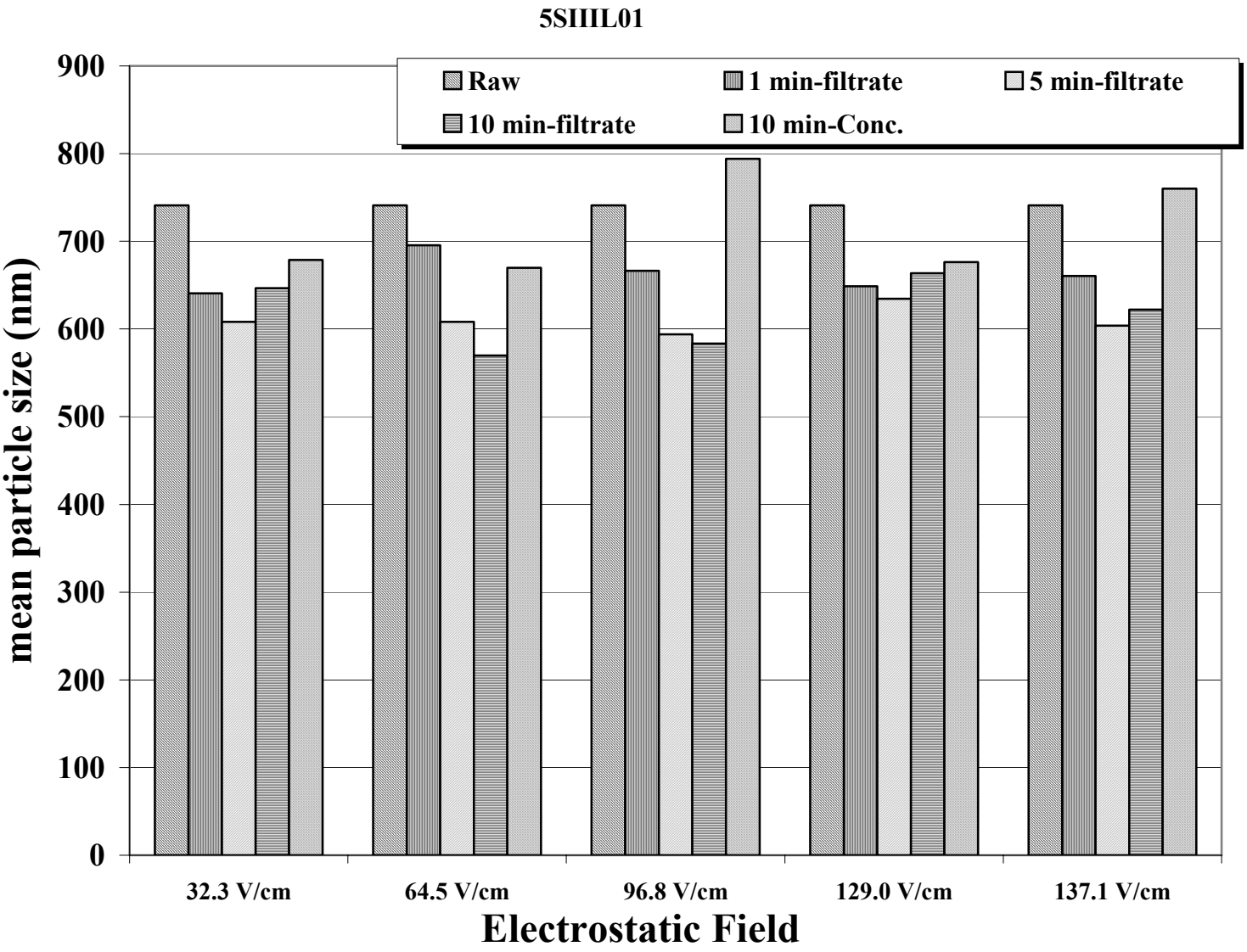

Figure 26. Distribution of particle size as affected by electrostatic field.
Experimental condition: pH = 6.6, initial turbidity = 422 NTU; Sample: 5SIIIL01

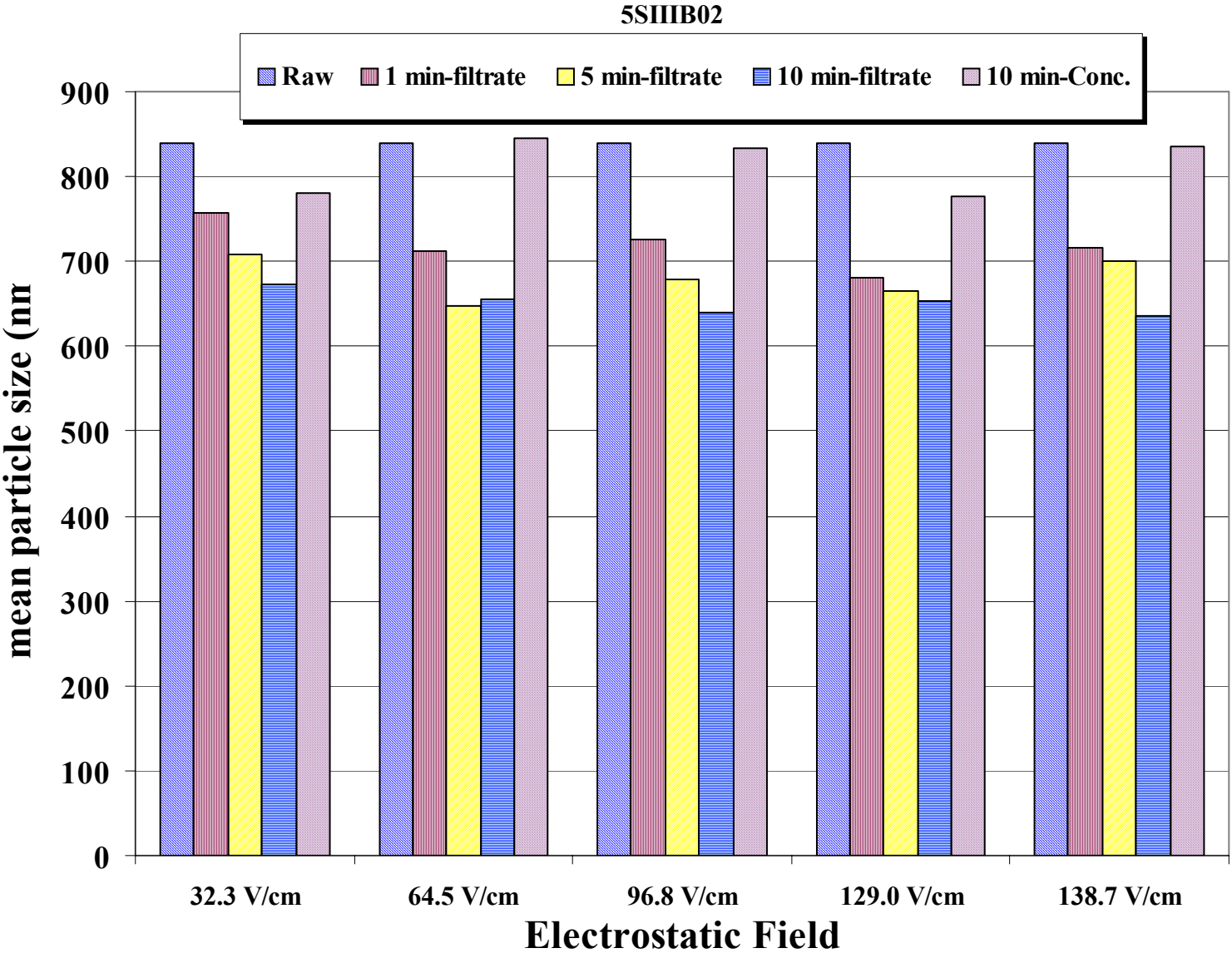

Figure 27. Distribution of particle size as affected by electrostatic field.
Experimental condition: pH = 6.8, initial turbidity = 750 NTU; Sample: 5SIIIB02

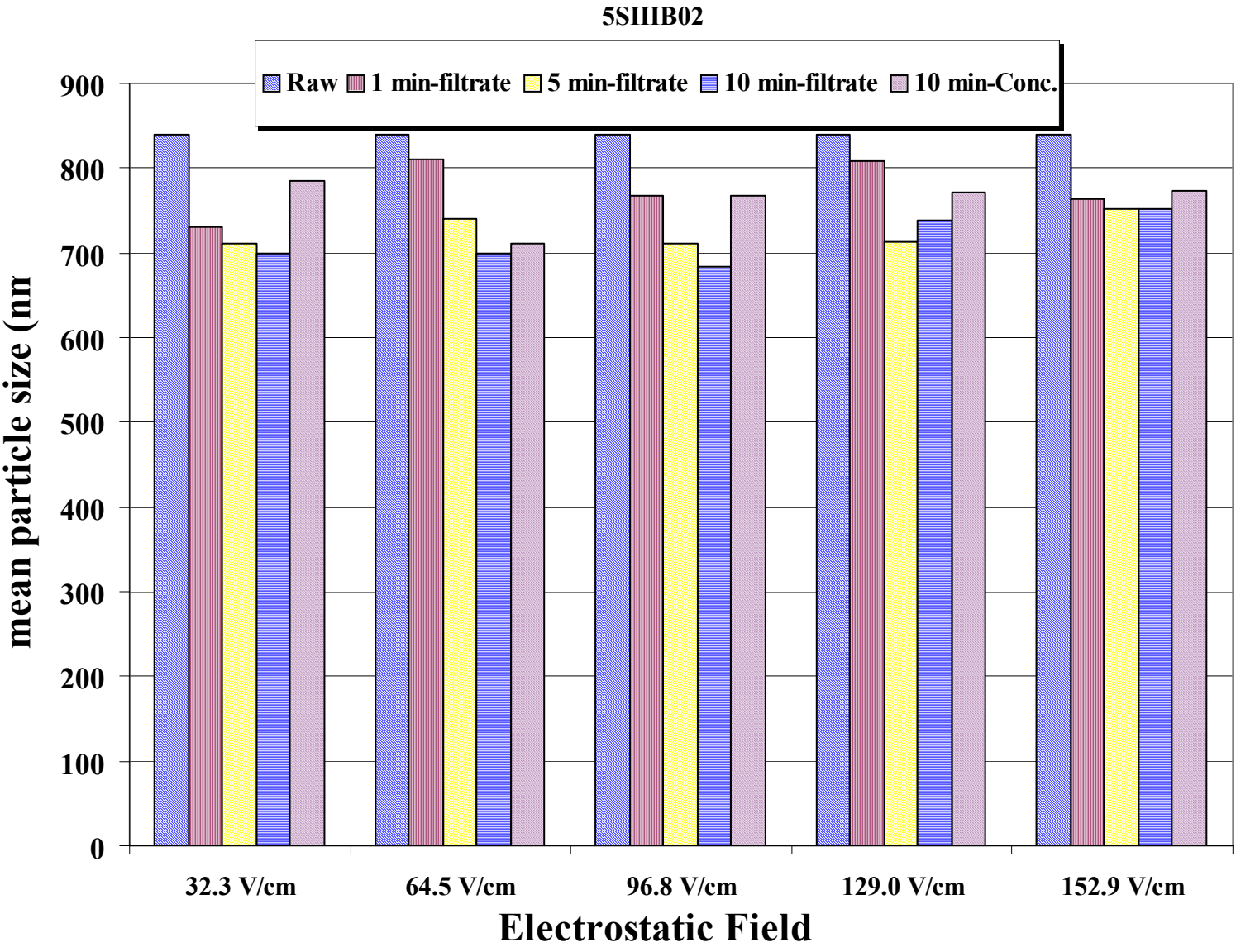

Figure 28. Distribution of particle size as affected by electrostatic field.
Experimental condition: pH = 668, initial turbidity = 390 NTU; Sample: 5SIIIB02

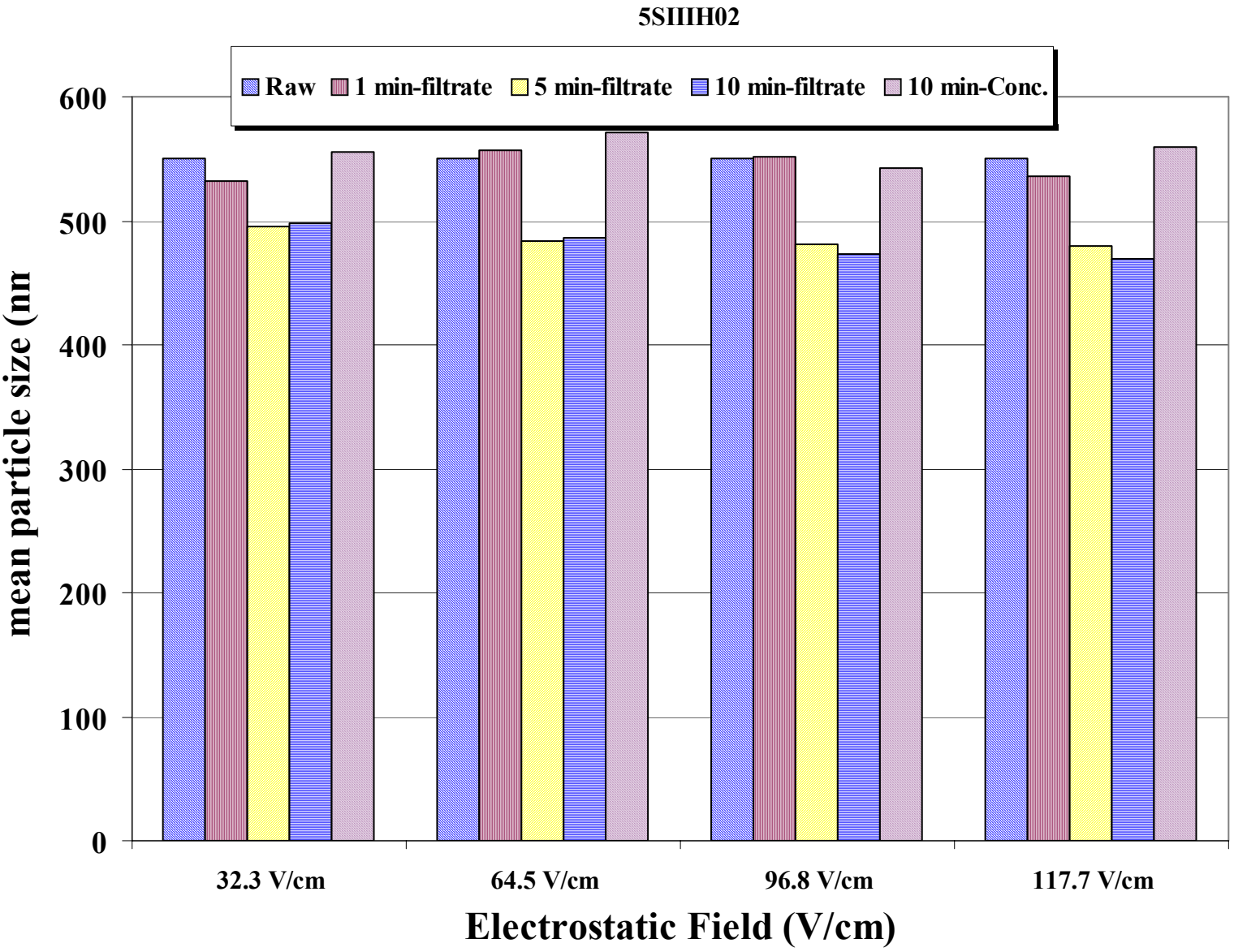

Figure 29. Distribution of particle size as affected by electrostatic field. Experimental condition: pH = 7.1, initial turbidity = 720 NTU; Sample: 5SIIIH02

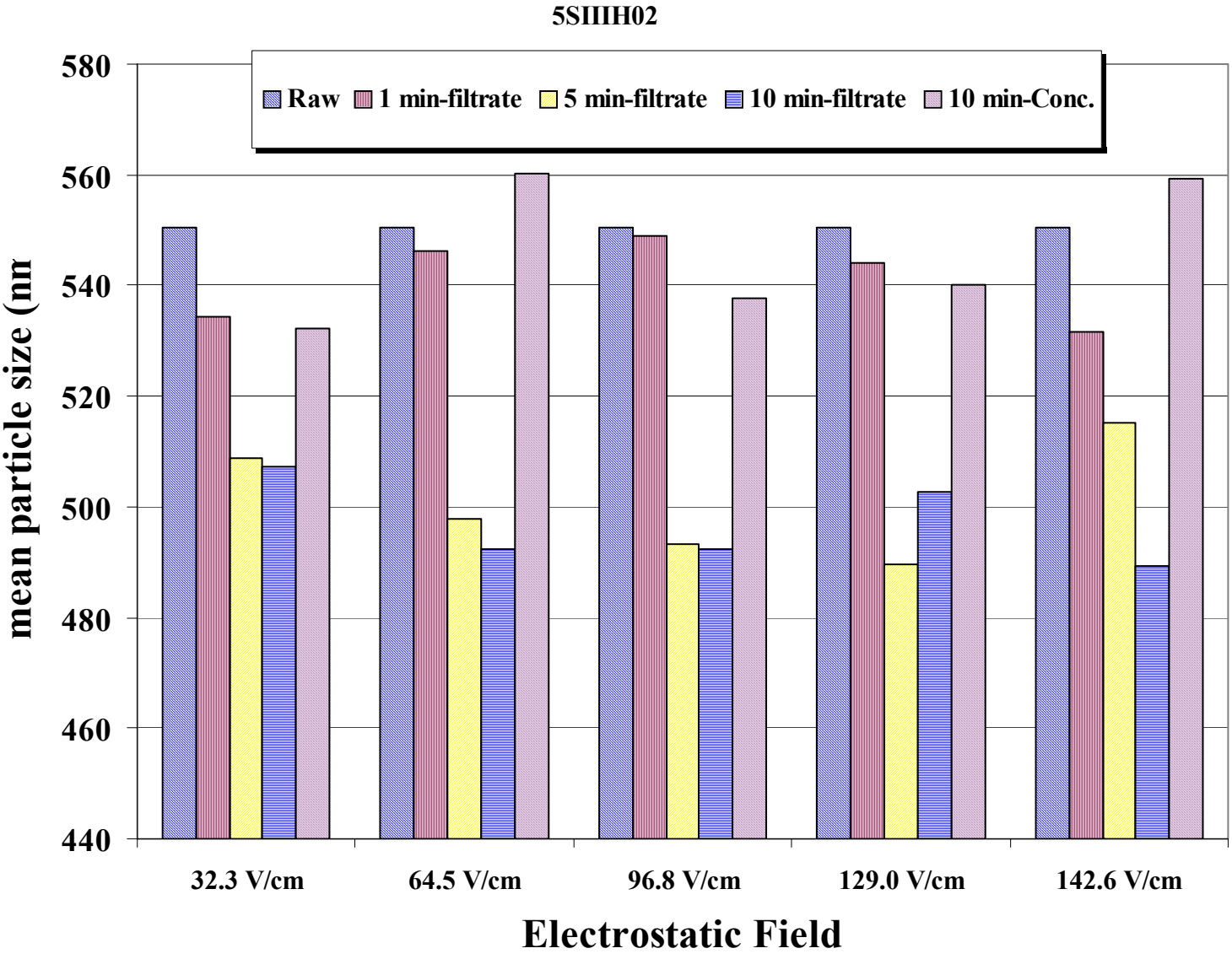

Figure 30. Distribution of particle size as affected by electrostatic field.
Experimental condition: pH = 6.8, initial turbidity = 285 NTU; Sample: 5SIIIH02

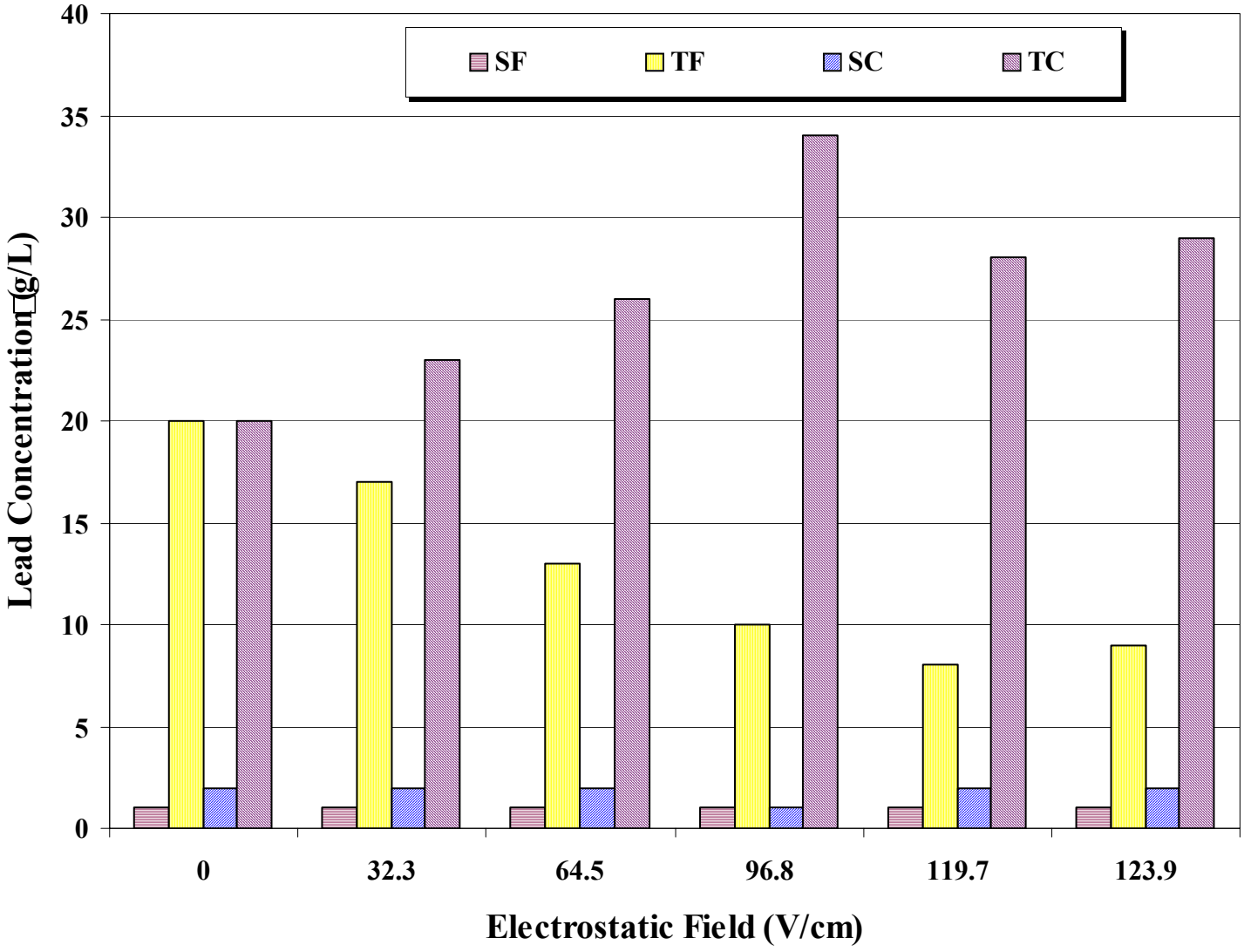

Figure 31. Distribution of led concentration as affected by electrostatic field. Experimental condition: pH = 6.8; initial turbidity = 680 NTU; Sample: 5SIIIL01. SF: soluble concentration of filtrate; TF: total concentration of filtrate; SC: soluble concentration of concentrate; TC: total concentration of concentrate.

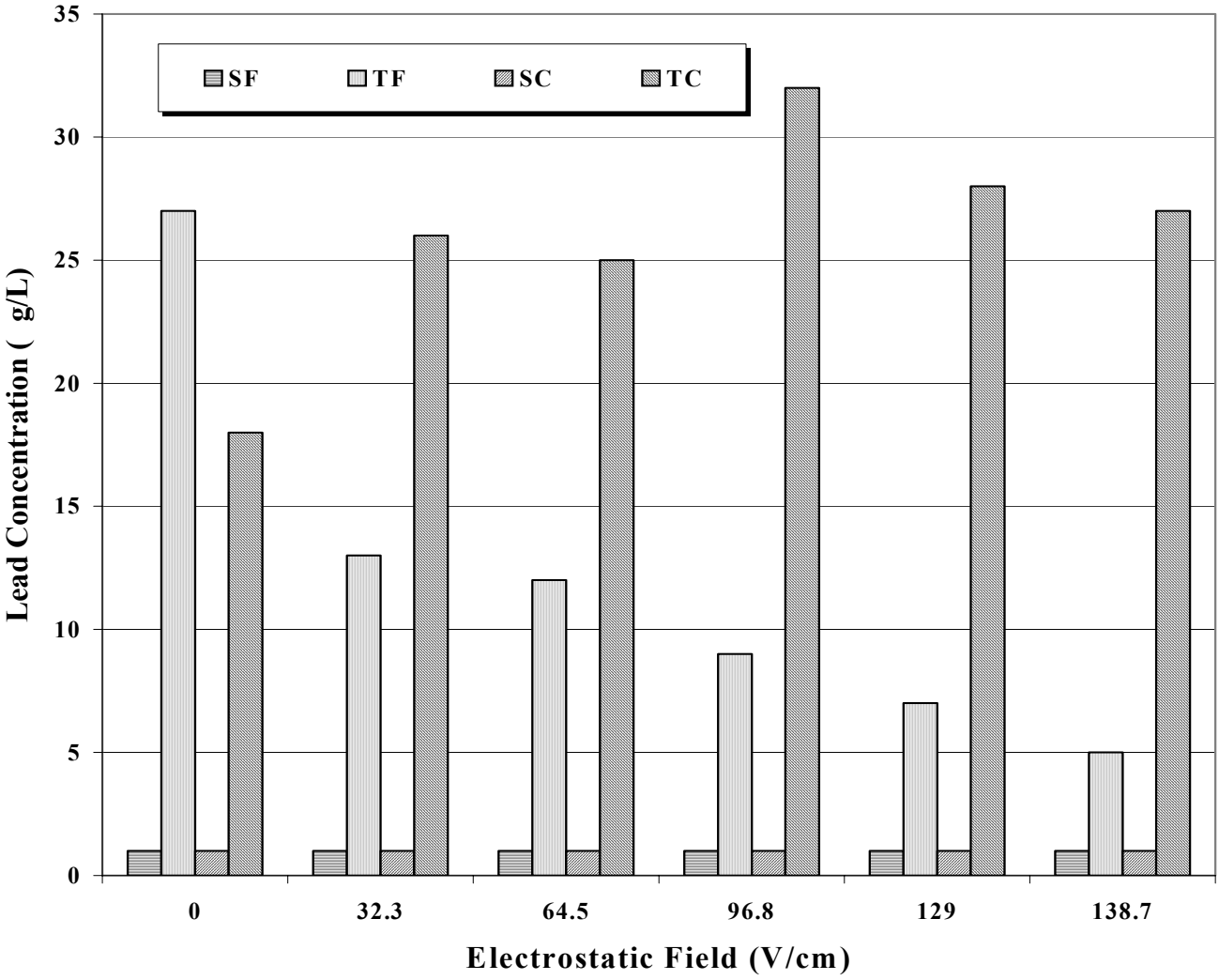

Figure 32. Distribution of led concentration as affected by electrostatic field. Experimental condition: pH = 6.8; initial turbidity = 750 NTU; Sample: 5SIIIB02. SF: soluble concentration of filtrate; TF: total concentration of filtrate; SC: soluble concentration of concentrate; TC: total concentration of concentrate.

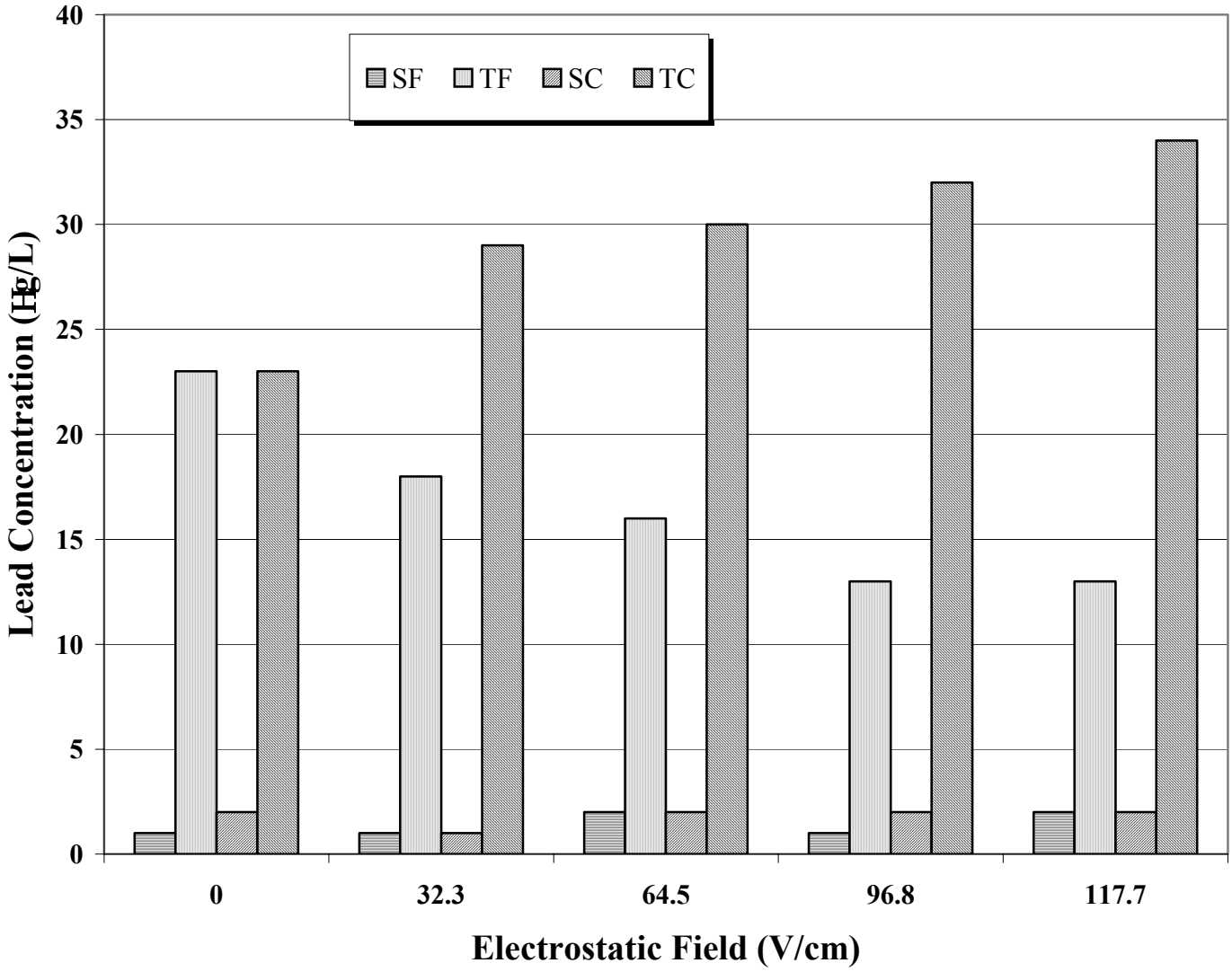

Figure 33. Distribution of led concentration as affected by electrostatic field. Experimental condition: pH = 7.1; initial turbidity = 720 NTU; Sample: 5SIIIH02. SF: soluble concentration of filtrate; TF: total concentration of filtrate; SC: soluble concentration of concentrate; TC: total concentration of concentrate.

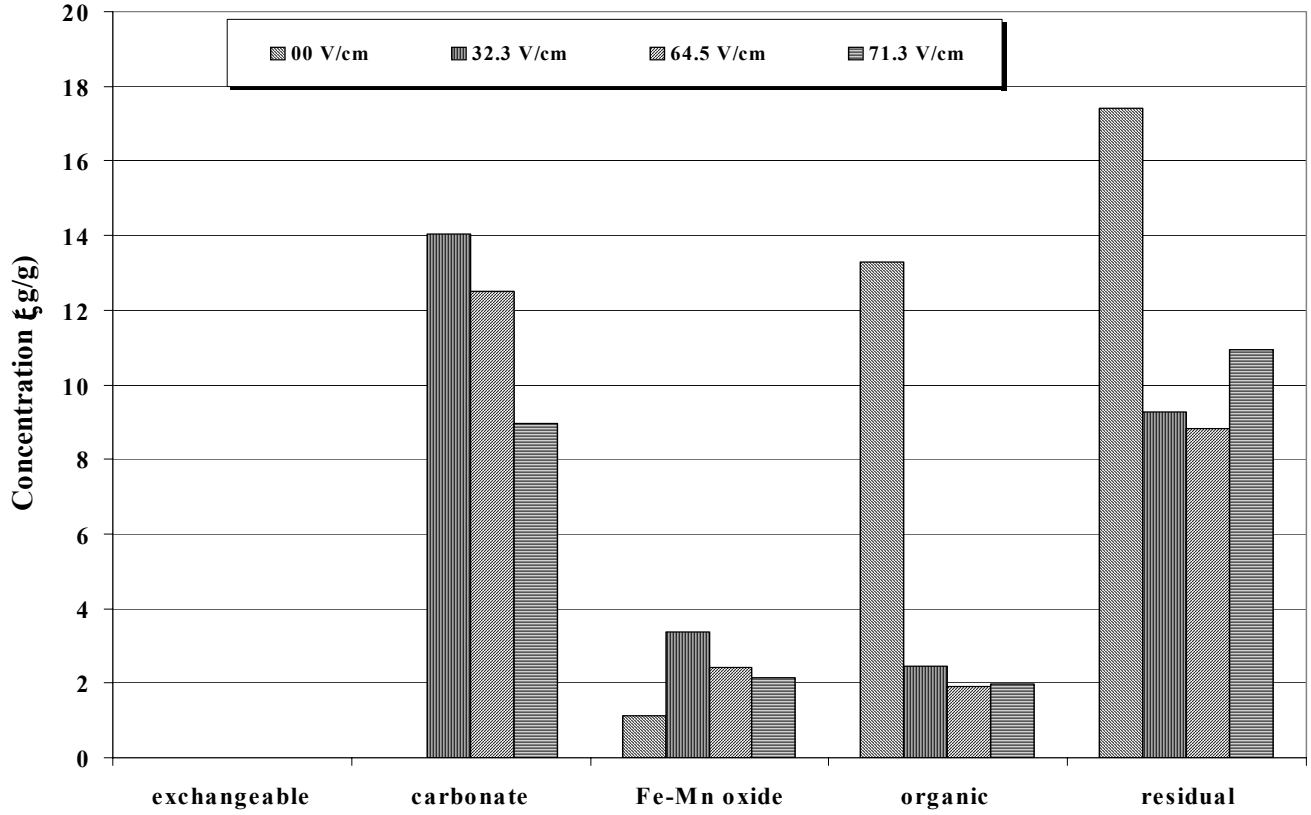

Figure 34. Distribution of lead species in particulate collected from well water sample as affected by electrostatic field (I). Experimental condition: pH = 6.8; Sample: 10IIB02

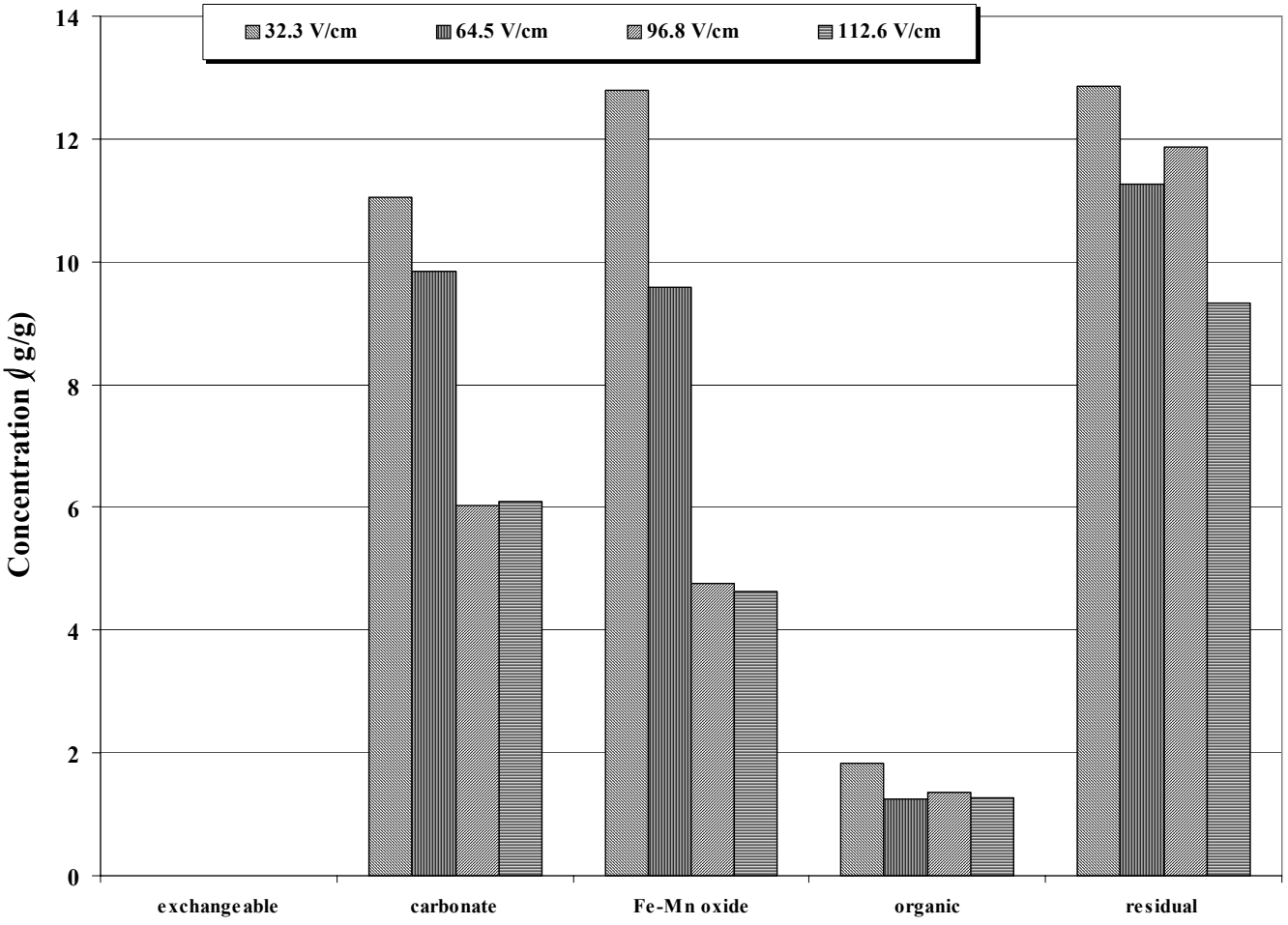

Figure 35. Distribution of lead species in particulate collected from well water sample as affected by electrostatic field (II). Experimental condition: pH = 6.8; Sample = 10IIB02

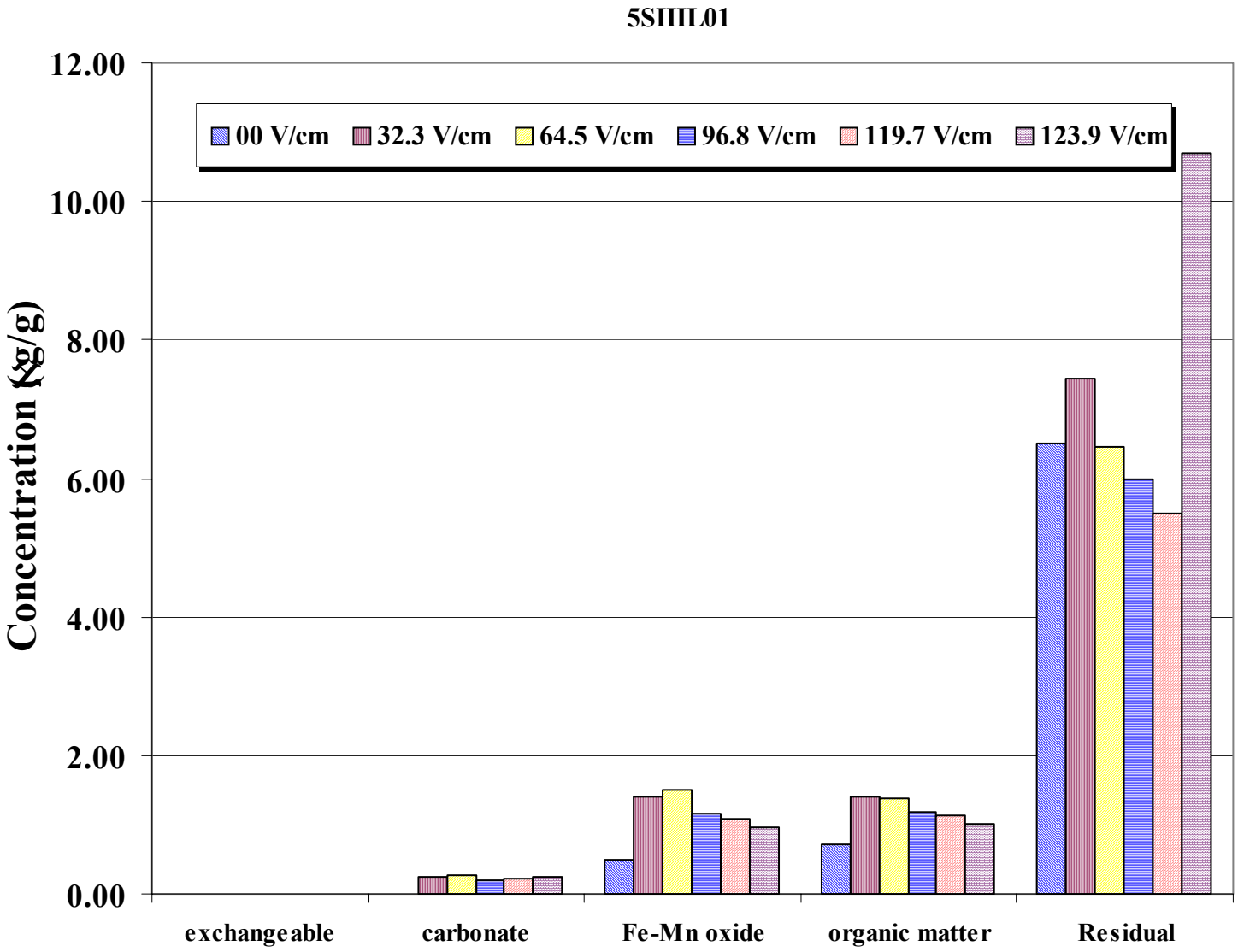

Figure 36. Distribution of lead species in particulate collected from well water sample as affected by electrostatic field (I). Experimental condition: pH = 6.8; initial turbidity = 680 NTU; Sample: 5SIIIL01.

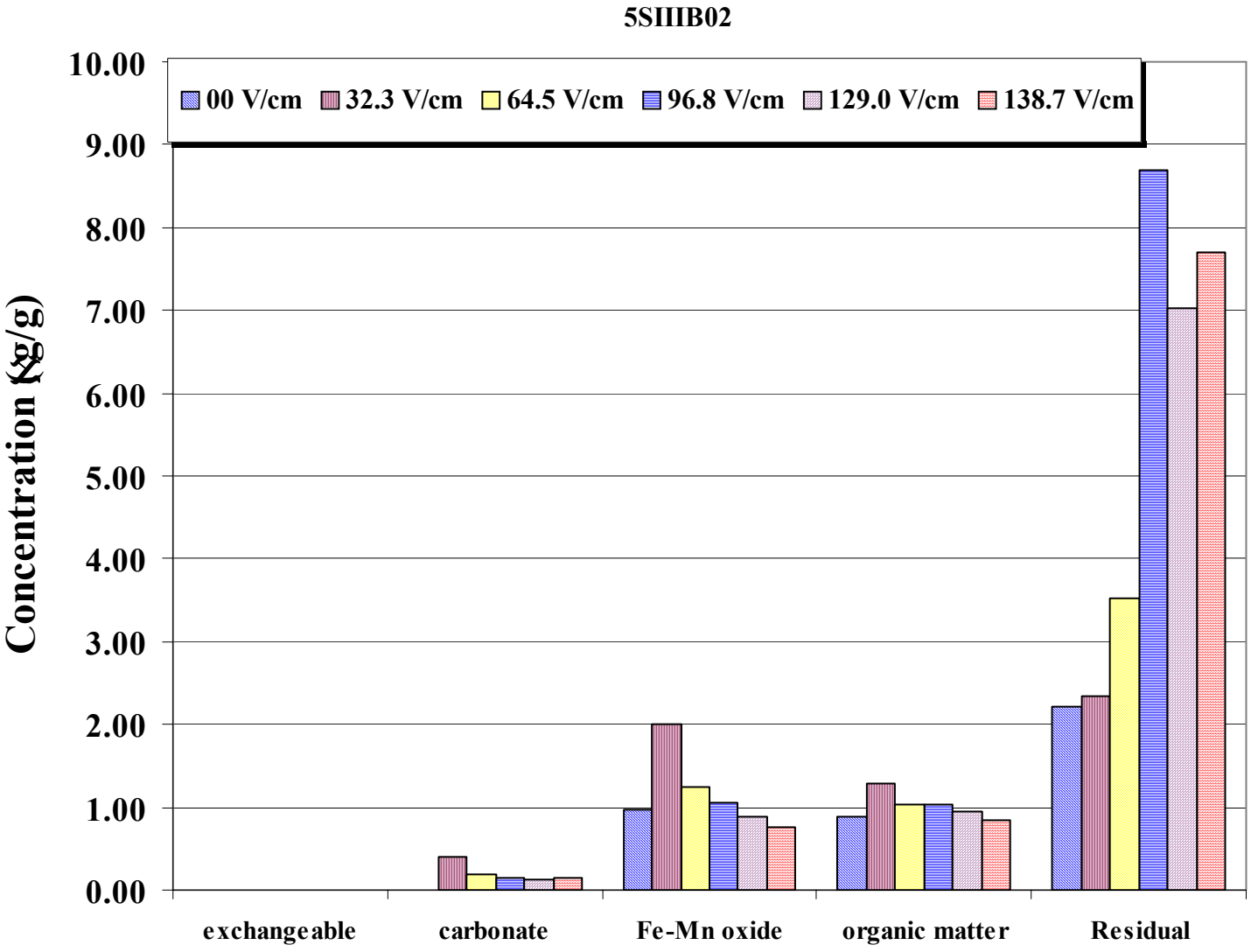

Figure 37. Distribution of lead species in particulate collected from well water sample as affected by electrostatic field. Experimental condition: pH = 6.8; initial turbidity = 750 NTU; Sample: 5SIIIB02.

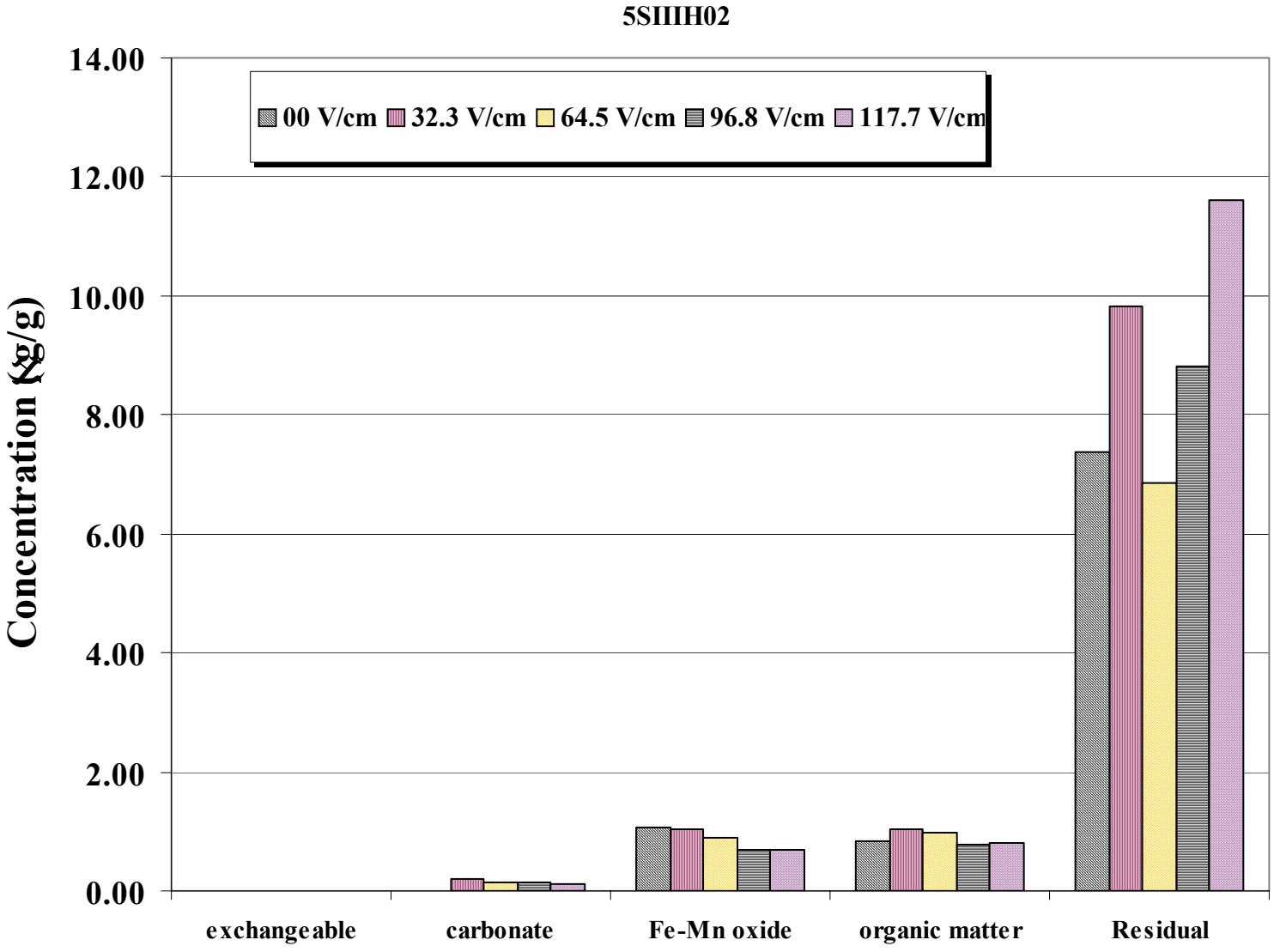

Figure 38. Distribution of lead species in particulate collected from well water sample as affected by electrostatic field. Experimental condition: pH = 7.1; initial turbidity = 720 NTU; Sample: 5SIIIH02.

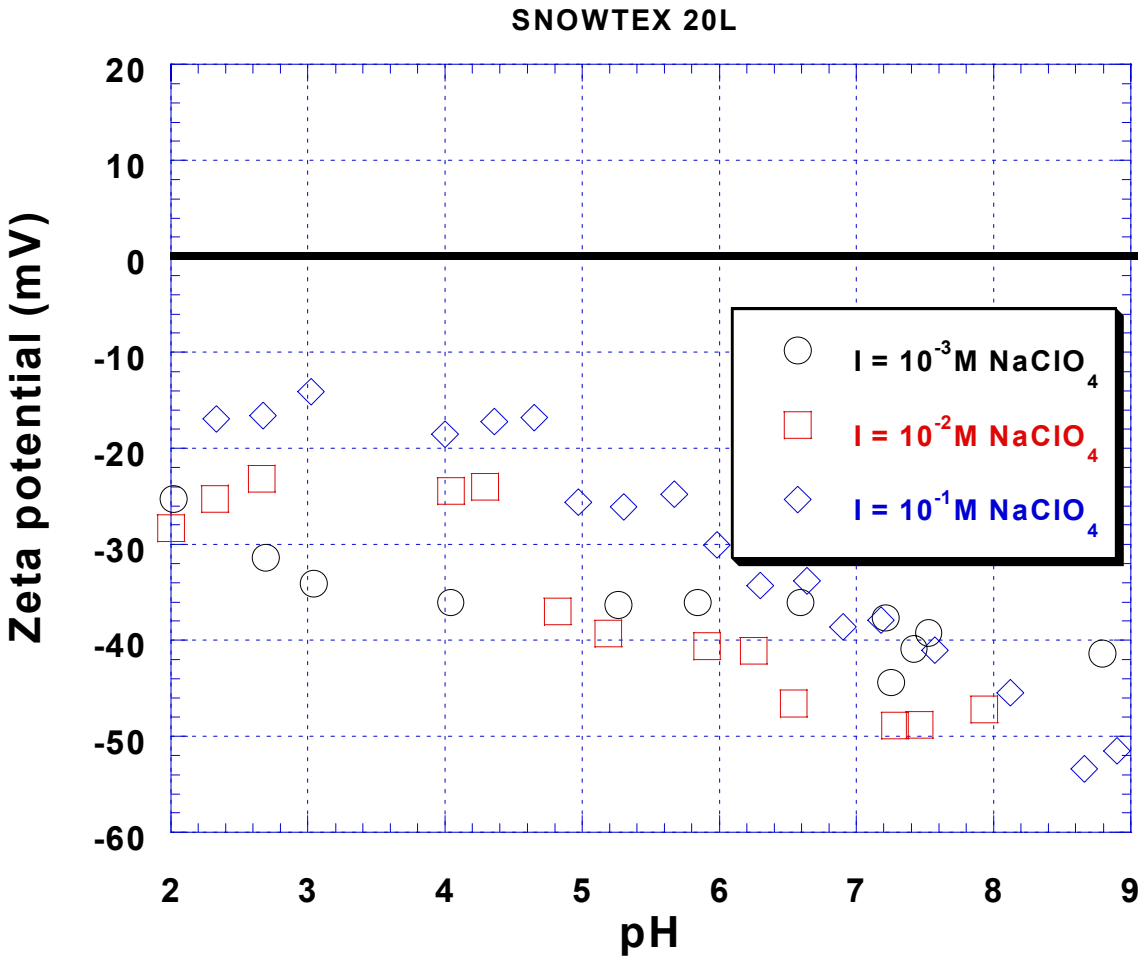

Figure 39. Zeta potential as a function of pH (Snowtex 20L).

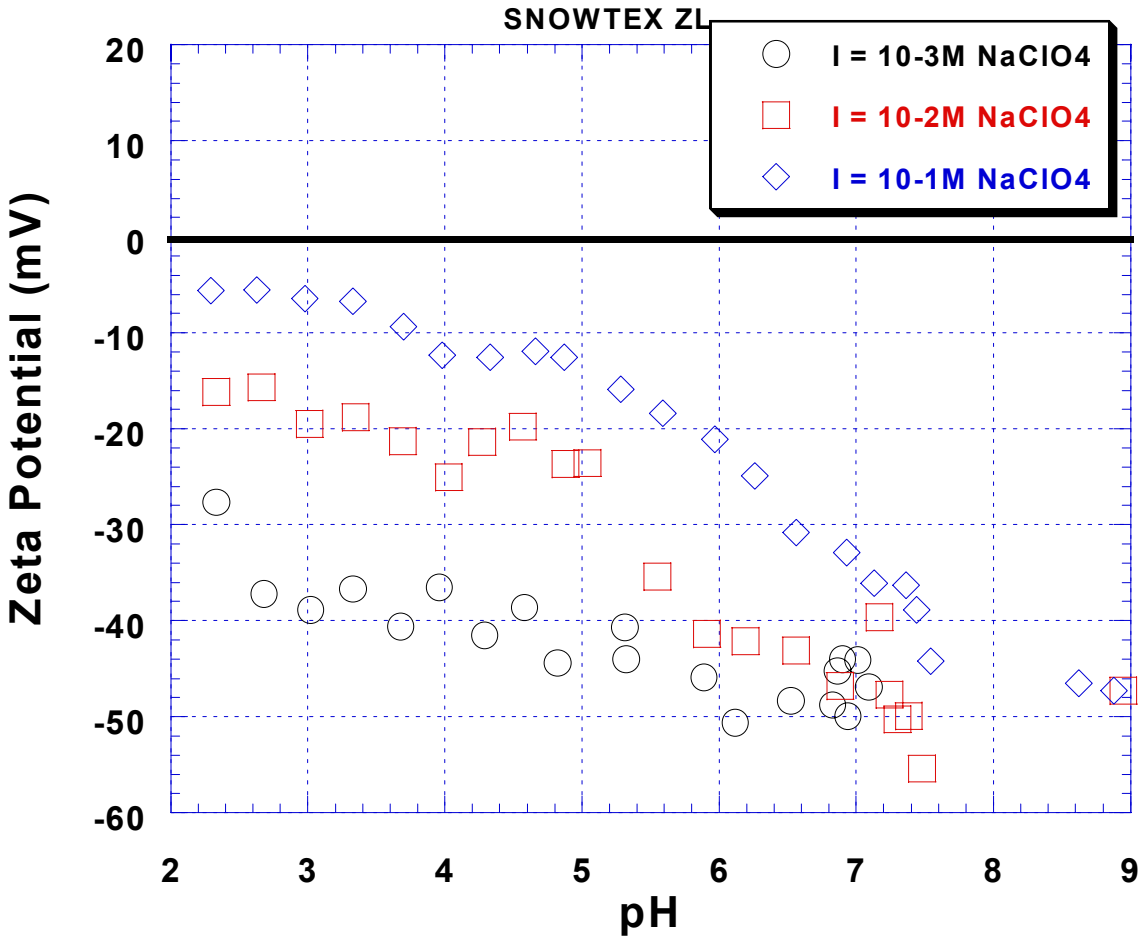

Figure 40. Zeta potential as a function of pH (Snowtex ZL).

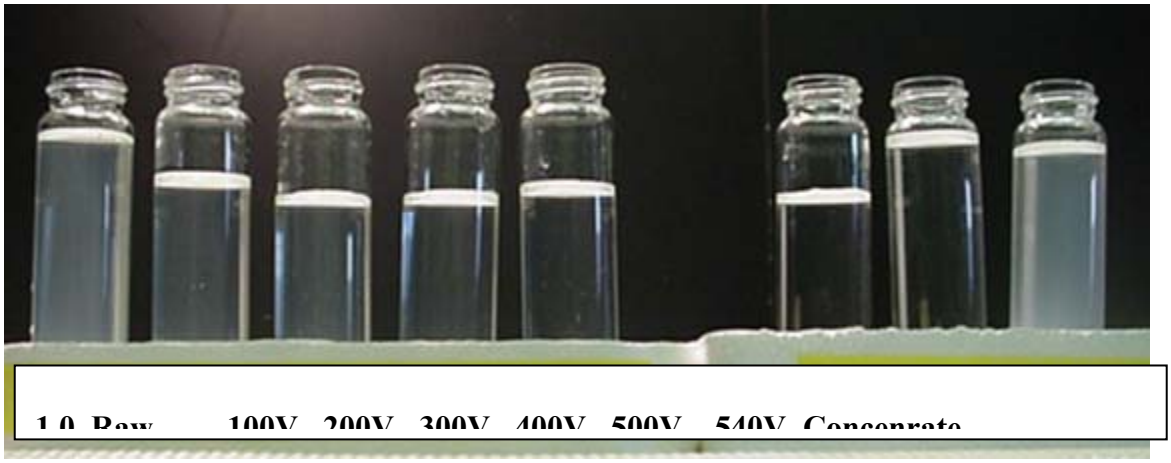

Figure 41. Visual comparison of colloidal silica sample on the various electrostatic field.

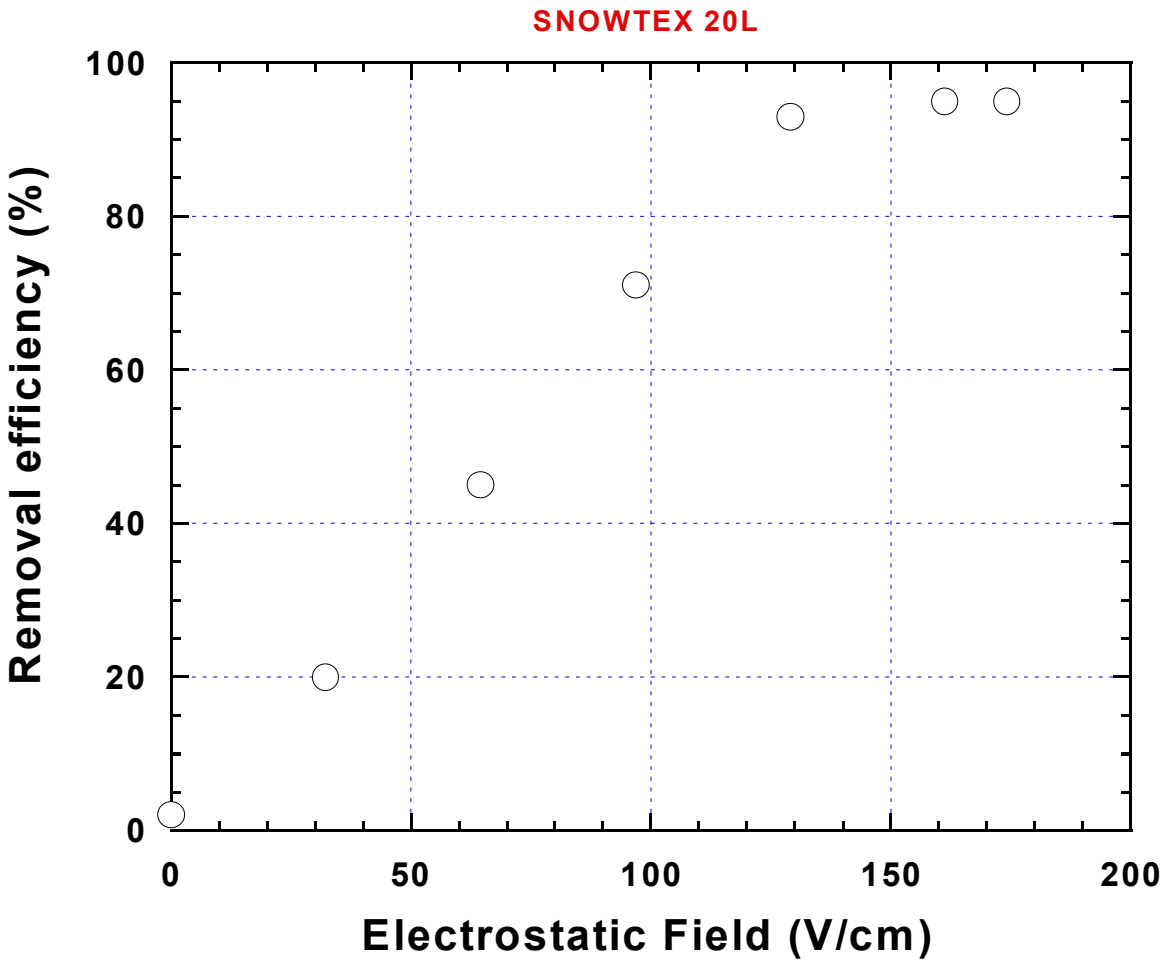

Figure 42. Effect of electrostatic field on removal of colloidal silica (II). Experimental condition: pH = 6.2; Sample: Snowtex 20L

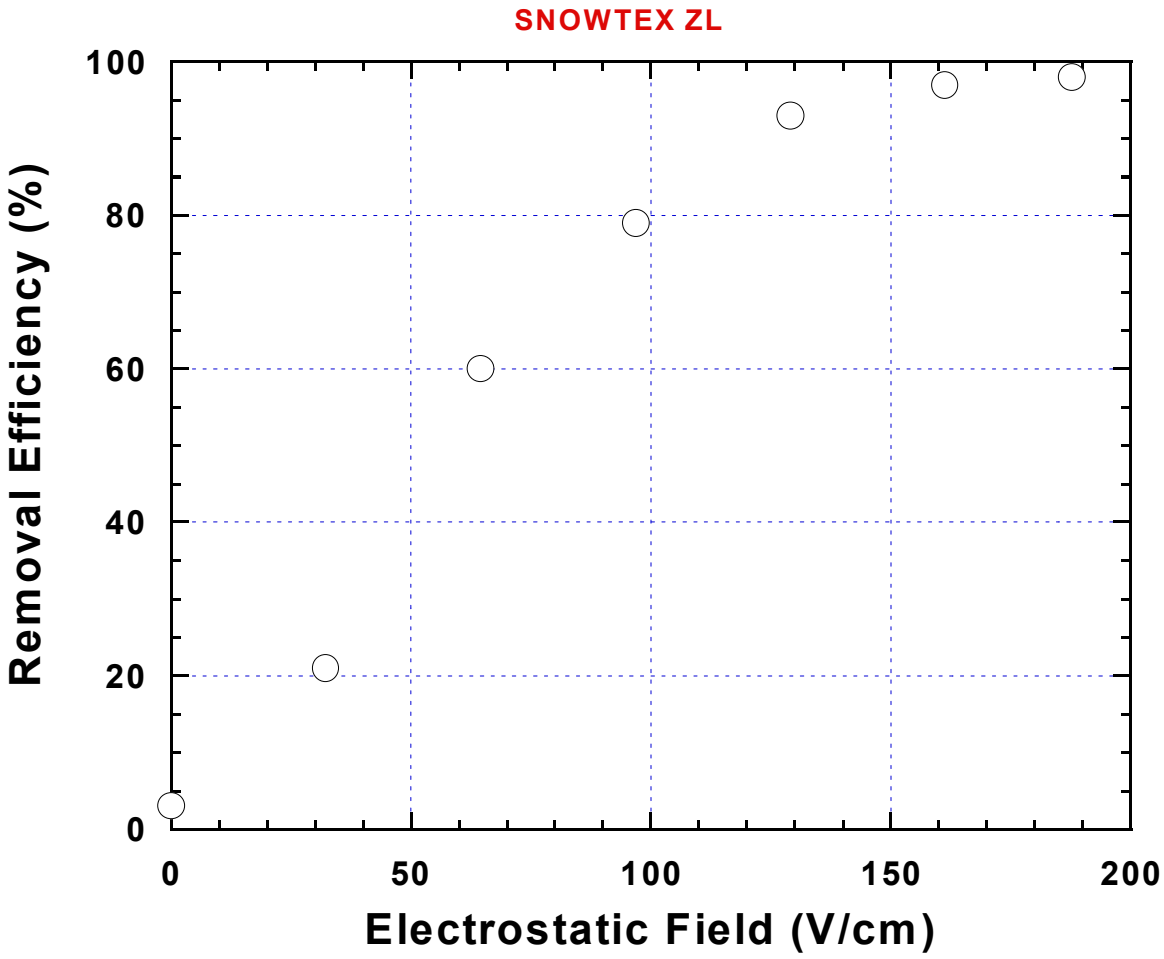

Figure 43. Effect of electrostatic field on removal of colloidal silica (II). Experimental condition: pH = 5; Sample: Snowtex ZL

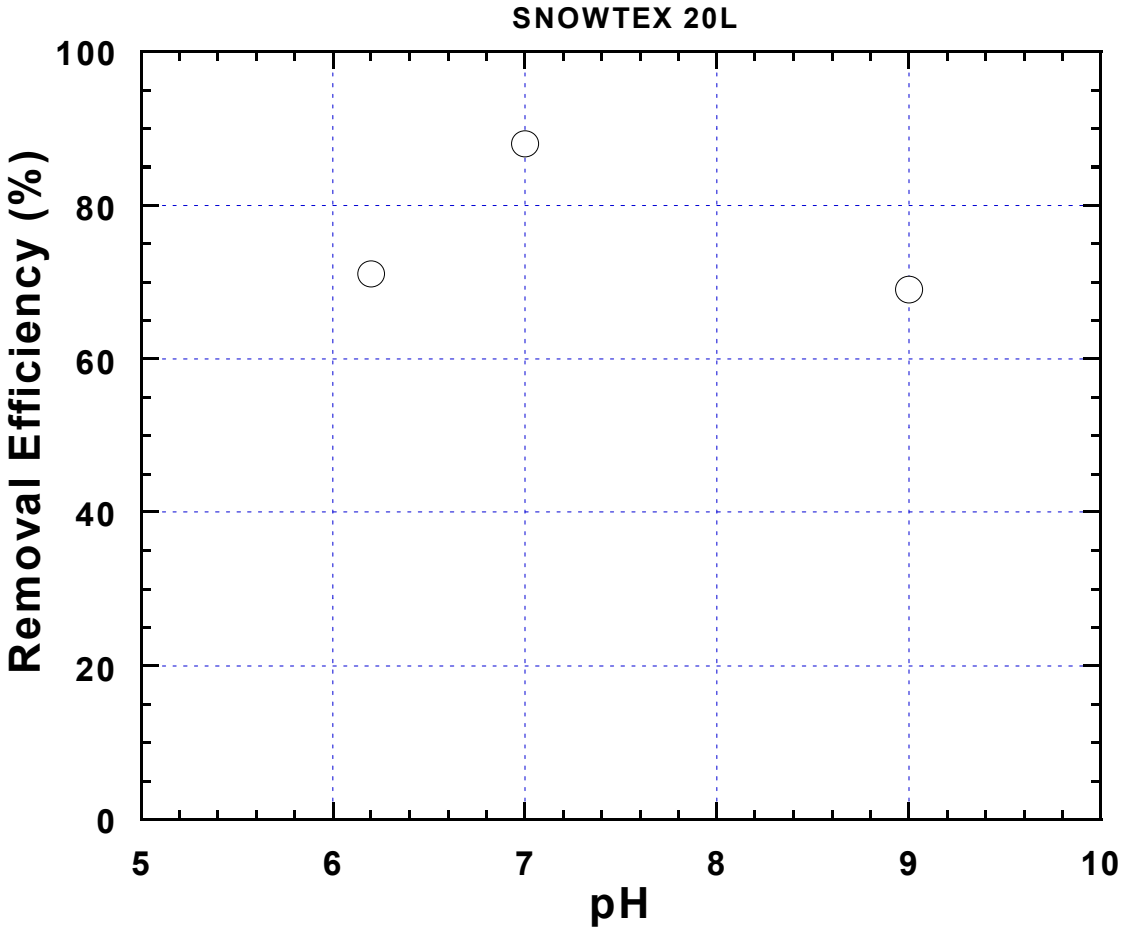

Figure 44. Steady state removal efficiency as a function of pH. Experimental condition: electrostatic field = 96.8 V/cm; Sample: Snowtex ZL

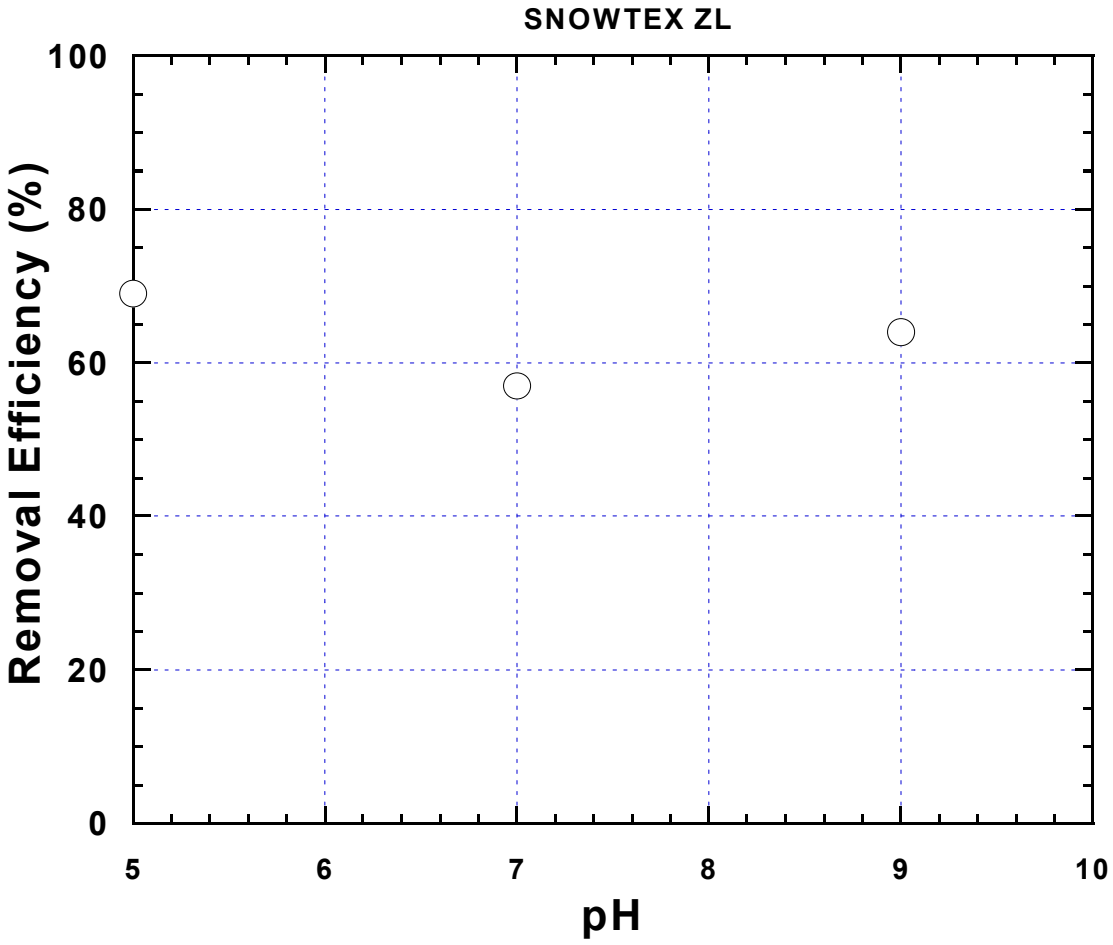

Figure 45. Steady state removal efficiency as a function of pH. Experimental condition: electrostatic field = 96.8 V/cm; Sample: Snowtex ZL

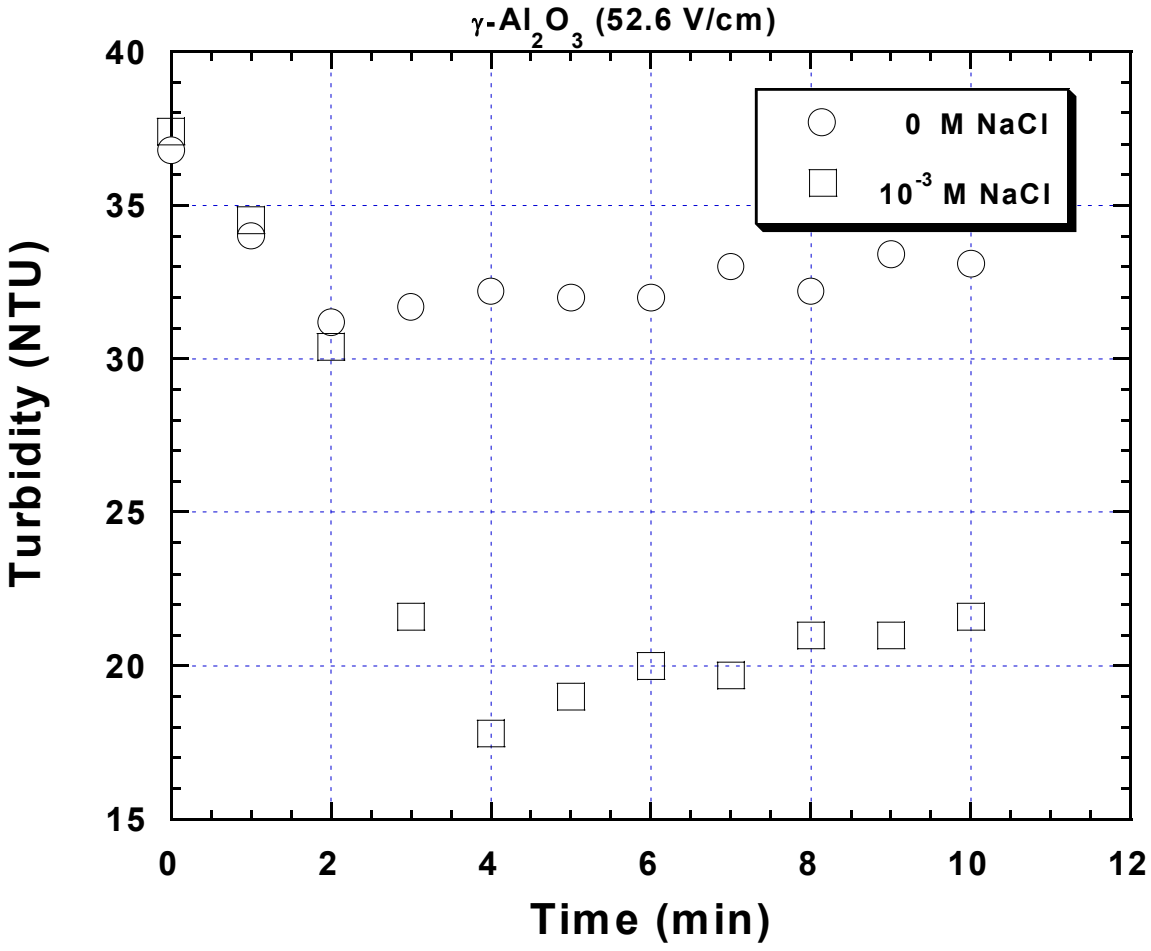

Figure 46. Change of filtrate turbidity as a function of time under various salt concentrations. Experimental condition: electrostatic field = 52.6 V/cm; pH = 5; Sample: γ-Al_2O_3

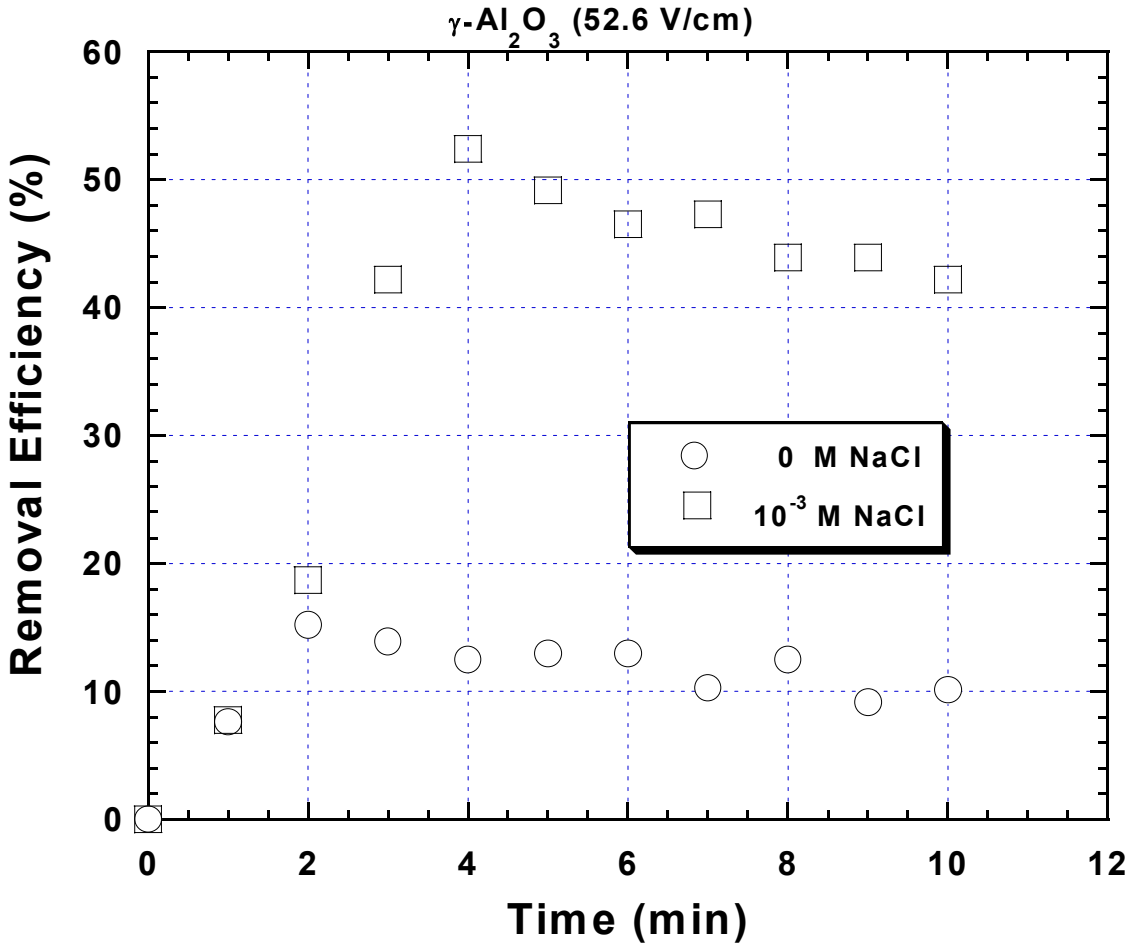

Figure 47. Removal efficiency as a function of time at various salt concentrations. Experimental condition: electrostatic field = 52.6 V/cm; pH = 5; Sample: γ-Al_2O_3

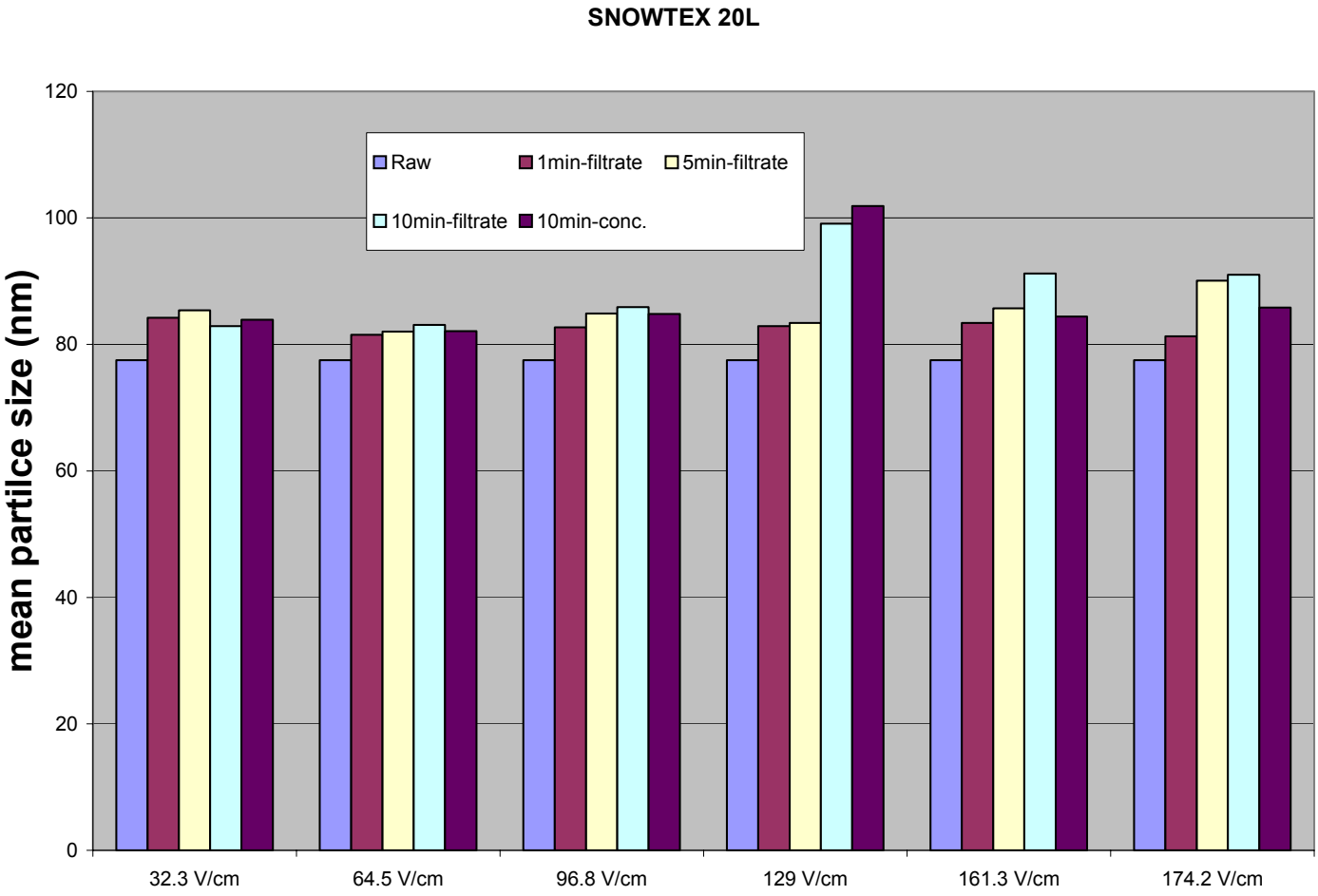

Figure 48. Distribution of particle size as affect by electrostatic field. Experimental condition: pH = 6.2; Sample: Ssnowtex 20L

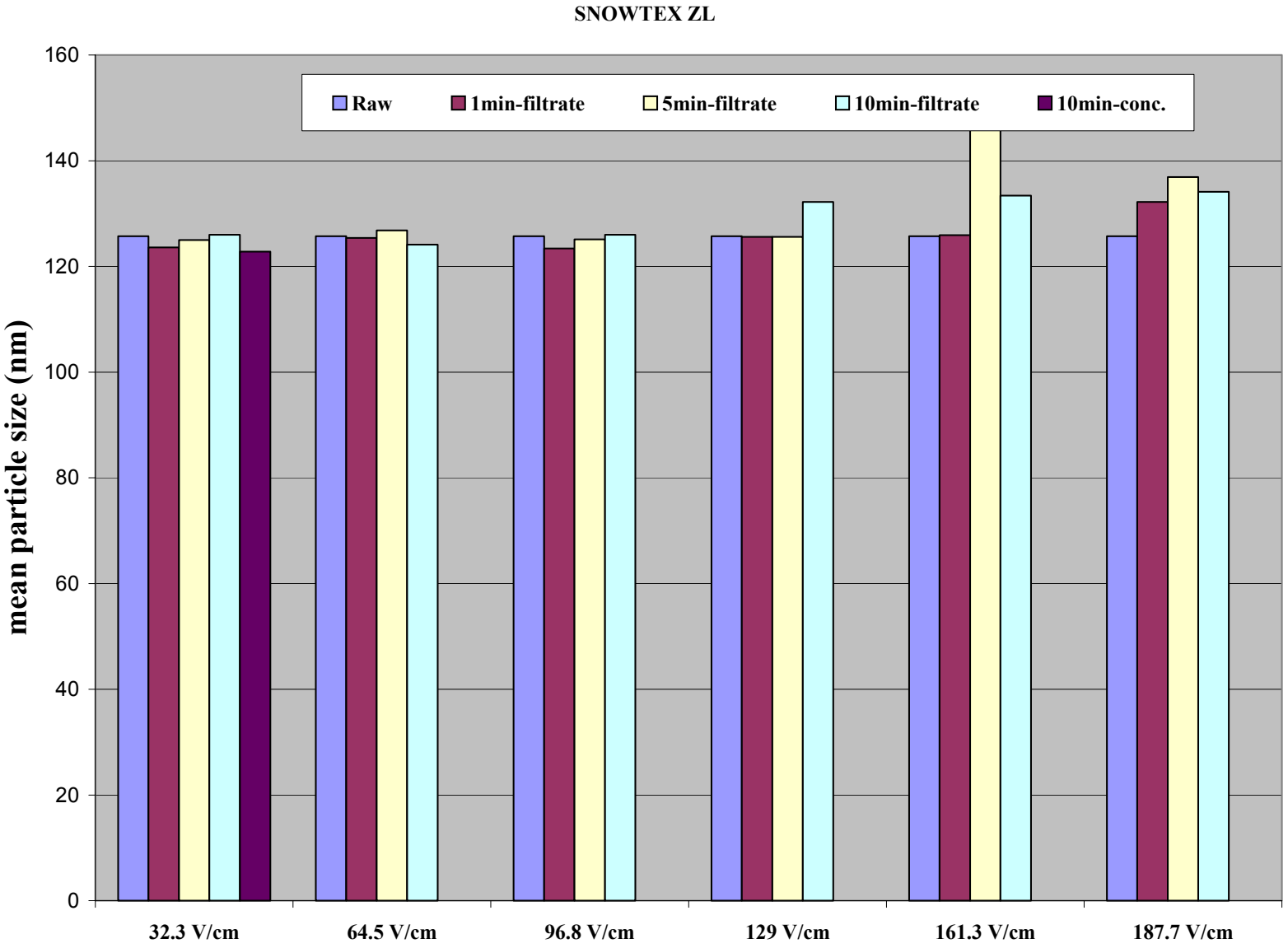

Figure 49. Distribution of particle size as affected by electrostatic field. Experimental condition: pH = 5; Sample: Snowtex ZL.

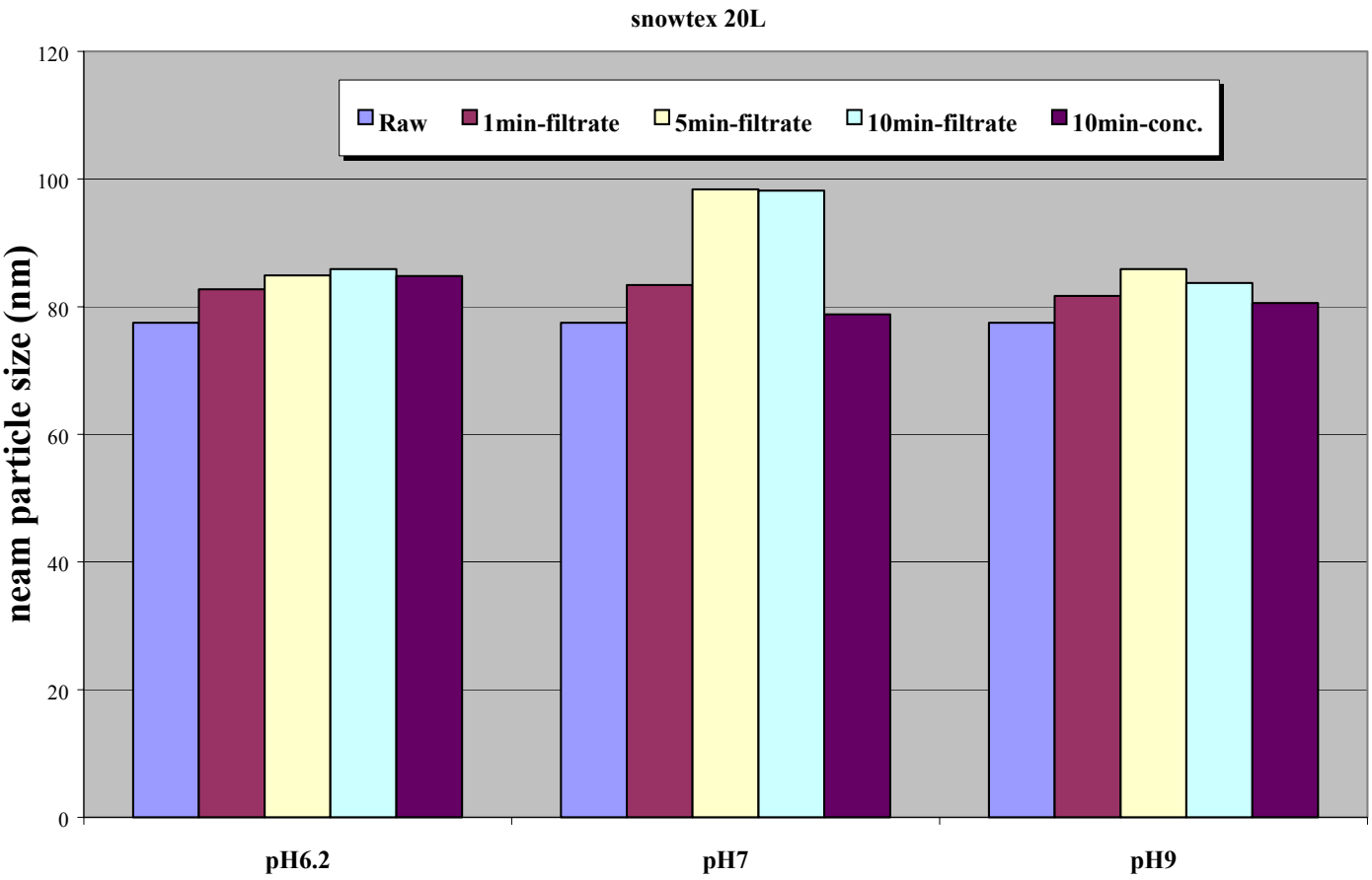

Figure 50. Distribution of particle size as affected by pH. Experimental condition: electrostatic field = 96.8 V/cm; Sample: Snowtex 20L

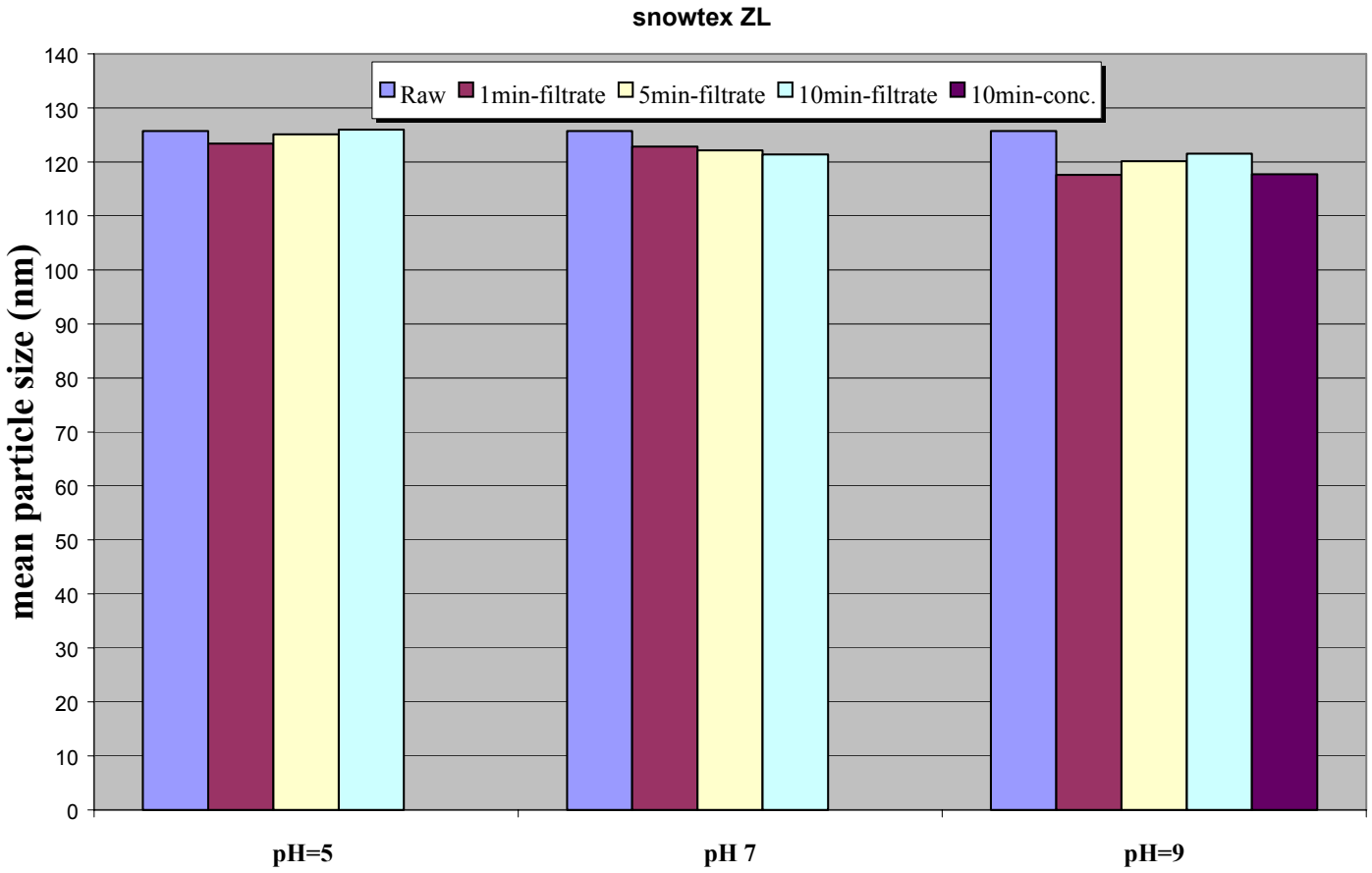

Figure 51. Distribution of particle size as affected by pH. Experimental condition: electrostatic field = 96.8 V/cm; Sample: Snowtex ZL.

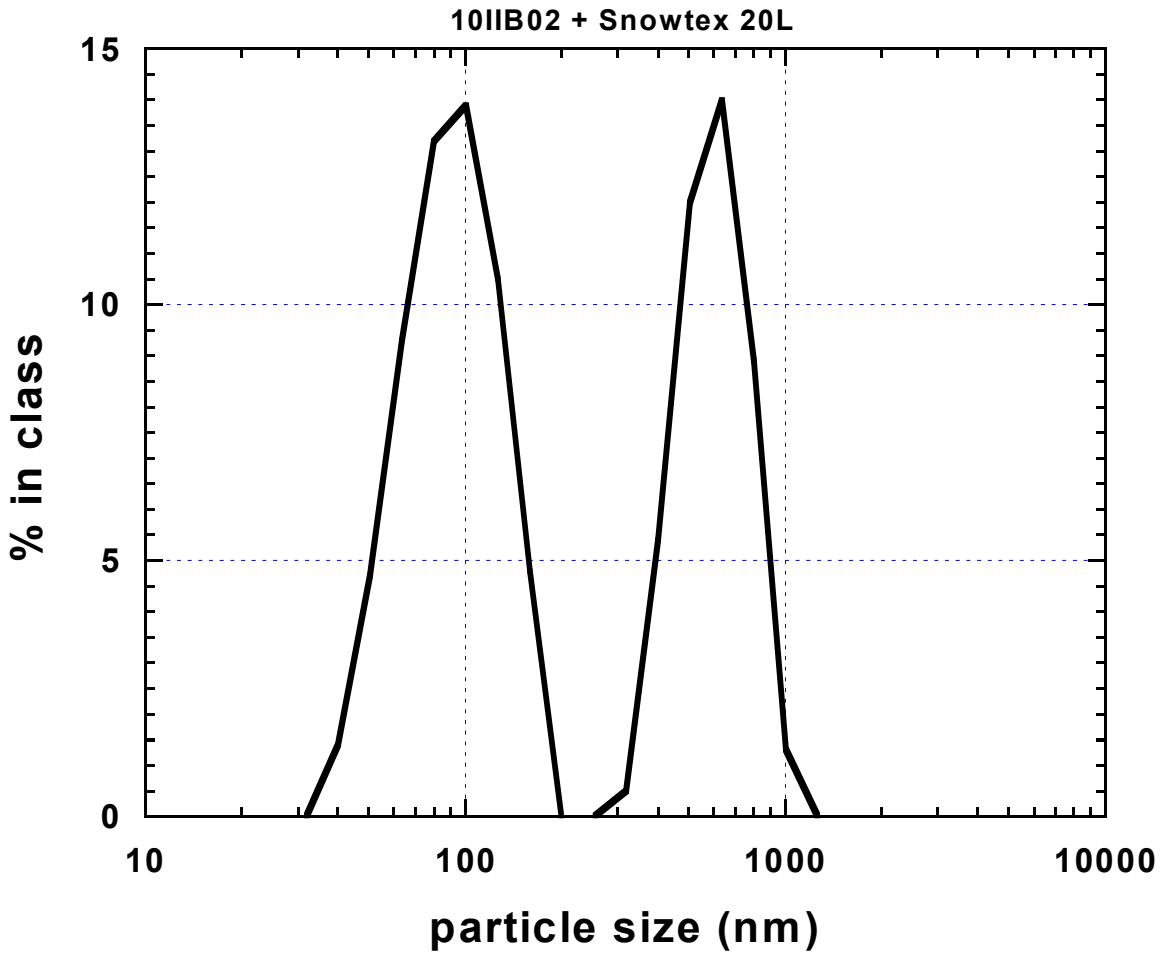

Figure 52. Bimodal distribution (10IIB02 + Snowtex 20L)

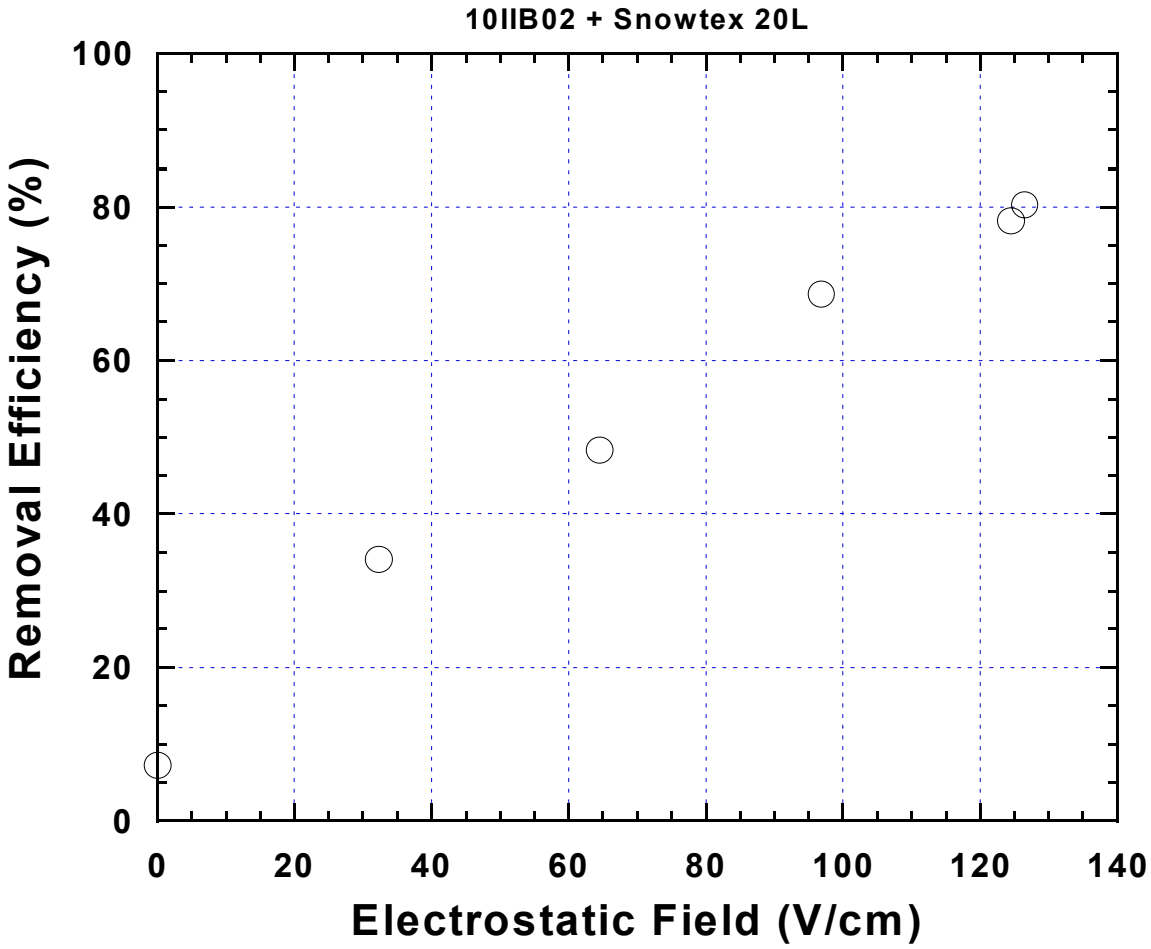

Figure 53. Effect of electrostatic field on removal of naturally occurring particle and colloidal silica. Experimental condition: 8.2; Sample: 10IIB02 + Snowtex 20L

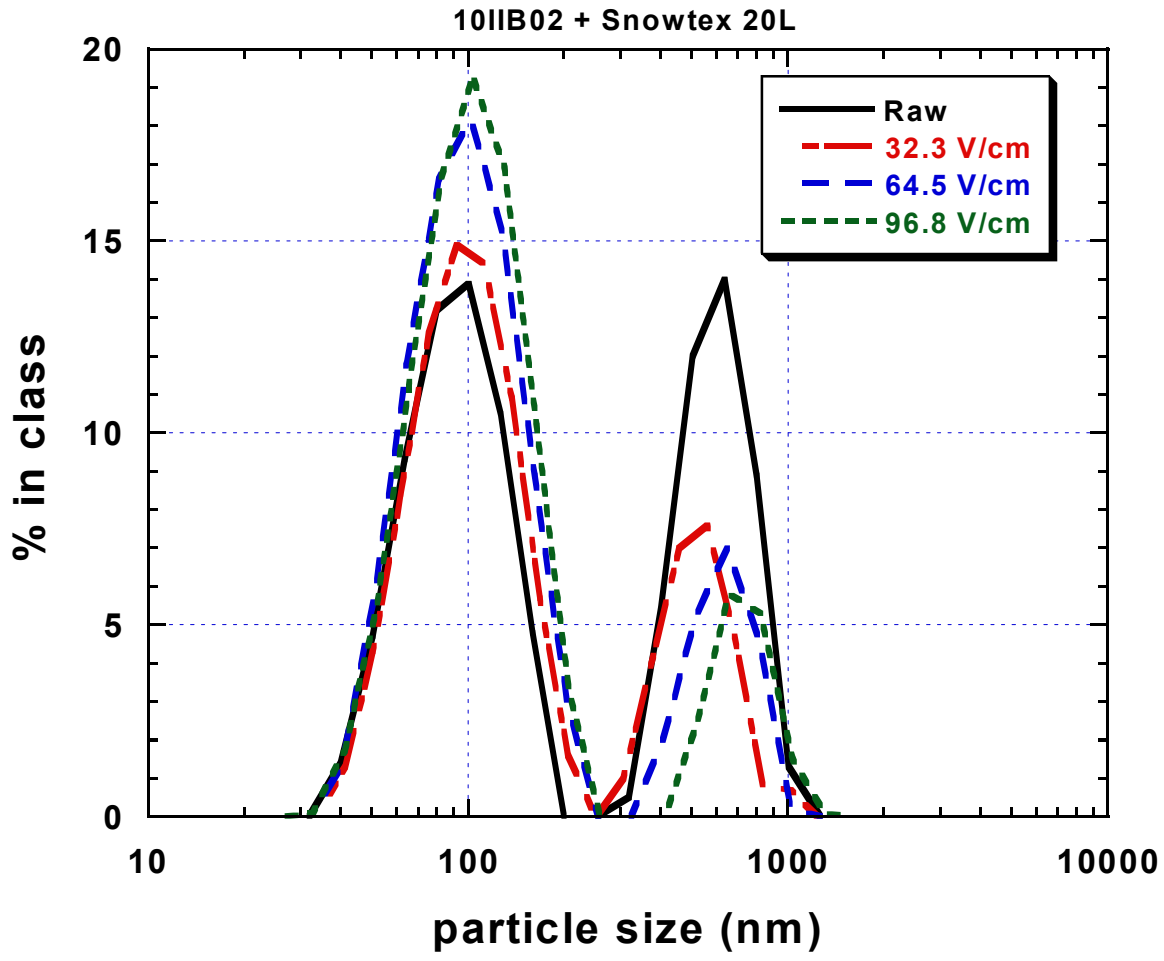

Figure 54. Distribution of particle size as affect by electrostatic field. Experimental condition: pH = 8.2; Sample: 10IIB02 + Snowtex 20L

Table A1. The effect of electrostatic field on the change of turbidity (Sample: 10IIB02)

Time (min)	Turbidity (NTU)			
	E = 00V/cm (V = 00)	E = 32.3 V/cm (V = 100)	E = 64.5 V/cm (V = 200)	E = 71.3 V/cm (V = 221)
0	206.6	206.6	206.6	206.6
1	200.0	196.0	177.0	189.0
2	196.0	143.0	113.0	141.0
3	191.0	127.0	97.4	104.0
4	193.0	131.0	96.4	83.6
5	193.0	130.0	104.0	72.9
6	193.0	133.0	103.0	69.2
7	193.0	135.0	96.4	69.6
8	195.0	137.0	95.7	72.4
9	196.0	139.0	95.5	73.0
10	195.0	142.0	94.4	74.4

Experimental conditions: initial total solid concentration = 0.26 g/L; pH = 6.8;
Sample: 10IIB02

Table A2. The effect of electrostatic field on the removal of colloidal silica (Sample: 10IIB02)

Time (min)	Removal Efficiency (%)			
	E = 00V/cm (V = 00)	E = 32.3 V/cm (V = 100)	E = 64.5 V/cm (V = 200)	E = 71.3 V/cm (V = 221)
0	0.0	0.0	0.0	0.0
1	3.2	5.1	14.3	8.5
2	5.1	30.8	45.3	31.8
3	7.6	38.5	52.9	49.7
4	6.6	36.6	53.3	59.5
5	6.6	37.1	49.7	64.7
6	6.6	35.6	50.1	66.5
7	6.6	34.7	53.3	66.3
8	5.6	33.7	53.7	65.0
9	5.1	32.7	53.8	64.7
10	5.6	31.3	54.3	64.0

Experimental conditions: initial total solid concentration = 0.26 g/L; pH = 6.8;
Sample: 10IIB02
Removal efficiency = $(T_0-T_i)/T_0*100\%$
T_0: Turbidity of filtrate at 0 minute
T_i: Turbidity of filtrate at i minute

Table A3. Effect of electrostatic field on the change of turbidity (Sample: 10IIB02)

Time (min)	Turbidity (NTU)				
	E = 00V/cm (V = 00)	E = 32.3 V/cm (V = 100)	E = 64.5 V/cm (V = 200)	E = 96.8 V/cm (V = 300)	E = 112.6 V/cm (V=349)
0	98.3	98.3	98.3	98.3	98.3
1	95.0	95.0	88.1	86.3	37.4
2	94.0	76.7	47.4	41.4	37.0
3	94.0	60.4	38.3	29.4	29.9
4	94.0	59.3	40.7	30.9	26.5
5	94.0	59.7	43.0	32.1	26.4
6	94.1	60.7	44.5	32.6	26.1
7	93.9	61.8	45.5	33.2	25.4
8	94.2	63.1	46.1	33.5	25.0
9	93.8	63.2	45.7	33.3	25.5
10	94.0	63.7	47.6	33.0	25.4

Experimental conditions: initial total solid concentration = 0.12 g/L; pH = 6.8; Sample: 10IIB02

Table A4. Effect of electrostatic field on the removal of colloidal silica (Sample: 10IIB02)

Time (min)	Removal Efficiency (%)				
	E = 00V/cm (V = 00)	E = 32.3 V/cm (V = 100)	E = 64.5 V/cm (V = 200)	E = 96.8 V/cm (V = 300)	E = 112.6 V/cm (V=349)
0	0.0	0.0	0.0	0.0	0.0
1	3.4	3.4	10.4	12.2	62.0
2	4.4	22.0	51.8	57.9	62.4
3	4.4	38.6	61.0	70.1	69.6
4	4.4	39.7	58.6	68.6	73.0
5	4.4	39.3	56.3	67.3	73.1
6	4.3	38.3	54.7	66.8	73.4
7	4.5	37.1	53.7	66.2	74.2
8	4.2	35.8	53.1	65.9	74.6
9	4.6	35.7	53.5	66.1	74.1
10	4.4	35.2	51.6	66.4	74.2

Experimental conditions: initial total solid concentration = 0.12 g/L; pH = 6.8; Sample: 10IIB02
Removal efficiency = $(T_0-T_i)/T_0*100\%$
T_0: Turbidity of filtrate at 0 minute
T_i: Turbidity of filtrate at i minute

Table A5. The effect of electrostatic field on the change of turbidity (Sample: 10IIL02)

Time (min)	Turbidity (NTU)		
	E = 00V/cm (V = 00)	E = 32.3 V/cm (V = 100)	E = 60.3 V/cm (V = 187)
0	31.3	31.3	31.3
1	30.8	30.4	25.7
2	30.5	28.3	18.2
3	30.3	20.8	13.5
4	30.3	16.3	11.2
5	30.1	16.3	11.3
6	29.9	17.3	11.3
7	30.1	17.9	11.5
8	30.5	18.4	11.5
9	30.8	18.6	11.6
10	30.7	19	11.4

Experimental conditions: initial total solid concentration = 0.13 g/L; pH = 7.1; Sample: 10IIL02

Table A6. The effect of electrostatic field on the removal of colloidal silica (Sample: 10IIL02)

Time (min)	Removal Efficiency (%)		
	E = 00V/cm (V = 00)	E = 32.3 V/cm (V = 100)	E = 60.3 V/cm (V = 187)
0	0.0	0.0	0.0
1	1.6	2.9	17.9
2	2.6	9.6	41.9
3	3.2	33.5	56.9
4	3.2	47.9	64.2
5	3.8	47.9	63.9
6	4.5	44.7	63.9
7	3.8	42.8	63.3
8	2.6	41.2	63.3
9	1.6	40.6	62.9
10	1.9	39.3	63.6

Experimental conditions: initial total solid concentration = 0.13 g/L; pH = 7.1; Sample: 10IIL02

Removal efficiency = $(T_0-T_i)/T_0*100\%$

T_0: Turbidity of filtrate at 0 minute

T_i: Turbidity of filtrate at i minute

Table A7. Effect of electrostatic field on the change of turbidity
(Sample: 10IIB02 + Snowtex 20L)

Time (min)	Turbidity (NTU)					
	E = 00V/cm (V = 00)	E = 32.3 V/cm (V = 100)	E = 64.5 V/cm (V = 200)	E = 96.8 V/cm (V = 300)	E = 124.5 V/cm (V=386)	E = 126.5 V/cm (V=392)
0	72.0	72.0	72.0	72.0	71.3	71.3
1	64.1	65.8	56.0	57.1	39.8	31.0
2	64.4	54.0	37.1	35.0	25.7	19.6
3	66.1	45.8	32.4	22.1	17.8	15.2
4	66.6	44.7	33.1	19.9	14.3	13.7
5	67.7	45.1	34.4	20.8	13.8	13.1
6	67.8	45.7	35.1	21.7	12.4	12.7
7	66.1	46.5	35.1	21.7	14.6	13.7
8	66.7	46.5	35.0	22.3	14.9	13.7
9	66.9	47.0	36.1	22.5	15.4	14.5
10	66.8	47.5	37.2	22.6	15.6	14.1

Experimental condition: pH = 8.2

Table A8. Effect of electrostatic field on the removal of colloidal silica
(Sample: 10IIB02 + Snowtex 20L)

Time (min)	Removal Efficiency (%)					
	E = 00V/cm (V = 00)	E = 32.3 V/cm (V = 100)	E = 64.5 V/cm (V = 200)	E = 96.8 V/cm (V = 300)	E = 124.5 V/cm (V=386)	E = 126.5 V/cm (V=392)
0	0.0	0.0	0.0	0.0	0.0	0.0
1	11.0	8.6	22.2	20.7	44.2	56.5
2	10.6	25.0	48.5	51.4	64.0	72.5
3	8.2	36.4	55.0	69.3	75.0	78.7
4	7.5	37.9	54.0	72.4	79.9	80.8
5	6.0	37.4	52.2	71.1	80.6	81.6
6	5.8	36.5	51.3	69.9	82.6	82.2
7	8.2	35.4	51.3	69.9	79.5	80.8
8	7.4	35.4	51.4	69.0	79.1	80.8
9	7.1	34.7	49.9	68.8	78.4	79.7
10	7.2	34.0	48.3	68.6	78.1	80.2

Experimental condition: pH = 8.2
Removal efficiency = $(T_0-T_i)/T_0*100\%$
T_0: Turbidity of filtrate at 0 minute
T_i: Turbidity of filtrate at i minute

Table A9. The effect of electrostatic field on the change of turbidity
(Sample: 5SIIIL01)

Time (min)	Turbidity (NTU)					
	E = 00V/cm (V = 00)	E = 32.3 V/cm (V = 100)	E = 64.5 V/cm (V = 200)	E = 96.8 V/cm (V = 300)	E = 119.7 V/cm (V = 371)	E = 123.9 V/cm (V = 384)
0	680	680	680	680	680	680
1	520	660	662	630	592	664
2	553	586	479	411	381	339
3	585	481	343	308	285	275
4	614	422	307	259	264	229
5	629	399	302	249	241	240
6	635	397	298	245	214	217
7	618	407	306	244	195	207
8	635	400	305	227	170	194
9	633	404	309	229	160	182
10	632	411	311	213	149	169

Experimental conditions: initial total solid concentration = 0.68 g/L; pH = 6.8; sample: 5SIIIL01

Table A10. The effect of electrostatic field on the removal efficiency (Sample: 5SIIIL01)

Time (min)	Removal Efficiency (%)					
	E = 00V/cm (V = 00)	E = 32.3 V/cm (V = 100)	E = 64.5 V/cm (V = 200)	E = 96.8 V/cm (V = 300)	E = 119.7 V/cm (V = 371)	E = 123.9 V/cm (V = 384)
0	0.0	0.0	0.0	0.0	0.0	0.0
1	23.5	2.9	2.6	7.4	12.9	2.4
2	18.7	13.8	29.6	39.6	44.0	50.1
3	14.0	29.3	49.6	54.7	58.1	59.6
4	9.7	37.9	54.9	61.9	61.2	66.3
5	7.5	41.3	55.6	63.4	64.6	64.7
6	6.6	41.6	56.2	64.0	68.5	68.1
7	9.1	40.1	55.0	64.1	71.3	69.6
8	6.6	41.2	55.1	66.6	75.0	71.5
9	6.9	40.6	54.6	66.3	76.5	73.2
10	7.1	39.6	54.3	68.7	78.1	75.1

Experimental conditions: initial total solid concentration = 0.68 g/L; pH = 6.8; sample: 5SIIIL01

Removal efficiency = $(T_0-T_i)/T_0*100\%$

T_0: Turbidity of filtrate at 0 minute

T_i: Turbidity of filtrate at the ith minute

Table A11. Effect of electrostatic field on the change of turbidity
(Sample: 5SIIIL01)

Time (min)	Turbidity (NTU)					
	E = 00V/cm (V = 00)	E = 32.3 V/cm (V = 100)	E = 64.5 V/cm (V = 200)	E = 96.8 V/cm (V = 300)	E = 129.0 V/cm (V = 400)	E = 137.1 V/cm (V = 425)
0	422	422	422	422	422	422
1	342	384	372	363	343	322
2	392	325	250	223	195	173
3	378	272	190	166	134	125
4	377	261	190	128	101	103
5	374	264	198	129	108	107
6	376	264	205	135	111	106
7	373	261	200	140	101	93
8	377	269	206	144	94	79
9	379	264	206	144	83	73
10	391	267	207	141	75	69

Experimental conditions: initial total solid concentration = 0.43 g/L; pH = 6.6; sample: 5SIIIL01

Table A12. Effect of electrostatic field on the removal efficiency
(Sample: 5SIIIL01)

Time (min)	Removal Efficiency (%)					
	E = 00V/cm (V = 00)	E = 32.3 V/cm (V = 100)	E = 64.5 V/cm (V = 200)	E = 96.8 V/cm (V = 300)	E = 129.0 V/cm (V = 400)	E = 137.1 V/cm (V = 425)
0	0.0	0.0	0.0	0.0	0.0	0.0
1	19.0	9.0	11.8	14.0	18.7	23.7
2	7.1	23.0	40.8	47.2	53.8	59.0
3	10.4	35.5	55.0	60.7	68.2	70.4
4	10.7	38.2	55.0	69.7	76.1	75.6
5	11.4	37.4	53.1	69.4	74.4	74.6
6	10.9	37.4	51.4	68.0	73.7	74.9
7	11.6	38.2	52.6	66.8	76.1	78.1
8	10.7	36.3	51.2	65.9	77.7	81.3
9	10.2	37.4	51.2	65.9	80.4	82.8
10	7.3	36.7	50.9	66.6	82.3	83.6

Experimental conditions: initial total solid concentration = 0.43 g/L; pH = 6.6; sample: 5SIIIL01
Removal efficiency = (T0-Ti)/T0*100%
T0: Turbidity of filtrate at 0 minute
Ti: Turbidity of filtrate at the ith minute

Table A13. The effect of electrostatic field on the change of turbidity (Sample: 5SIIIB02)

Time (min)	Turbidity (NTU)					
	E = 00V/cm (V = 00)	E = 32.3 V/cm (V = 100)	E = 64.5 V/cm (V = 200)	E = 96.8 V/cm (V = 300)	E = 129.0 V/cm (V = 400)	E = 138.7 V/cm (V = 430)
0	750	750	750	750	750	750
1	714	695	650	647	618	511
2	723	687	466	399	366	291
3	707	597	358	292	263	194
4	684	501	351	250	195	160
5	692	466	355	261	171	147
6	693	473	357	257	174	148
7	689	476	363	273	182	154
8	704	476	374	271	167	149
9	701	481	372	280	159	134
10	703	495	389	272	154	139

Experimental conditions: initial total solid concentration = 0.52 g/L; pH = 6.8; sample: 5SIIIB02

Table A14. The effect of electrostatic field on the removal efficiency (Sample: 5SIIIB02)

Time (min)	Removal Efficiency (%)					
	E = 00V/cm (V = 00)	E = 32.3 V/cm (V = 100)	E = 64.5 V/cm (V = 200)	E = 96.8 V/cm (V = 300)	E = 129.0 V/cm (V = 400)	E = 138.7 V/cm (V = 430)
0	0.0	0.0	0.0	0.0	0.0	0.0
1	4.8	7.3	13.3	13.7	17.6	31.9
2	3.6	8.4	37.9	46.8	51.2	61.2
3	5.7	20.4	52.3	61.1	64.9	74.1
4	8.8	33.2	53.2	66.7	74.0	78.7
5	7.7	37.9	52.7	65.2	77.2	80.4
6	7.6	36.9	52.4	65.7	76.8	80.3
7	8.1	36.5	51.6	63.6	75.7	79.5
8	6.1	36.5	50.1	63.9	77.7	80.1
9	6.5	35.9	50.4	62.7	78.8	82.1
10	6.3	34.0	48.1	63.7	79.5	81.5

Experimental conditions: initial total solid concentration = 0.52 g/L; pH = 6.8; sample: 5SIIIB02
Removal efficiency = (T0-Ti)/T0*100%
T0: Turbidity of filtrate at 0 minute
Ti: Turbidity of filtrate at the ith minute

Table A15. Effect of electrostatic field on the change of turbidity (Sample: 5SIIIB02)

Time (min)	Turbidity (NTU)					
	E = 00V/cm (V = 00)	E = 32.3 V/cm (V = 100)	E = 64.5 V/cm (V = 200)	E = 96.8 V/cm (V = 300)	E = 129.0 V/cm (V = 400)	E = 152.9 V/cm (V = 474)
0	390	390	390	390	390	390
1	350	389	362	356	349	307
2	370	346	261	226	205	152
3	363	289	192	153	125	105
4	347	261	182	127	84.9	72.8
5	363	253	187	127	79.6	60.7
6	351	258	189	132	81.1	60
7	349	265	192	134	86.1	63
8	348	269	198	137	82.6	61.5
9	358	276	200	135	83.6	54.4
10	351	274	204	142	77.6	50.4

Experimental conditions: initial total solid concentration = 0.27 g/L; pH = 6.6; sample: 5SIIIB02

Table A16. Effect of electrostatic field on the removal efficiency (Sample: 5SIIIB02)

Time (min)	Removal Efficiency (%)					
	E = 00V/cm (V = 00)	E = 32.3 V/cm (V = 100)	E = 64.5 V/cm (V = 200)	E = 96.8 V/cm (V = 300)	E = 129.0 V/cm (V = 400)	E = 152.9 V/cm (V = 474)
0	0.0	0.0	0.0	0.0	0.0	0.0
1	10.3	0.3	7.2	8.7	10.5	21.3
2	5.1	11.3	33.1	42.1	47.4	61.0
3	6.9	25.9	50.8	60.8	67.9	73.1
4	11.0	33.1	53.3	67.4	78.2	81.3
5	6.9	35.1	52.1	67.4	79.6	84.4
6	10.0	33.8	51.5	66.2	79.2	84.6
7	10.5	32.1	50.8	65.6	77.9	83.8
8	10.8	31.0	49.2	64.9	78.8	84.2
9	8.2	29.2	48.7	65.4	78.6	86.1
10	10.0	29.7	47.7	63.6	80.1	87.1

Experimental conditions: initial total solid concentration = 0.27 g/L; pH = 6.6; sample: 5SIIIB02

Removal efficiency = $(T_0-T_i)/T_0*100\%$

T_0: Turbidity of filtrate at 0 minute

T_i: Turbidity of filtrate at the ith minute

Table A17. Effect of electrostatic field on the change of turbidity (Sample: 5SIIIH02)

Time (min)	Turbidity (NTU)				
	E = 00V/cm (V = 00)	E = 32.3 V/cm (V = 100)	E = 64.5 V/cm (V = 200)	E = 96.8 V/cm (V = 300)	E = 117.7 V/cm (V = 365)
0	720	720	720	720	720
1	657	676	675	637	583
2	688	542	492	420	384
3	664	459	345	296	278
4	681	452	323	263	237
5	672	472	336	259	217
6	665	486	364	278	228
7	679	495	364	285	226
8	674	494	370	288	220
9	668	499	380	291	225
10	693	506	380	291	219

Experimental conditions: initial total solid concentration = 0.44 g/L; pH = 7.1; sample: 5SIIIH02

Table A18. Effect of electrostatic field on the removal efficiency (Sample: 5SIIIH02)

Time (min)	Removal Efficiency (%)				
	E = 00V/cm (V = 00)	E = 32.3 V/cm (V = 100)	E = 64.5 V/cm (V = 200)	E = 96.8 V/cm (V = 300)	E = 117.7 V/cm (V = 365)
0	0.0	0.0	0.0	0.0	0.0
1	8.8	6.1	6.3	11.5	19.0
2	4.4	24.7	31.7	41.7	46.7
3	7.8	36.3	52.1	58.9	61.4
4	5.4	37.2	55.1	63.5	67.1
5	6.7	34.4	53.3	64.0	69.9
6	7.6	32.5	49.4	61.4	68.3
7	5.7	31.3	49.4	60.4	68.6
8	6.4	31.4	48.6	60.0	69.4
9	7.2	30.7	47.2	59.6	68.8
10	3.8	29.7	47.2	59.6	69.6

Experimental conditions: initial total solid concentration = 0.44 g/L; pH = 7.1; sample: 5SIIIH02

Removal efficiency = $(T_0-T_i)/T_0*100\%$

T_0: Turbidity of filtrate at 0 minute

T_i: Turbidity of filtrate at the ith minute

Table A19. Effect of electrostatic field on the change of turbidity (Sample: 5SIIIH02)

Time (min)	Turbidity (NTU)					
	E = 00V/cm (V = 00)	E = 32.3 V/cm (V = 100)	E = 64.5 V/cm (V = 200)	E = 96.8 V/cm (V = 300)	E = 129.0 V/cm (V = 400)	E = 142.6 V/cm (V = 442)
0	285	285	285	285	285	285
1	285	257	275	217	241	238
2	284	234	183	213	150	143
3	269	194	133	116	109	90.1
4	268	172	117	88	68	66
5	271	169	115	93	61	56
6	269	171	120	98	63	56
7	266	175	121	107	70	58
8	262	180	126	112	70	62
9	267	179	125	117	72	59
10	267	181	126	112	72	57

Experimental conditions: initial total solid concentration = 0.18 g/L; pH = 6.8; sample: 5SIIIH02

Table A20. Effect of electrostatic field on the removal efficiency
(Sample: 5SIIIH02)

Time (min)	Removal Efficiency (%)					
	E = 00V/cm (V = 00)	E = 32.3 V/cm (V = 100)	E = 64.5 V/cm (V = 200)	E = 96.8 V/cm (V = 300)	E = 129.0 V/cm (V = 400)	E = 142.6 V/cm (V = 442)
0	0.0	0.0	0.0	0.0	0.0	0.0
1	0.0	9.8	3.5	23.9	15.4	16.5
2	0.4	17.9	35.8	25.3	47.4	49.8
3	5.6	31.9	53.3	59.3	61.8	68.4
4	6.0	39.6	58.9	69.1	76.0	76.8
5	4.9	40.7	59.6	67.4	78.8	80.3
6	5.6	40.0	57.9	65.7	77.9	80.3
7	6.7	38.6	57.5	62.5	75.6	79.6
8	8.1	36.8	55.8	60.7	75.6	78.4
9	6.3	37.2	56.1	58.9	74.8	79.4
10	6.3	36.5	55.8	60.7	74.8	80.1

Experimental conditions: initial total solid concentration = 0.18 g/L; pH = 6.8; sample: 5SIIIH02
Removal efficiency = $(T_0-T_i)/T_0*100\%$
T_0: Turbidity of filtrate at 0 minute
T_i: Turbidity of filtrate at the ith minute

Table A21. The effect of electrostatic field on the change of turbidity
(Sample: SNOWTEX 20L)

Time (min)	Turbidity (NTU)						
	E = 00V/cm (V = 00)	E = 32.3 V/cm (V = 100)	E = 64.5 V/cm (V = 200)	E = 96.8 V/cm (V = 300)	E = 129.0 V/cm (V=400)	E = 161.3 V/cm (V = 500)	E = 174.2 V/cm (v = 540)
0	35.3	35.3	35.3	35.3	35.3	35.3	35.3
1	33.8	30.8	30.6	26.8	24.2	17.0	15.2
2	34.6	29.2	23.7	20.4	18.0	13.1	10.6
3	34.7	27.9	18.1	12.8	9.8	6.6	6.4
4	34.4	28.0	16.4	9.0	6.1	4.9	4.8
5	34.5	27.9	16.5	8.2	4.5	3.7	3.6
6	32.8	28.0	16.7	8.1	3.8	2.0	3.0
7	33.5	28.3	18.3	8.8	2.8	1.8	2.5
8	34.5	28.2	18.5	9.7	2.7	2.1	2.2
9	34.4	28.1	19.1	9.5	2.4	1.5	1.8
10	34.6	28.1	19.3	10.1	2.3	1.7	1.6

Experimental conditions: pH = 6.2

Table A22. The effect of electrostatic field on the removal of colloidal silica (Sample: SNOWTEX 20L)

Time (min)	Removal Efficiency (%)						
	E = 00V/cm (V = 00)	E = 32.3 V/cm (V = 100)	E = 64.5 V/cm (V = 200)	E = 96.8 V/cm (V = 300)	E = 129.0 V/cm (V=400)	E = 161.3 V/cm (V = 500)	E = 174.2 V/cm (v = 540)
0	0.0	0.0	0.0	0.0	0.0	0.0	0.0
1	4.2	12.7	13.3	24.1	31.4	51.8	56.9
2	2.0	17.3	32.9	42.2	49.0	62.9	70.0
3	1.7	21.0	48.7	63.7	72.4	81.2	81.8
4	2.5	20.7	53.5	74.6	82.8	86.2	86.4
5	2.3	21.0	53.3	76.7	87.3	89.5	89.9
6	7.1	20.7	52.7	76.9	89.1	94.2	91.6
7	5.1	19.8	48.2	75.2	92.0	94.9	92.9
8	2.3	20.1	47.6	72.7	92.3	94.0	93.7
9	2.5	20.4	45.9	73.0	93.3	95.9	95.0
10	2.0	20.4	45.3	71.4	93.5	95.1	95.4

Experimental condition: pH = 6.2

Removal efficiency = $(T_0-T_i)/T_0*100\%$

T_0: Turbidity of filtrate at 0 minute

T_i: Turbidity of filtrate at i minute

Table A23. Effect of electrostatic field on the change of turbidity
(Sample: SNOWTEX ZL)

Time (min)	Turbidity (NTU)						
	E = 00V/cm (V = 00)	E = 32.3 V/cm (V = 100)	E = 64.5 V/cm (V = 200)	E = 96.8 V/cm (V = 300)	E = 129.0 V/cm (V=400)	E = 161.3 V/cm (V = 500)	E = 187.7 V/cm (v = 582)
0	58.0	58.0	58.0	58.0	58.0	58.0	58.0
1	51.9	55.6	51.8	50.8	50.0	42.2	20.6
2	52.0	51.0	39.0	34.6	36.7	27.4	12.5
3	52.1	48.1	29.1	18.8	19.9	14.2	6.2
4	54.4	48.1	26.5	11.9	12.7	8.1	3.7
5	55.0	48.2	26.3	8.6	9.0	4.8	2.6
6	55.9	48.1	22.0	7.8	6.8	3.5	2.2
7	55.9	47.2	19.5	8.7	6.0	2.9	2.0
8	57.1	46.0	20.1	10.9	5.1	2.6	1.6
9	56.6	46.1	21.7	14.0	4.3	2.1	1.4
10	56.4	45.9	23.1	17.7	4.0	1.9	1.4

Experimental condition: pH = 5

Table A24. Effect of electrostatic field on the removal of colloidal silica (Sample: SNOWTEX ZL)

Time (min)	Removal Efficiency (%)						
	E = 00V/cm (V = 00)	E = 32.3 V/cm (V = 100)	E = 64.5 V/cm (V = 200)	E = 96.8 V/cm (V = 300)	E = 129.0 V/cm (V=400)	E = 161.3 V/cm (V = 500)	E = 187.7 V/cm (v = 582)
0	0.0	0.0	0.0	0.0	0.0	0.0	0.0
1	10.5	4.1	10.7	12.4	13.8	27.2	64.5
2	10.3	12.1	32.8	40.3	36.7	52.8	78.4
3	10.2	17.1	49.8	67.6	65.7	75.5	89.3
4	6.2	17.1	54.3	79.5	78.1	86.1	93.6
5	5.2	16.9	54.7	85.2	84.5	91.8	95.5
6	3.6	17.1	62.1	86.6	88.3	94.1	96.2
7	3.6	18.6	66.4	84.9	89.7	95.1	96.5
8	1.6	20.7	65.3	81.2	91.3	95.5	97.3
9	2.4	20.5	62.6	75.9	92.5	96.4	97.5
10	2.8	20.9	60.2	69.5	93.1	96.8	97.6

Experimental condition: pH = 5

Removal efficiency = $(T_0-T_i)/T_0*100\%$

T_0: Turbidity of filtrate at 0 minute

T_i: Turbidity of filtrate at i minute

Table A25. The effect of pH on the change of turbidity
(Sample: SNOWTEX 20L)

Time (min)	Turbidity (NTU)		
	pH = 6.2	pH = 7	pH = 9
0	35.3	35.3	35.3
1	26.8	19.0	27.4
2	20.4	12.6	21.7
3	12.8	9.7	15.9
4	9.0	7.8	11.4
5	8.2	6.5	9.5
6	8.1	5.2	8.7
7	8.8	4.9	9.3
8	9.7	5.1	9.7
9	9.5	4.8	10.0
10	10.1	4.4	10.9

Table A26. The effect of pH on the removal efficiency
(Sample: SNOWTEX 20L)

Time (min)	Removal Efficiency (%)		
	pH = 6.2	pH = 7	pH = 9
0	0.0	0.0	0.0
1	24.1	46.2	22.4
2	42.2	64.3	38.5
3	63.7	72.6	55.0
4	74.6	77.9	67.7
5	76.7	81.5	73.2
6	76.9	85.3	75.5
7	75.2	86.0	73.7
8	72.7	85.6	72.5
9	73.0	86.3	71.7
10	71.4	87.5	69.1

Table A27. The effect of pH on the change of turbidity
(Sample: SNOWTEX ZL)

Time (min)	Turbidity (NTU)		
	pH = 5	pH = 7	pH = 9
0	58.0	58.0	58.0
1	50.8	47.7	52.5
2	34.6	40.5	38.6
3	18.8	28.4	31.2
4	11.9	18.6	27.8
5	8.6	15.4	22.8
6	7.8	17.1	20.5
7	8.7	21.1	20.1
8	10.9	25.1	20.7
9	14.0	27.2	22.6
10	17.7	28.9	24.3

Table A28. The effect of pH on the removal efficiency
(Sample: SNOWTEX ZL)

Time (min)	Turbidity (NTU)		
	pH = 5	pH = 7	pH = 9
0	0.0	0.0	0.0
1	12.4	17.8	9.5
2	40.3	30.2	33.4
3	67.6	51.0	46.2
4	79.5	67.9	52.1
5	85.2	73.4	60.7
6	86.6	70.5	64.7
7	84.9	63.6	65.3
8	81.2	56.7	64.3
9	75.9	53.1	61.0
10	69.5	50.2	58.1

Figure A1. Field trip for groundwater sampling (well #5S)

Figure A2. Setup for on-site water quality monitoring

Figure A3. Low flow purging sampling pumping system.

Figure A4. The controller of low flow purging pump system.

Figure A5. Bailer.

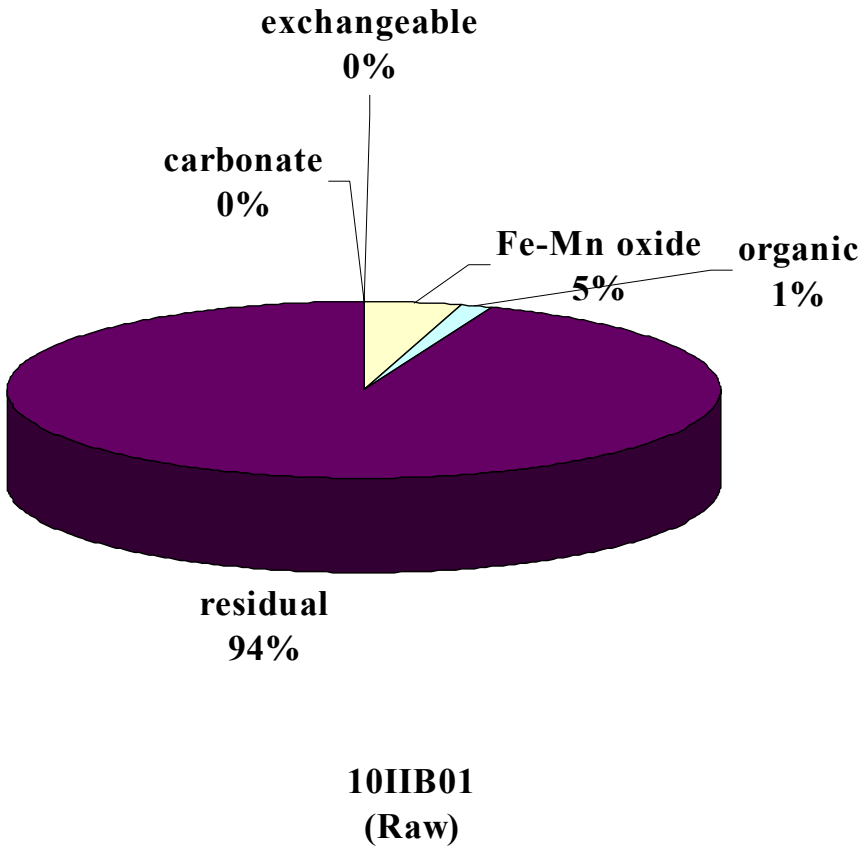

Figure A6. Distribution of lead species in particulate collected from well sample 10IIB01

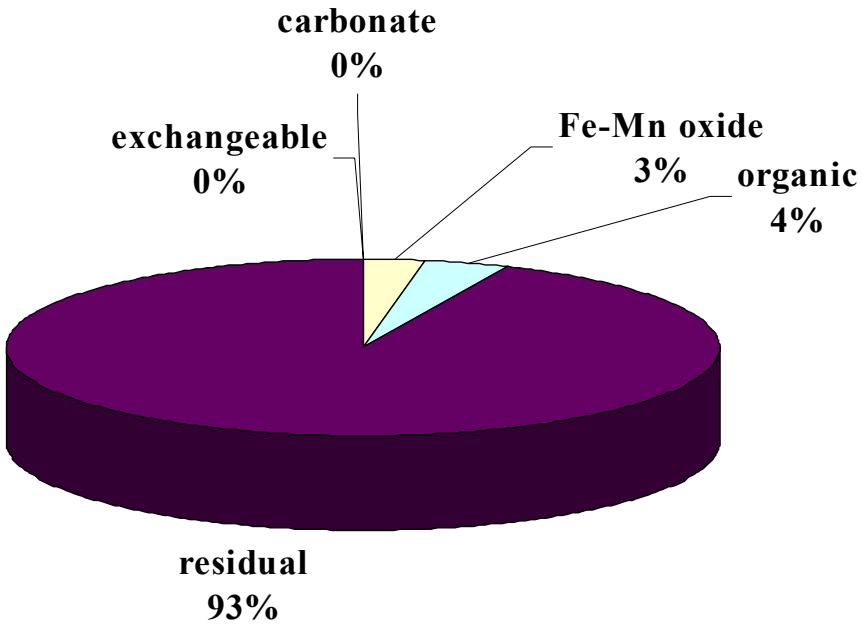

Figure A7. Distribution of lead species in particulate collected from well sample 10IIB02

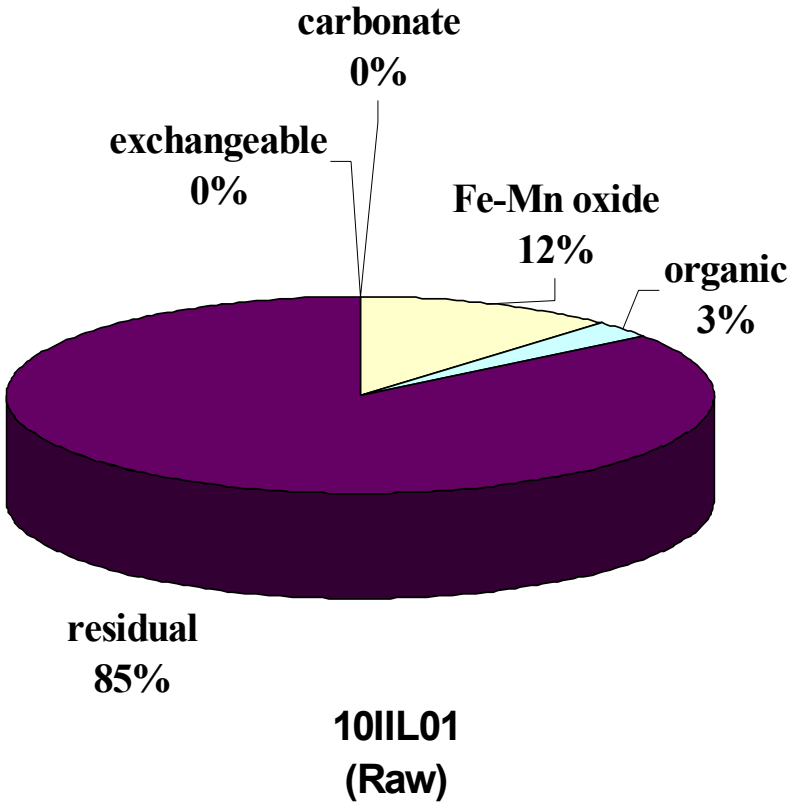

Figure A8. Distribution of lead species in particulate collected from well sample 10IIL01

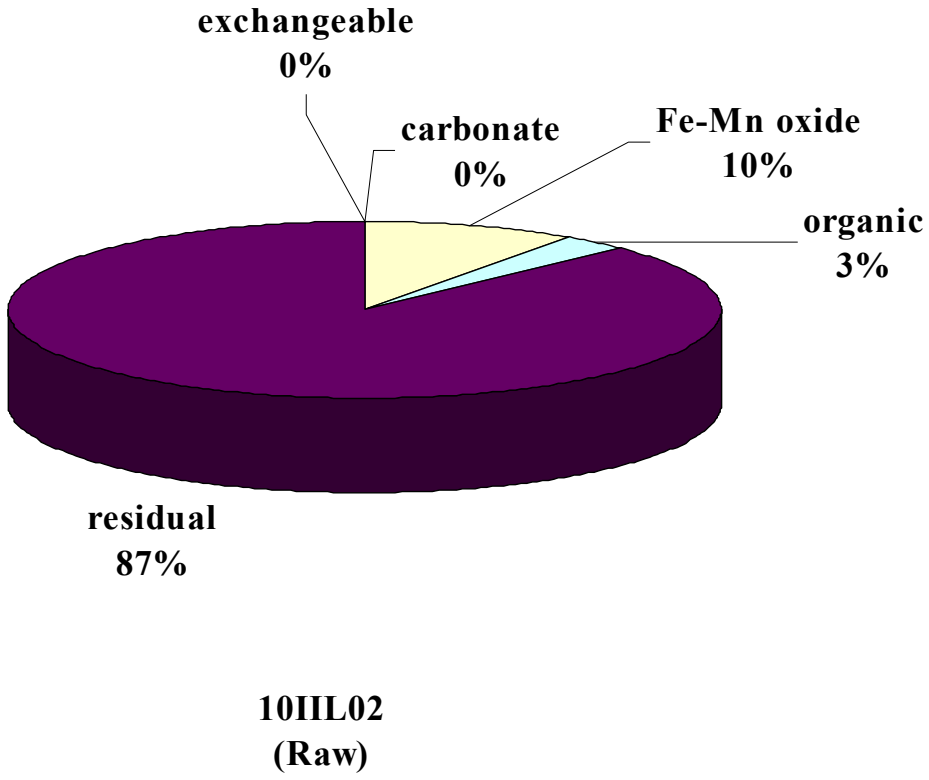

Figure A9. Distribution of lead species in particulate collected from well sample

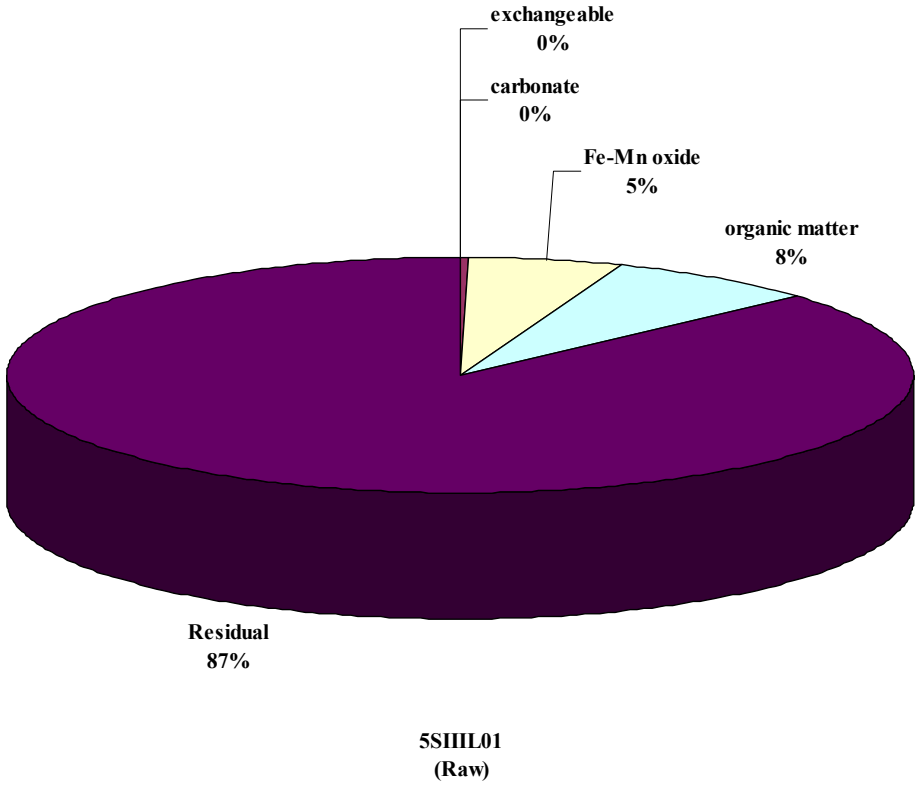

Figure A10. Distribution of lead species in particulate collected from well sample 5SIIIL01

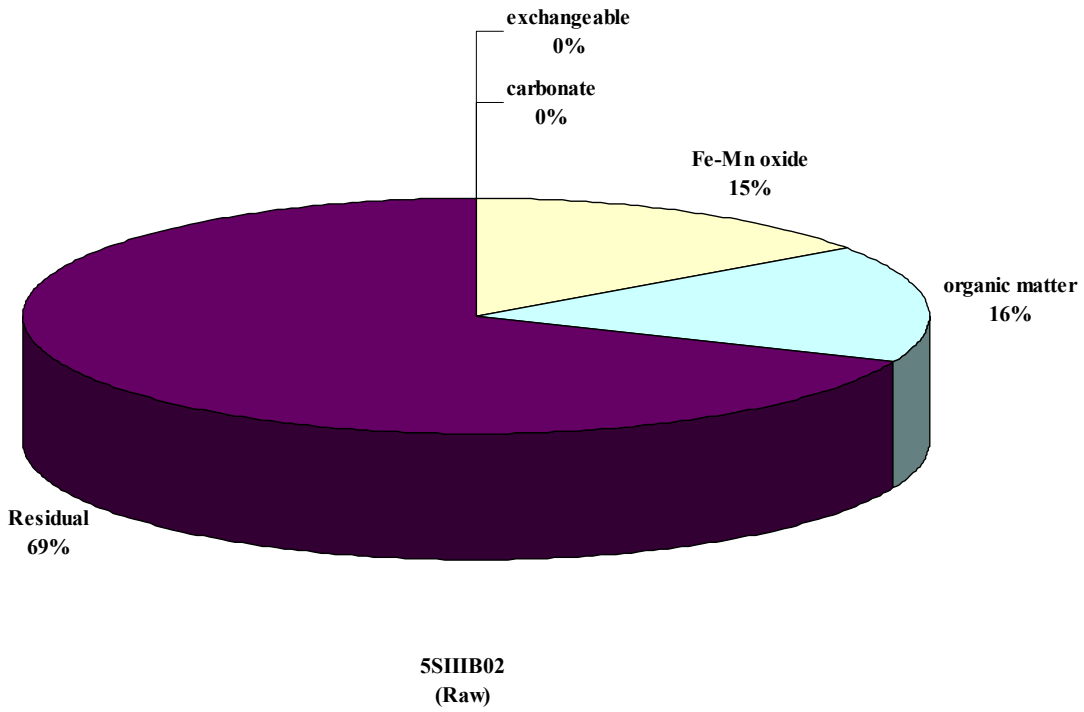

Figure A11. Distribution of lead species in particulate collected from well sample 5SIIIB02

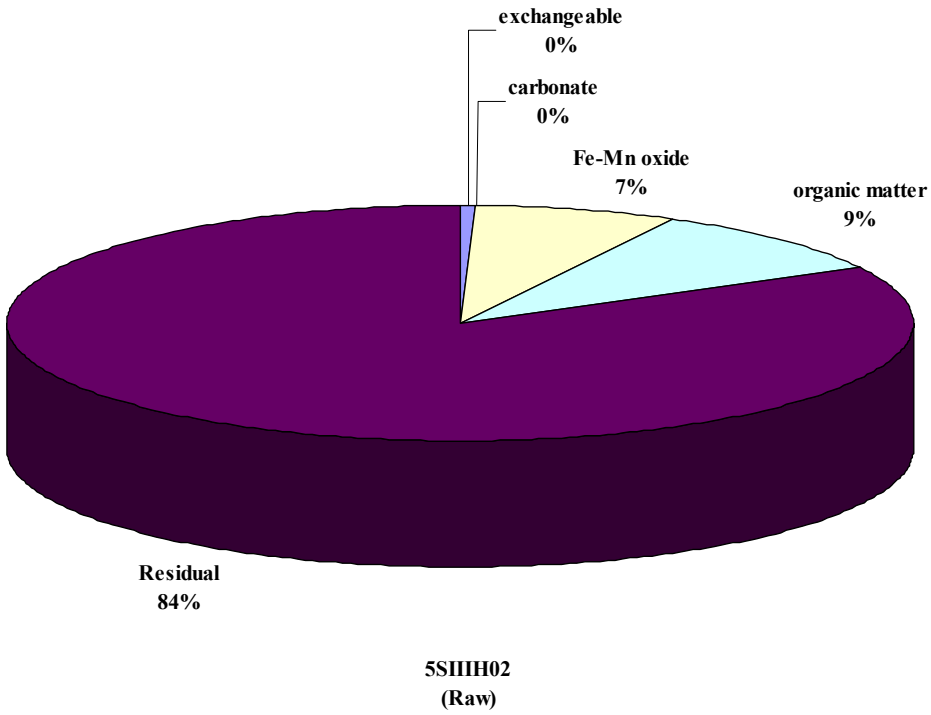

Figure A12. Distribution of lead species in particulate collected from well sample 5SIIIH02

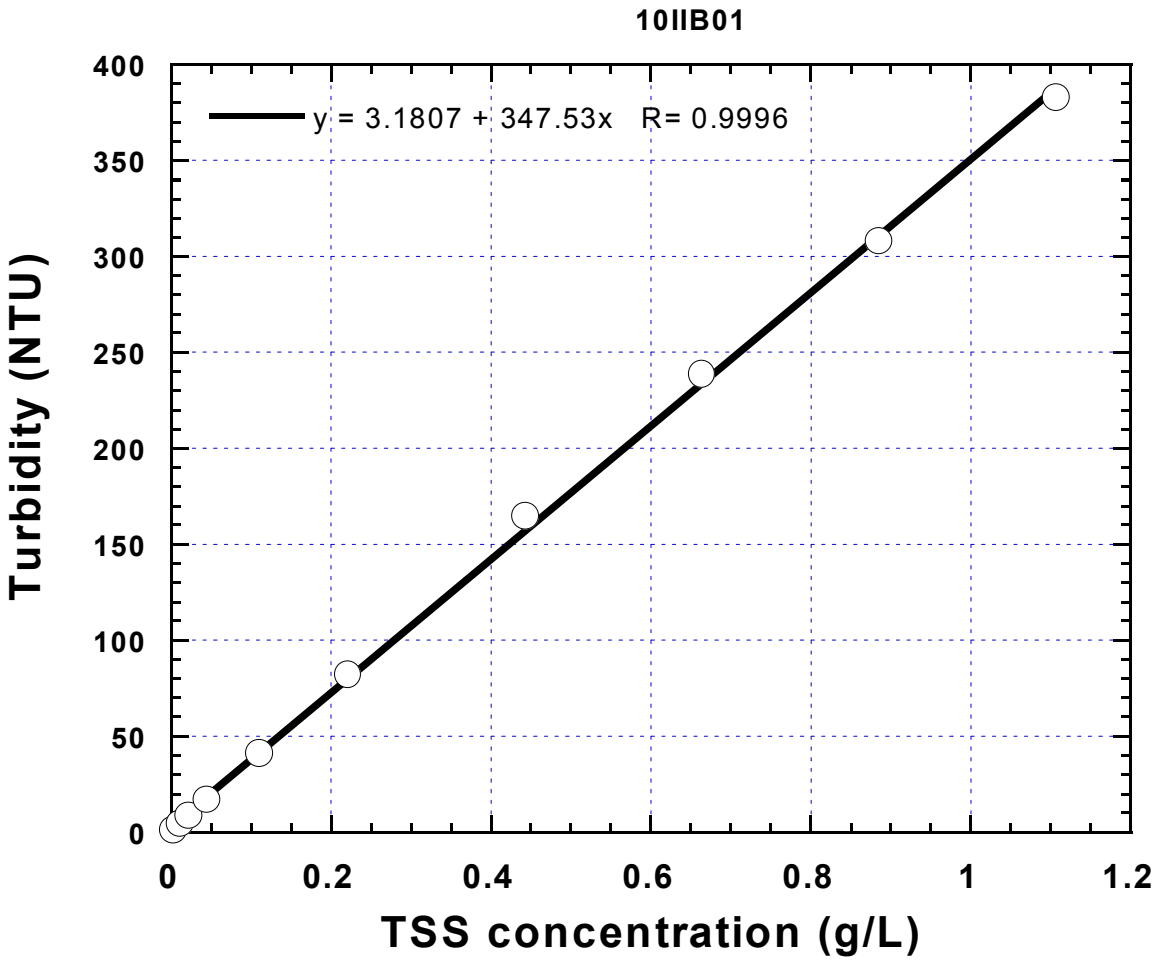

Figure A13. Calibration curve for turbidity (NTU) and particulate concentration of well water (well #10, bailing sample, 10IIB01)

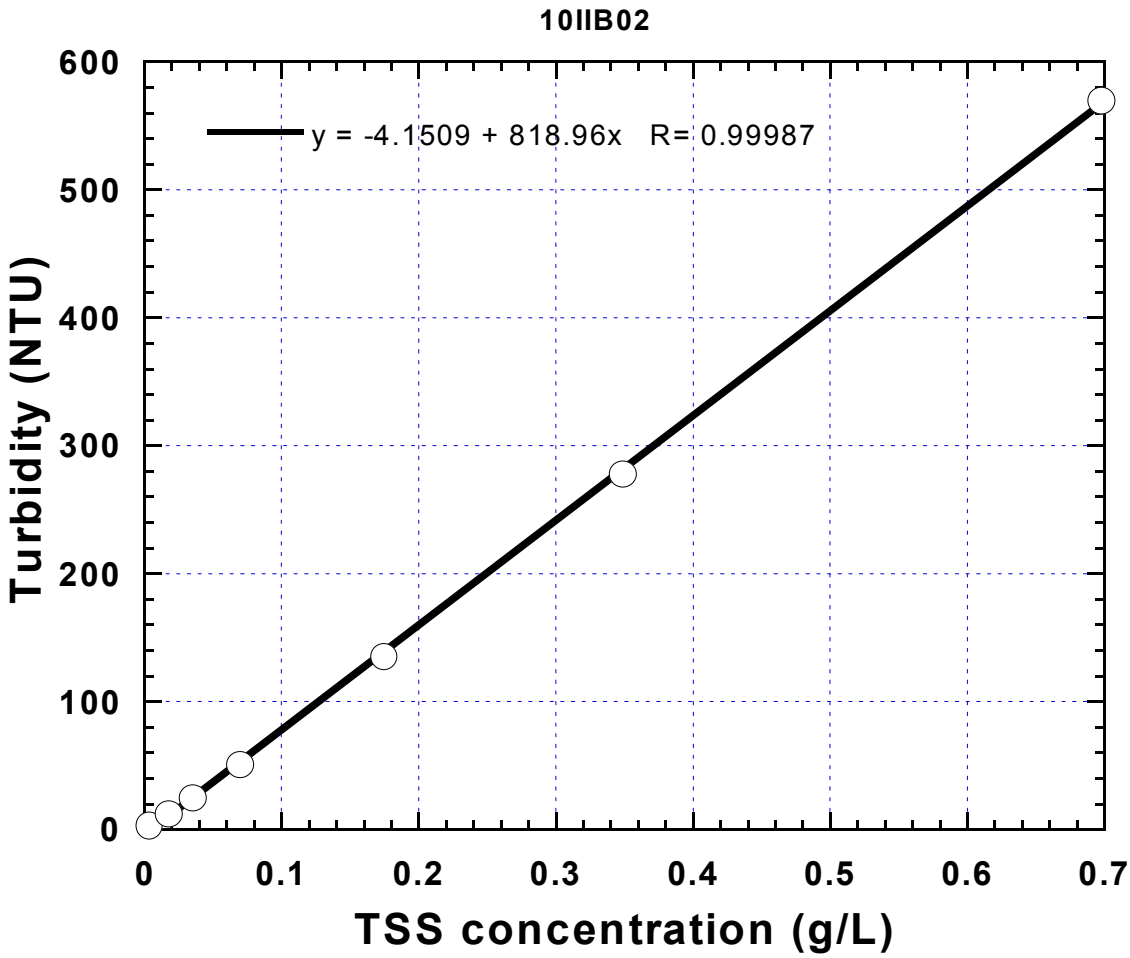

Figure A14. Calibration curve for turbidity (NTU) and particulate concentration of well water (well #10, bailing sample, 10IIB02)

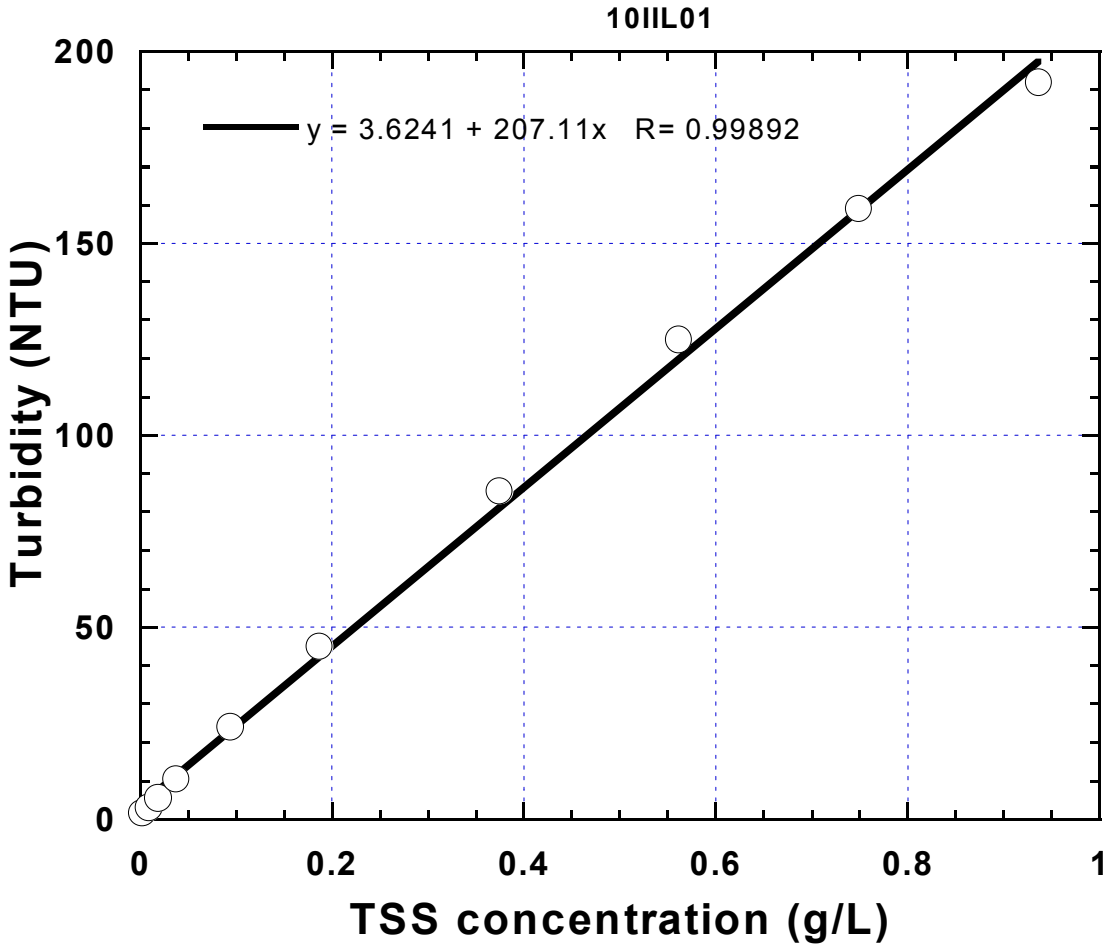

Figure A15. Calibration curve for turbidity (NTU) and particulate concentration of well water (well #10, low flow purging sample, 10IIL01)

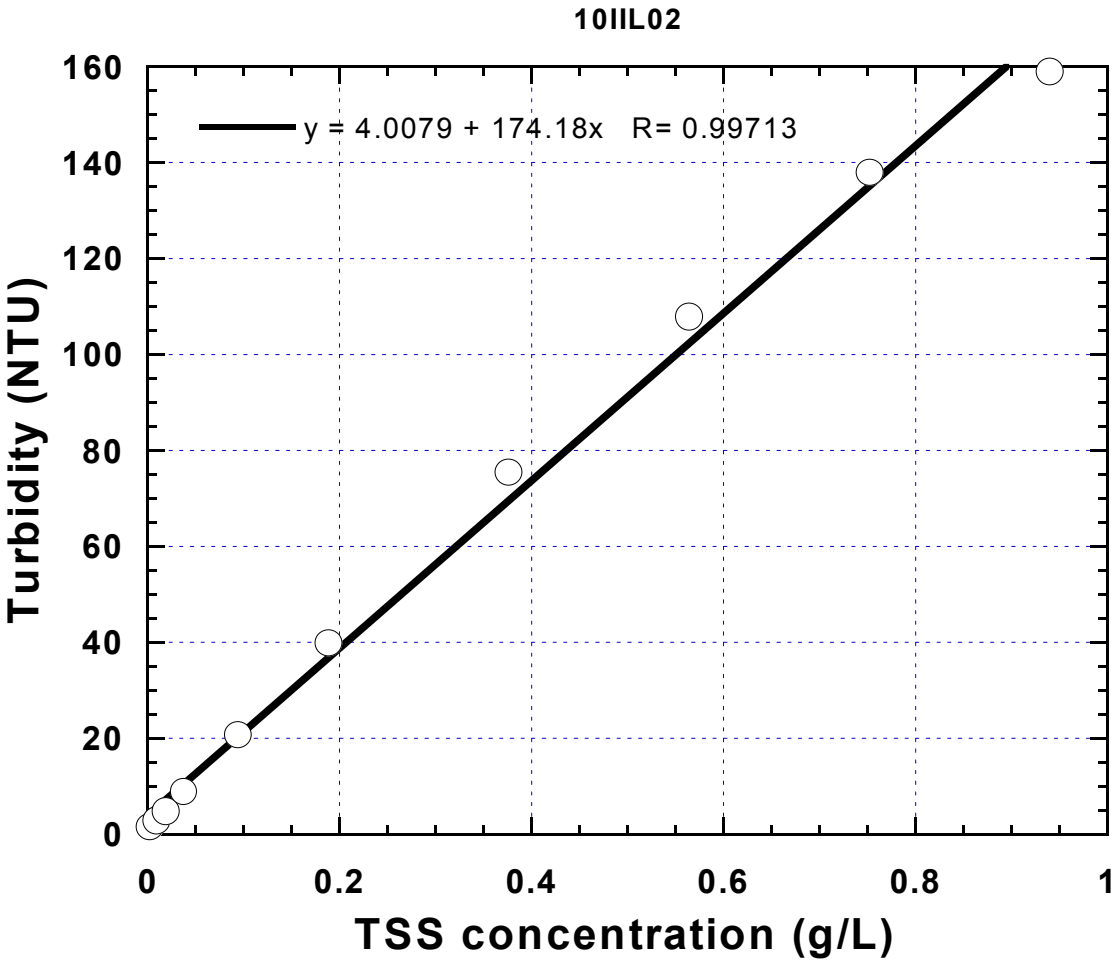

Figure A16. Calibration curve for turbidity (NTU) and particulate concentration of well water (well #10, low flow purging sample, 10IIL02)

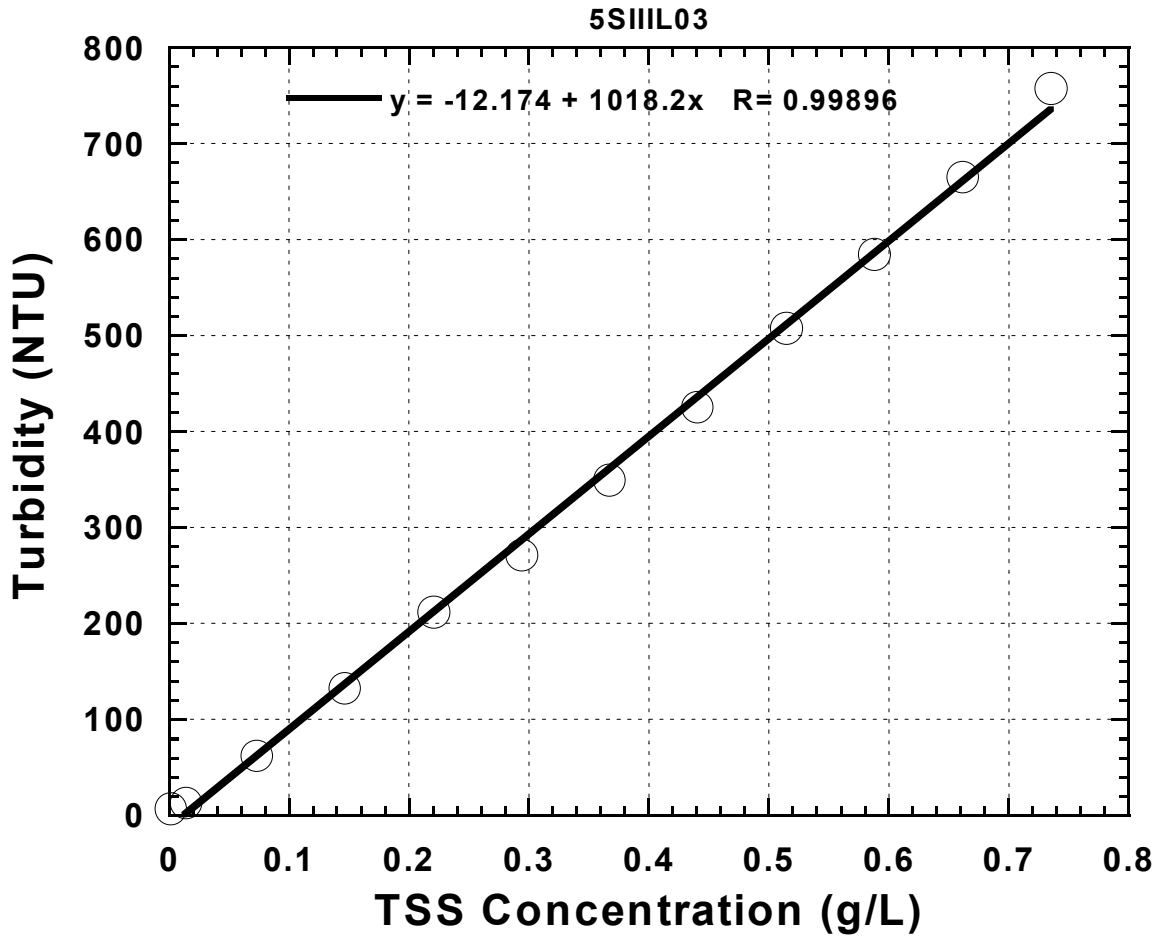

Figure A17. Calibration curve for turbidity (NTU) and particulate concentration of well water (well #5S, low flow purging sample, 5SIIIL03)

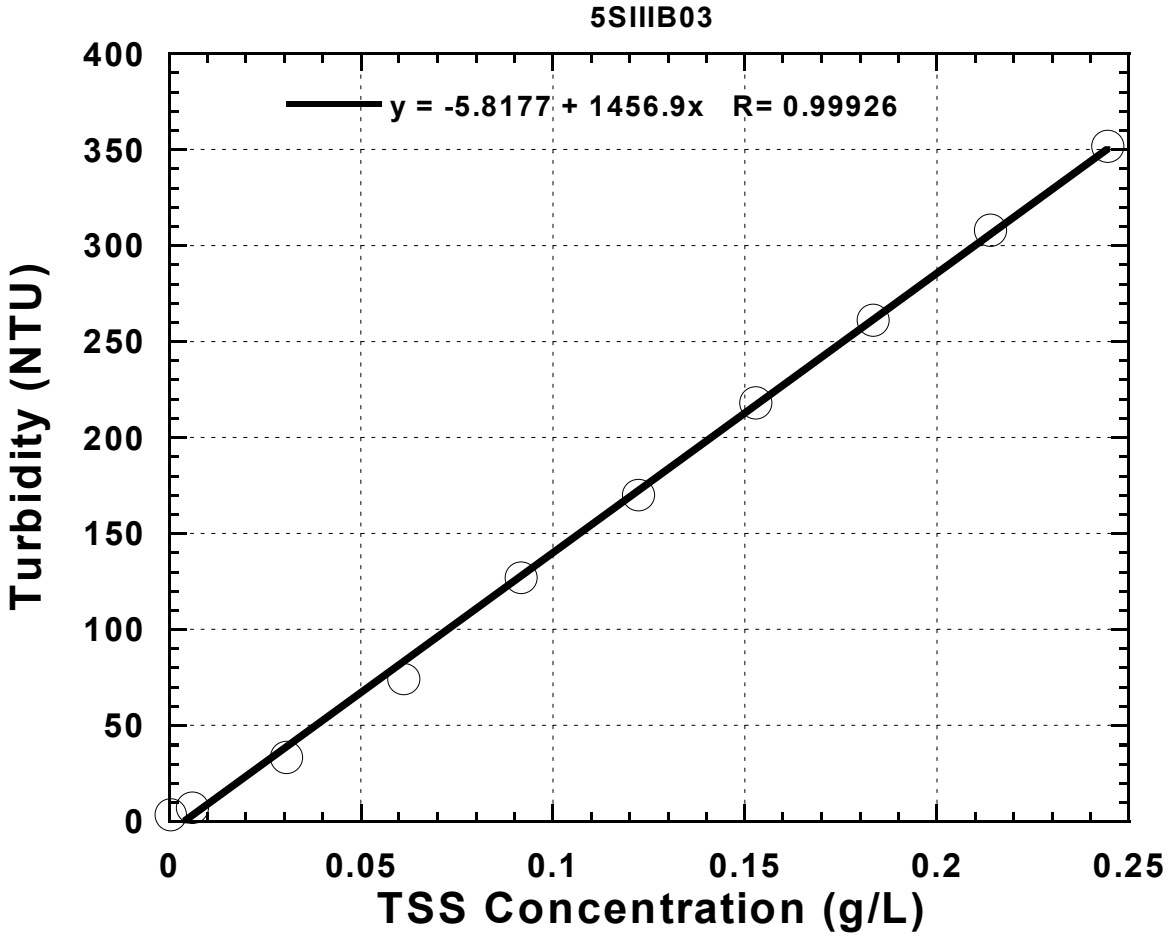

Figure A18. Calibration curve for turbidity (NTU) and particulate concentration of well water (well #5S, bailing sample, 5SIIIB03)

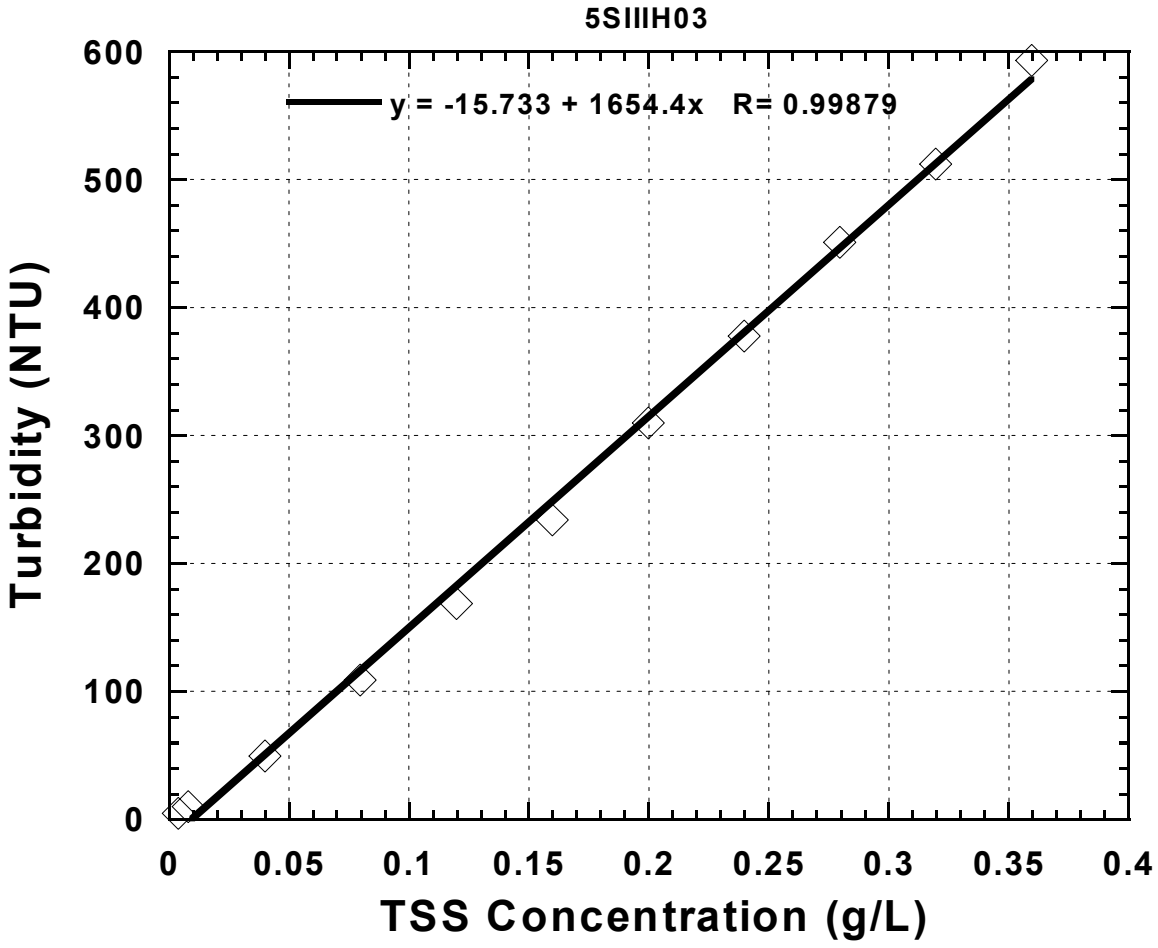

Figure A19. Calibration curve for turbidity (NTU) and particulate concentration of well water (well #5S, high flow purging sample, 5SIIIH03)

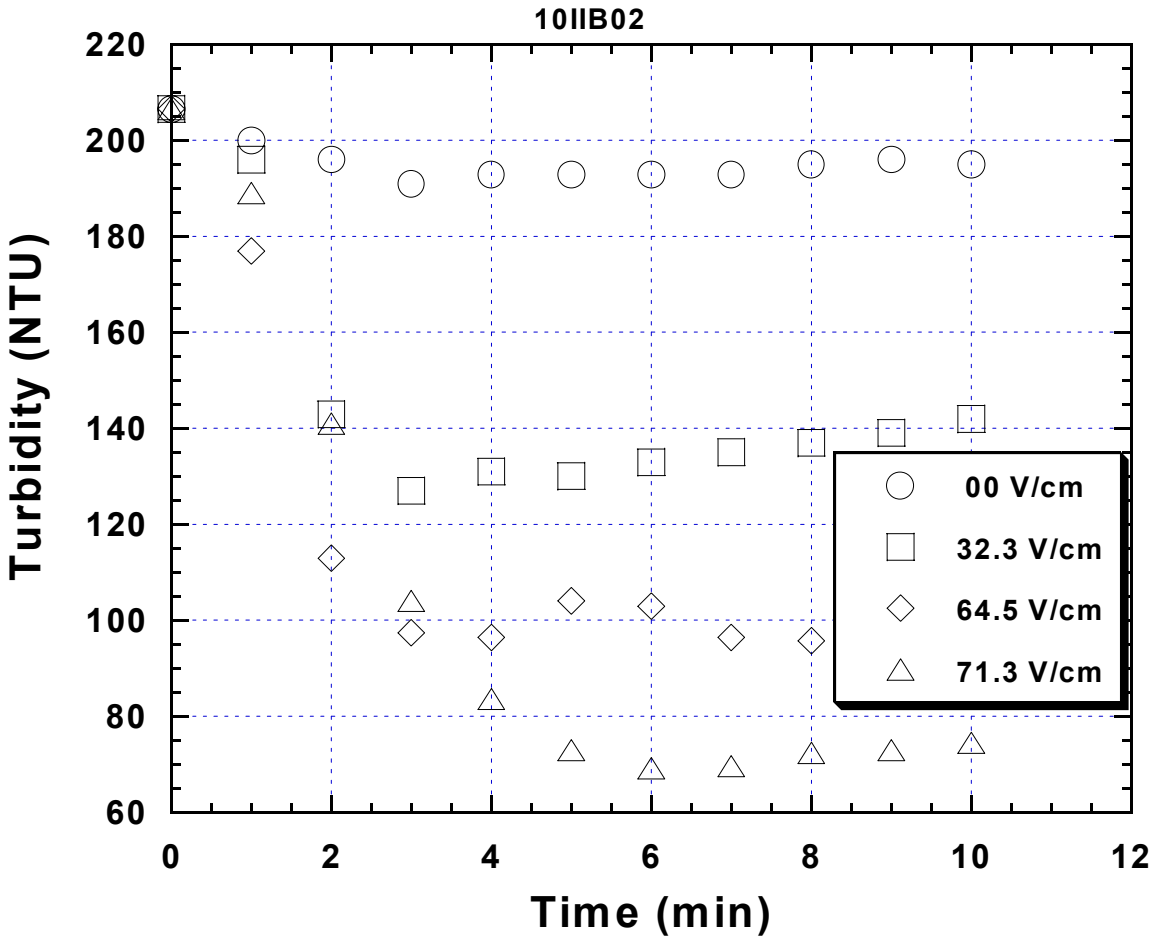

Figure A20. Turbidity changes as a function of time at various electrostatic field values (I). Experimental condition: pH = 6.8; Sample: 10IIB02

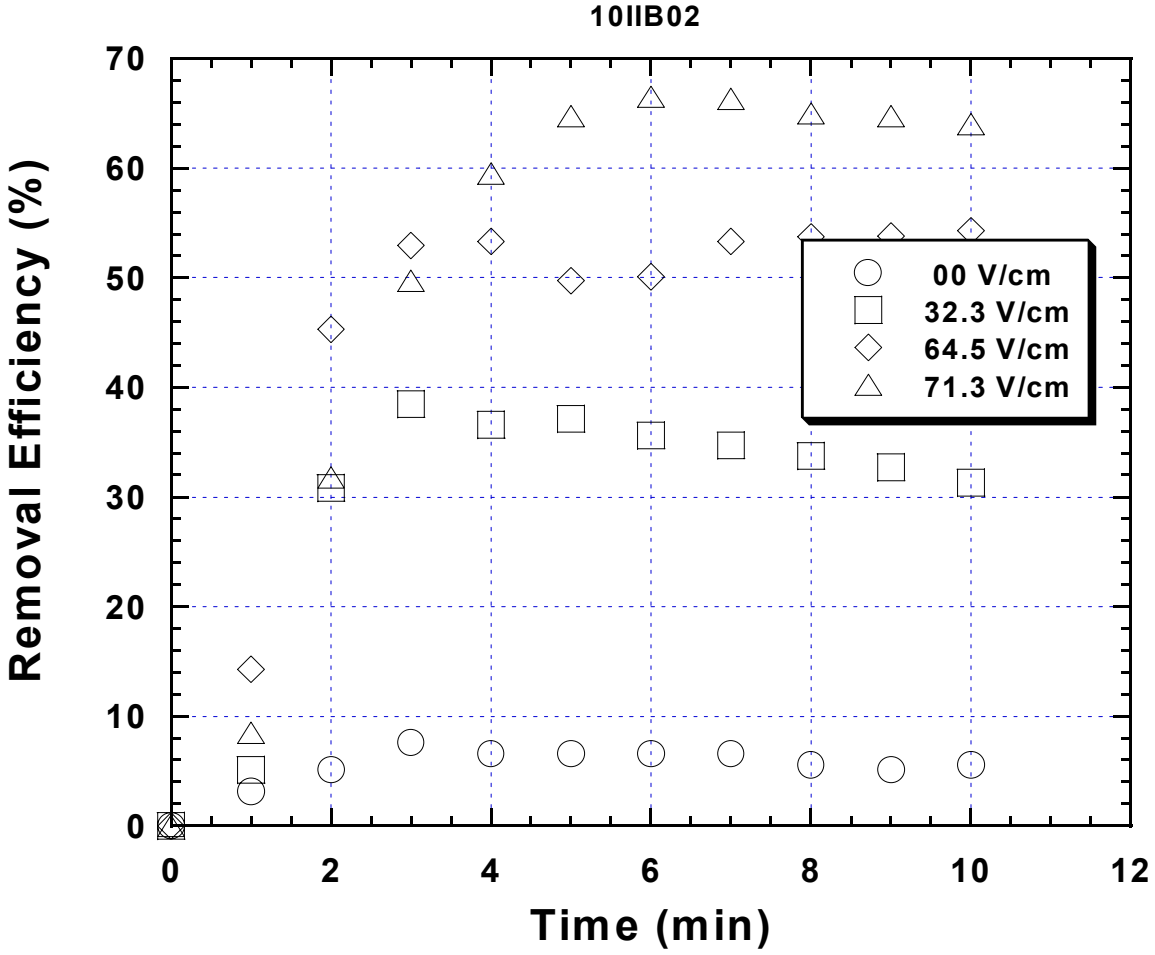

Figure A21. Removal efficiency as a function of time at various electrostatic field values (I). Experimental condition: pH = 6.8; Sample: 10IIB02

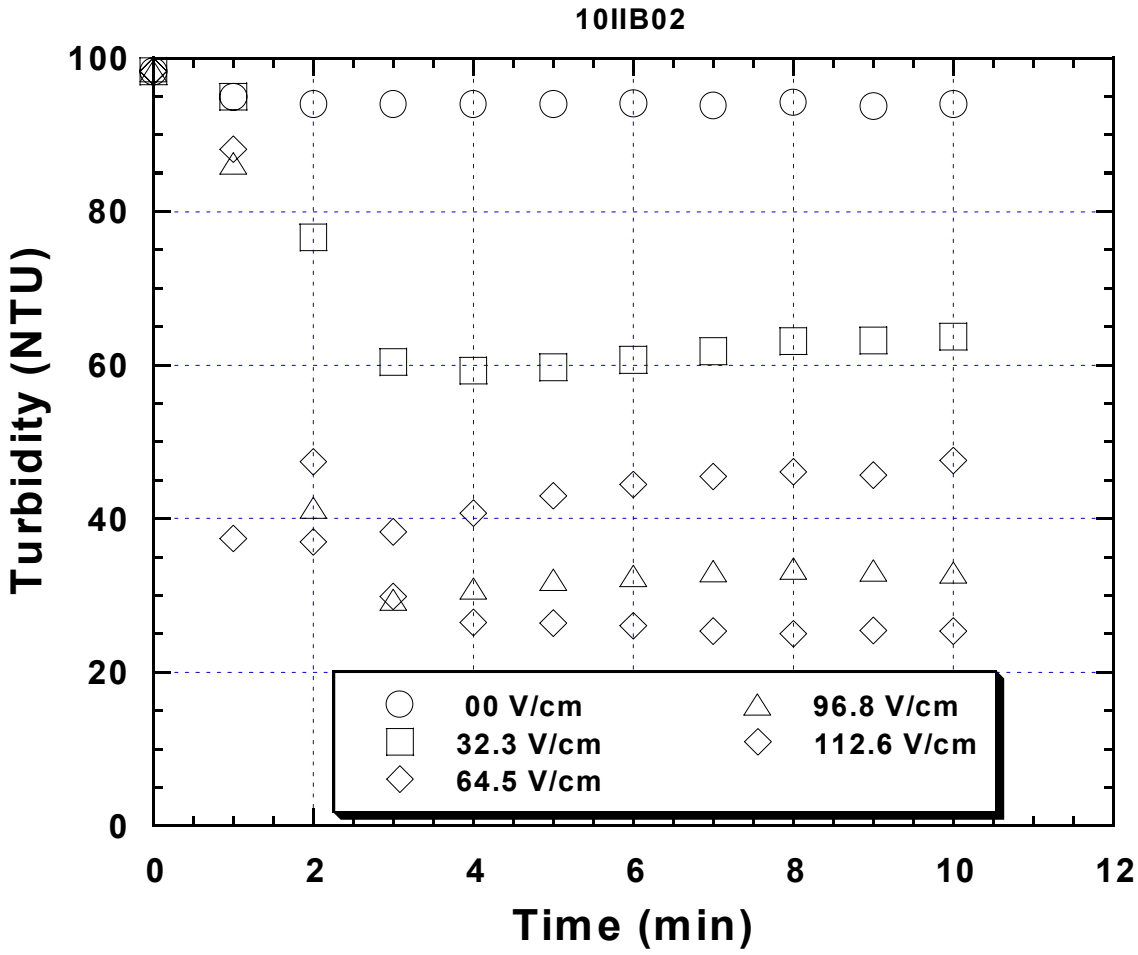

Figure A22. Turbidity changes as a function of time at various electrostatic field values (II). Experimental condition: pH = 6.8; Sample: 10IIB02

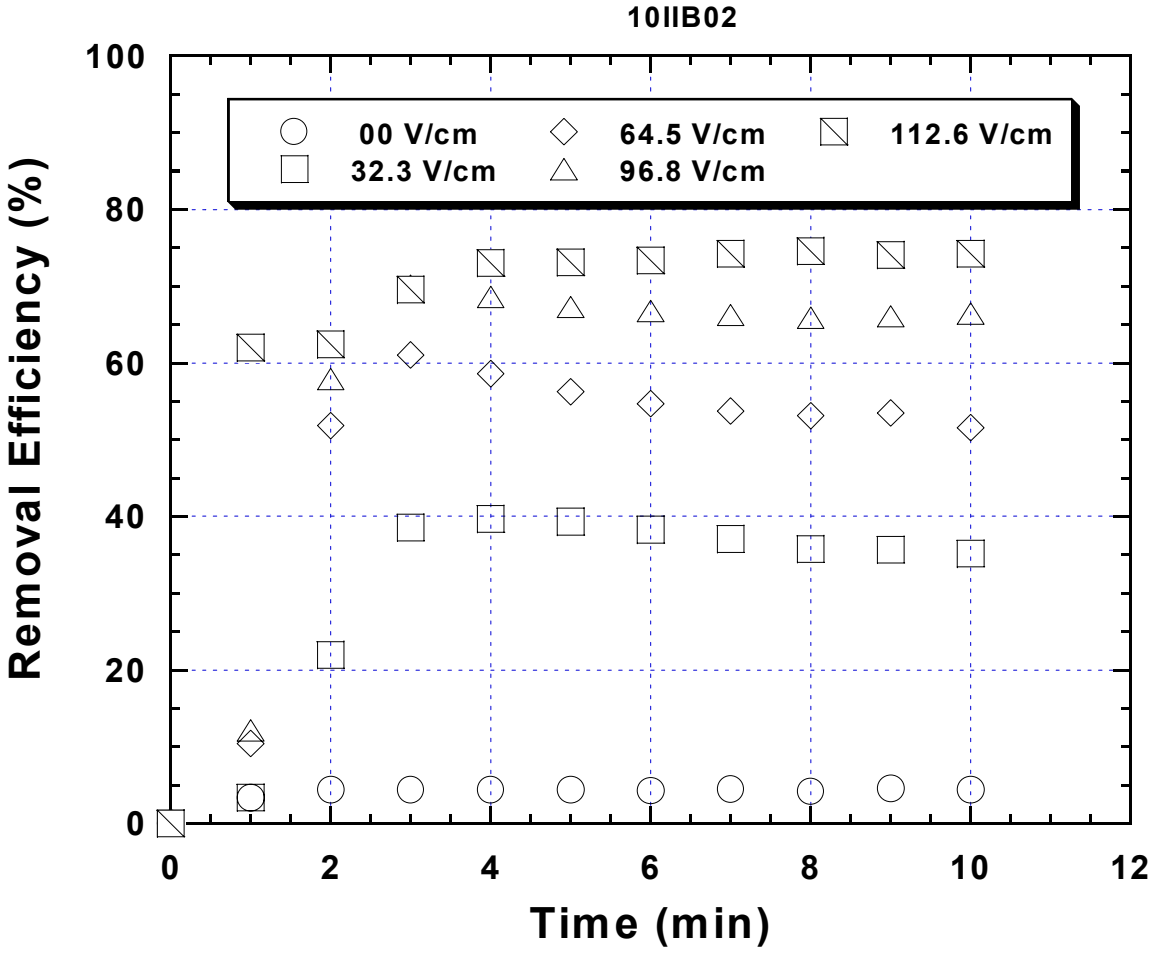

Figure A23. Removal efficiency as a function of time at various electrostatic field values (II). Experimental condition: pH = 6.8; Sample: 10IIB02

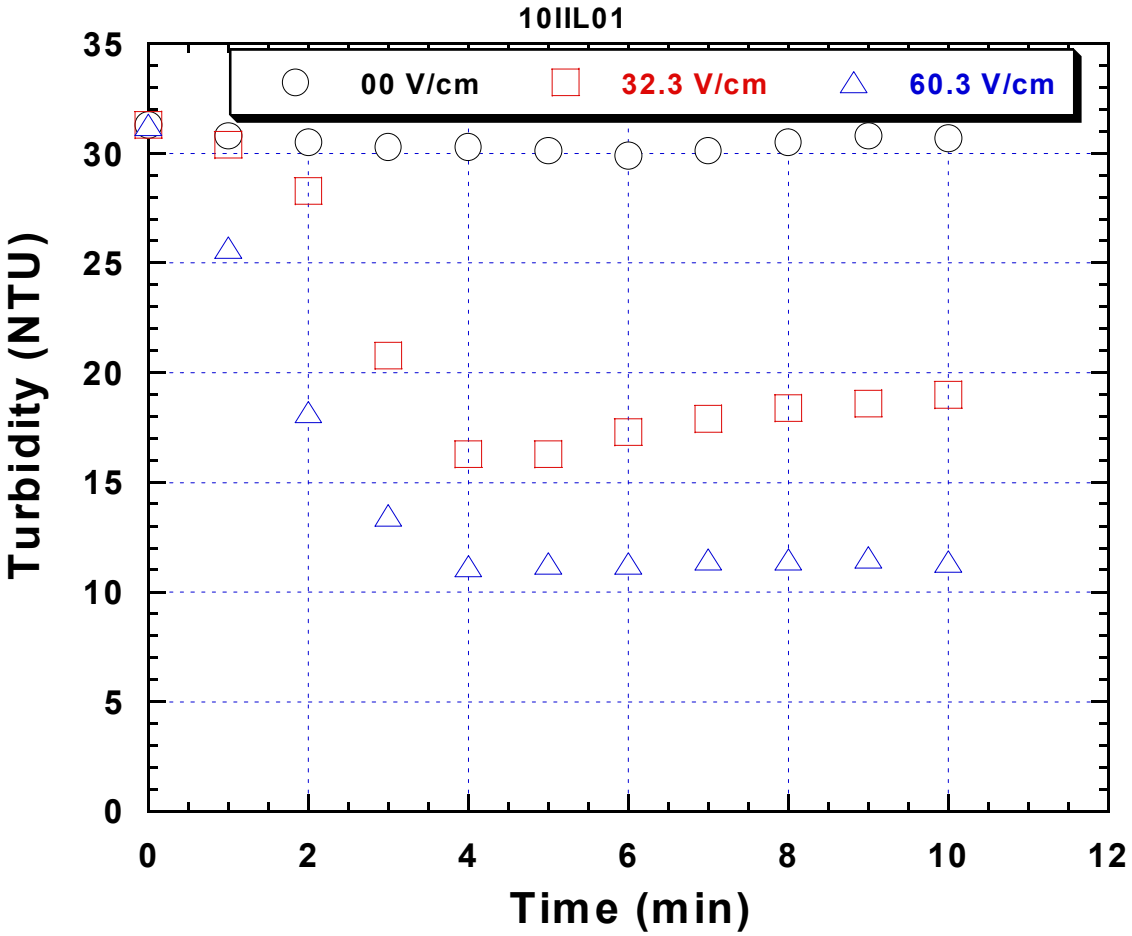

Figure A24. Turbidity changes as a function of time at various electrostatic field values. Experimental condition: pH = 7.1; Sample: 10IIL02

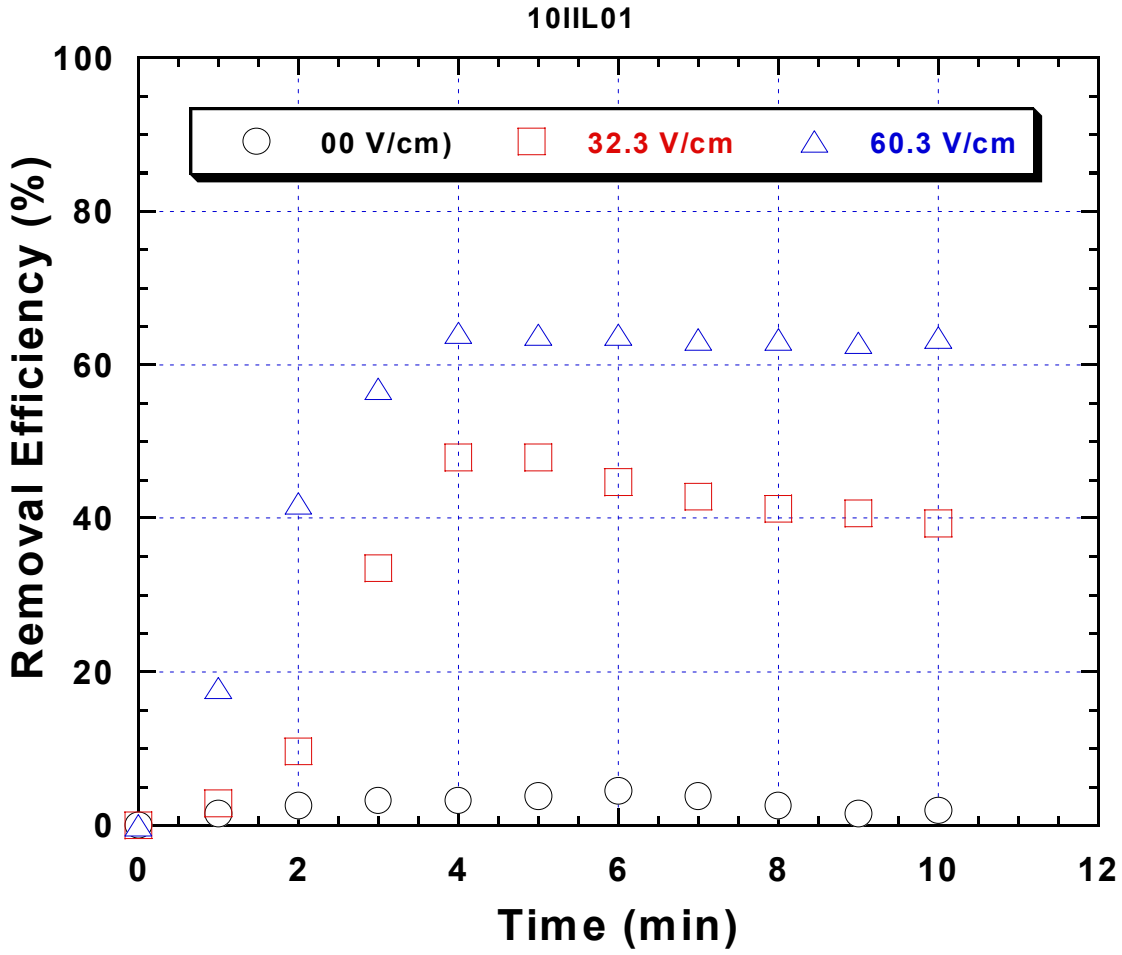

Figure A25. Removal efficiency as a function of time at various electrostatic field values. Experimental condition: pH = 7.1; Sample: 10IIL02

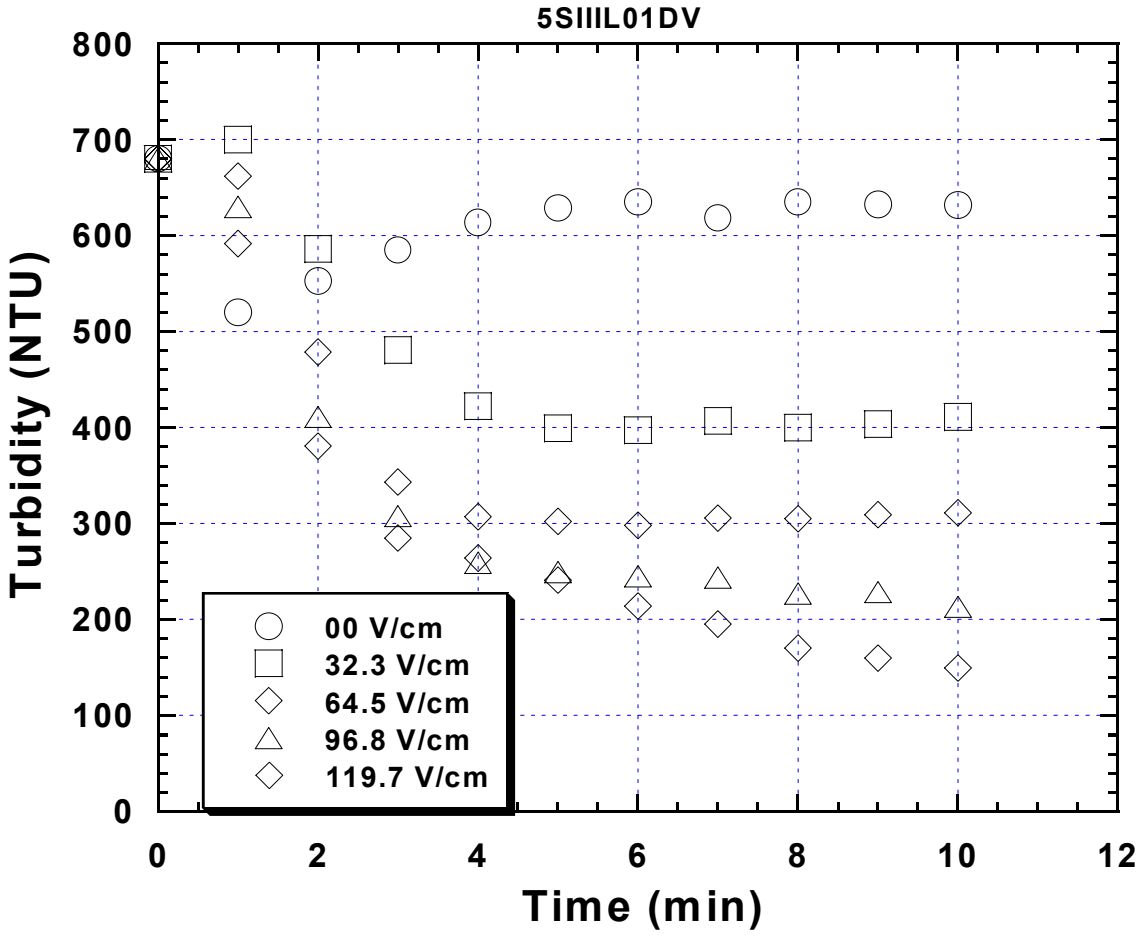

Figure A26. Turbidity changes as a function of time at various electrostatic field values. Experimental condition: pH = 6.8; initial turbidity = 680; Sample: 5SIIIL01

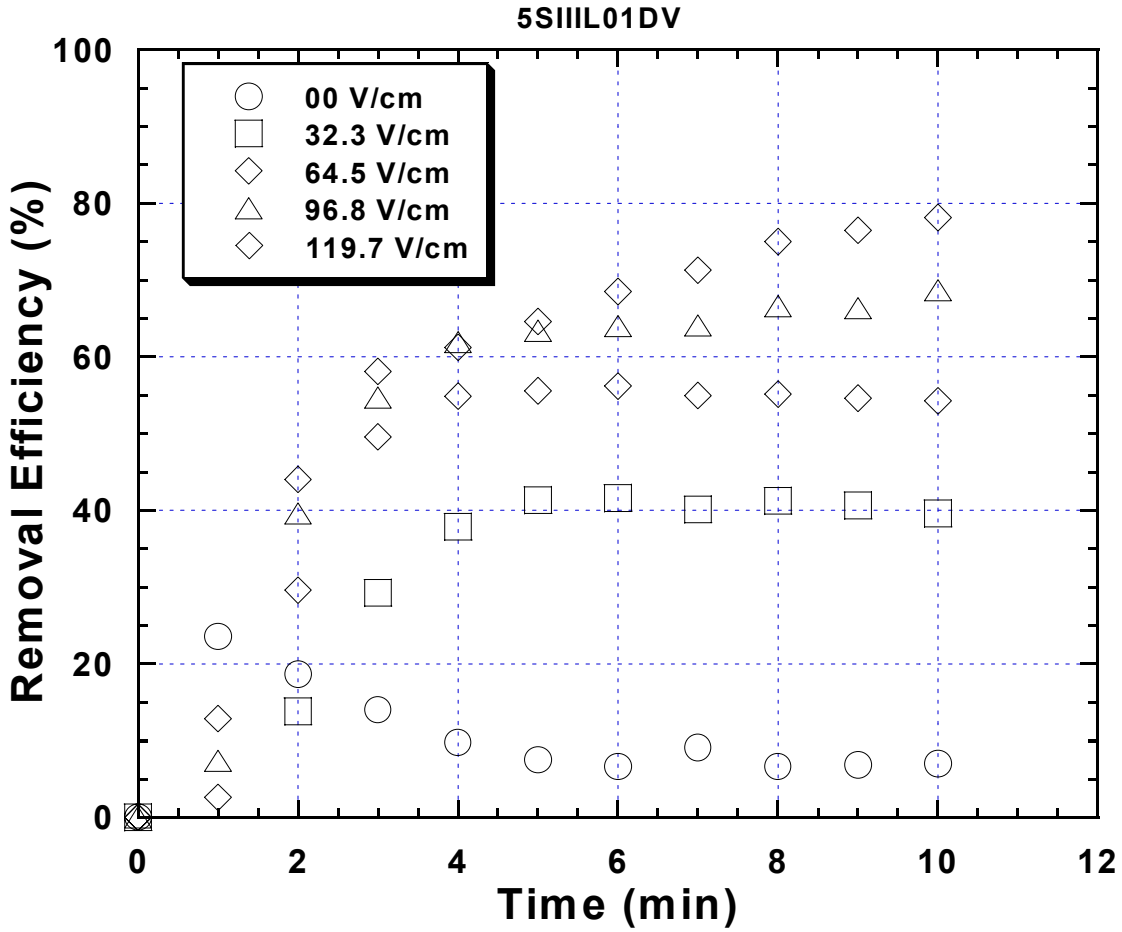

Figure A27. Removal Efficiency as a function of time at various electrostatic field values. Experimental condition: pH = 6.8; initial turbidity = 680; Sample: 5SIIIL01

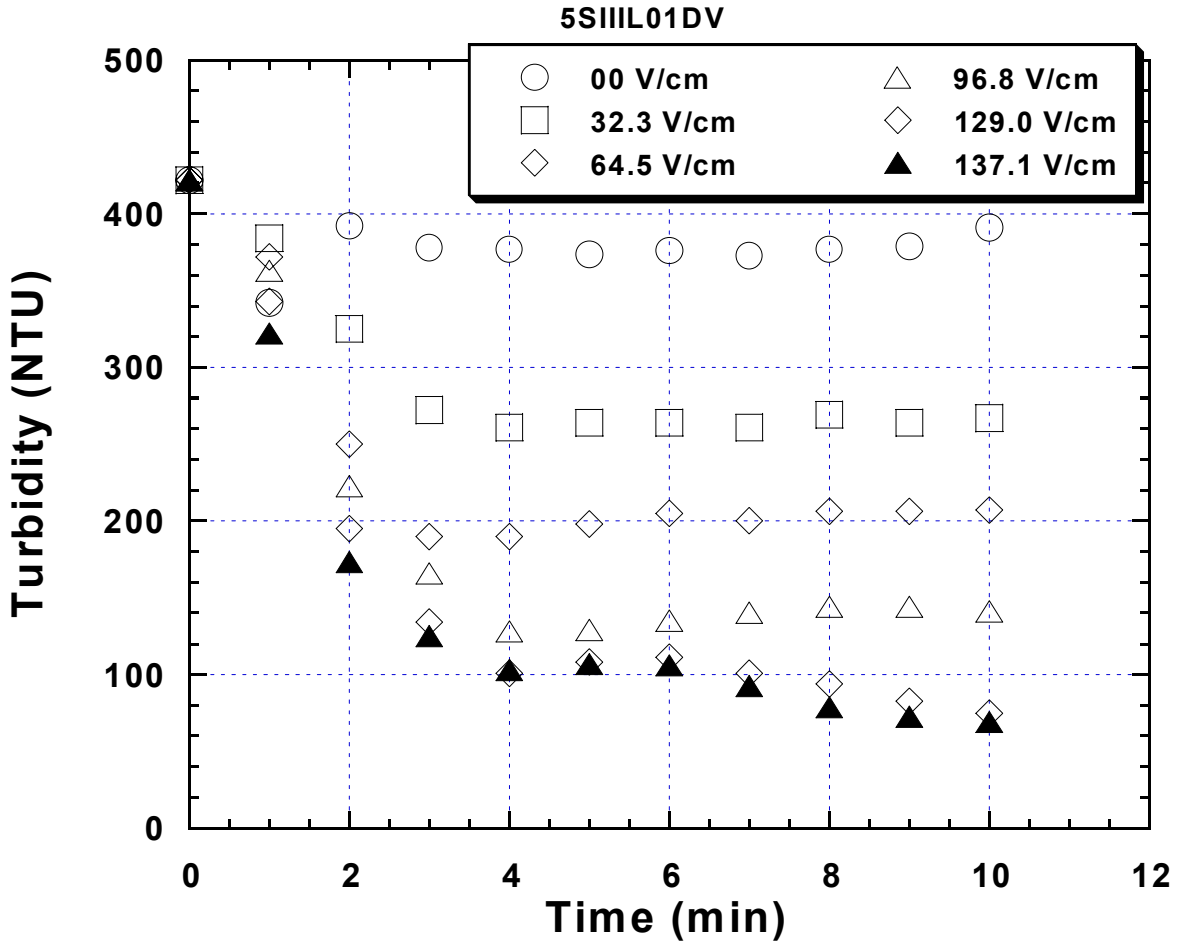

Figure A28. Turbidity changes as a function of time at various electrostatic field values. Experimental condition: pH = 6.6; initial turbidity = 422; Sample: 5SIIIL01

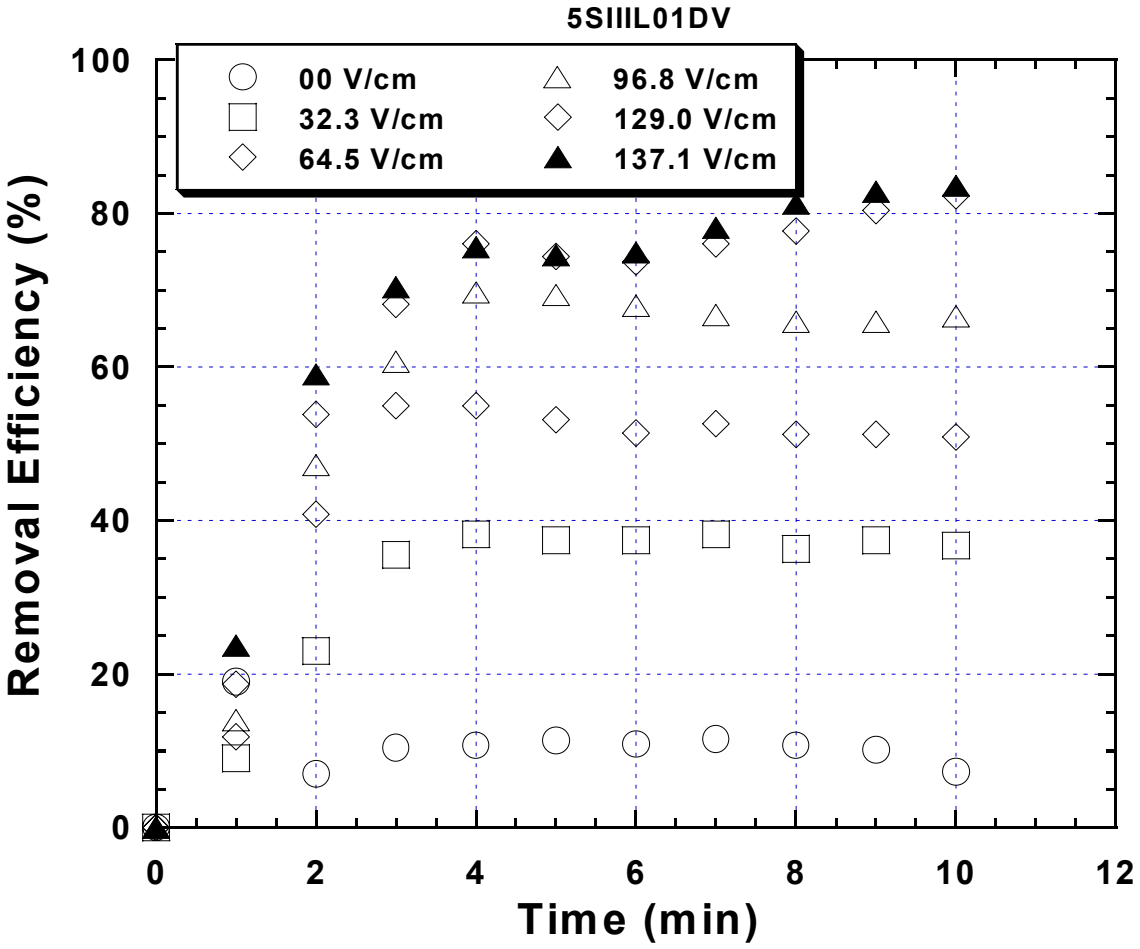

Figure A29. Removal Efficiency as a function of time at various electrostatic field values. Experimental condition: pH = 6.6; initial turbidity = 422; Sample: 5SIIIL01

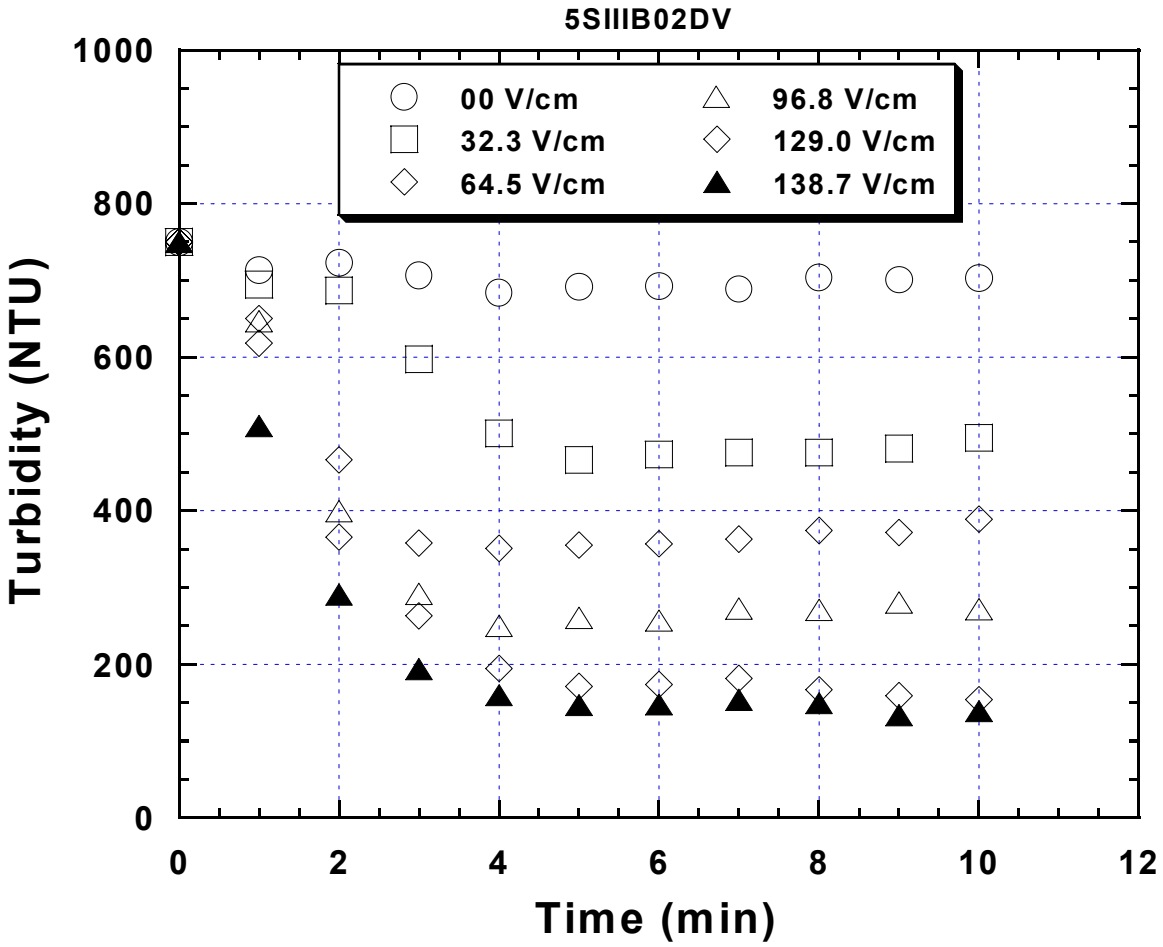

Figure A30. Turbidity changes as a function of time at various electrostatic field values. Experimental condition: pH = 6.8; initial turbidity = 750; Sample: 5SIIIB02

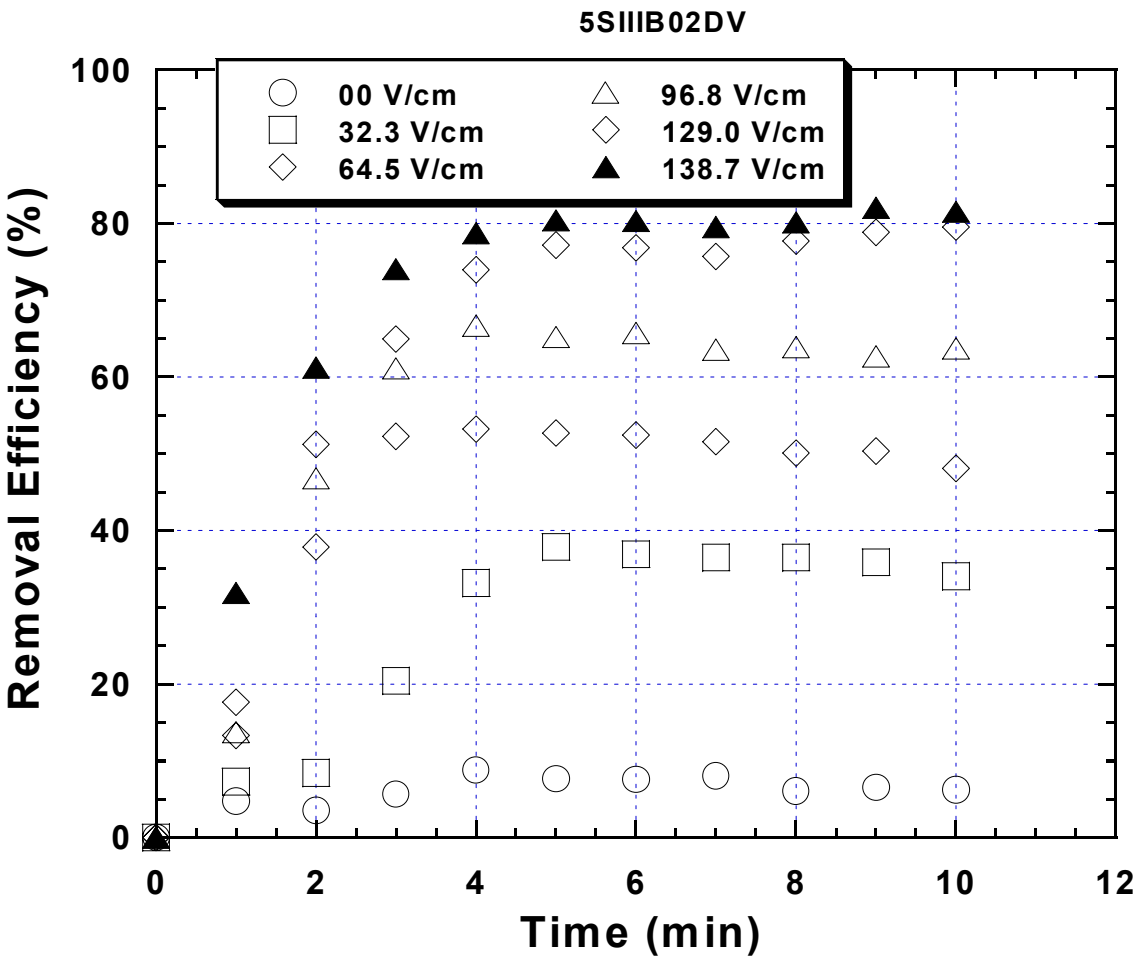

Figure A31. Removal Efficiency as a function of time at various electrostatic field values. Experimental condition: pH = 6.8; initial turbidity = 750; Sample: 5SIIIB02

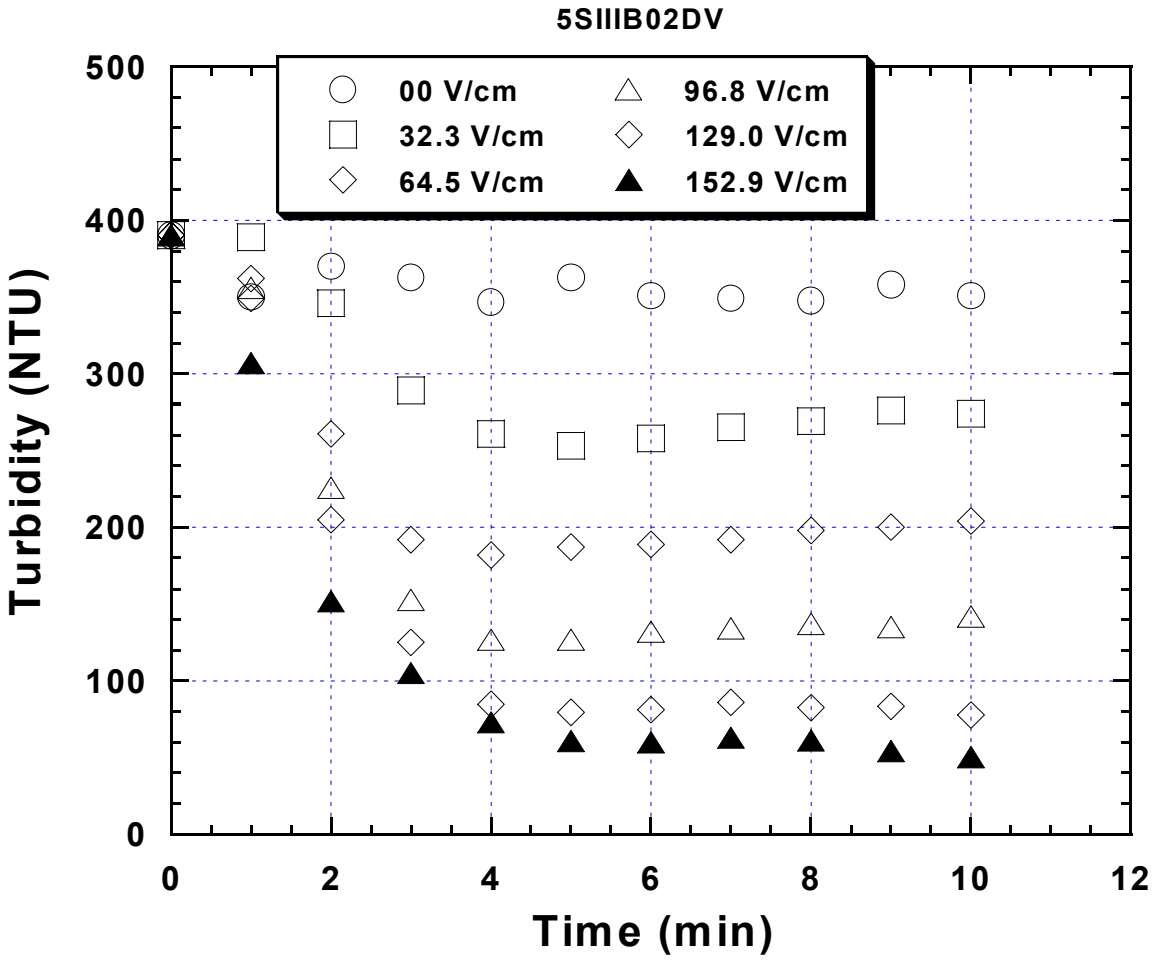

Figure A32. Turbidity changes as a function of time at various electrostatic field values. Experimental condition: pH = 6.6; initial turbidity = 390; Sample: 5SIIIB02

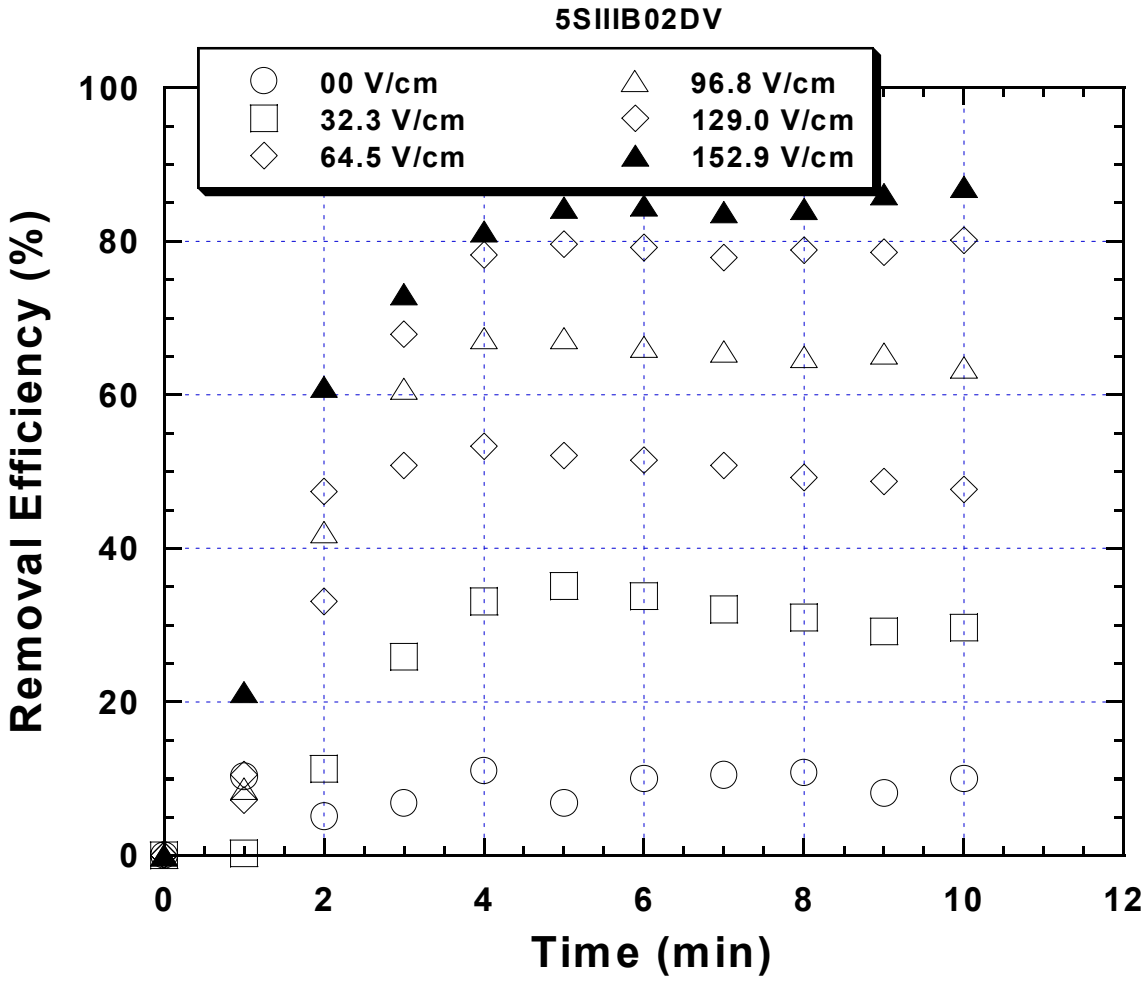

Figure A33. Removal Efficiency as a function of time at various electrostatic field values. Experimental condition: pH = 6.6; initial turbidity = 390; Sample: 5SIIIB02

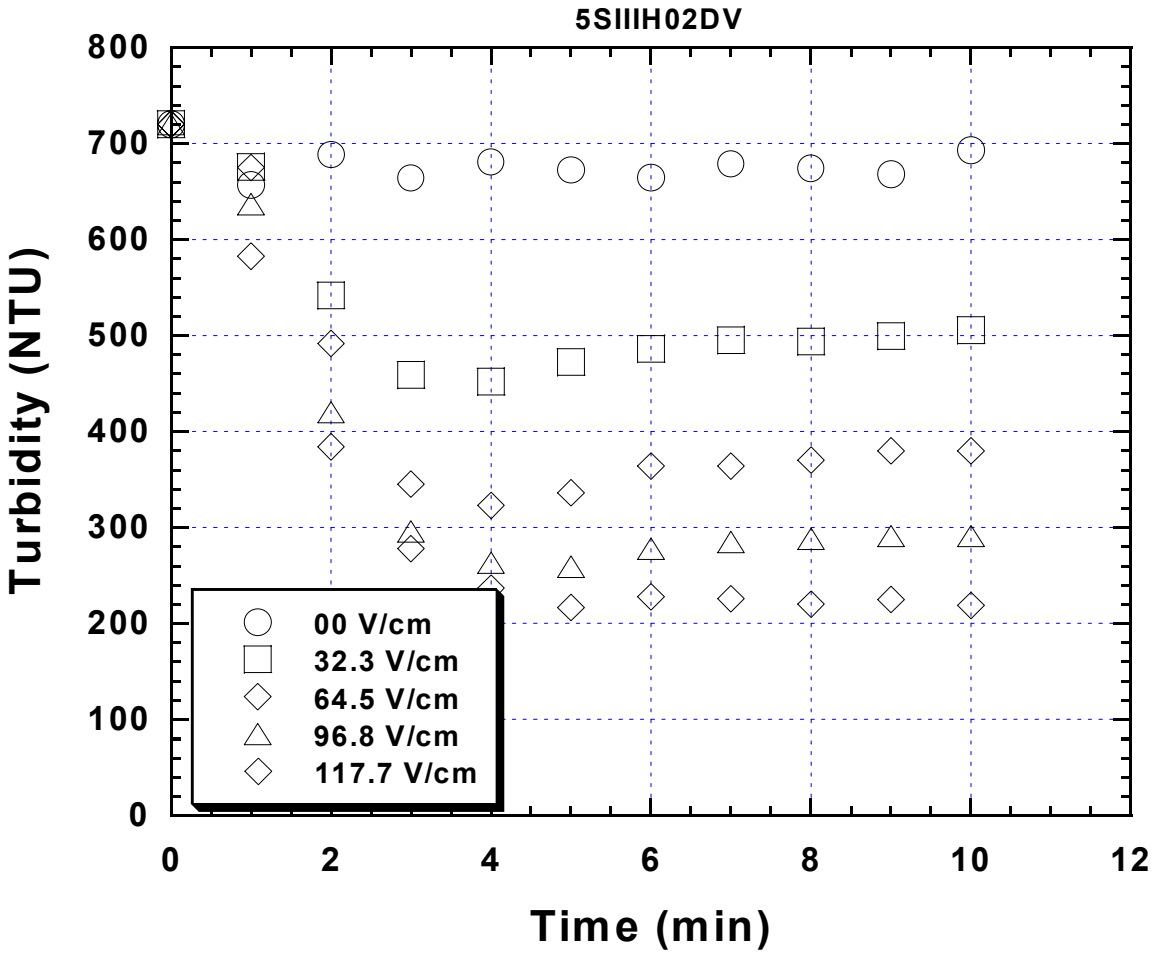

Figure A34. Turbidity changes as a function of time at various electrostatic field values. Experimental condition: pH = 7.1; initial turbidity = 720; Sample: 5SIIIH02

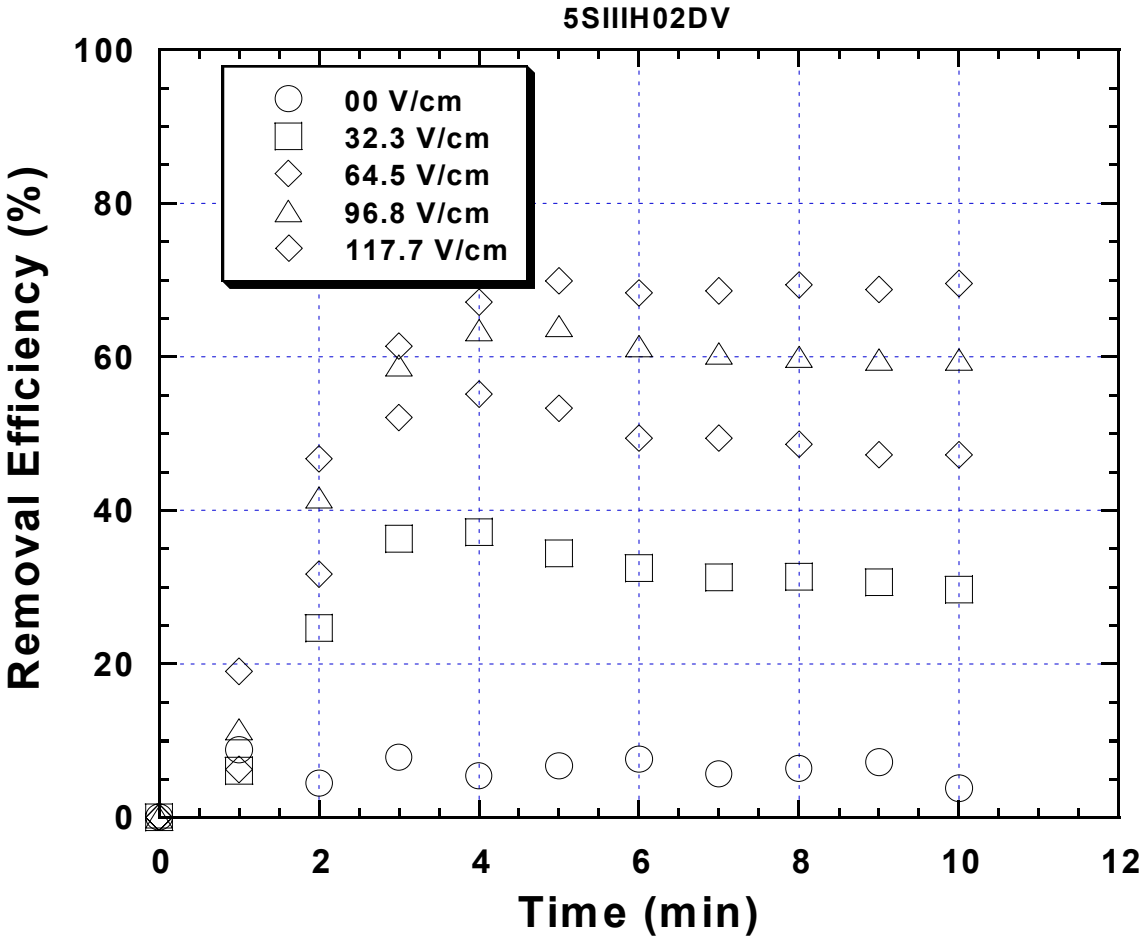

Figure A35. Removal Efficiency as a function of time at various electrostatic field values. Experimental condition: pH = 7.1; initial turbidity = 720; Sample: 5SIIIH02

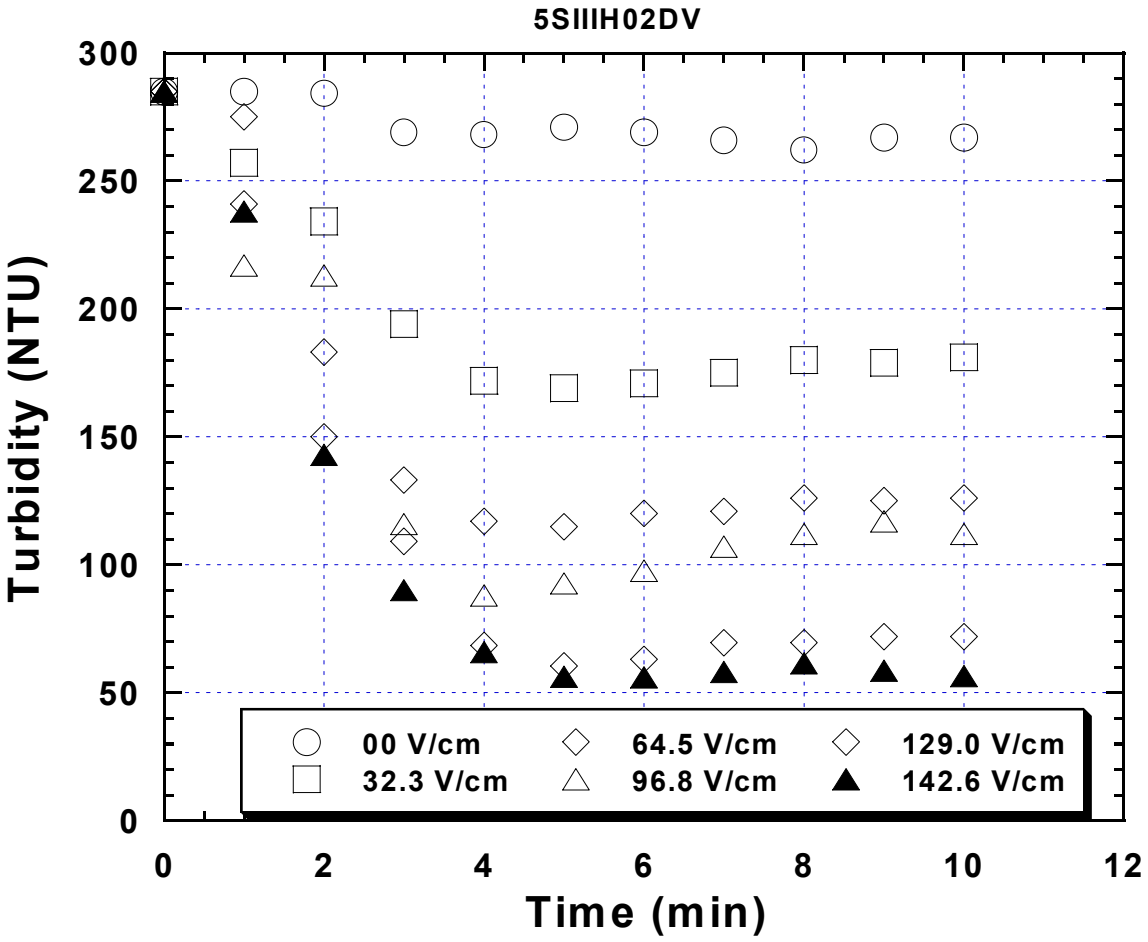

Figure A36. Turbidity changes as a function of time at various electrostatic field values. Experimental condition: pH = 6.8; initial turbidity = 285; Sample: 5SIIIH02

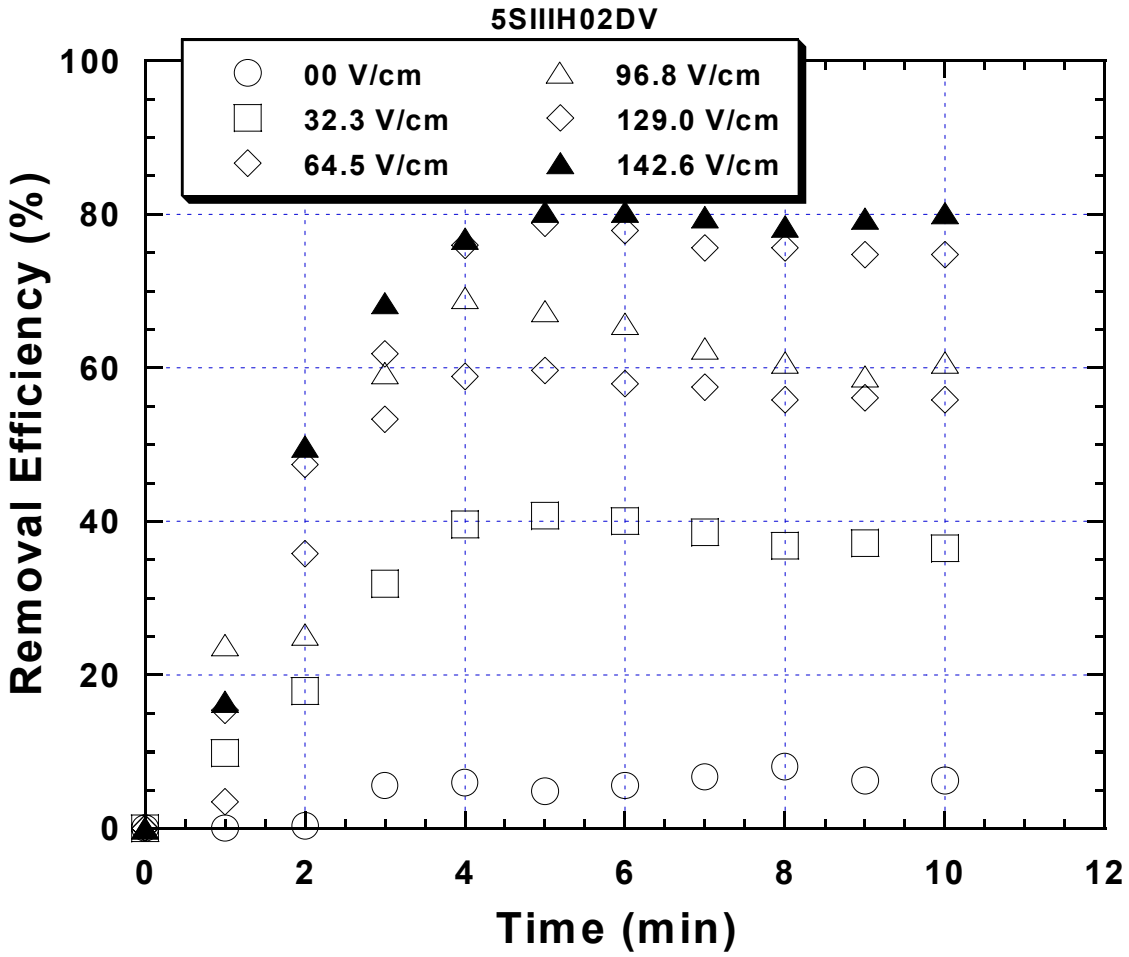

Figure A37. Removal Efficiency as a function of time at various electrostatic field values. Experimental condition: pH = 6.8; initial turbidity = 285; Sample: 5SIIIH02

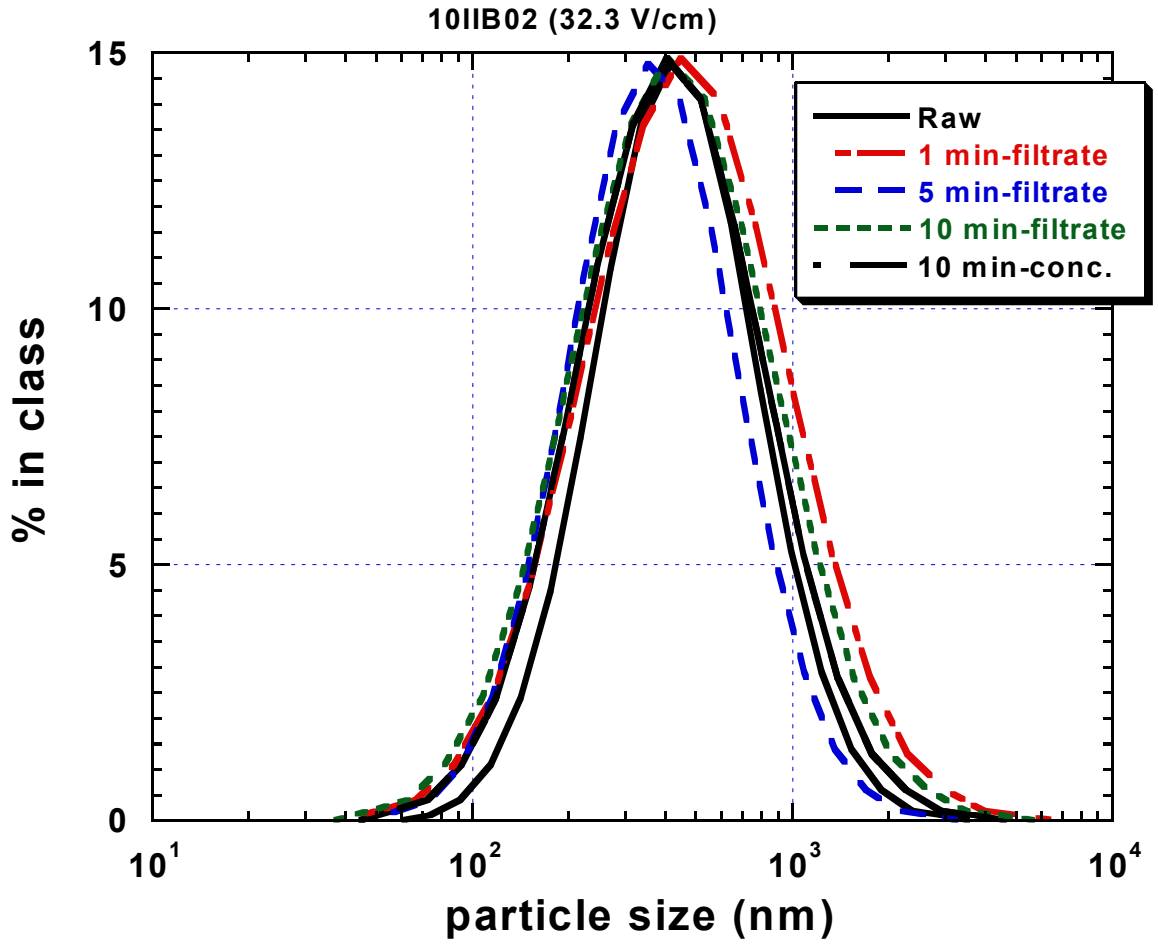

Figure A38. Change in particle size distribution during filtration operation. Experimental conditions: electrostatic field = 32.3 V/cm; pH = 6.8; Sample: 10IIB02.

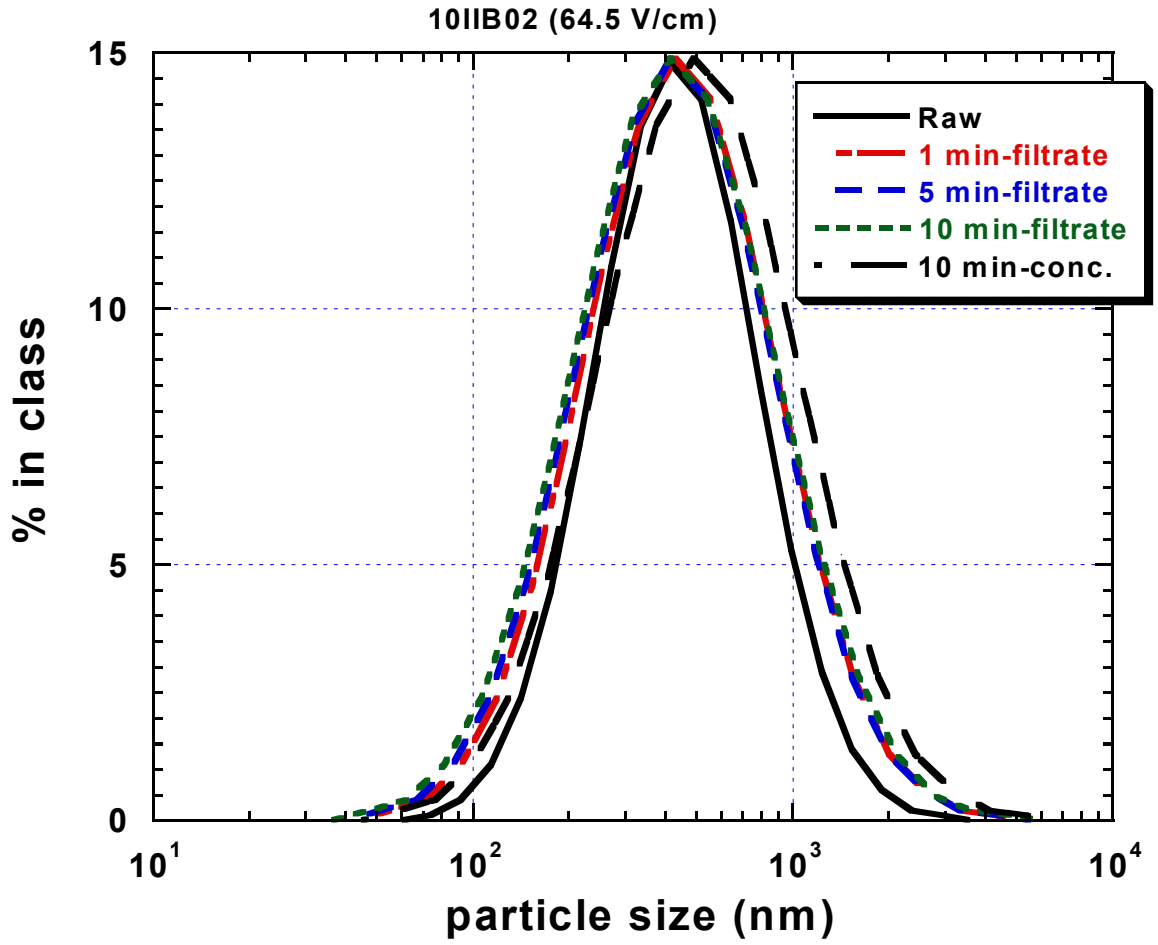

Figure A39. Change in particle size distribution during filtration operation. Experimental conditions: electrostatic field = 64.5 V/cm; pH = 6.8; Sample: 10IIB02.

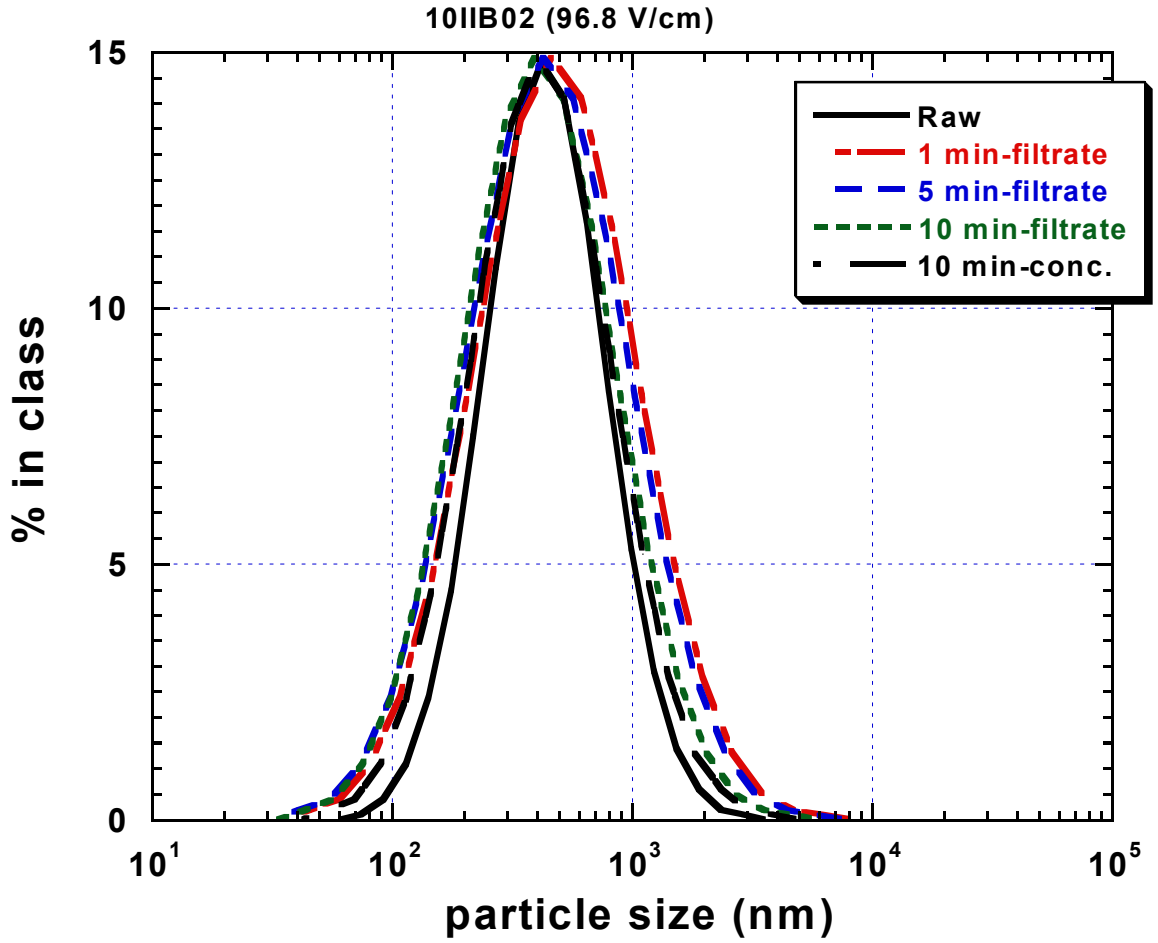

Figure A40. Change in particle size distribution during filtration operation. Experimental conditions: electrostatic field = 96.8 V/cm; pH = 6.8; Sample: 10IIB02.

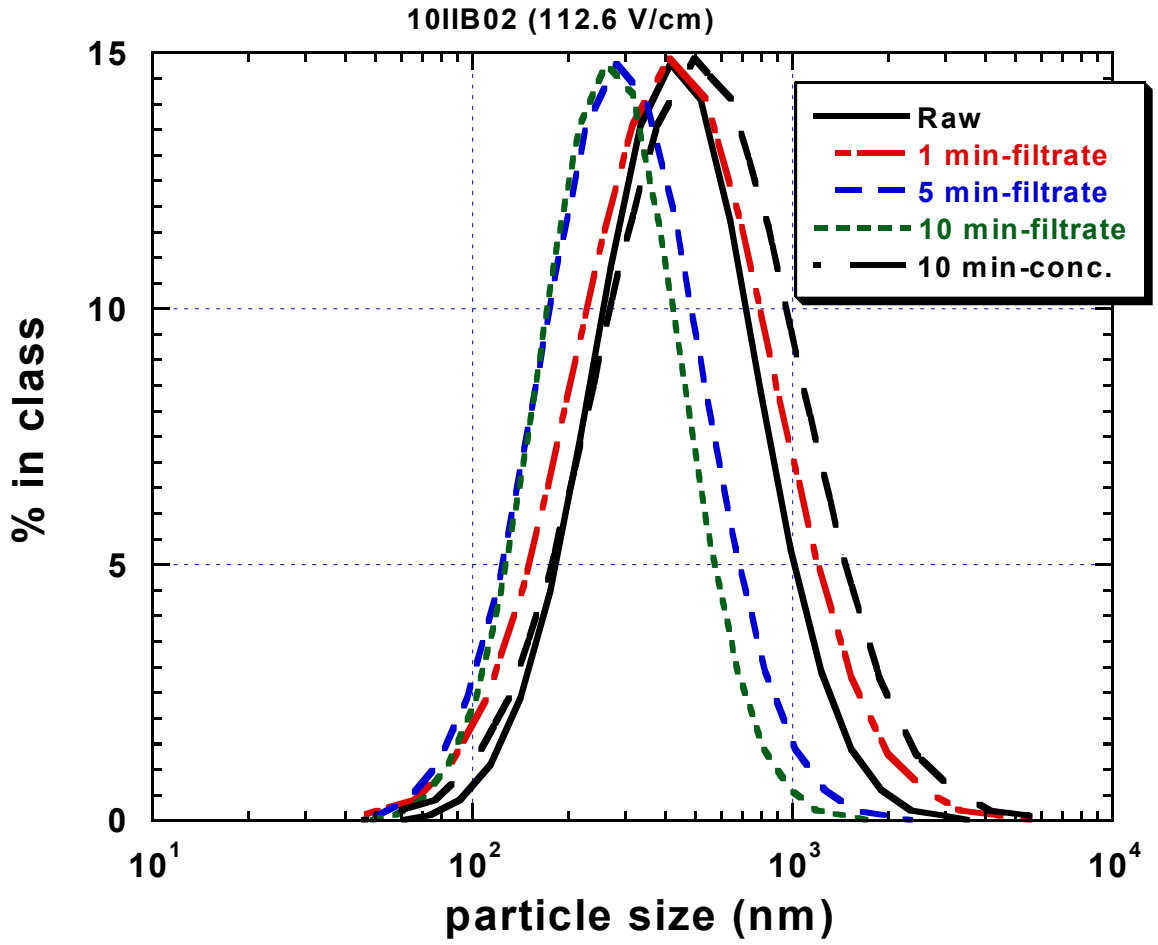

Figure A41. Change in particle size distribution during filtration operation. Experimental conditions: electrostatic field = 112.6 V/cm; pH = 6.8; Sample: 10IIB02.

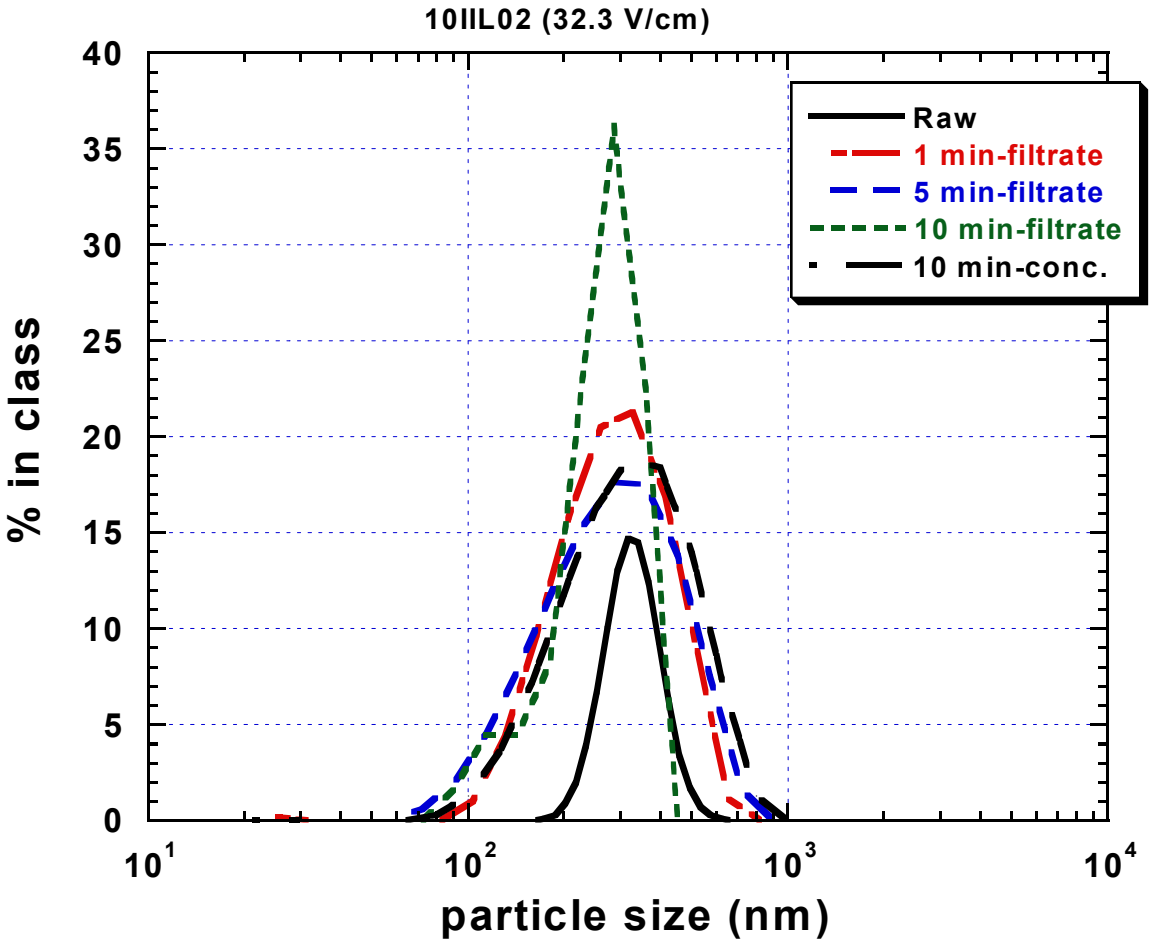

Figure A42. Change in particle size distribution during filtration operation. Experimental conditions: electrostatic field = 32.3 V/cm; pH = 7.1; Sample: 10IIL02.

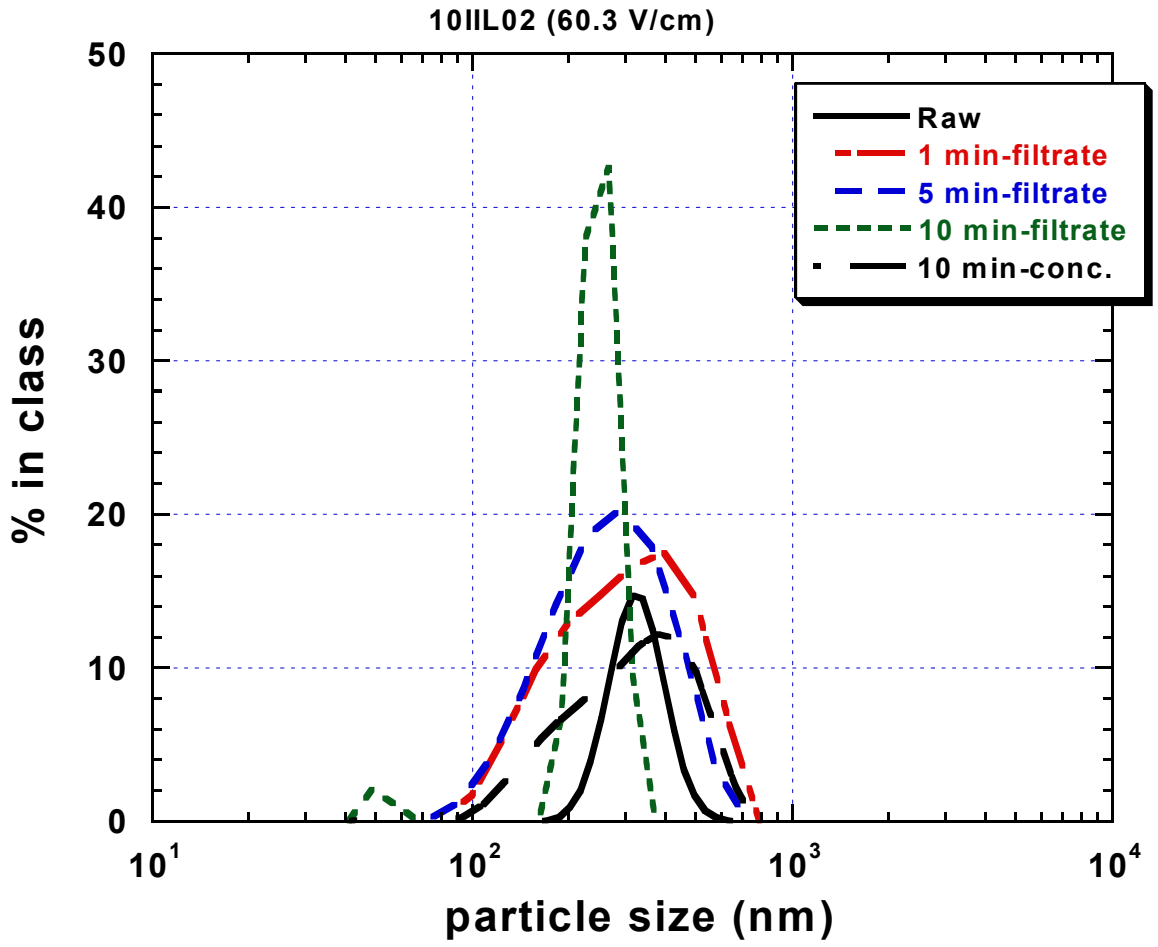

Figure A43. Change in particle size distribution during filtration operation. Experimental conditions: electrostatic field = 60.3 V/cm; pH = 7.1; Sample: 10IIL02.

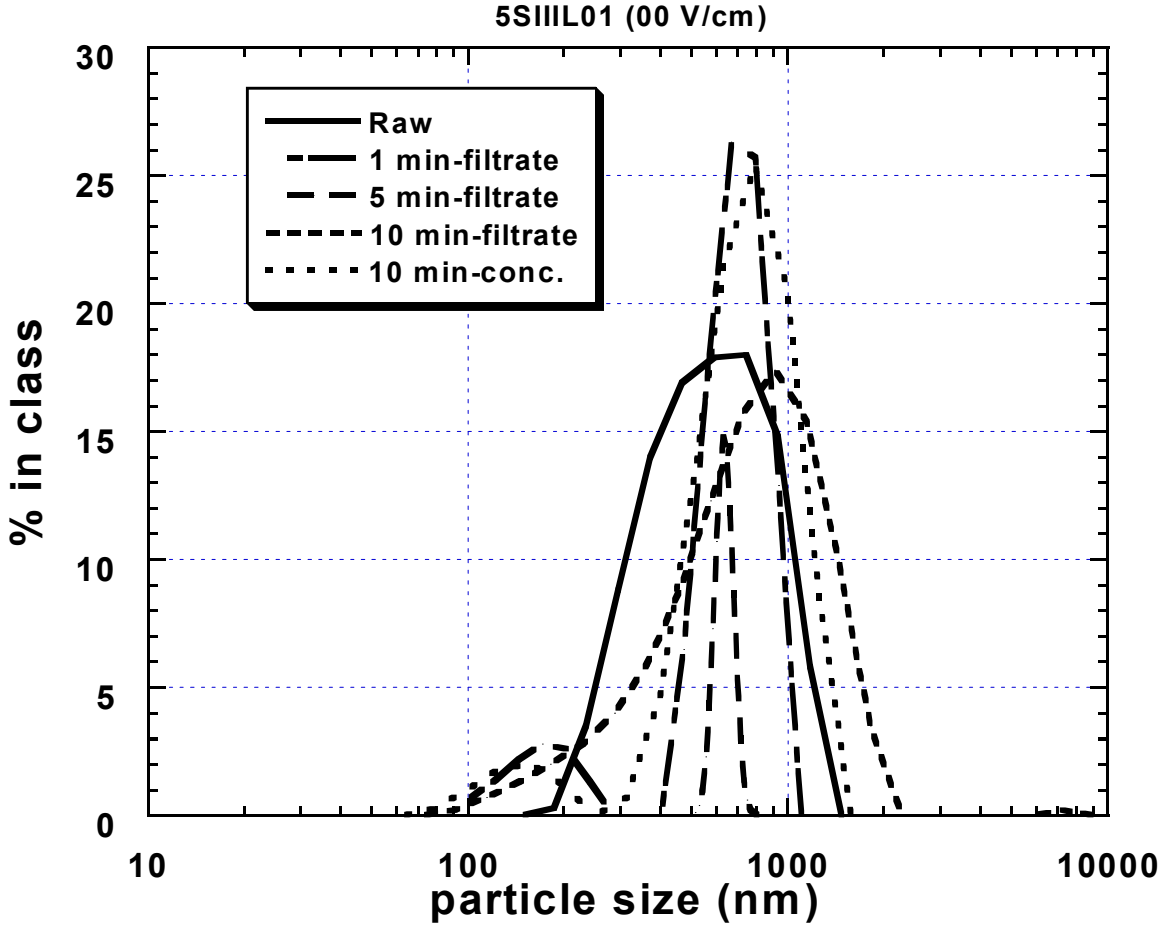

Figure A44. Change in particle size distribution during filtration operation. Experimental conditions: electrostatic field = 00 V/cm; pH = 6.8; Sample: 5SIIIL01

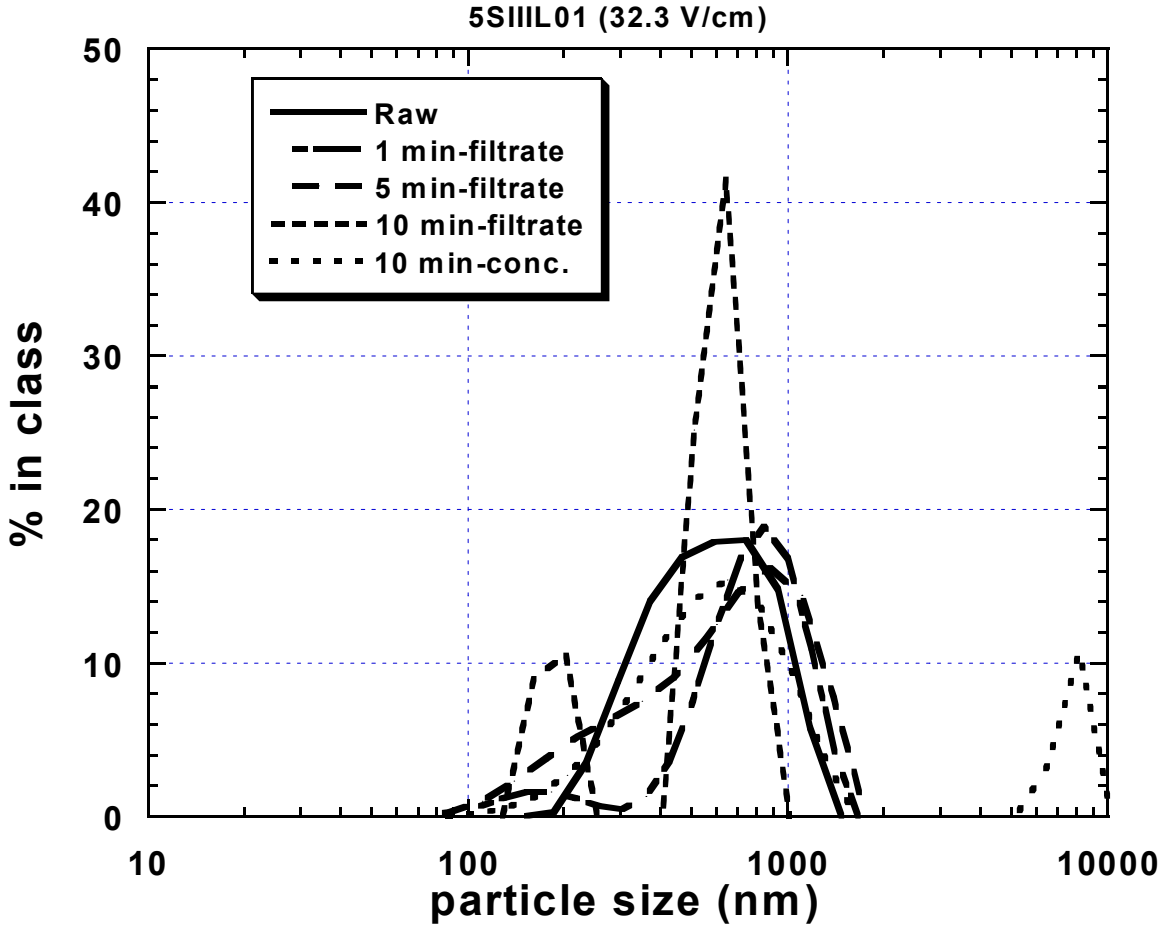

Figure A45. Change in particle size distribution during filtration operation. Experimental conditions: electrostatic field = 32.3 V/cm; pH = 6.8; Sample: 5SIIIL01

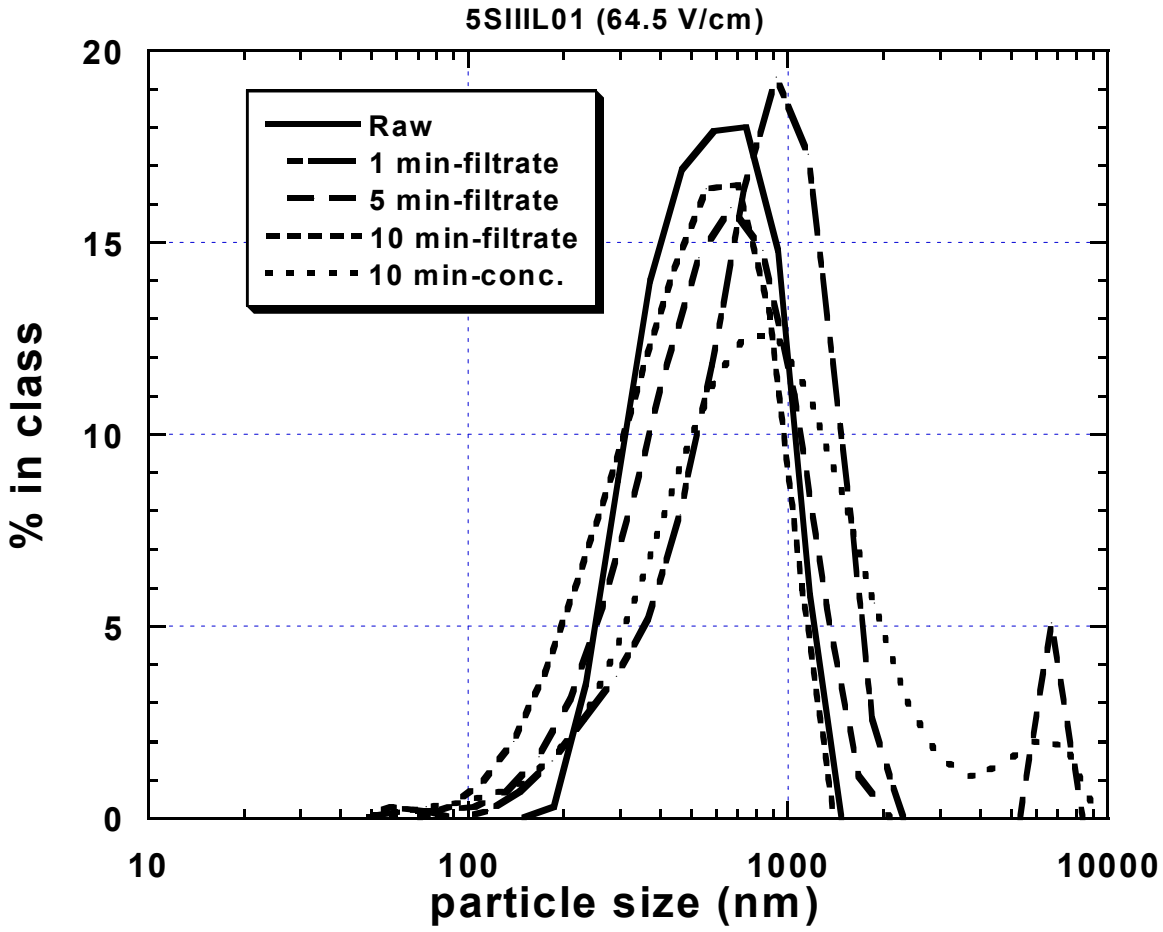

Figure A46. Change in particle size distribution during filtration operation. Experimental conditions: electrostatic field = 64.5 V/cm; pH = 6.8; Sample: 5SIIIL01

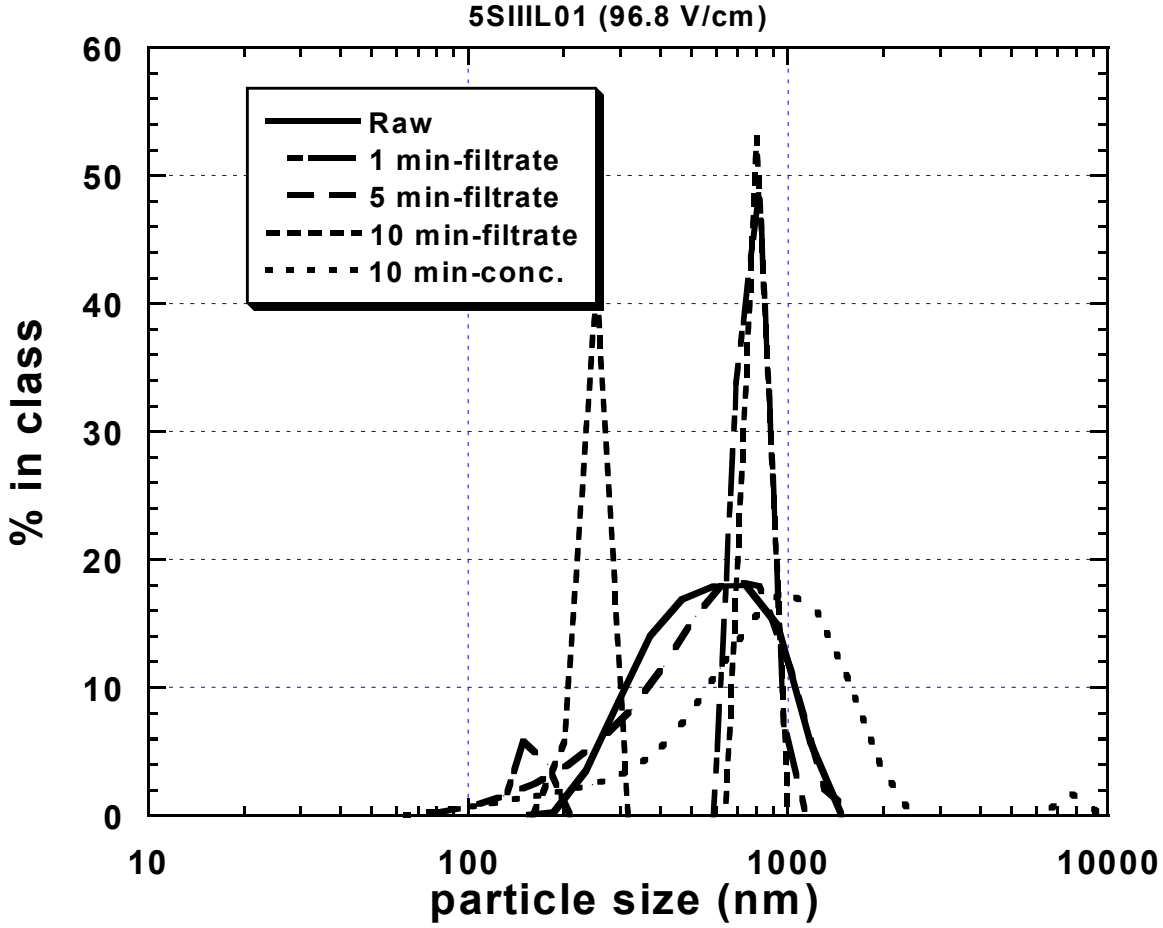

Figure A47. Change in particle size distribution during filtration operation. Experimental conditions: electrostatic field = 96.8 V/cm; pH = 6.8; Sample: 5SIIIL01

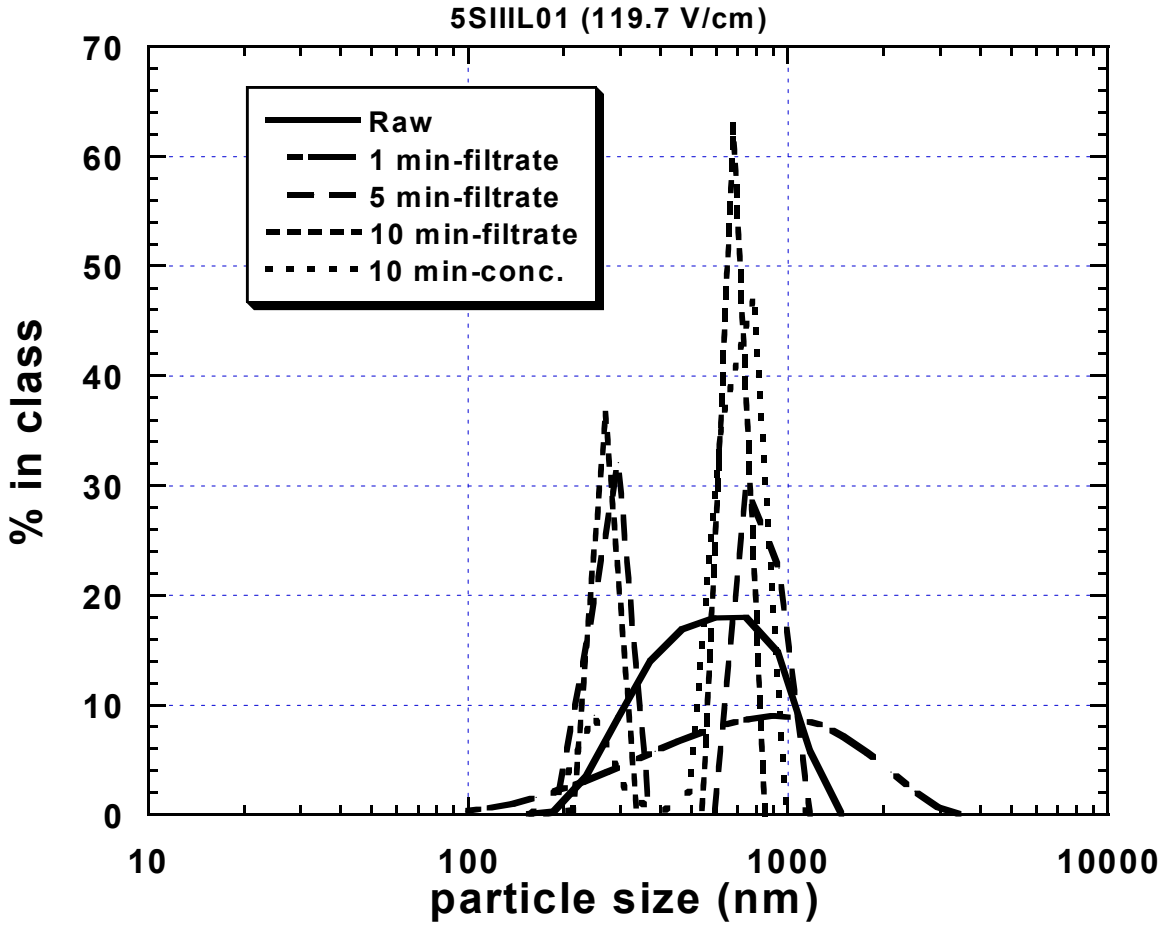

Figure A48. Change in particle size distribution during filtration operation. Experimental conditions: electrostatic field = 119.7 V/cm; pH = 6.8; Sample: 5SIIIL01

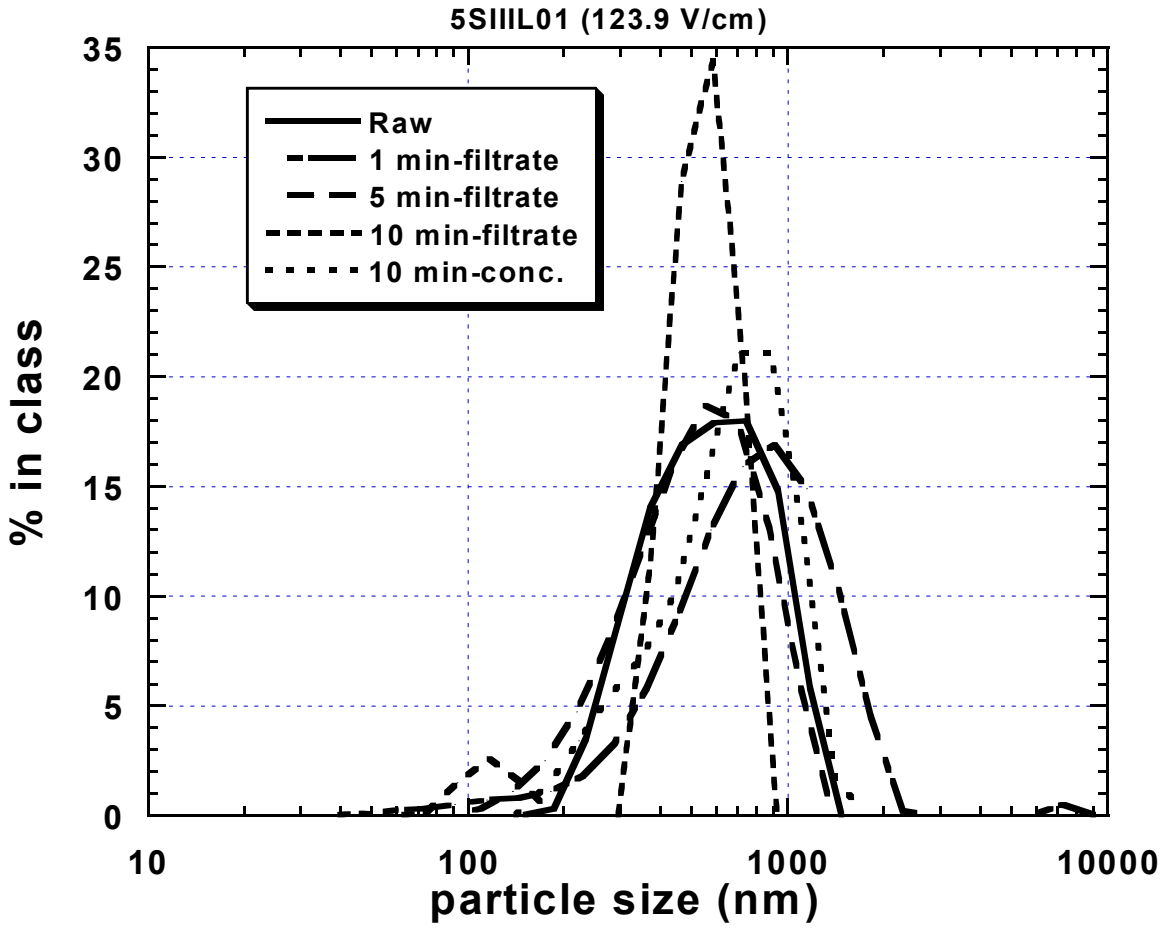

Figure A49. Change in particle size distribution during filtration operation. Experimental conditions: electrostatic field = 123.9 V/cm; pH = 6.8; Sample: 5SIIIL01

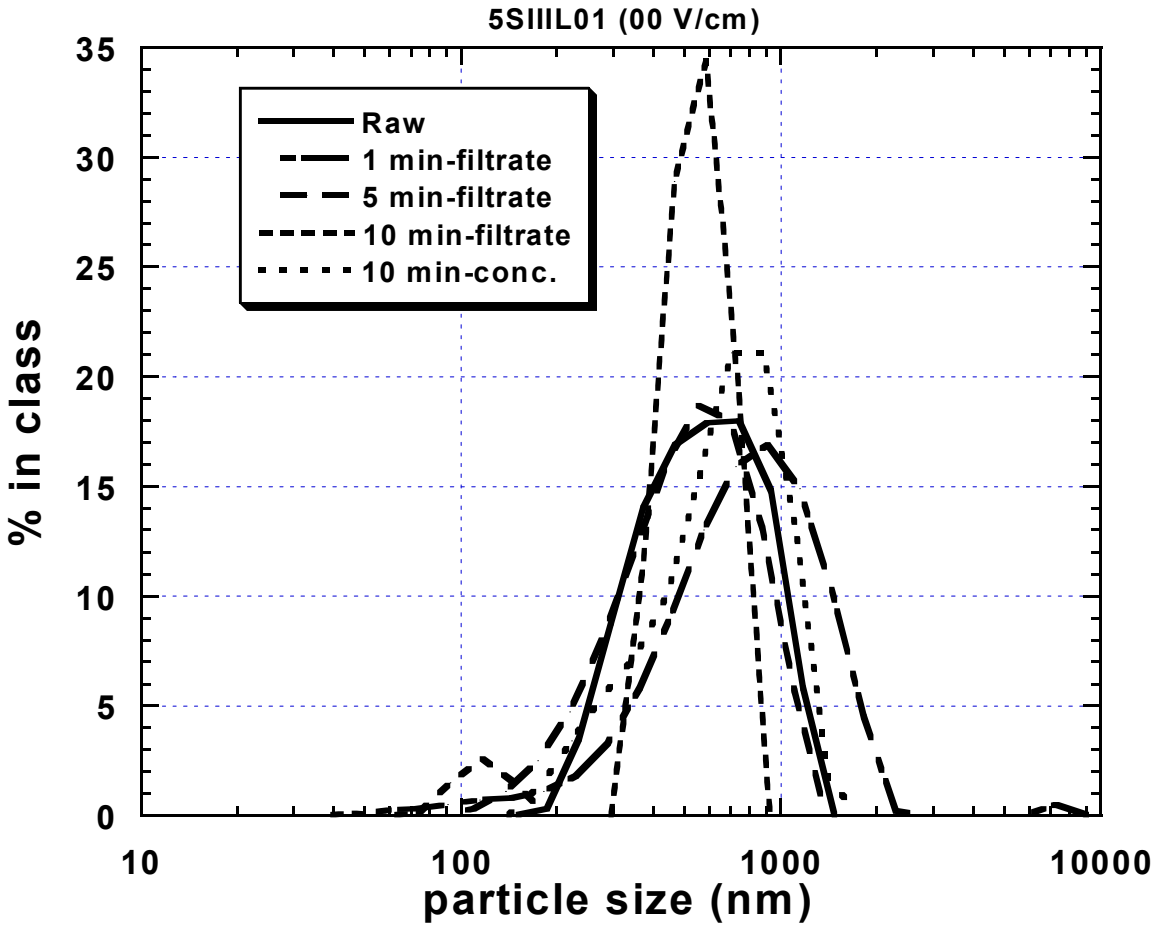

Figure A50. Change in particle size distribution during filtration operation. Experimental conditions: electrostatic field = 00 V/cm; pH = 6.6; Sample: 5SIIIL01

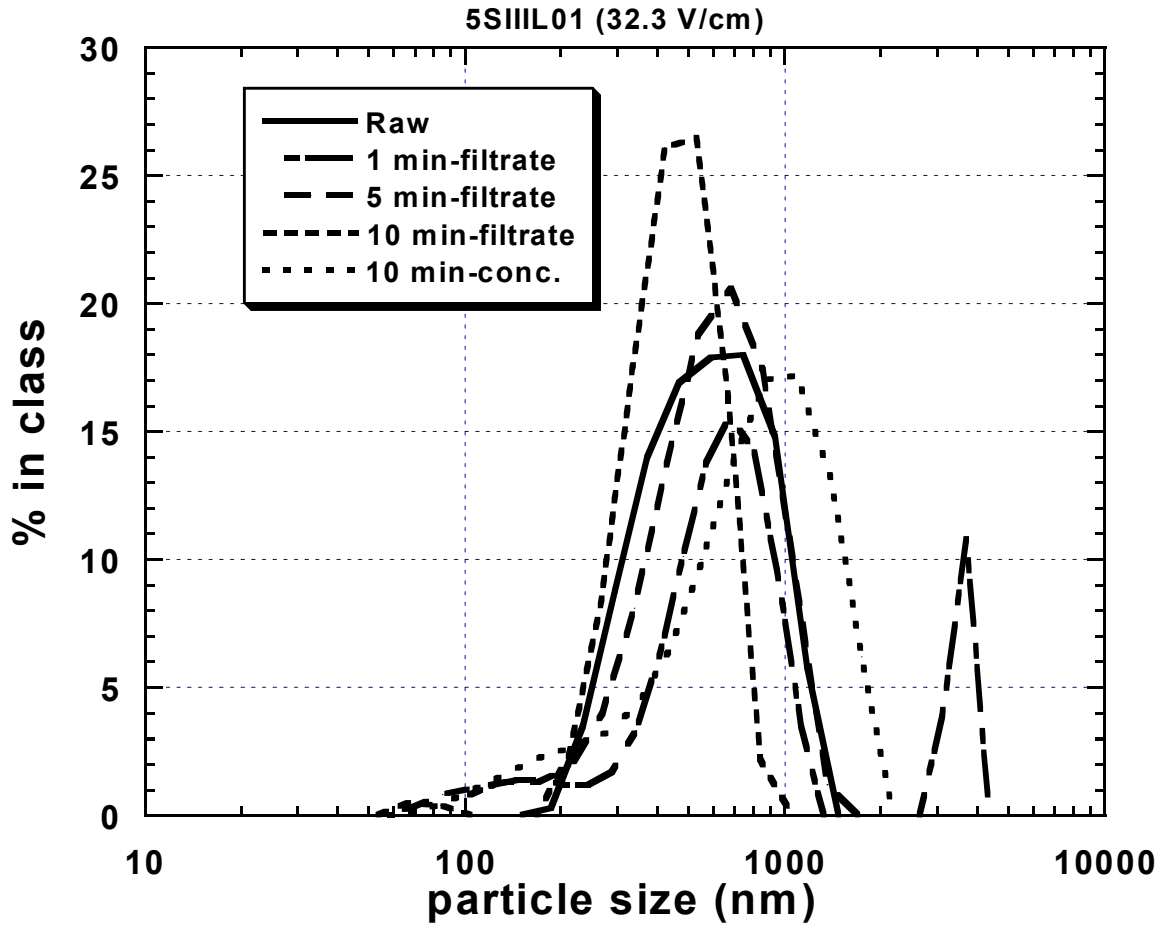

Figure A51. Change in particle size distribution during filtration operation. Experimental conditions: electrostatic field = 32.3 V/cm; pH = 6.6; Sample: 5SIIIL01

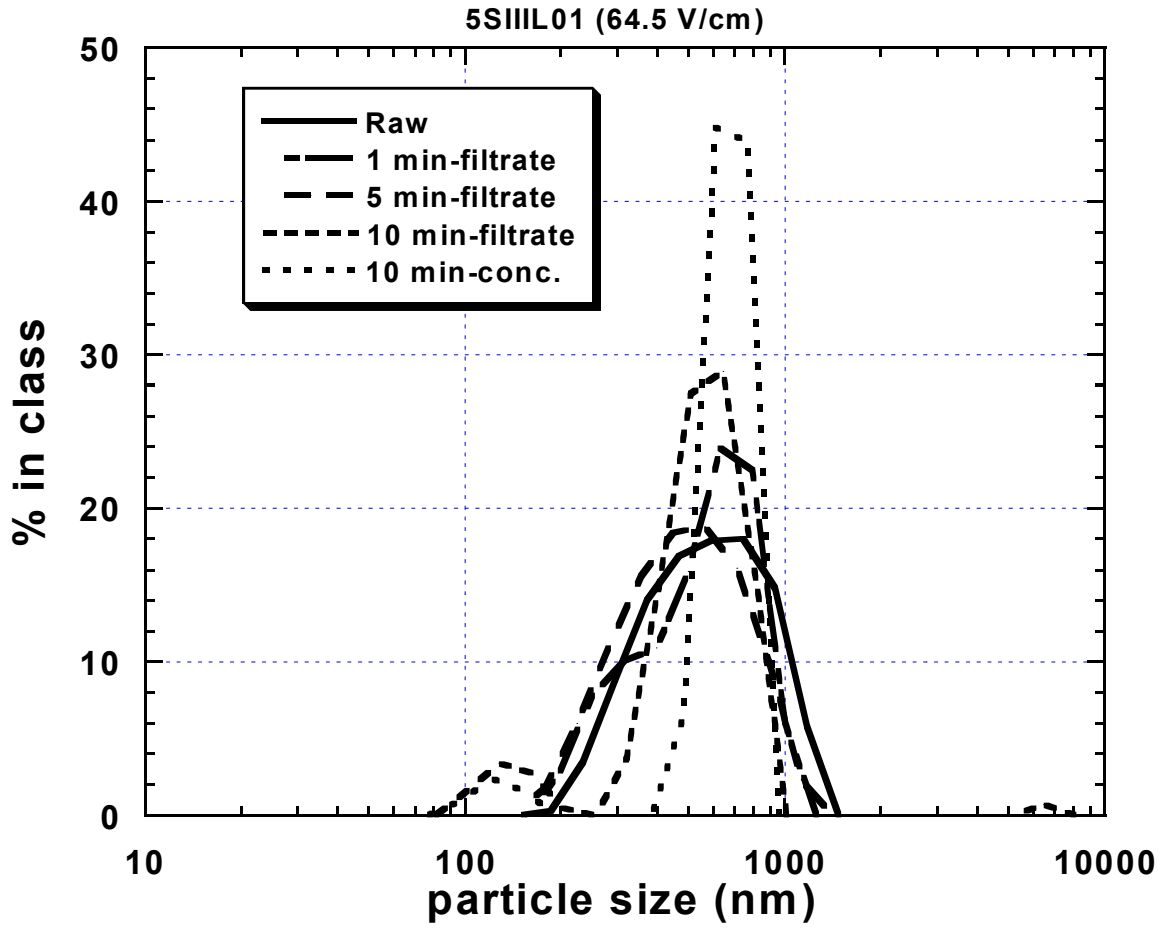

Figure A52. Change in particle size distribution during filtration operation. Experimental conditions: electrostatic field = 64.5 V/cm; pH = 6.6; Sample: 5SIIIL01

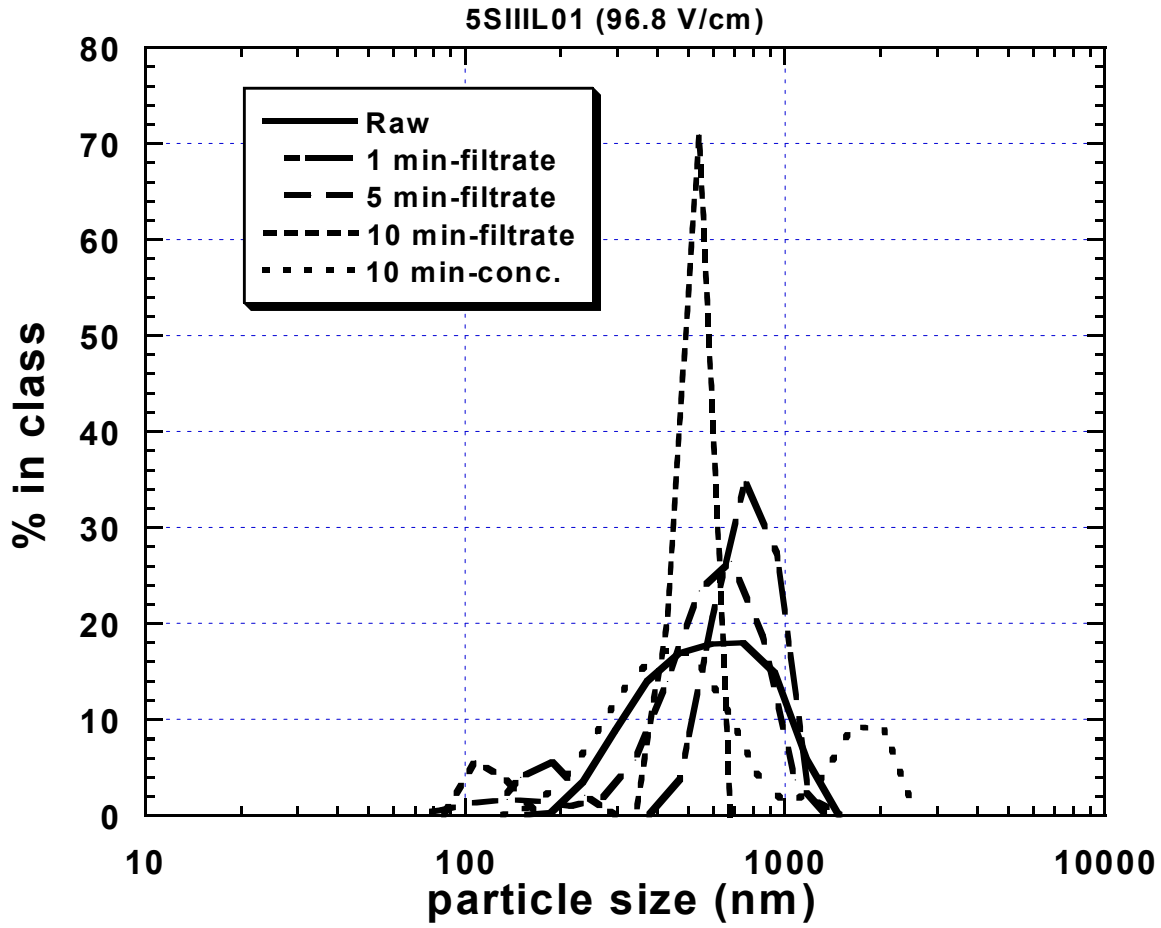

Figure A53. Change in particle size distribution during filtration operation. Experimental conditions: electrostatic field = 96.8 V/cm; pH = 6.6; Sample: 5SIIIL01

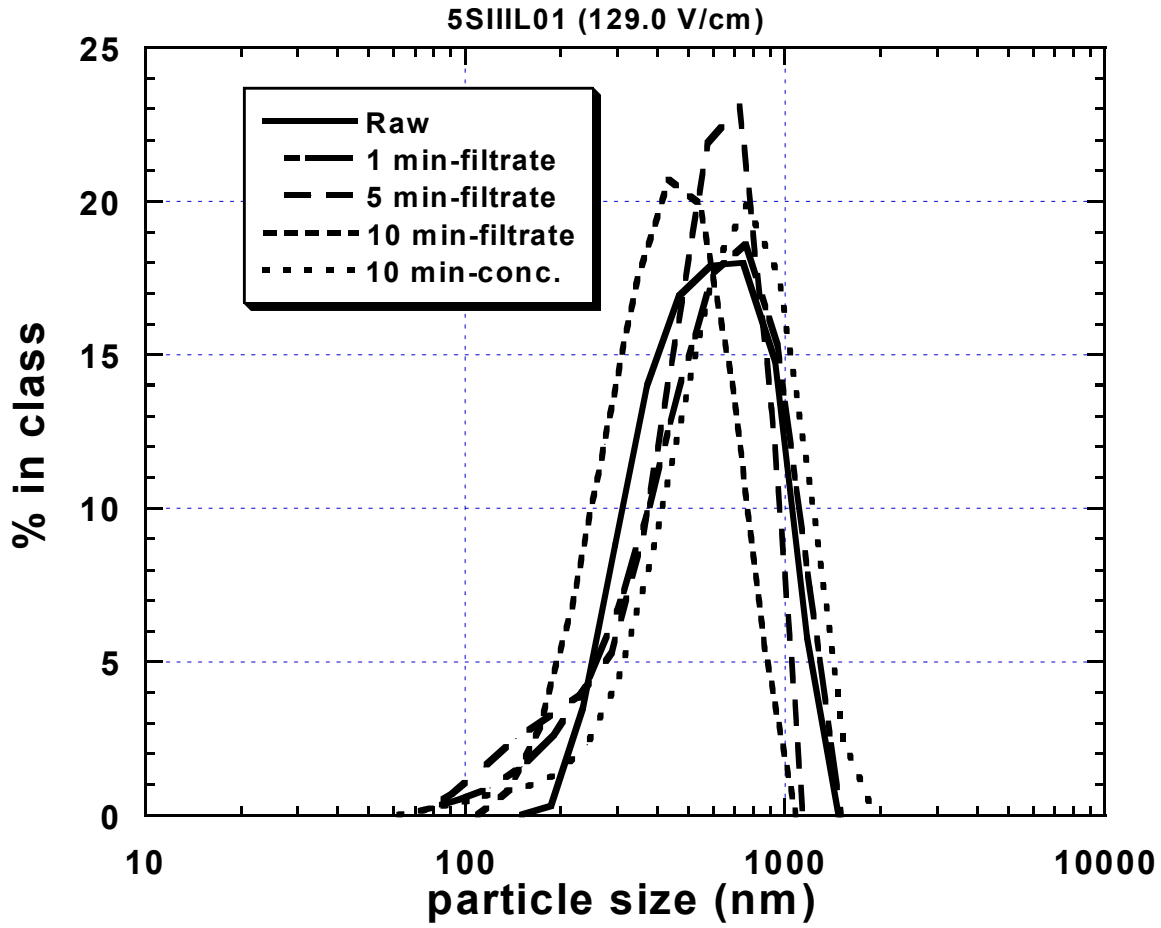

Figure A54. Change in particle size distribution during filtration operation. Experimental conditions: electrostatic field = 129.0 V/cm; pH = 6.6; Sample: 5SIIIL01

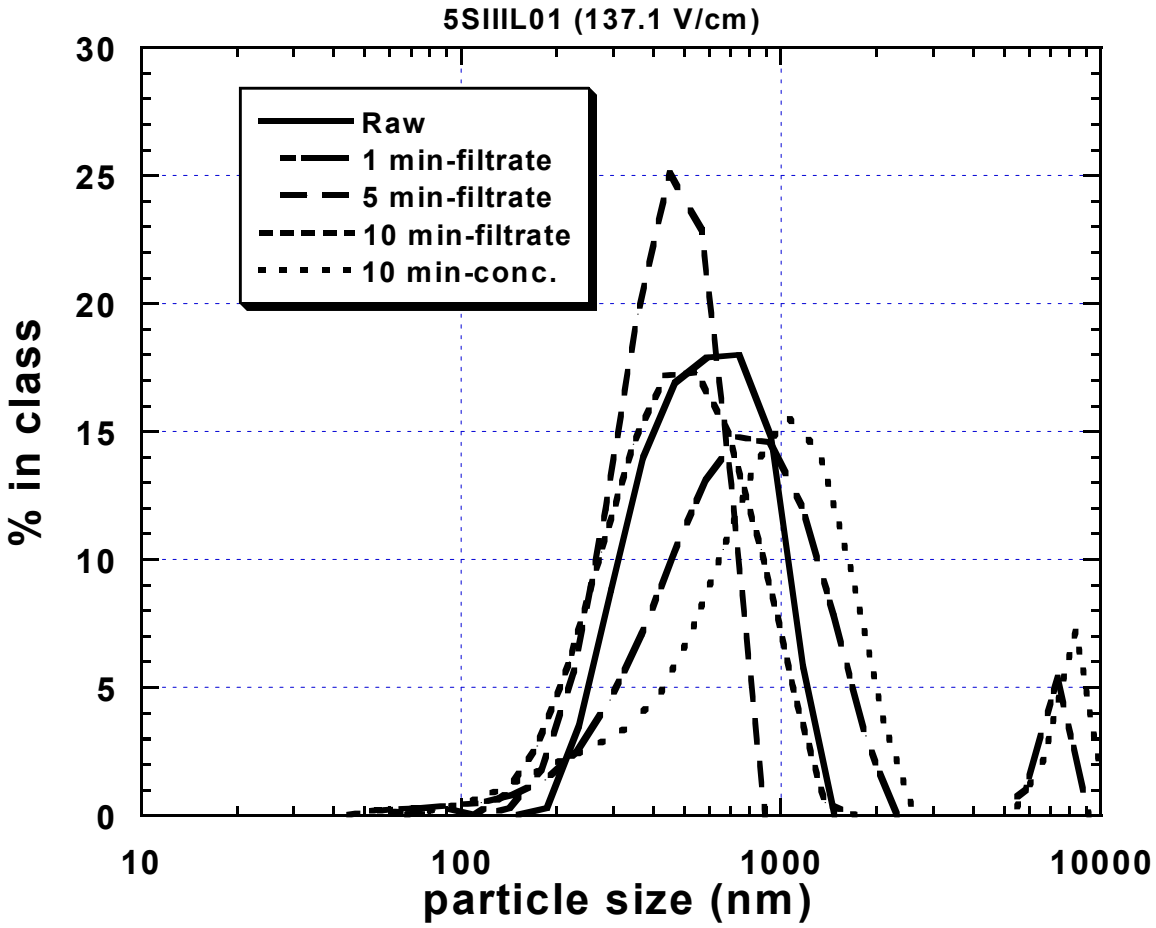

Figure A55. Change in particle size distribution during filtration operation. Experimental conditions: electrostatic field = 137.1 V/cm; pH = 6.6; Sample: 5SIIIL01

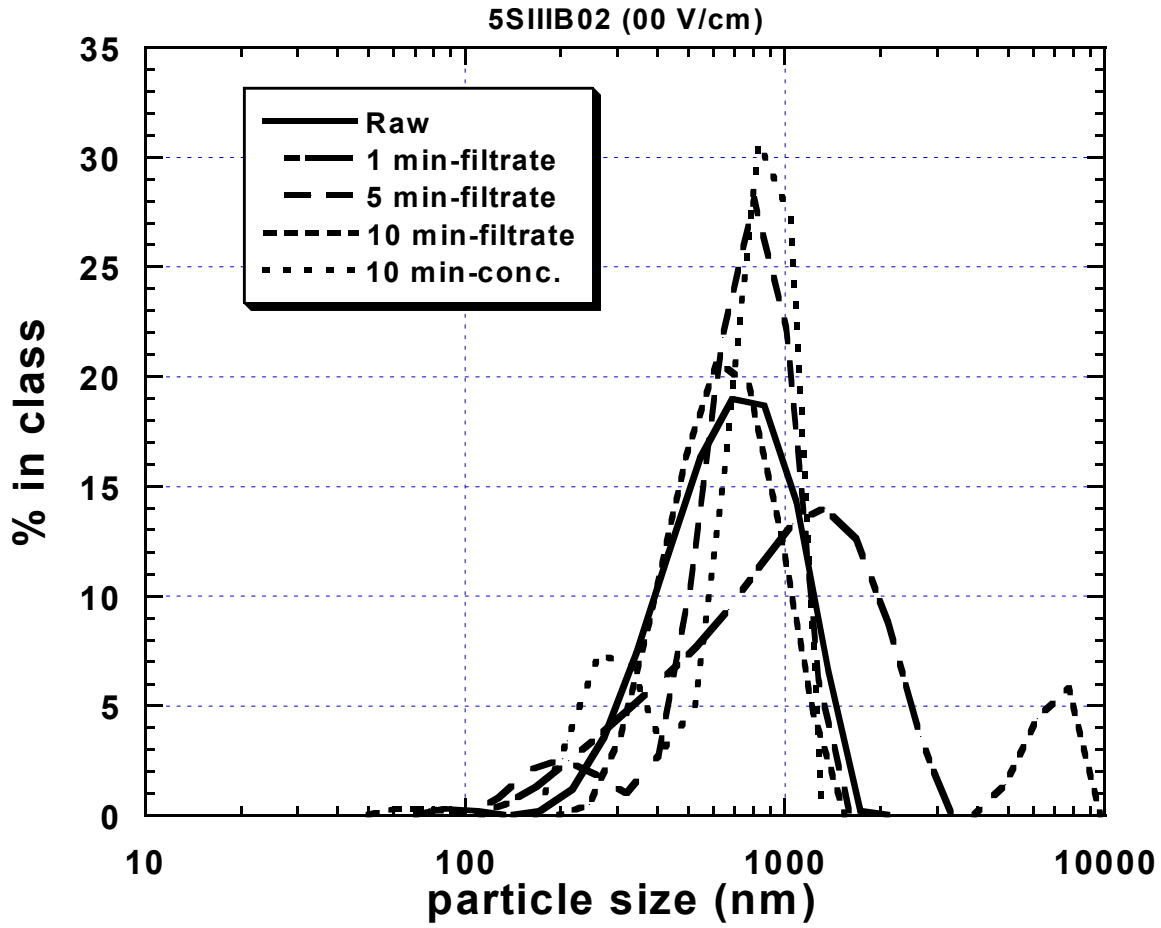

Figure A56. Change in particle size distribution during filtration operation. Experimental conditions: electrostatic field = 00 V/cm; pH = 6.8; Sample: 5SIIIB02

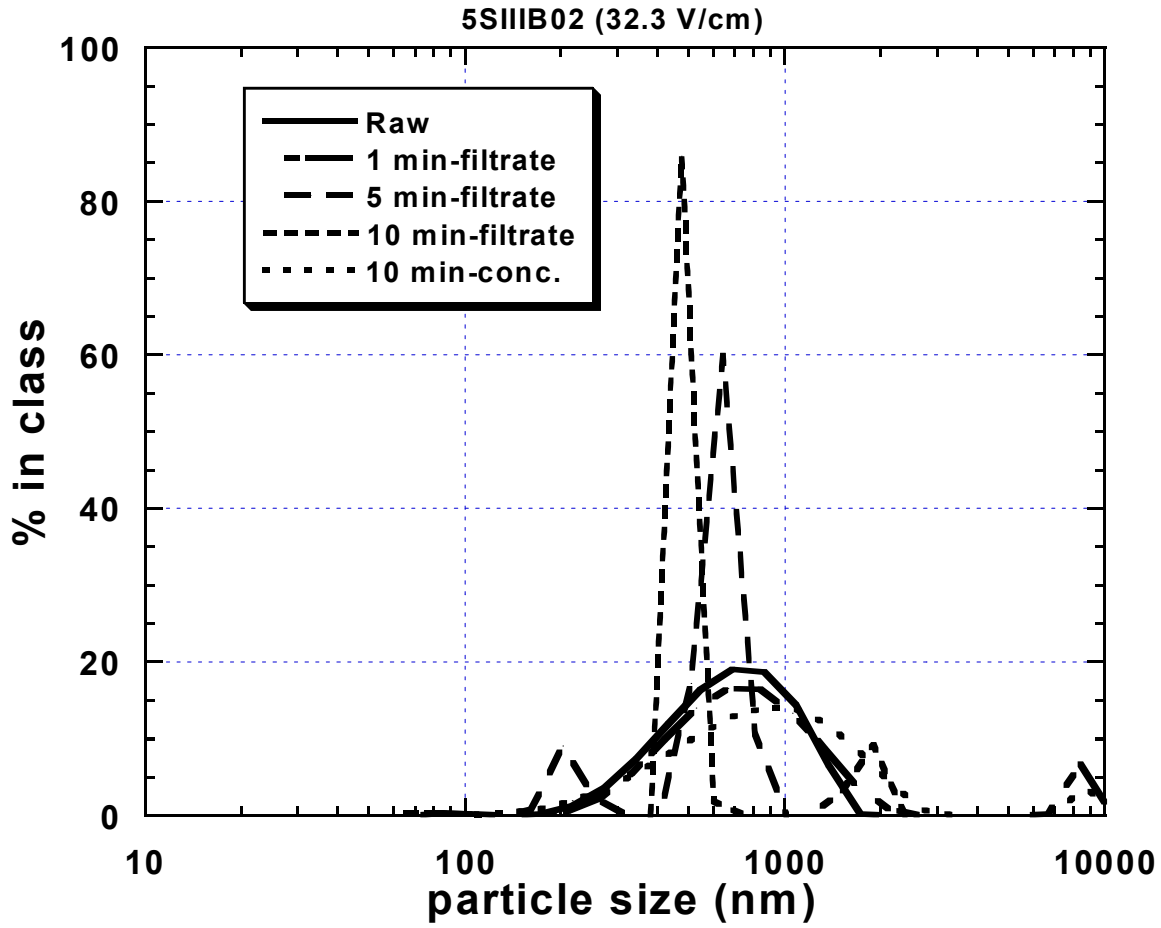

Figure A57. Change in particle size distribution during filtration operation. Experimental conditions: electrostatic field = 32.3 V/cm; pH = 6.8; Sample: 5SIIIB02

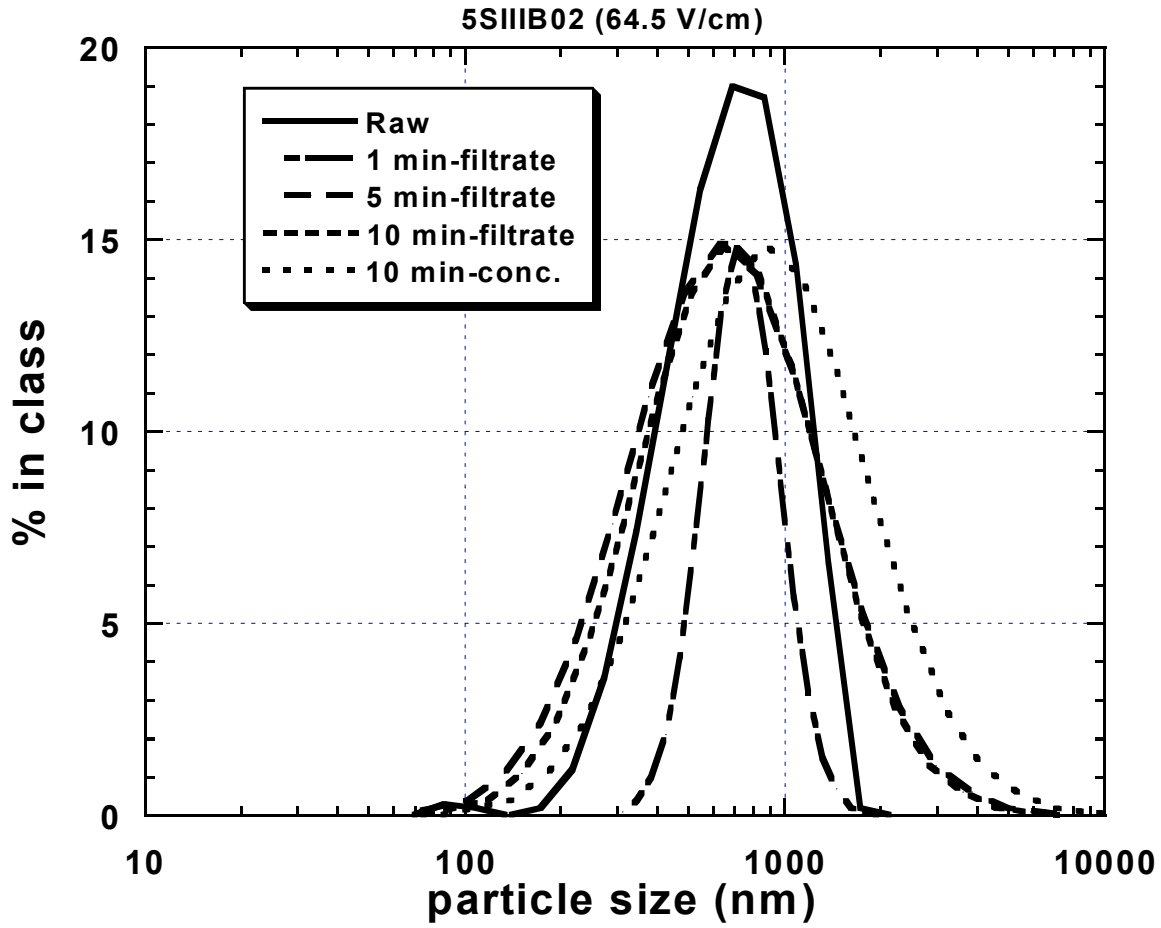

Figure A58. Change in particle size distribution during filtration operation. Experimental conditions: electrostatic field = 64.5 V/cm; pH = 6.8; Sample: 5SIIIB02

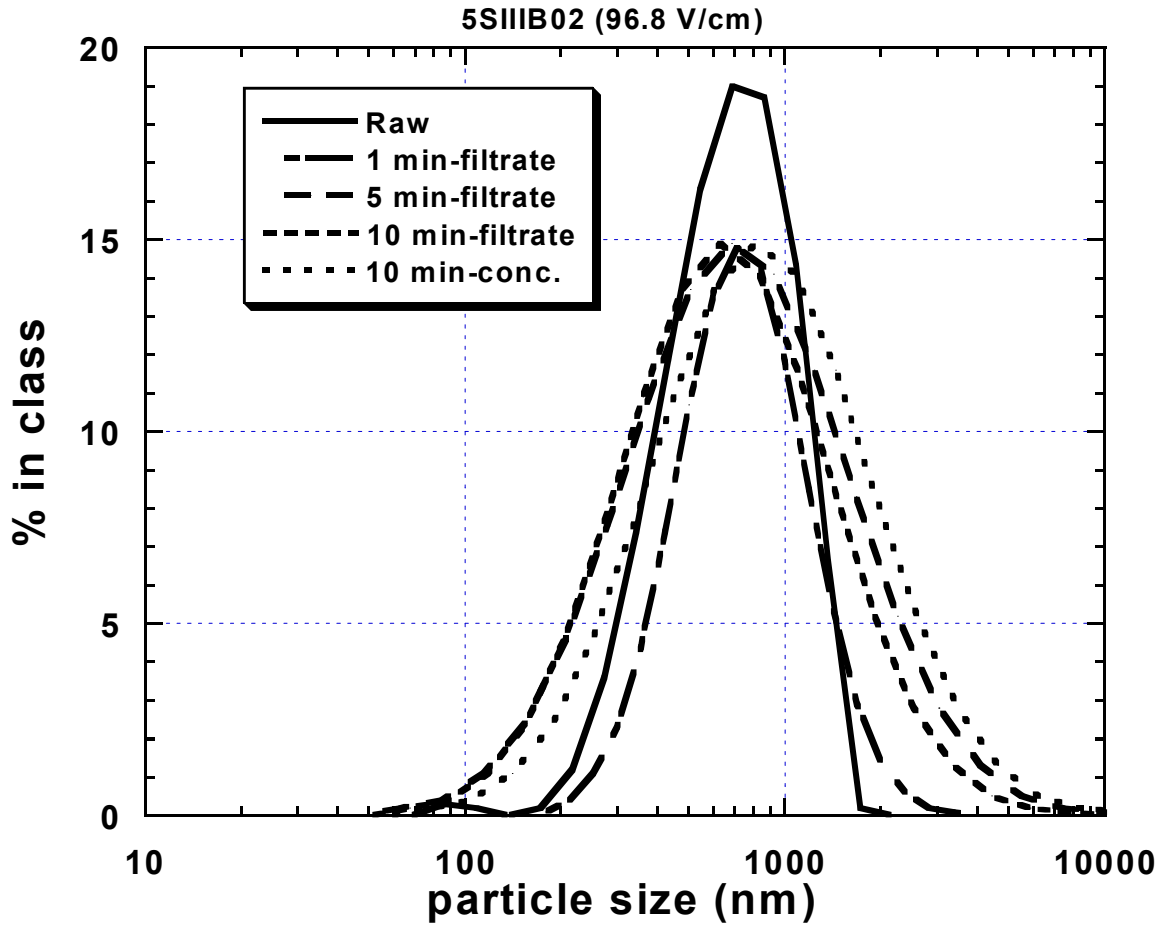

Figure A59. Change in particle size distribution during filtration operation. Experimental conditions: electrostatic field = 96.8 V/cm; pH = 6.8; Sample: 5SIIIB02

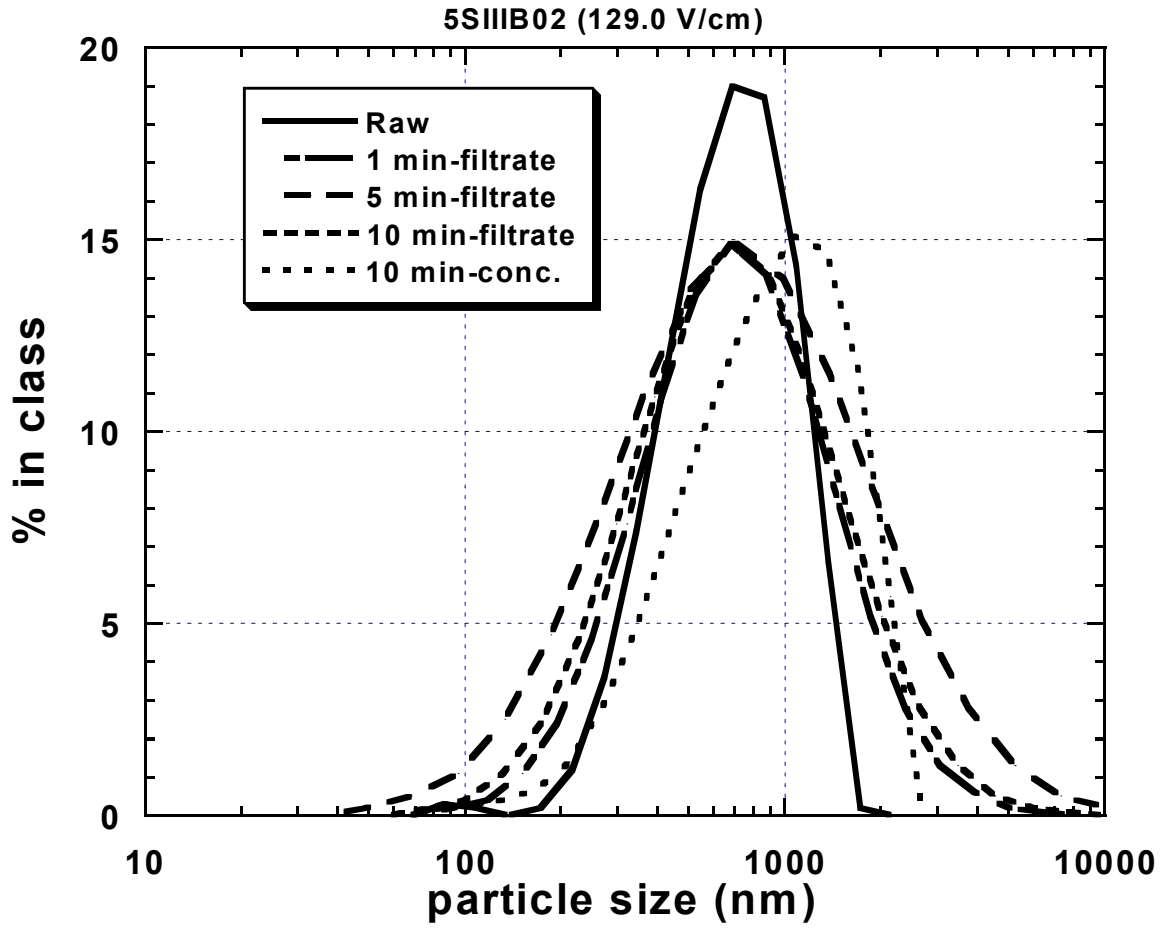

Figure A60. Change in particle size distribution during filtration operation. Experimental conditions: electrostatic field = 129.0 V/cm; pH = 6.8; Sample: 5SIIIB02

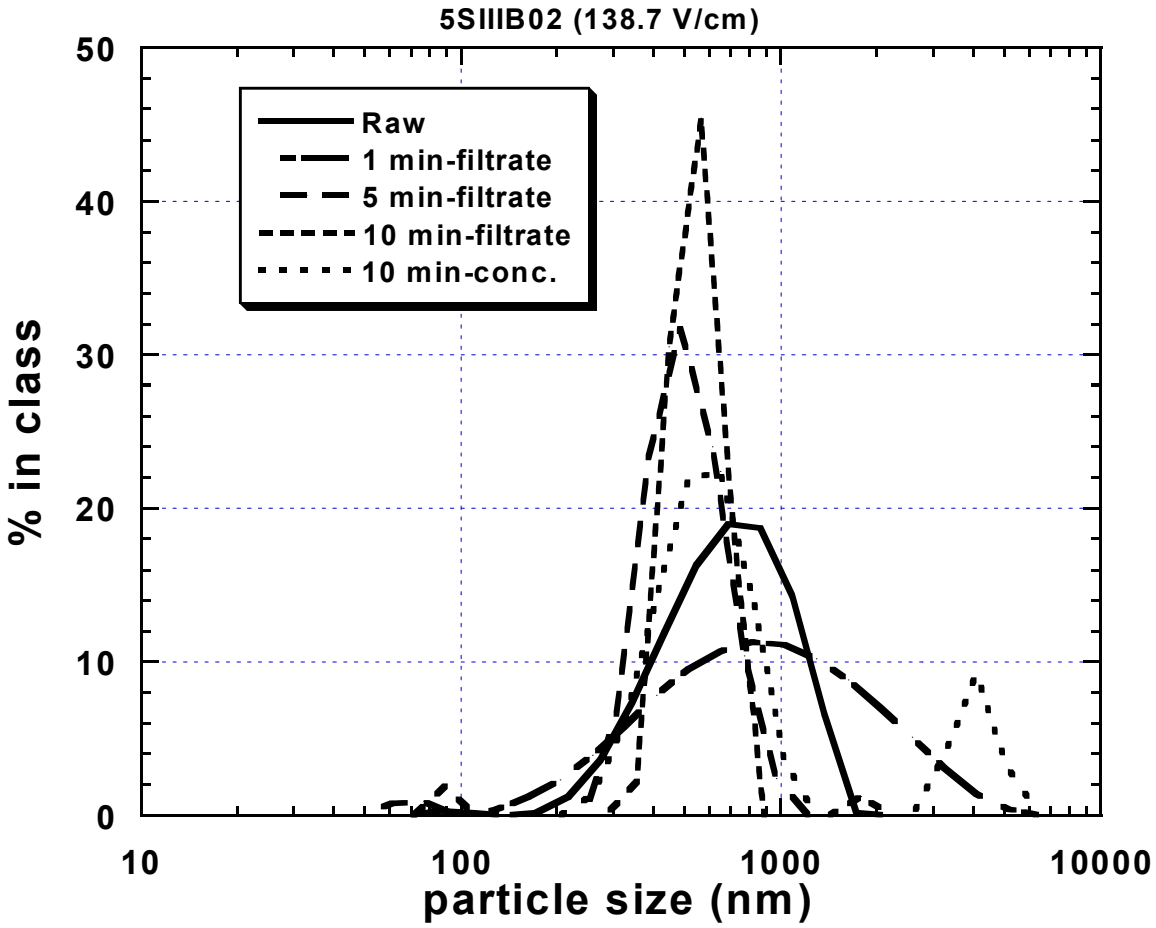

Figure A61. Change in particle size distribution during filtration operation. Experimental conditions: electrostatic field 138.7 V/cm; pH = 6.8; Sample: 5SIIIB02

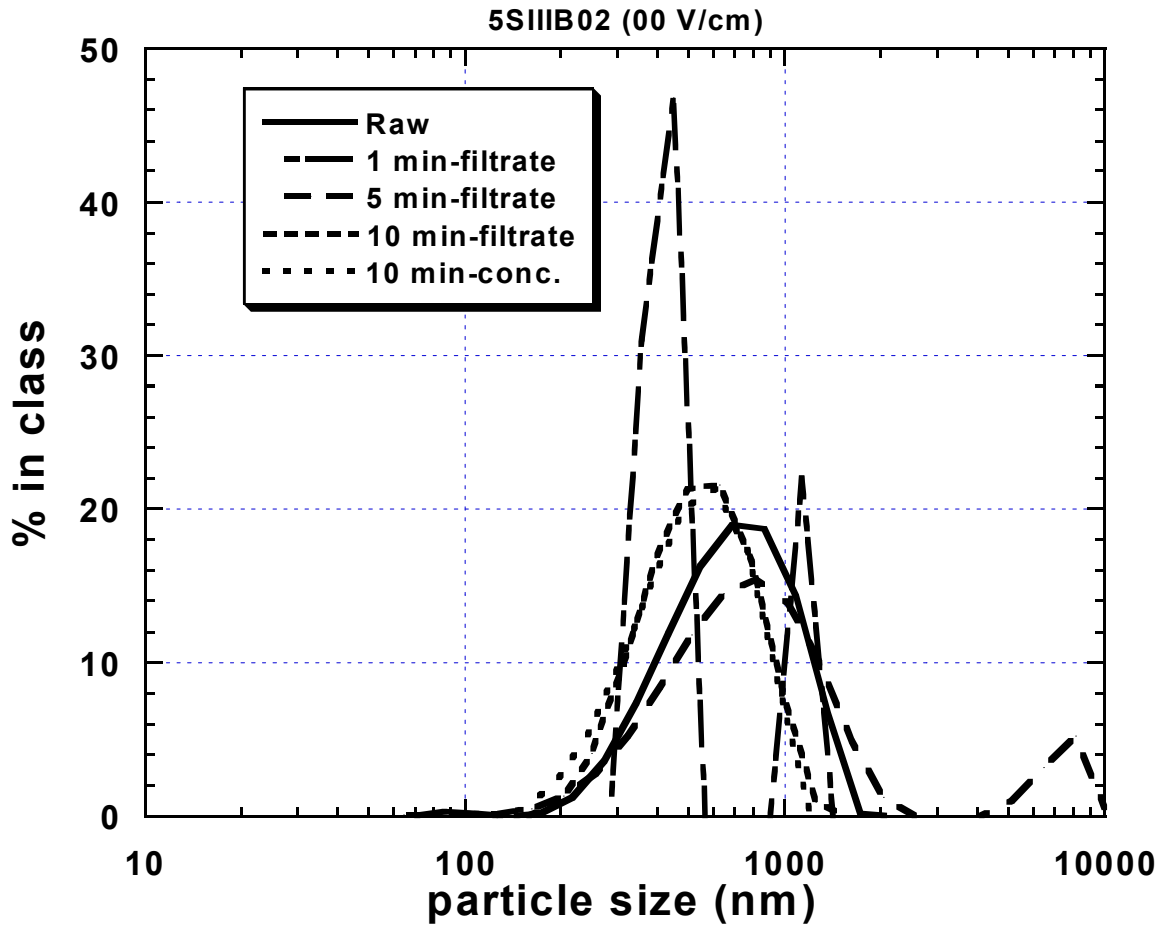

Figure A62. Change in particle size distribution during filtration operation. Experimental conditions: electrostatic field = 00 V/cm; pH = 6.6; Sample: 5SIIIB02

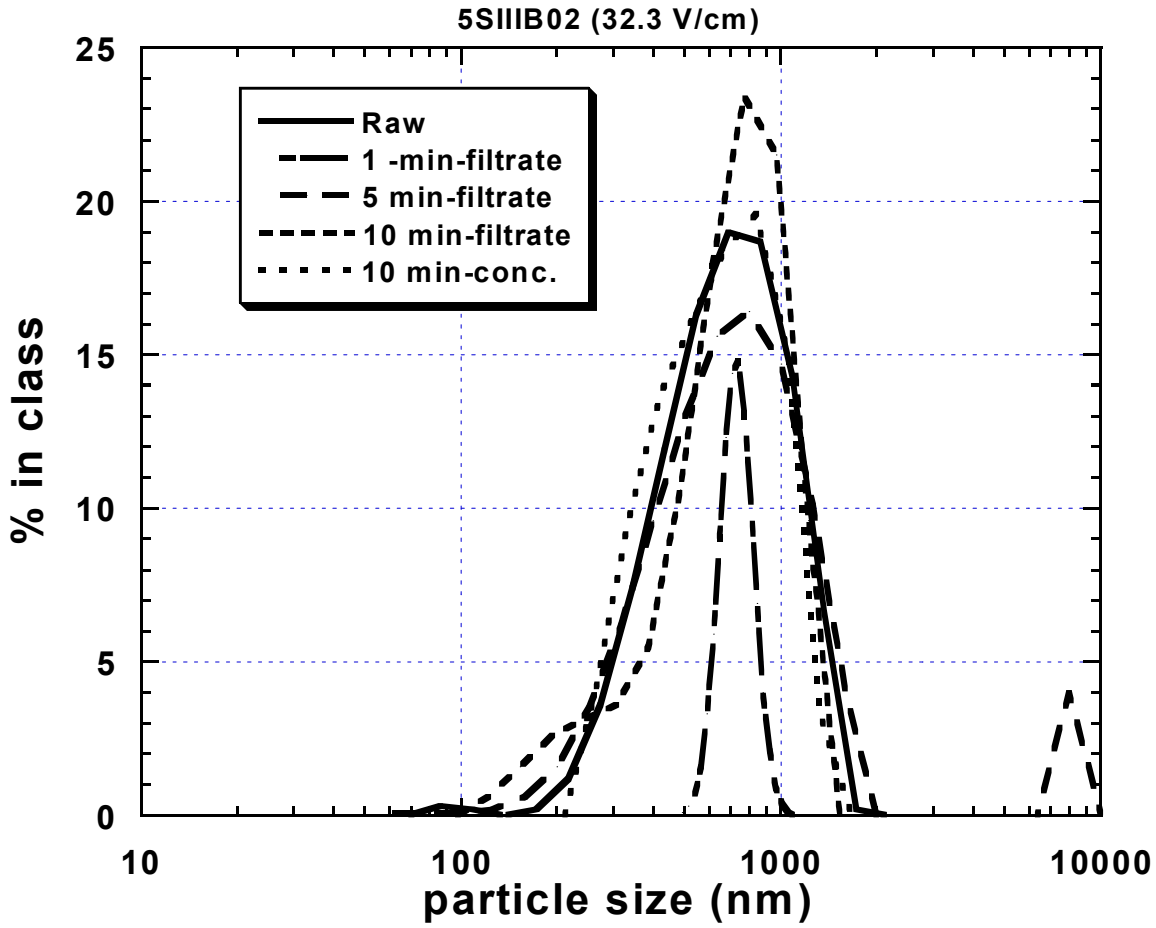

Figure A63. Change in particle size distribution during filtration operation. Experimental conditions: electrostatic field = 32.3 V/cm; pH = 6.6; Sample: 5SIIIB02

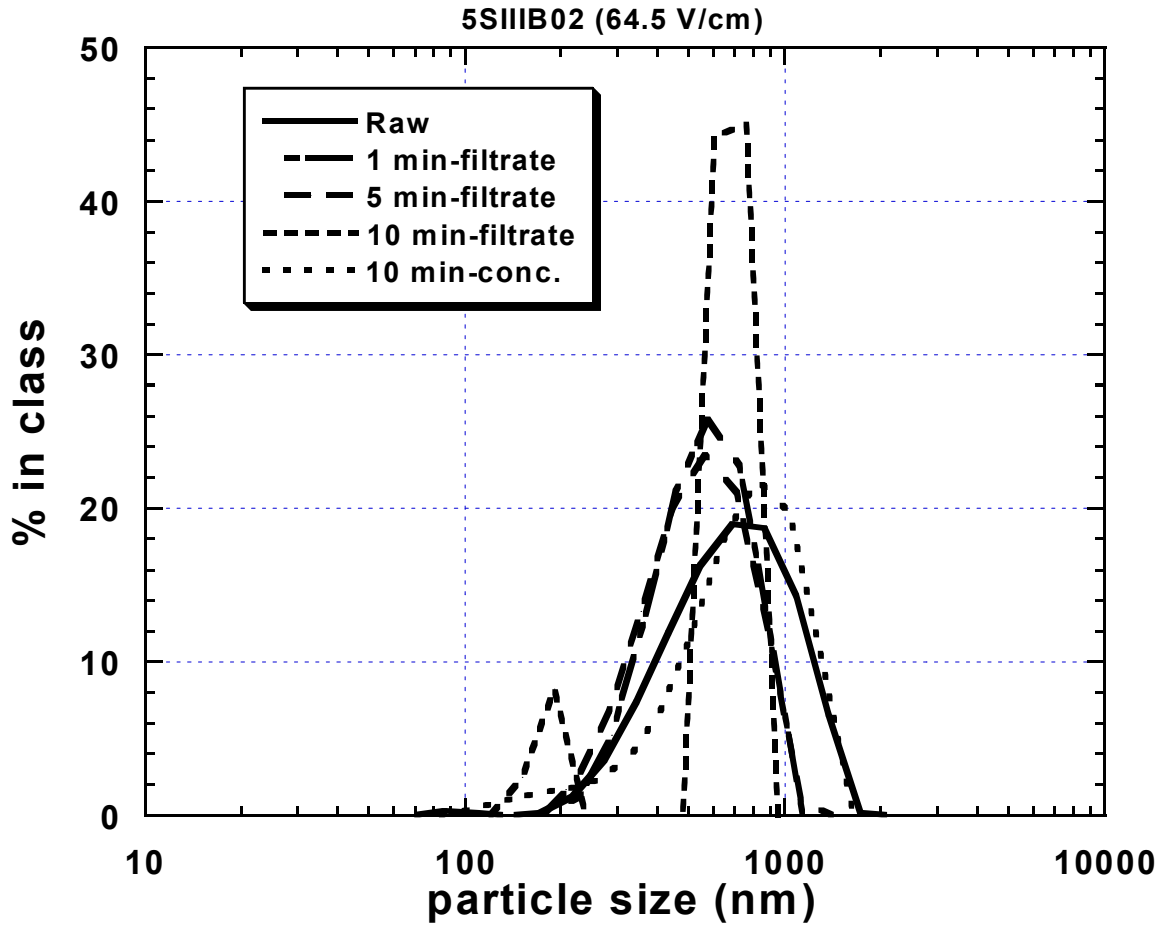

Figure A64. Change in particle size distribution during filtration operation. Experimental conditions: electrostatic field = 64.5 V/cm; pH = 6.6; Sample: 5SIIIB02

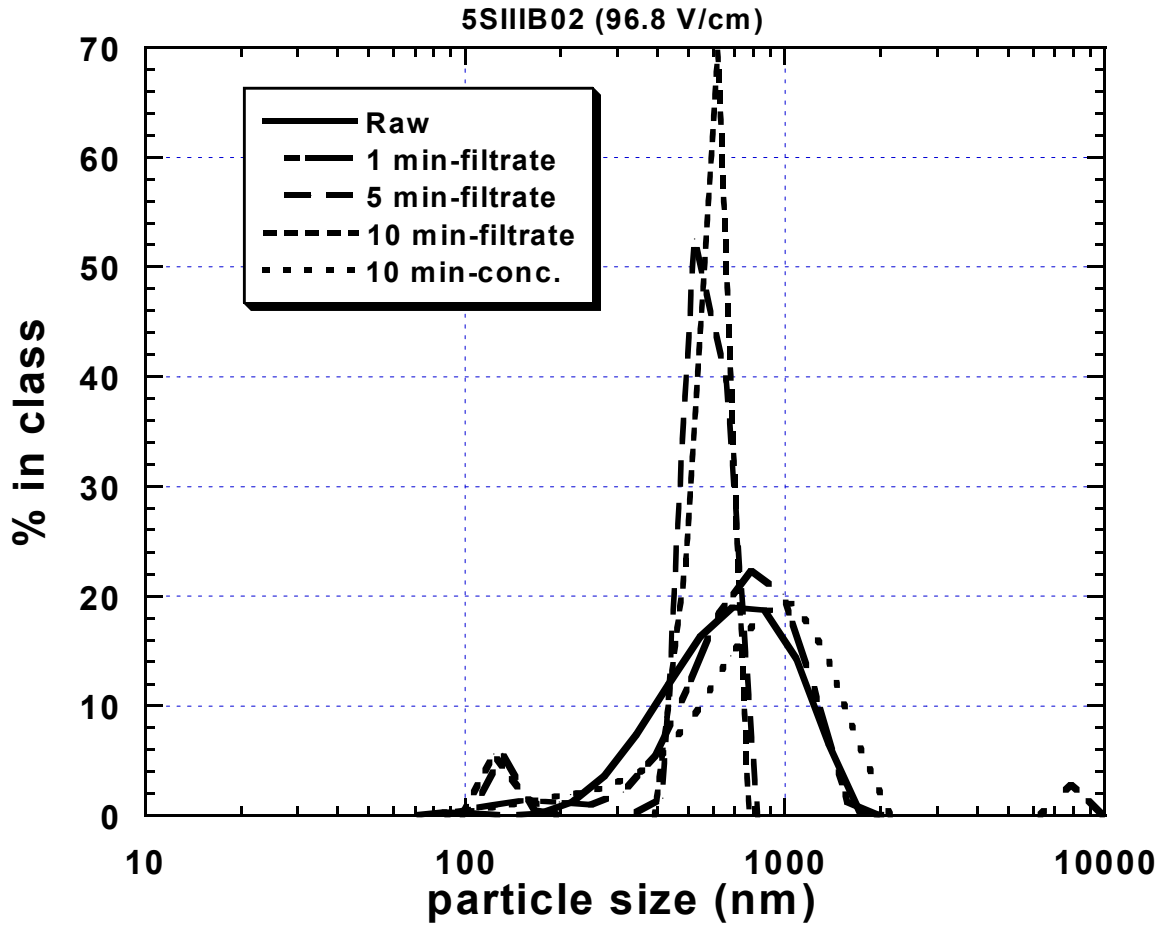

Figure A65. Change in particle size distribution during filtration operation. Experimental conditions: electrostatic field = 96.8 V/cm; pH = 6.6; Sample: 5SIIIB02

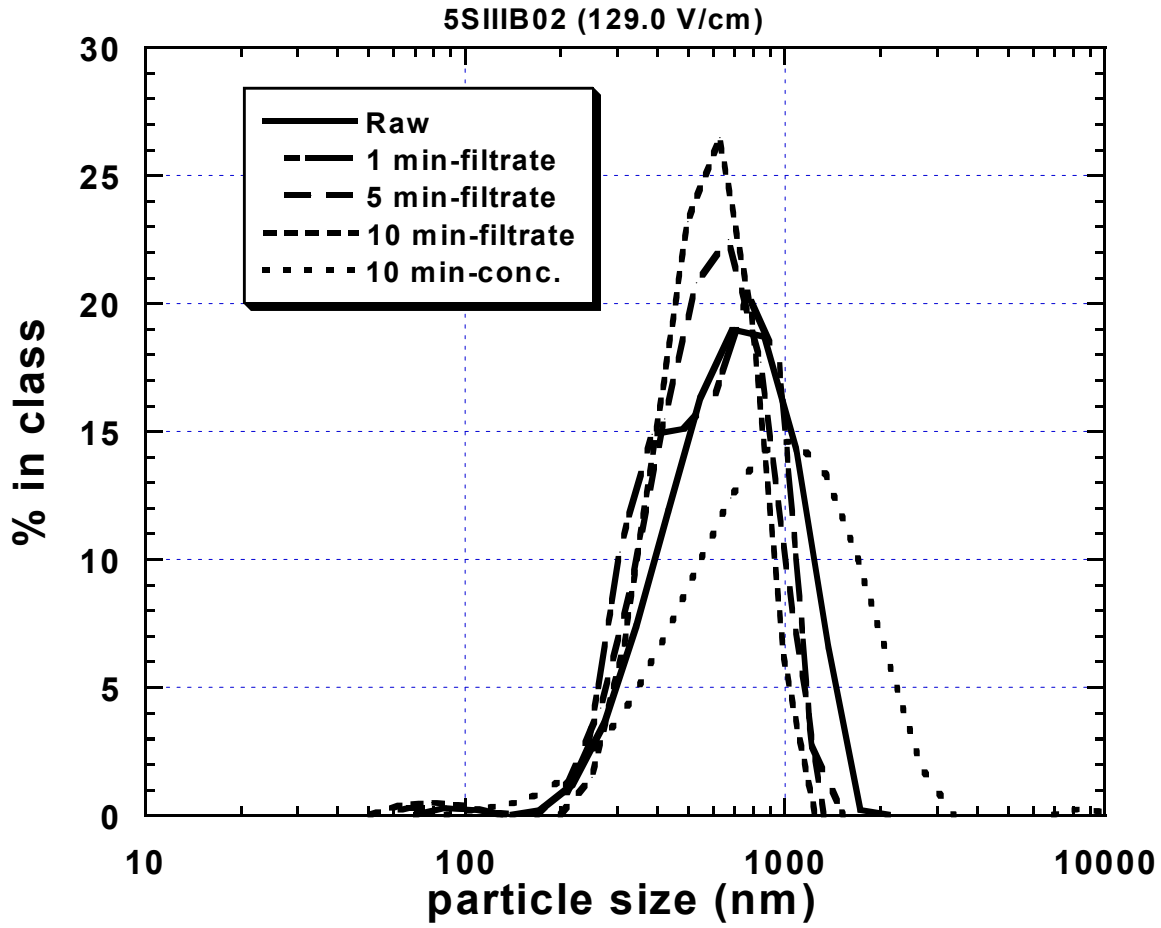

Figure A66. Change in particle size distribution during filtration operation. Experimental conditions: electrostatic field = 129.0V/cm; pH = 6.6; Sample: 5SIIIB02

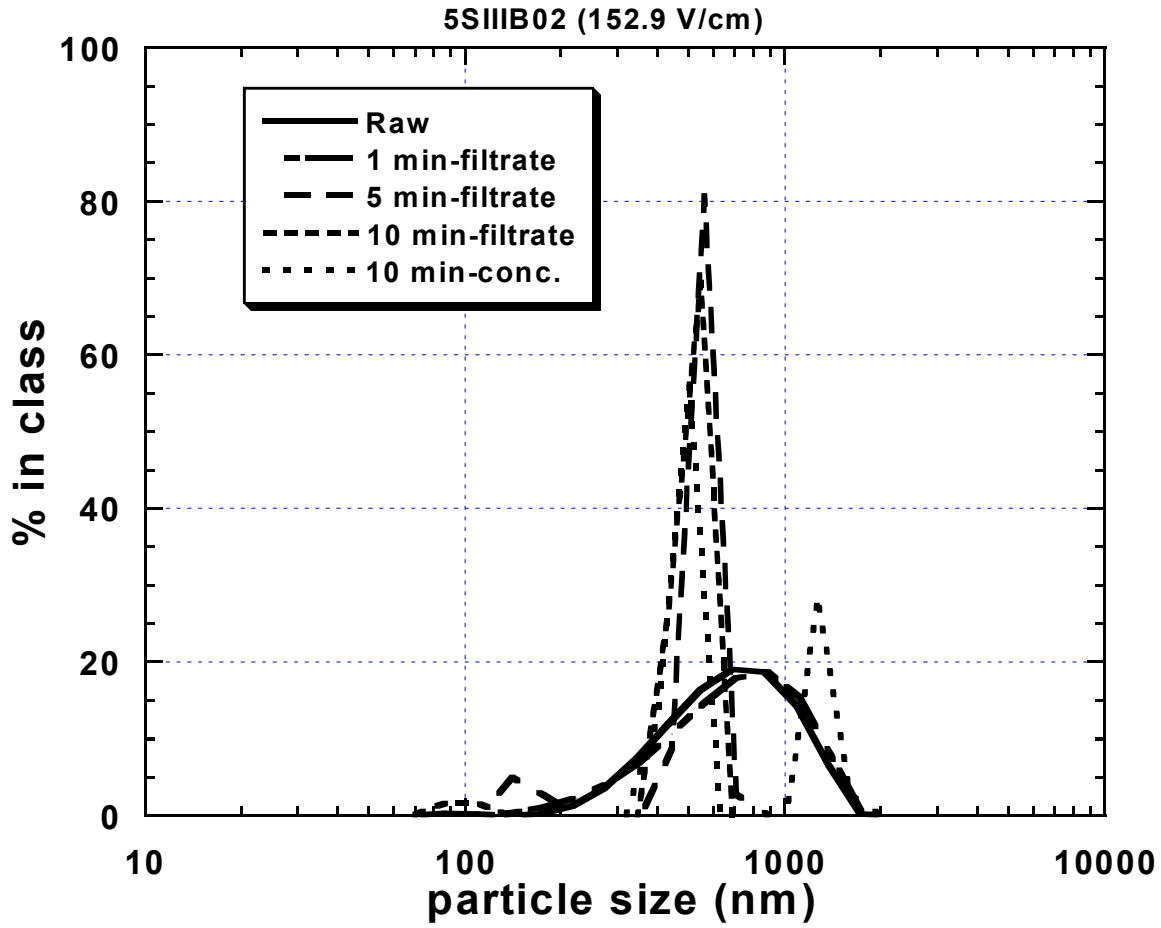

Figure A67. Change in particle size distribution during filtration operation. Experimental conditions: electrostatic field = 152.9 V/cm; pH = 6.6; Sample: 5SIIIB02

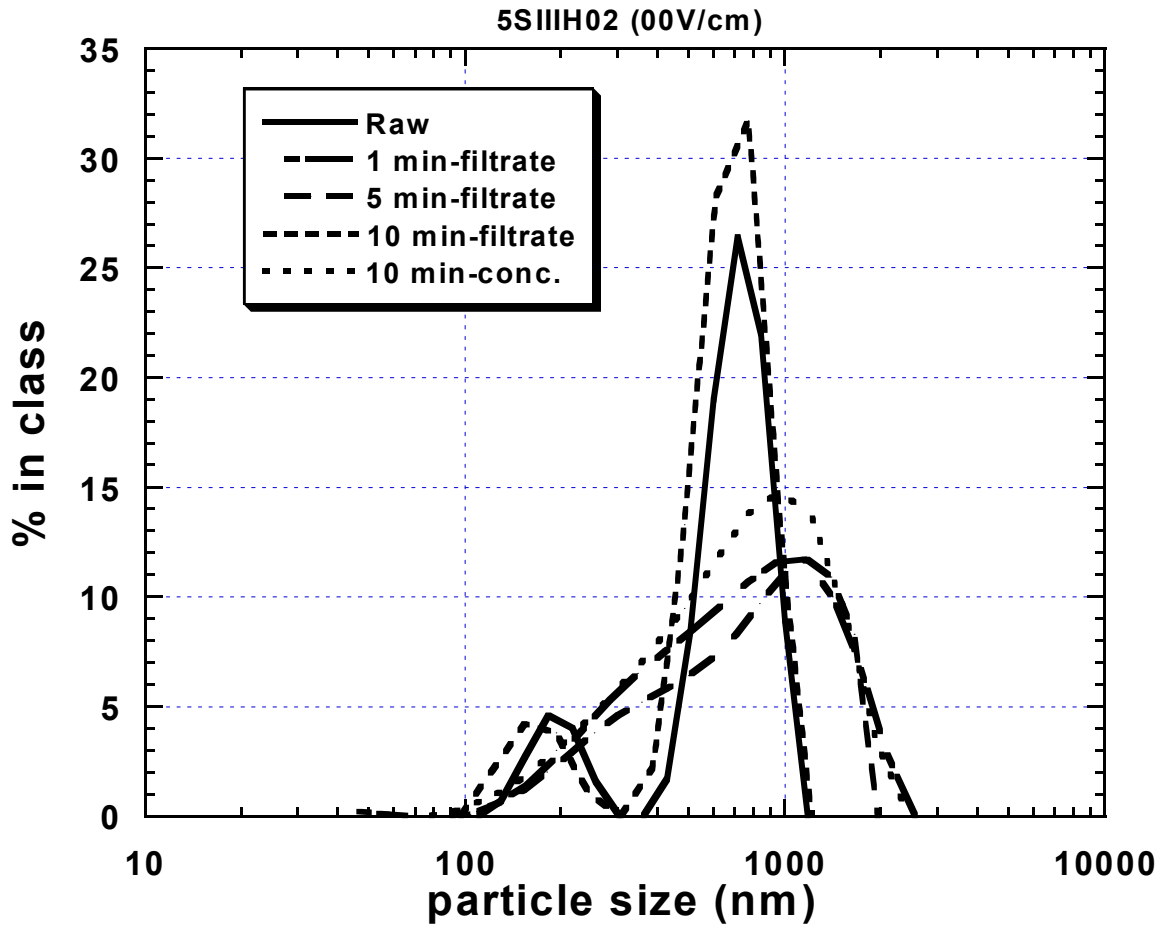

Figure A68. Change in particle size distribution during filtration operation. Experimental conditions: electrostatic field = 00 V/cm; pH = 7.1; Sample: 5SIIIH02

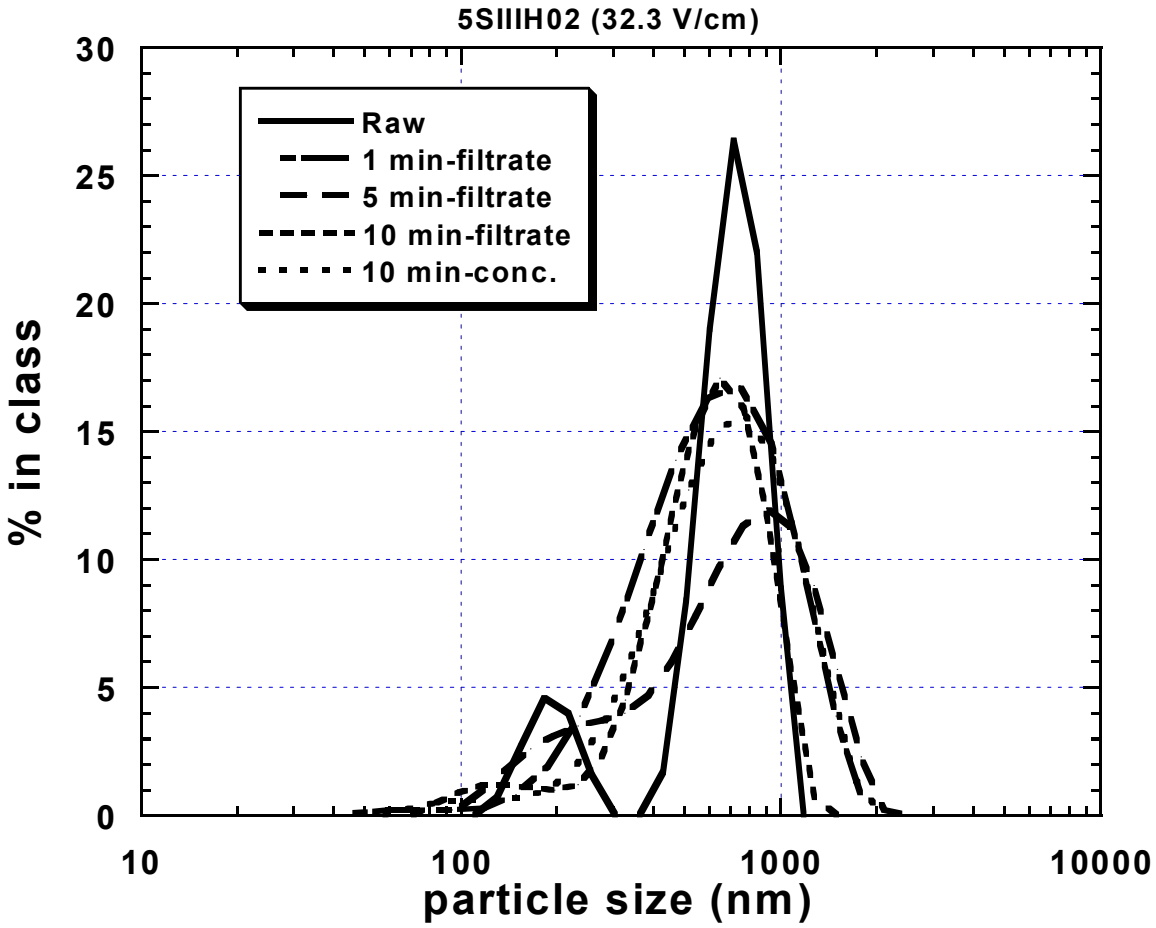

Figure A69. Change in particle size distribution during filtration operation. Experimental conditions: electrostatic field = 32.3 V/cm; pH = 7.1; Sample: 5SIIIH02

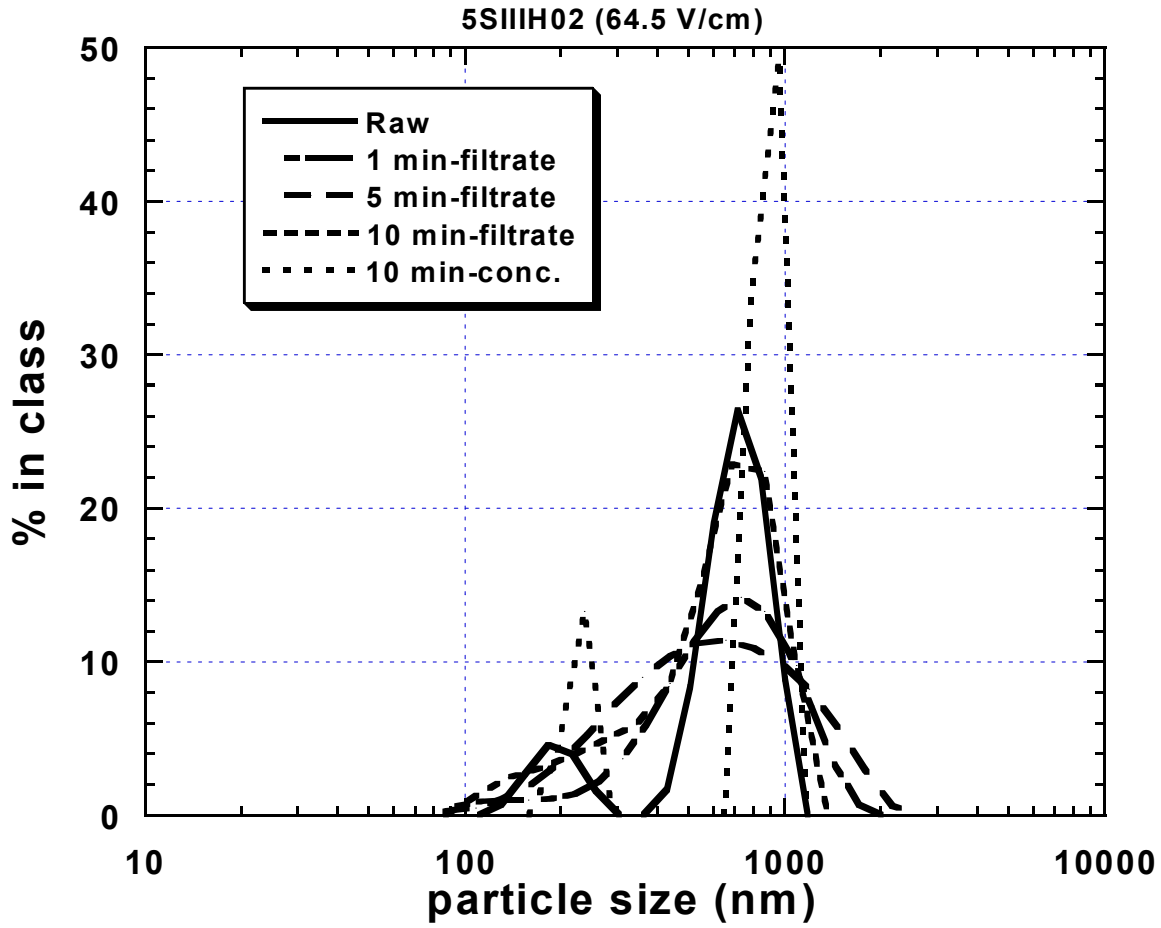

Figure A70. Change in particle size distribution during filtration operation. Experimental conditions: electrostatic field = 64.5 V/cm; pH = 7.1; Sample: 5SIIIH02

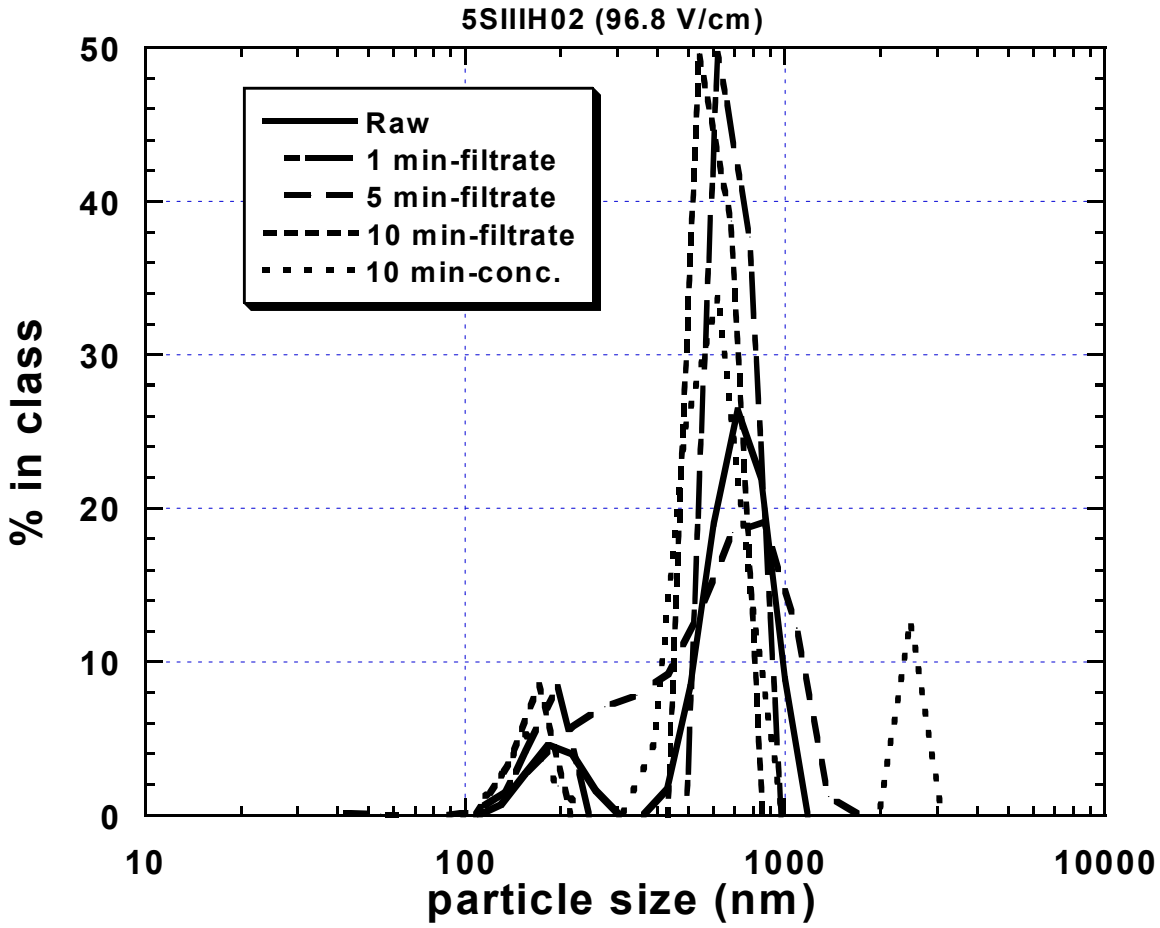

Figure A71. Change in particle size distribution during filtration operation. Experimental conditions: electrostatic field = 96.8 V/cm; pH = 7.1; Sample: 5SIIIH02

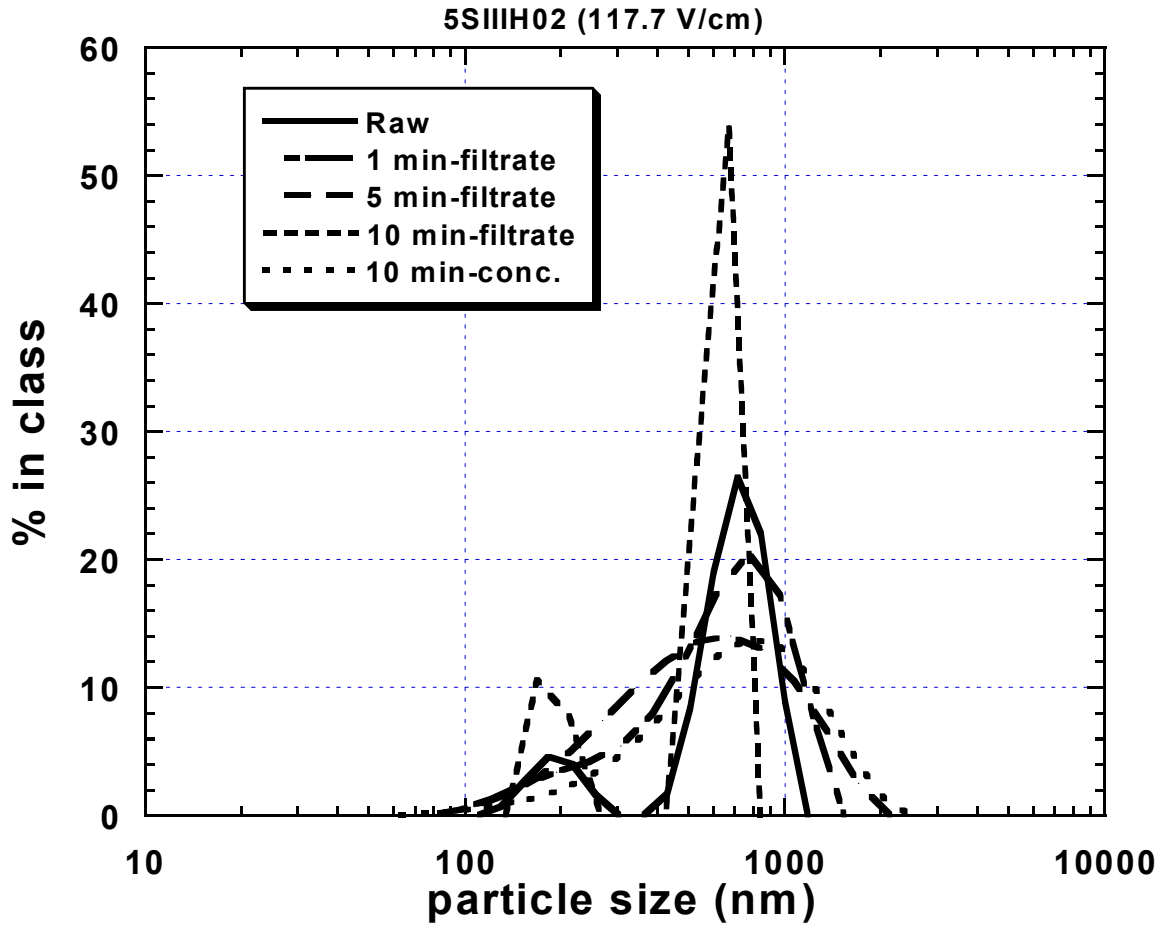

Figure A72. Change in particle size distribution during filtration operation. Experimental conditions: electrostatic field = 117.7 V/cm; pH = 7.1; Sample: 5SIIIH02

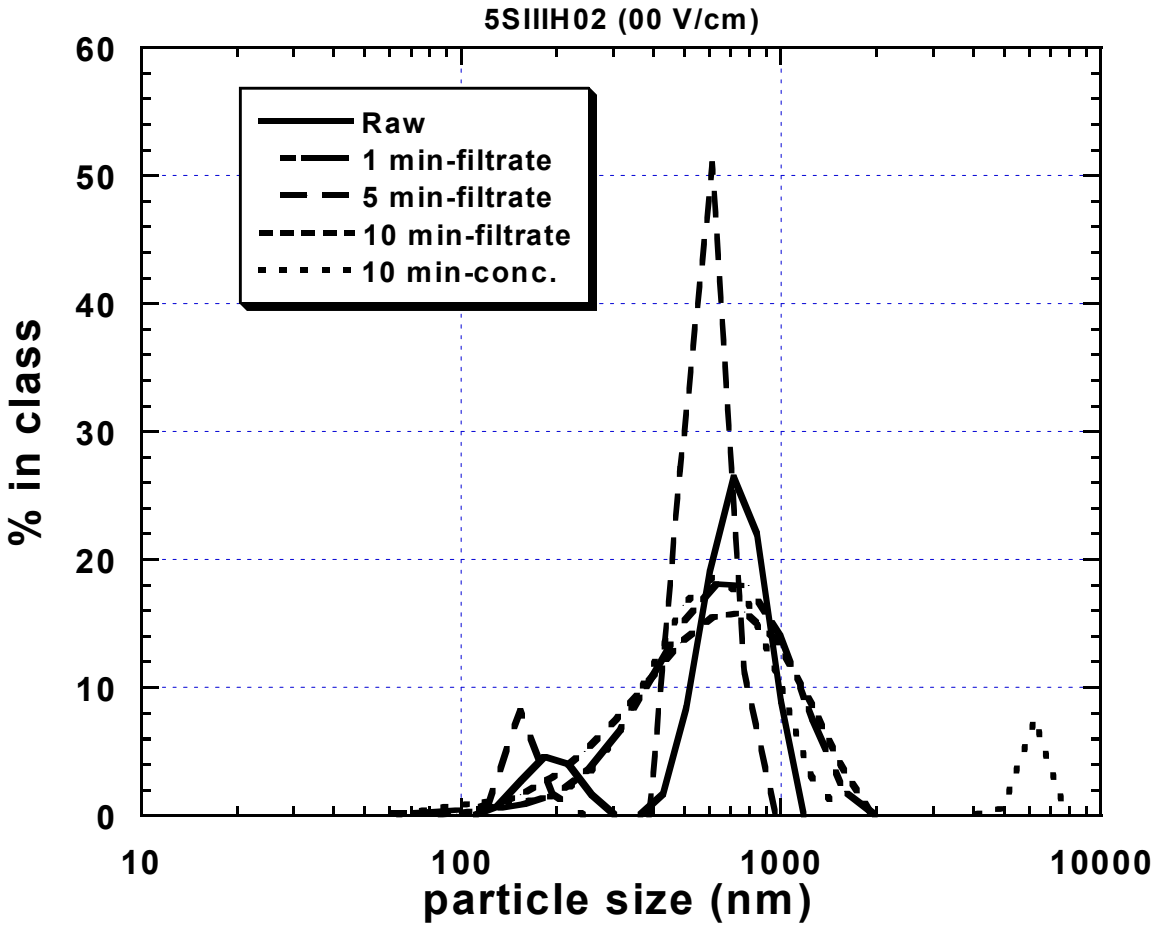

Figure A73. Change in particle size distribution during filtration operation. Experimental conditions: electrostatic field = 00 V/cm; pH = 6.8; Sample: 5SIIIH02

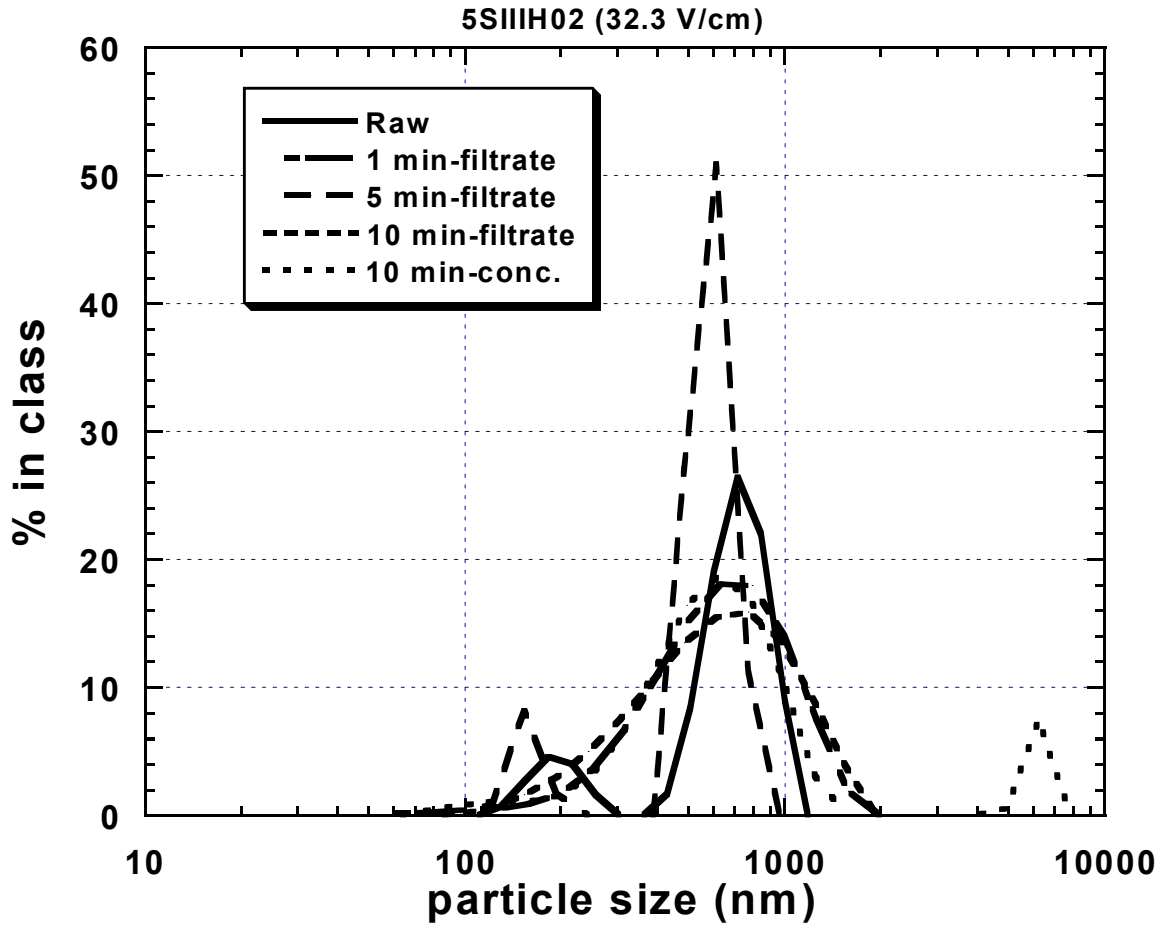

Figure A74. Change in particle size distribution during filtration operation. Experimental conditions: electrostatic field = 32.3 V/cm; pH = 6.8; Sample: 5SIIIH02

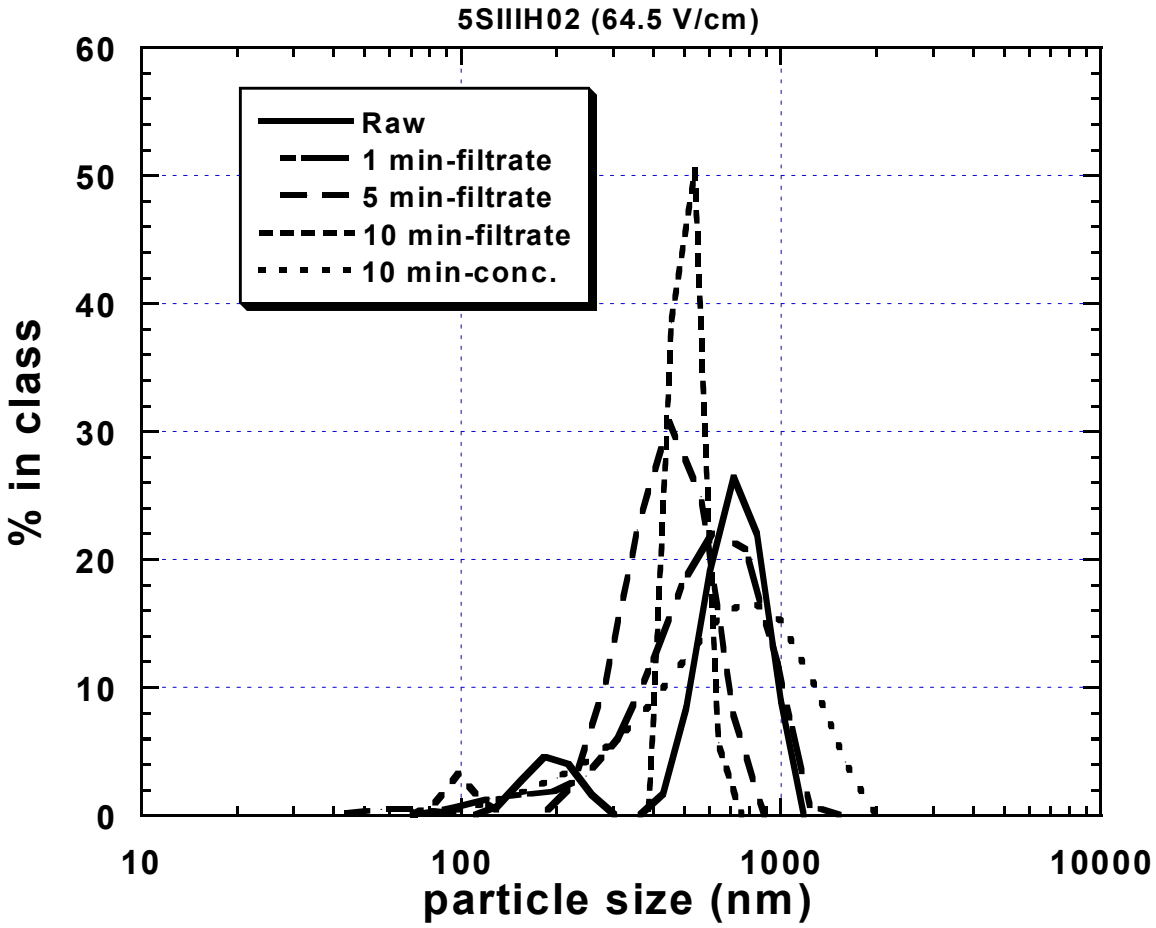

Figure A75. Change in particle size distribution during filtration operation. Experimental conditions: electrostatic field = 64.5 V/cm; pH = 6.8; Sample: 5SIIIH02

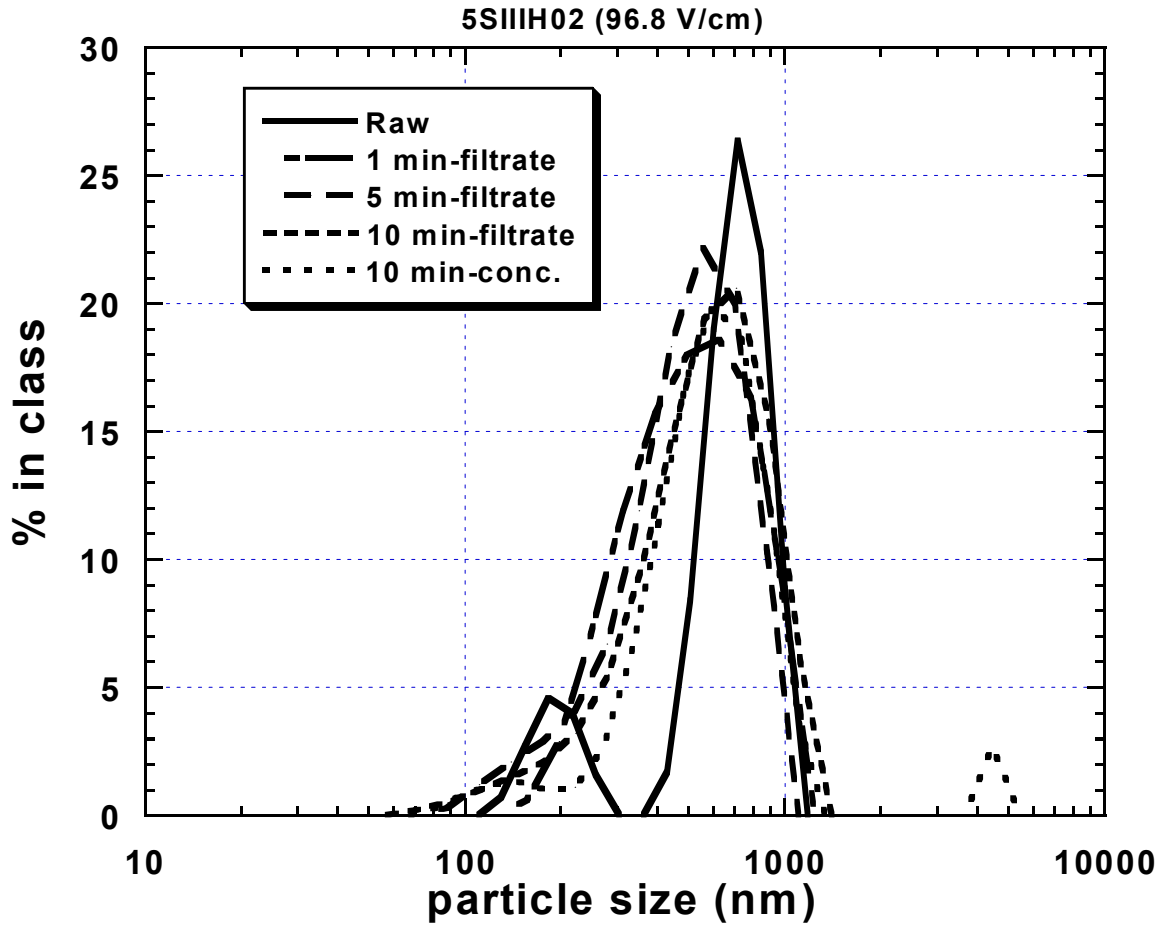

Figure A76. Change in particle size distribution during filtration operation. Experimental conditions: electrostatic field = 96.8 V/cm; pH = 6.8; Sample: 5SIIIH02

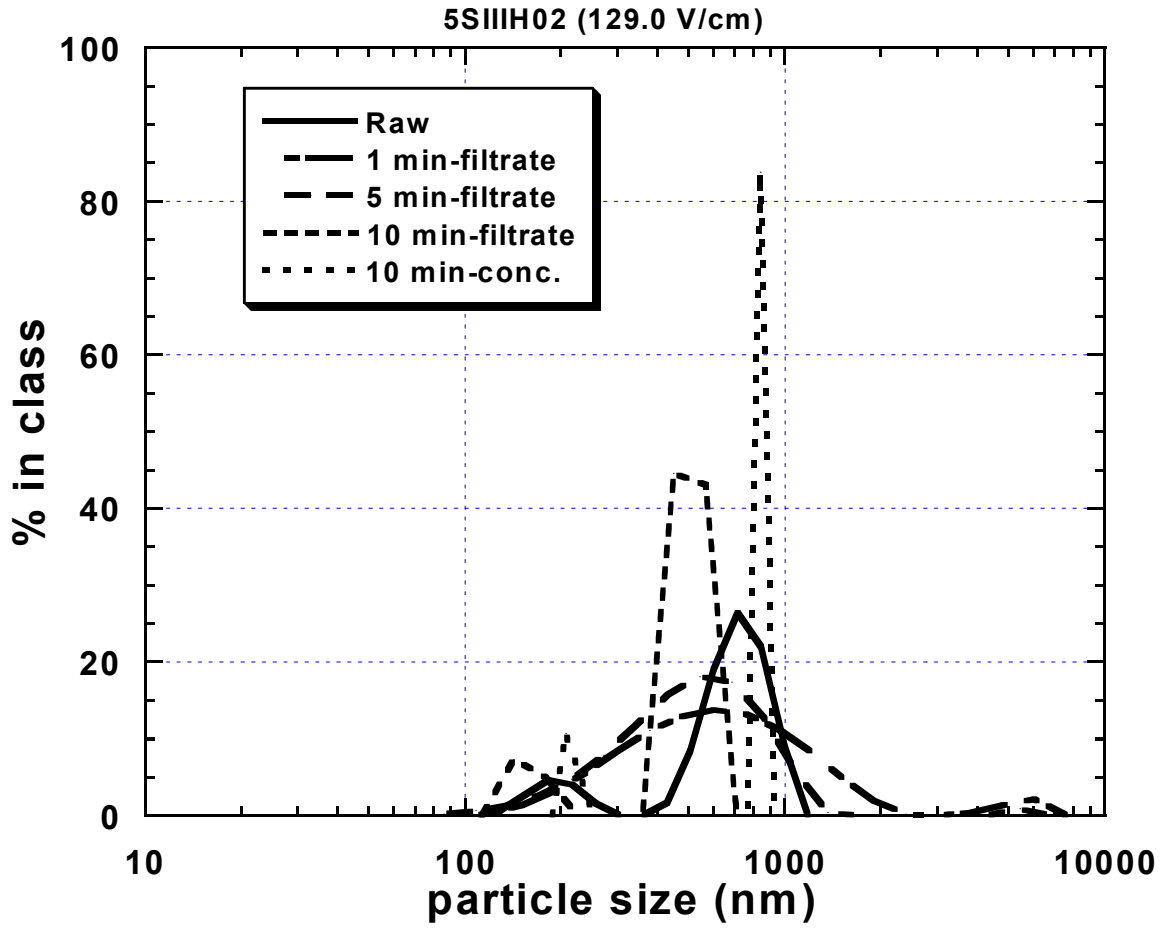

Figure A77. Change in particle size distribution during filtration operation. Experimental conditions: electrostatic field = 129.0 V/cm; pH = 6.8; Sample: 5SIIIH02

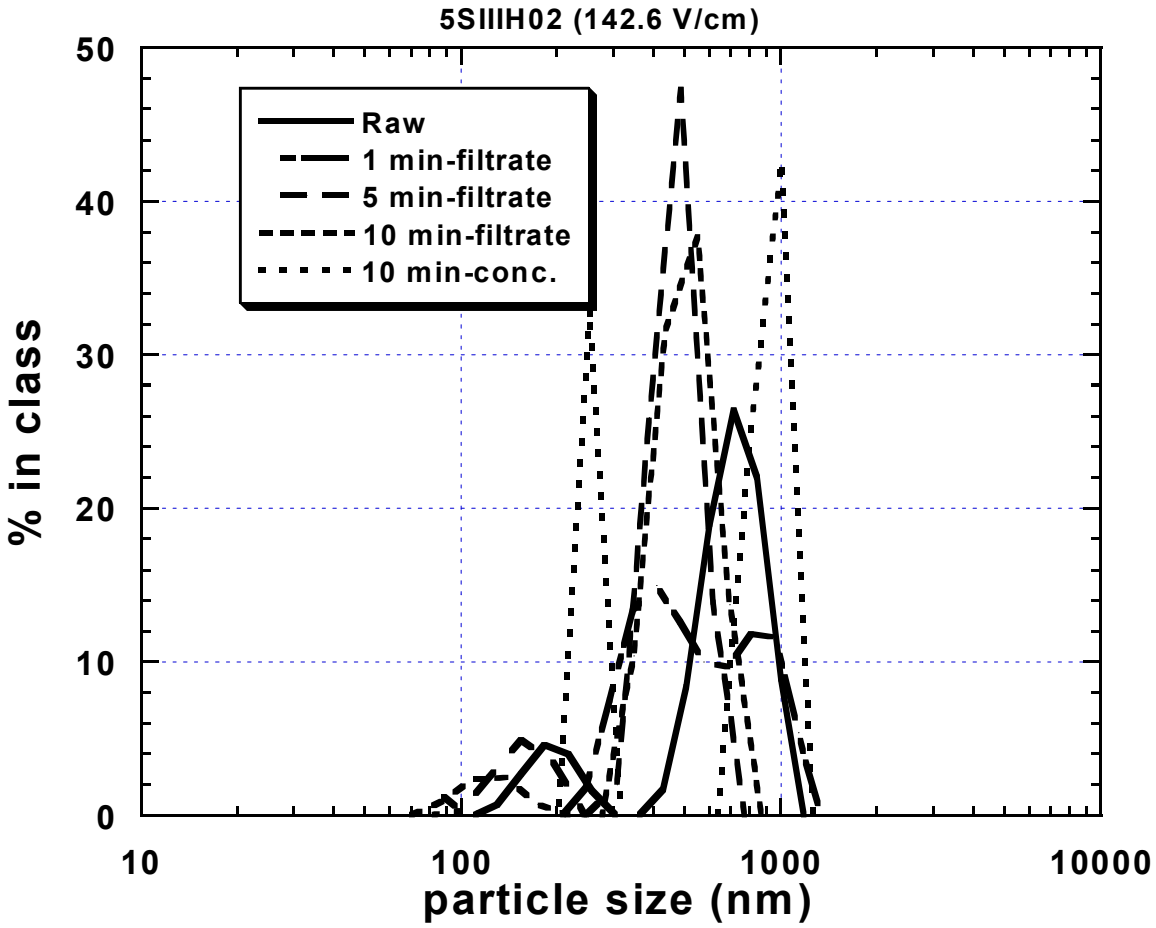

Figure A78. Change in particle size distribution during filtration operation. Experimental conditions: electrostatic field =142.6 V/cm; pH = 6.8; Sample: 5SIIIH02

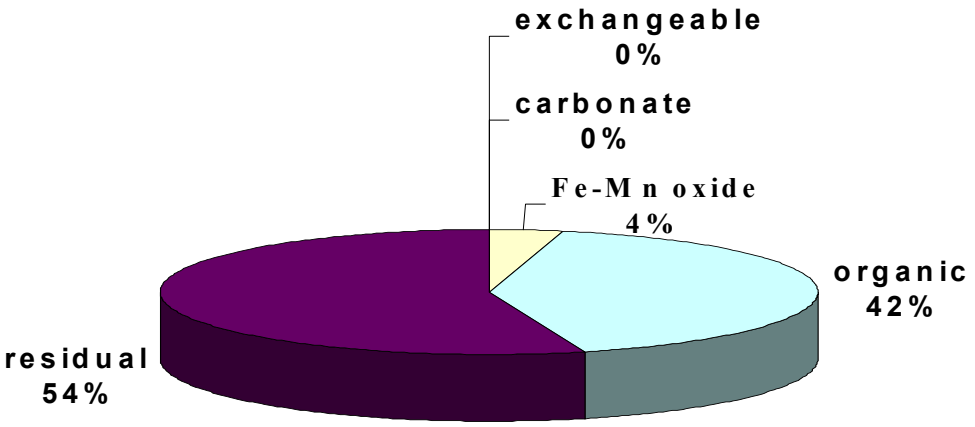

Figure A79. Distribution of lead species in particulate collected from well water sample at constant electrostatic field. Experimental conditions: pH = 6.8; electrostatic field = 00 V/cm; Sample: 10IIB02

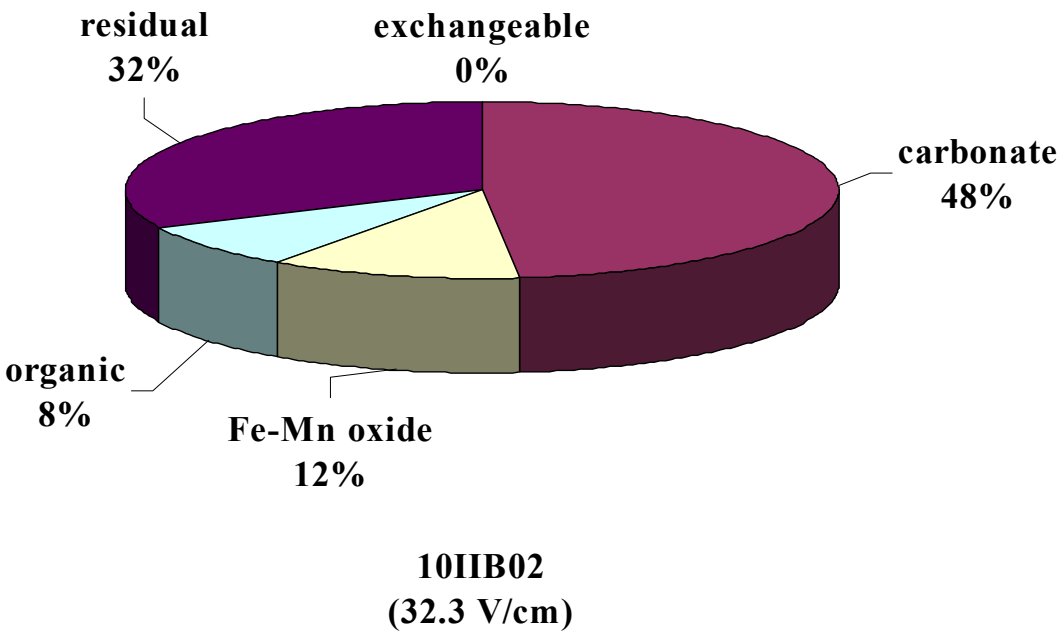

Figure A80. Distribution of lead species in particulate collected from well water sample at constant electrostatic field. Experimental conditions: pH = 6.8; electrostatic field = 32.3 V/cm; Sample: 10IIB02

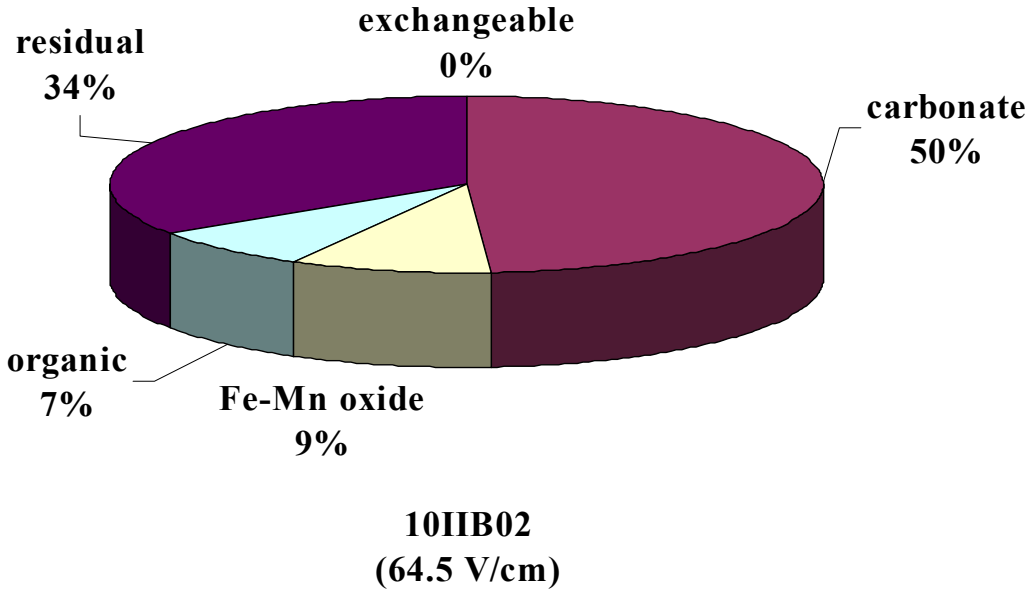

Figure A81. Distribution of lead species in particulate collected from well water sample at constant electrostatic field. Experimental conditions: pH = 6.8; electrostatic field = 64.5 V/cm; Sample: 10IIB02

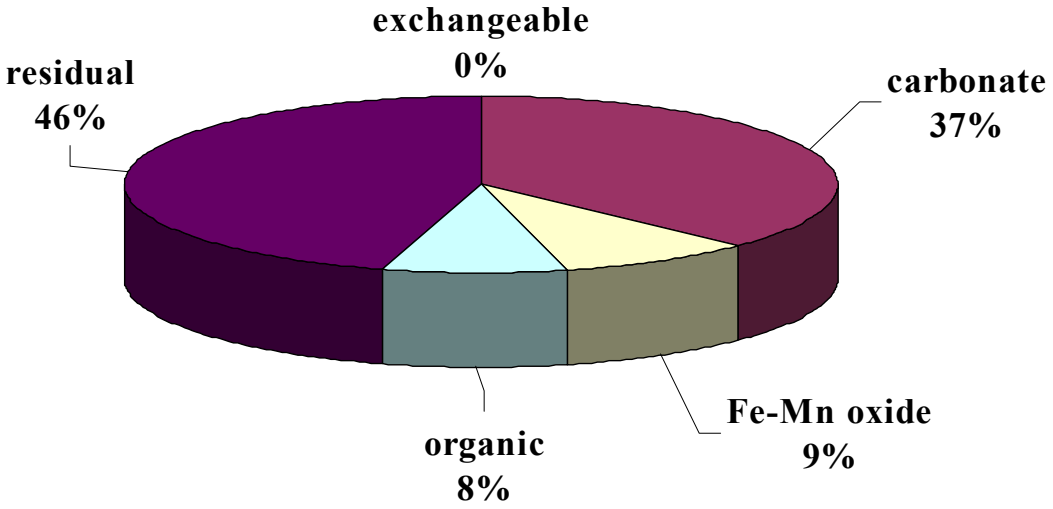

Figure A82. Distribution of lead species in particulate collected from well water sample at constant electrostatic field. Experimental conditions: pH = 6.8; electrostatic field = 71.3 V/cm; Sample: 10IIB02

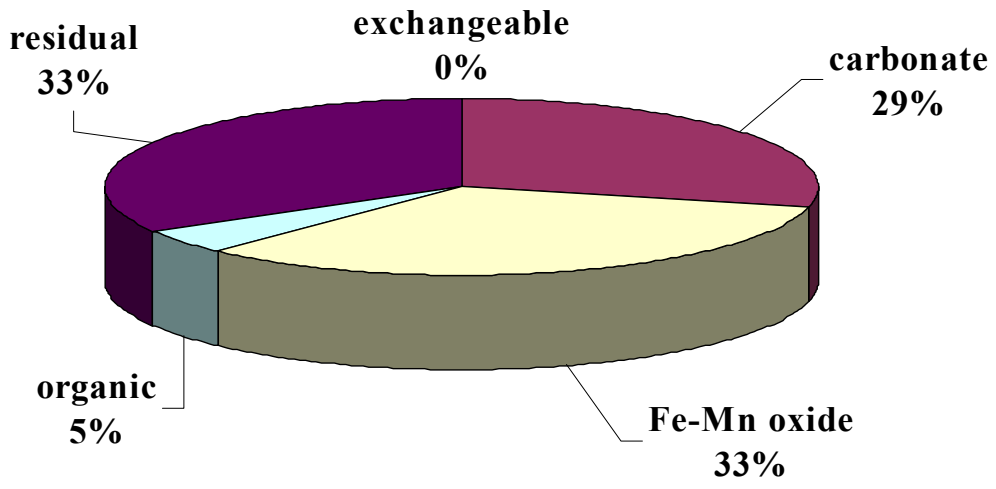

Figure A83. Distribution of lead species in particulate collected from well water sample at constant electrostatic field. Experimental conditions: pH = 6.8; electrostatic field = 32.3 V/cm; Sample: 10IIB02

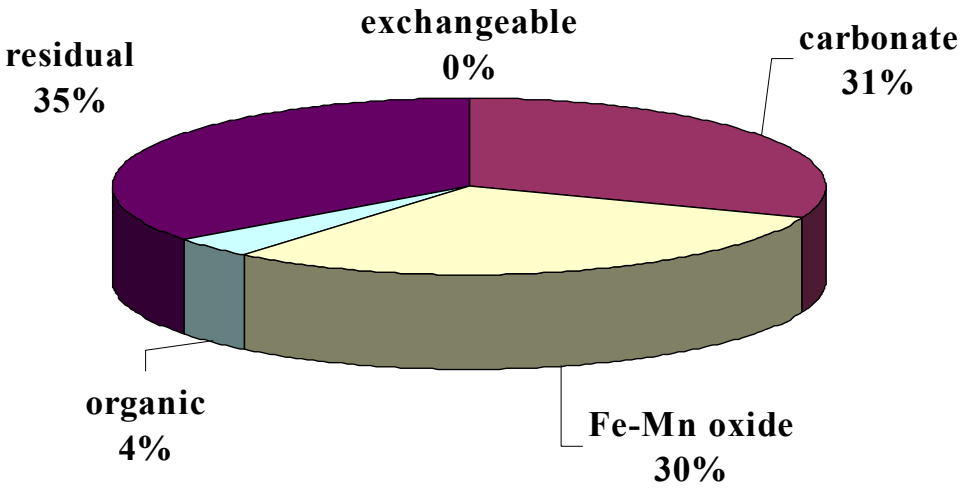

Figure A84. Distribution of lead species in particulate collected from well water sample at constant electrostatic field. Experimental conditions: pH = 6.8; electrostatic field = 64.5 V/cm; Sample: 10IIB02

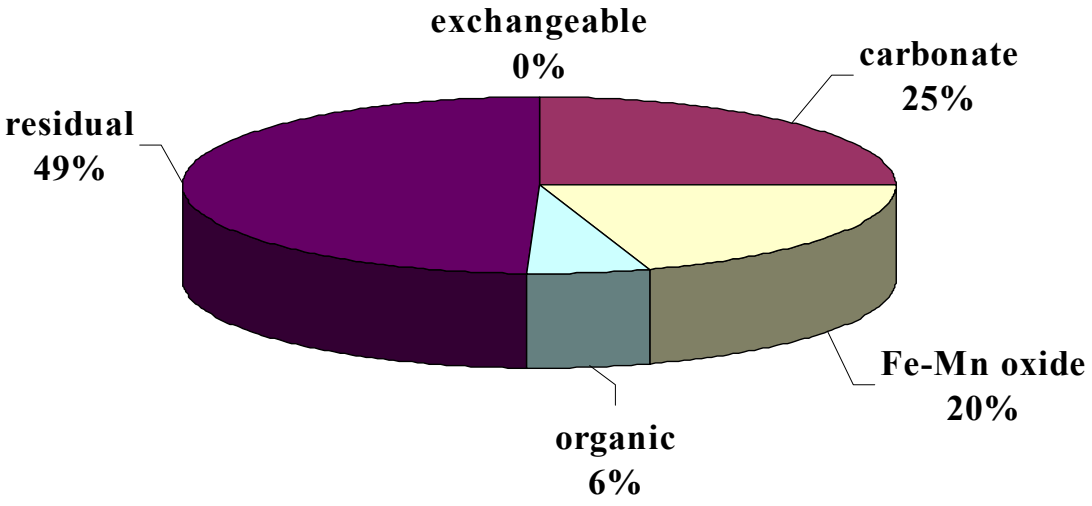

Figure A85. Distribution of lead species in particulate collected from well water sample at constant electrostatic field. Experimental conditions: pH = 6.8; electrostatic field = 96.8 V/cm; Sample: 10IIB02

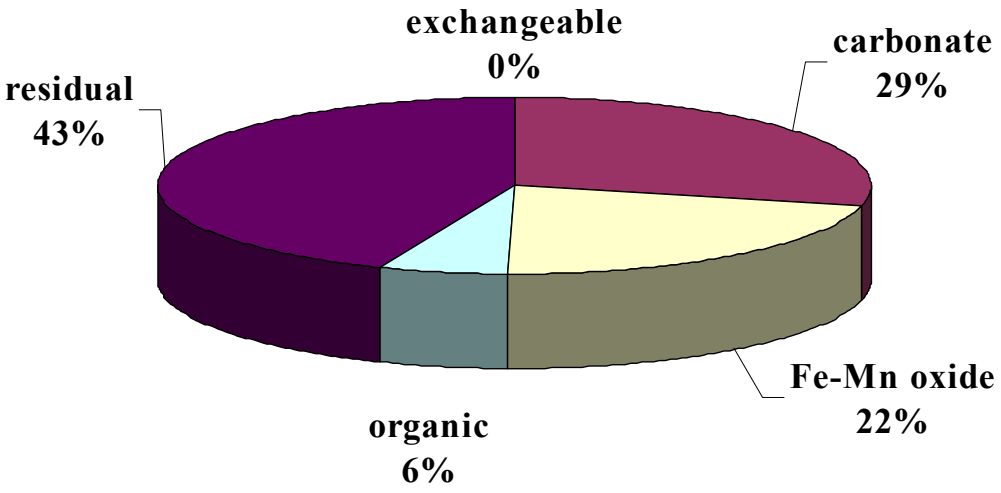

Figure A86. Distribution of lead species in particulate collected from well water sample at constant electrostatic field. Experimental conditions: pH = 6.8; electrostatic field = 96.8 V/cm; Sample: 10IIB02

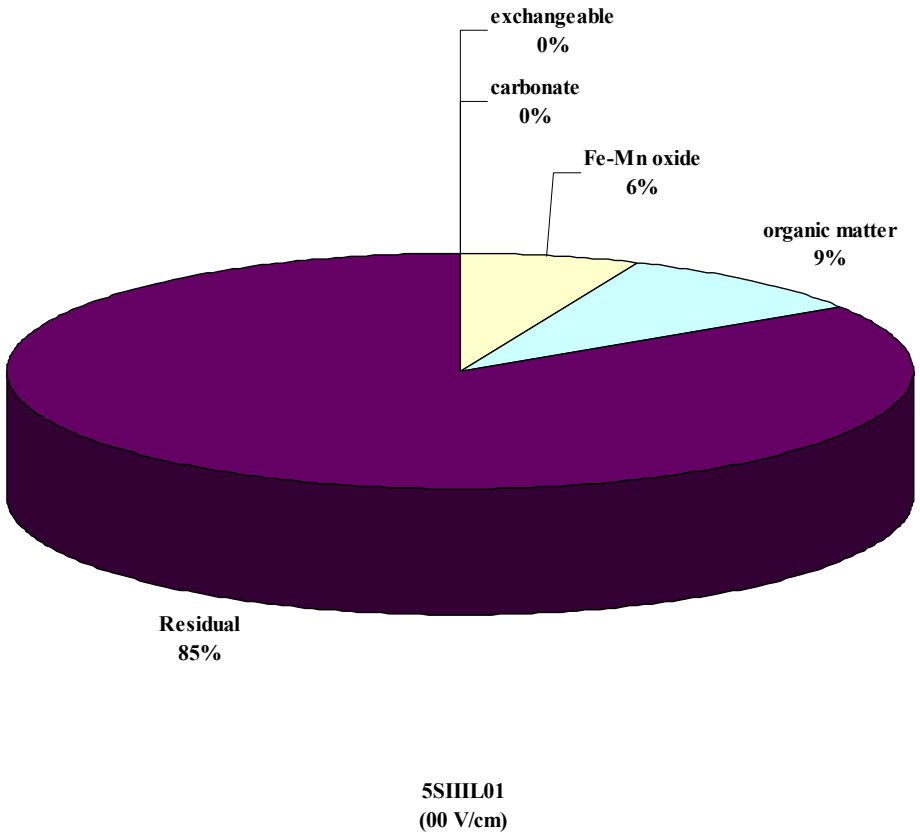

Figure A87. Distribution of lead species in particulate collected from well water sample at constant electrostatic field. Experimental condition: pH = 6.8; initial turbidity = 680 NTU; electrostatic field = 00 V/cm; Sample: 5SIIIL01.

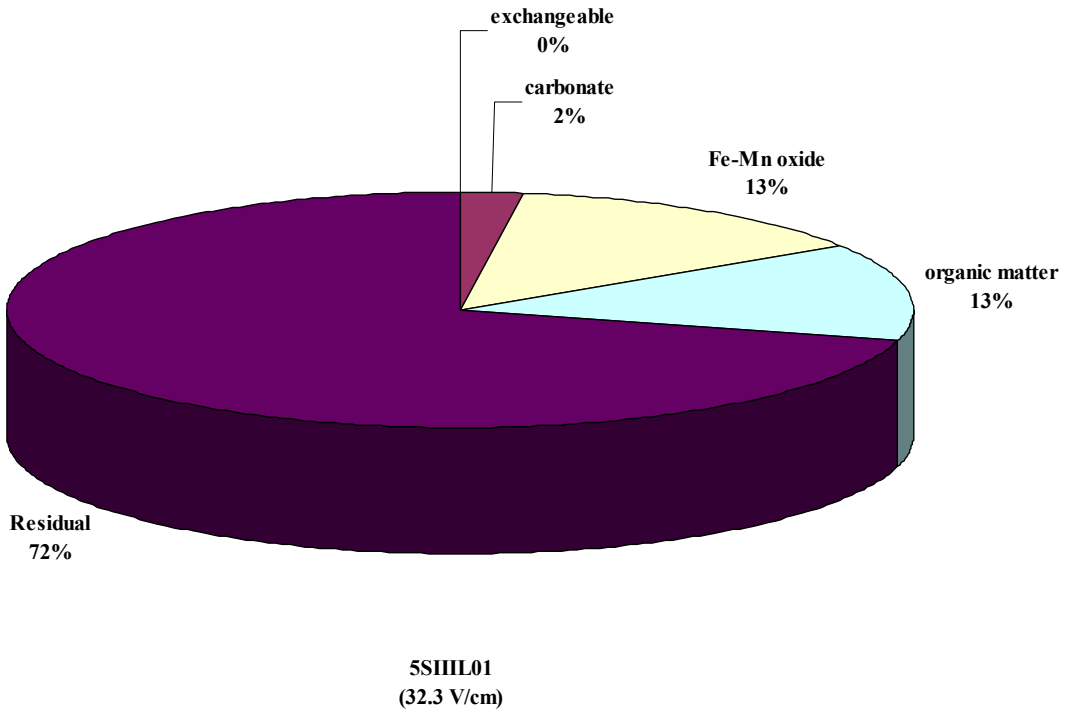

Figure A88. Distribution of lead species in particulate collected from well water sample at constant electrostatic field. Experimental condition: pH = 6.8; initial turbidity = 680 NTU; electrostatic field = 32.3 V/cm; Sample: 5SIIIL01.

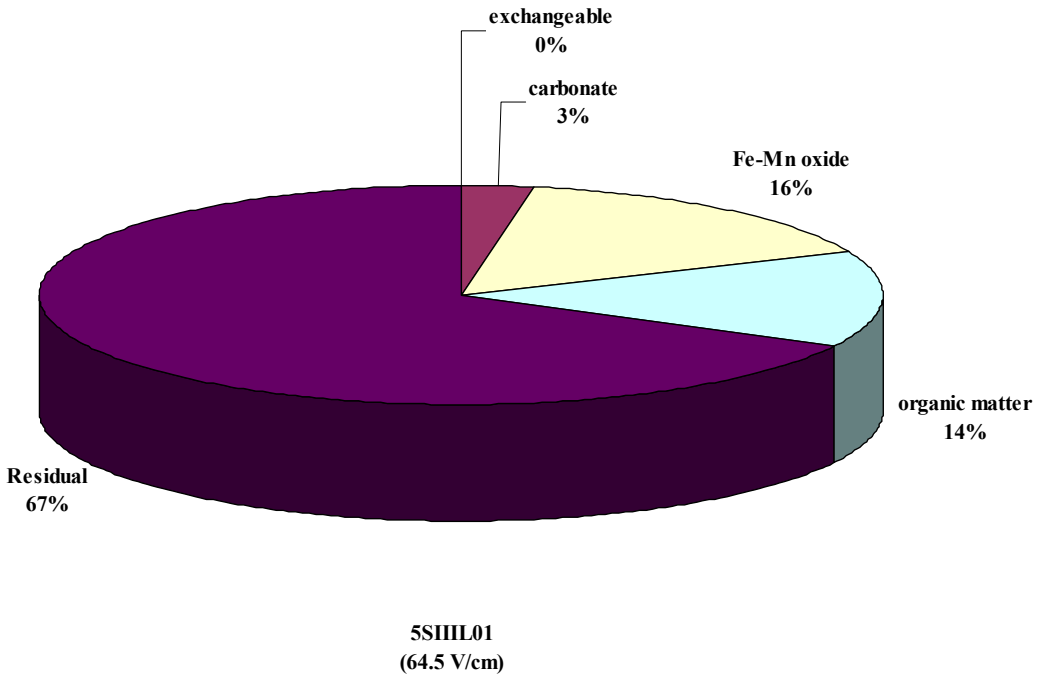

Figure A89. Distribution of lead species in particulate collected from well water sample at constant electrostatic field. Experimental condition: pH = 6.8; initial turbidity = 680 NTU; electrostatic field = 64.5 V/cm; Sample: 5SIIIL01.

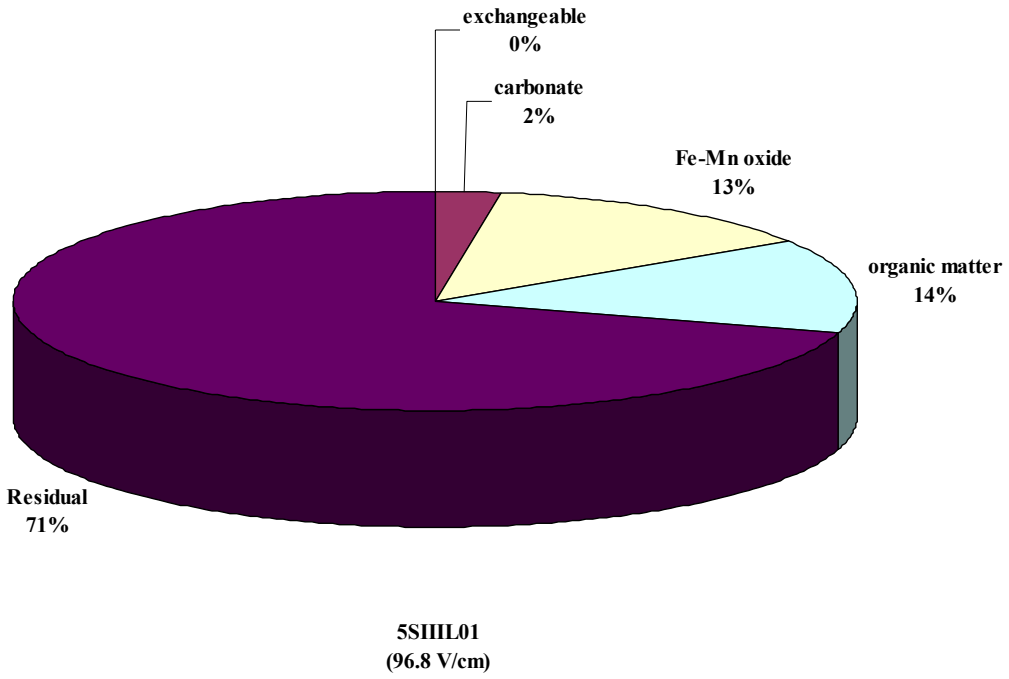

Figure A90. Distribution of lead species in particulate collected from well water sample at constant electrostatic field. Experimental condition: pH = 6.8; initial turbidity = 680 NTU; electrostatic field = 96.8 V/cm; Sample: 5SIIIL01.

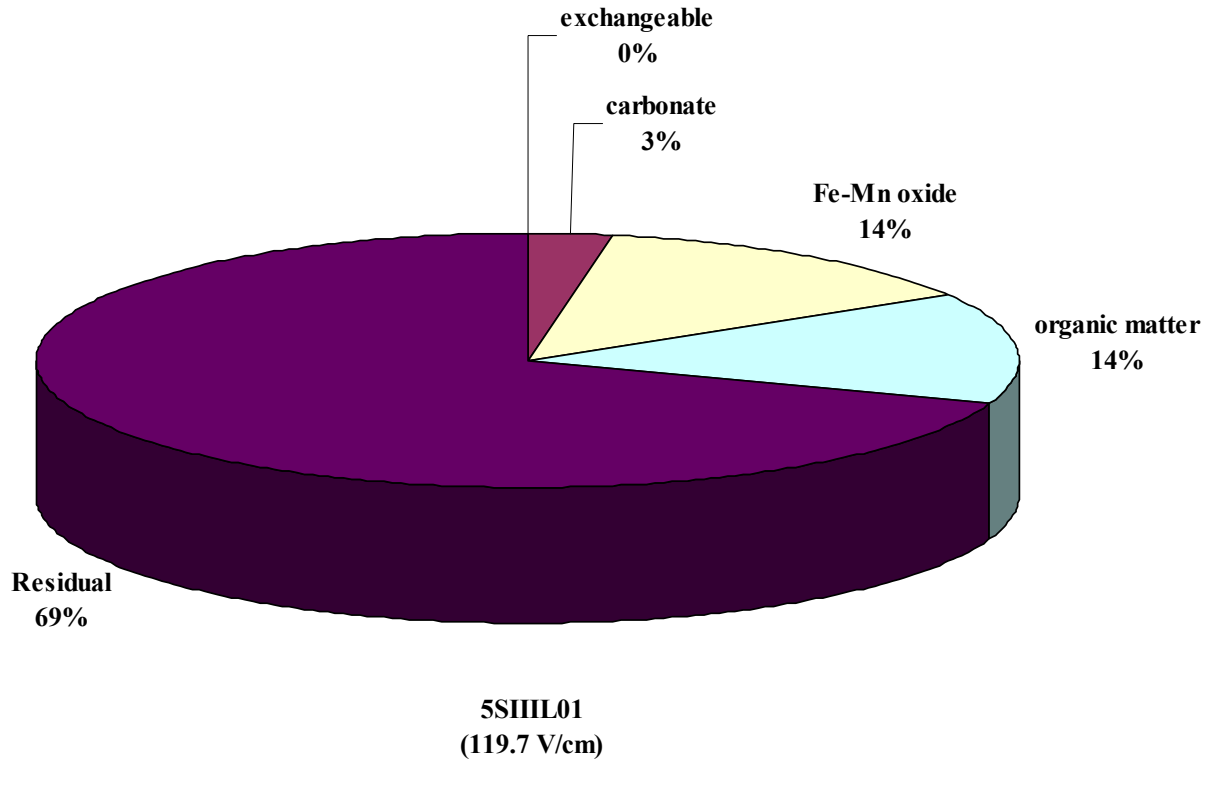

Figure A91. Distribution of lead species in particulate collected from well water sample at constant electrostatic field. Experimental condition: pH = 6.8; initial turbidity = 680 NTU; electrostatic field = 119.7 V/cm; Sample: 5SIIIL01.

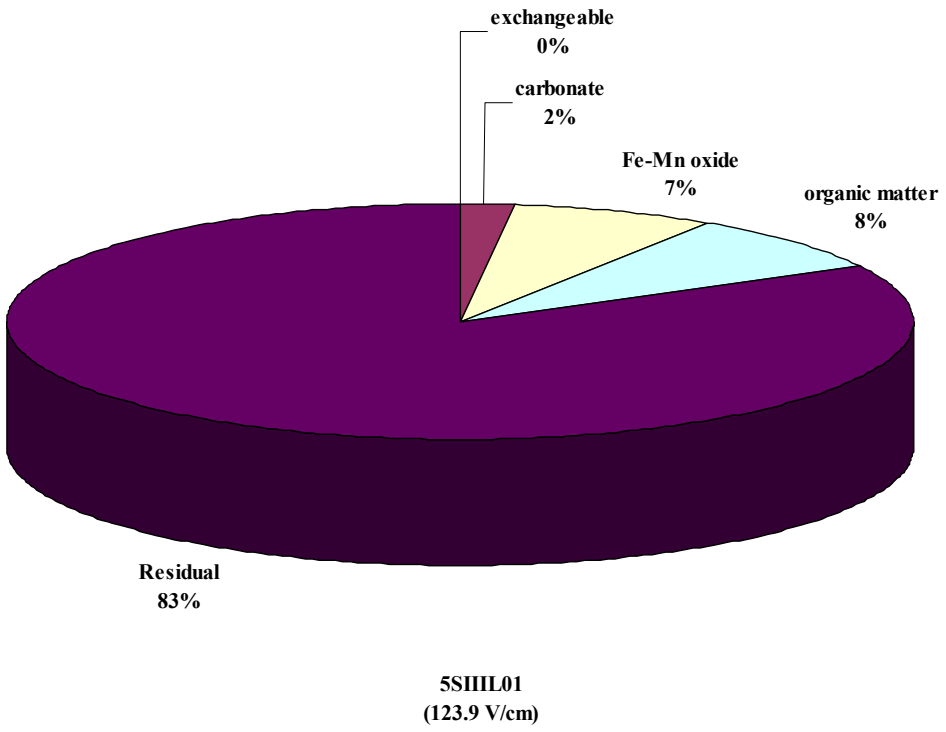

Figure A92. Distribution of lead species in particulate collected from well water sample at constant electrostatic field. Experimental condition: pH = 6.8; initial turbidity = 680 NTU; electrostatic field = 123.9 V/cm; Sample: 5SIIIL01.

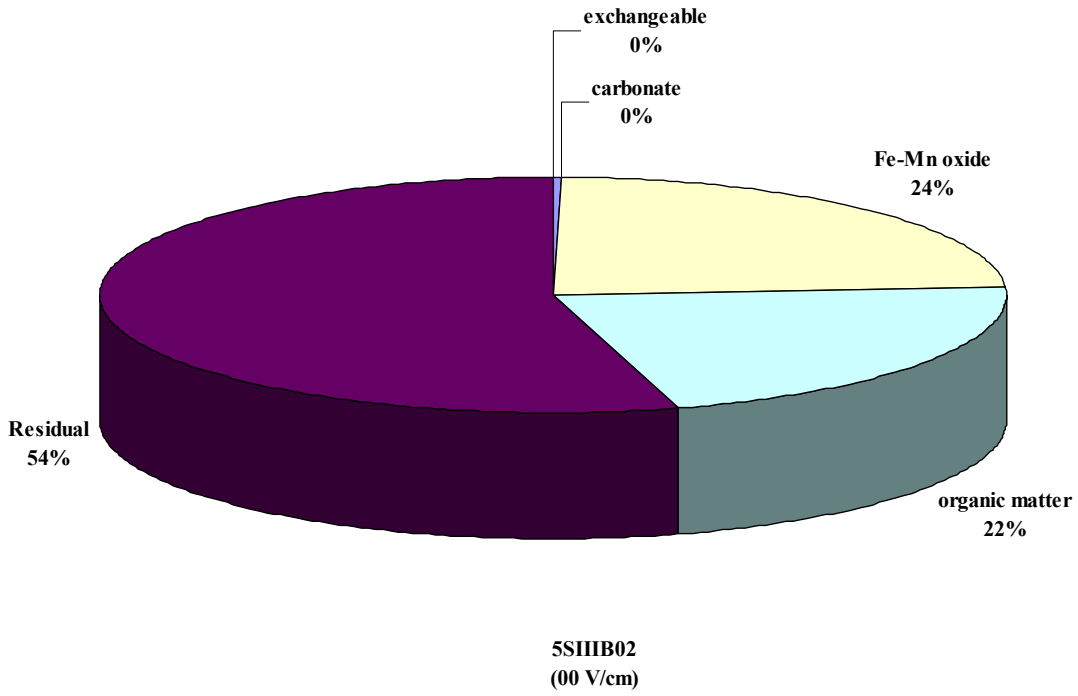

Figure A93. Distribution of lead species in particulate collected from well water sample at constant electrostatic field. Experimental condition: pH = 6.8; initial turbidity = 750 NTU; electrostatic field = 00 V/cm; Sample: 5SIIIB02.

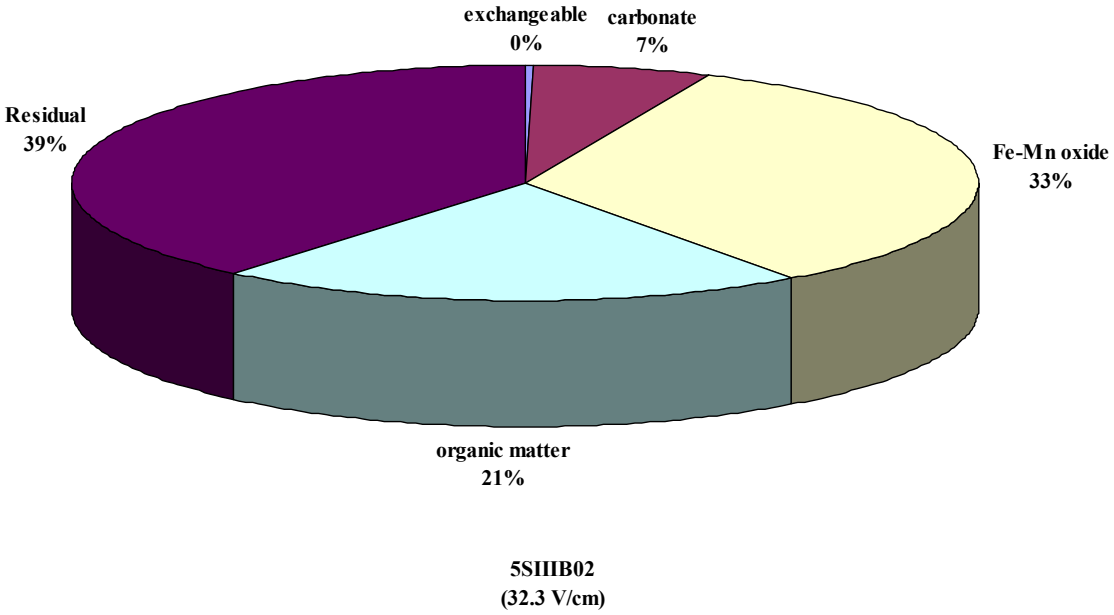

Figure A94. Distribution of lead species in particulate collected from well water sample at constant electrostatic field. Experimental condition: pH = 6.8; initial turbidity = 750 NTU; electrostatic field = 32.3 V/cm; Sample: 5SIIIB02.

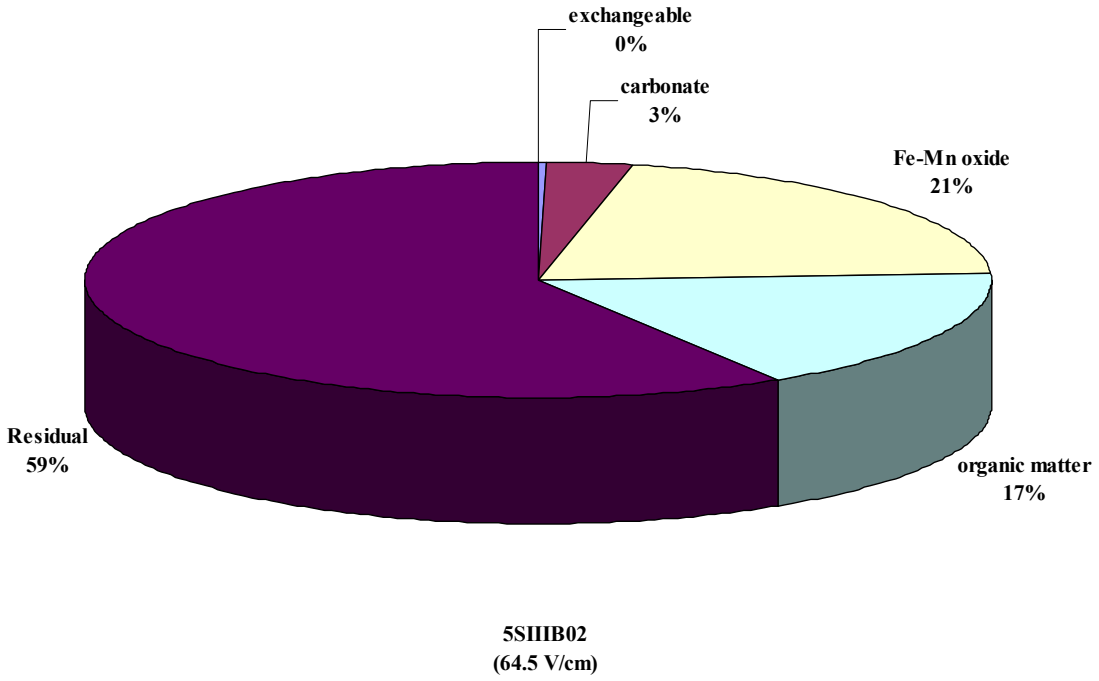

Figure A95. Distribution of lead species in particulate collected from well water sample at constant electrostatic field. Experimental condition: pH = 6.8; initial turbidity = 750 NTU; electrostatic field = 64.5 V/cm; Sample: 5SIIIB02.

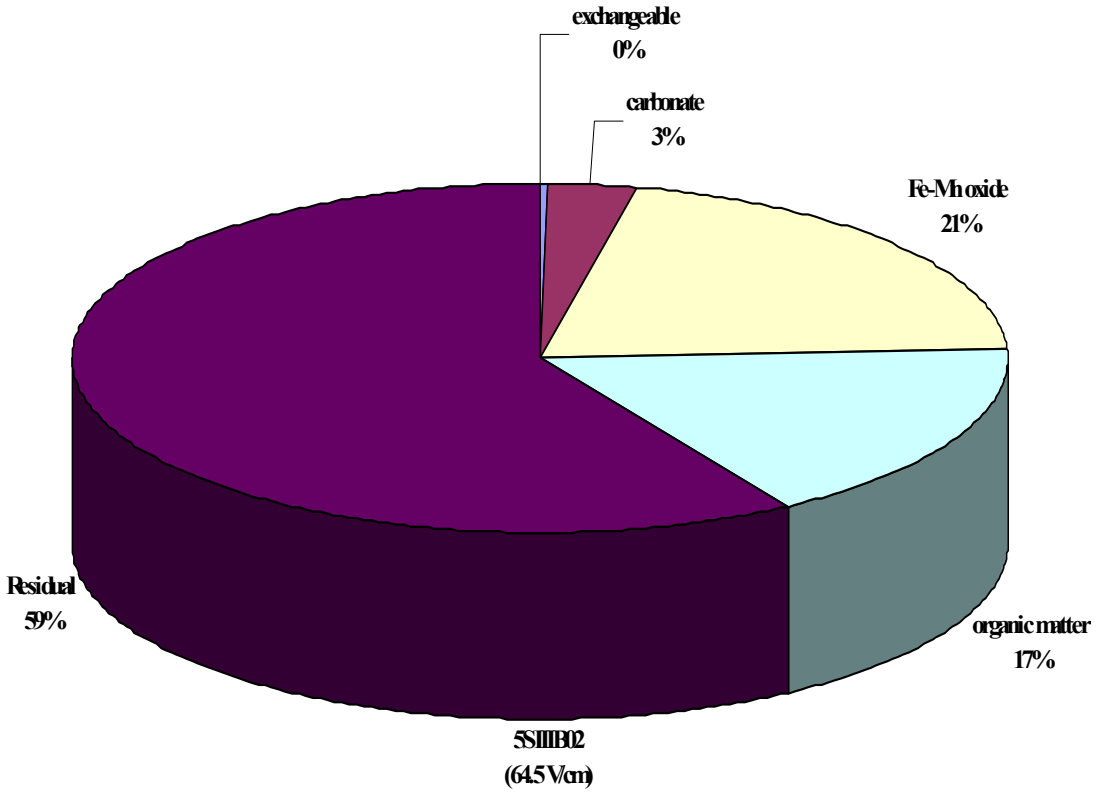

Figure A96. Distribution of lead species in particulate collected from well water sample at constant electrostatic field. Experimental condition: pH = 6.8; initial turbidity = 750 NTU; electrostatic field = 96.8 V/cm; Sample: 5SIIIB02.

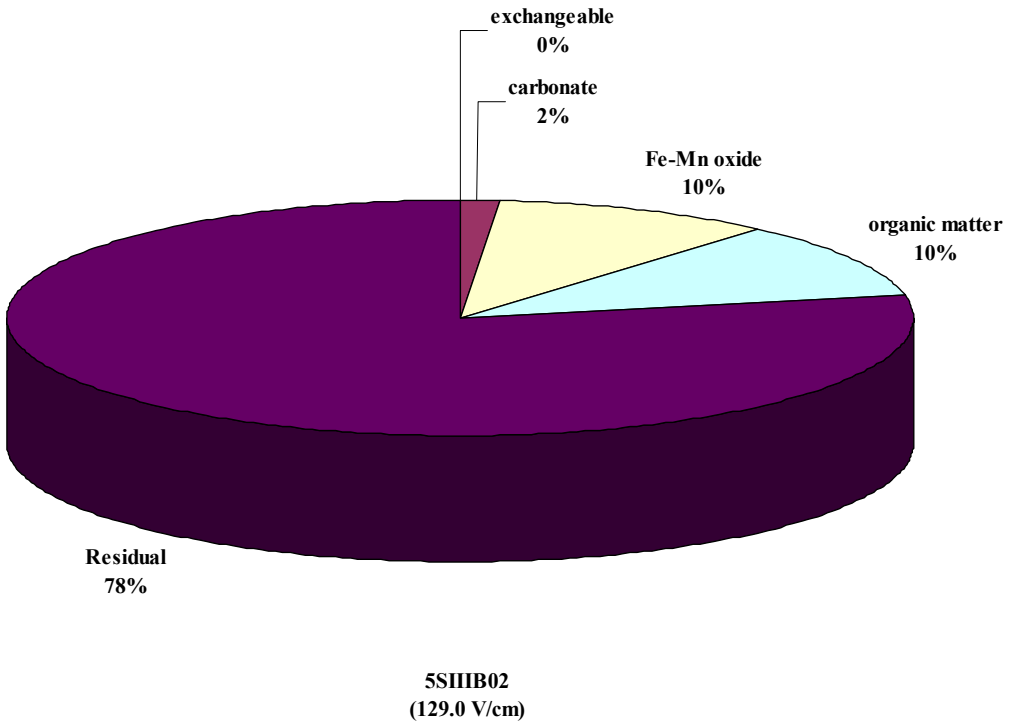

Figure A97. Distribution of lead species in particulate collected from well water sample at constant electrostatic field. Experimental condition: pH = 6.8; initial turbidity = 750 NTU; electrostatic field = 129.0 V/cm; Sample: 5SIIIB02.

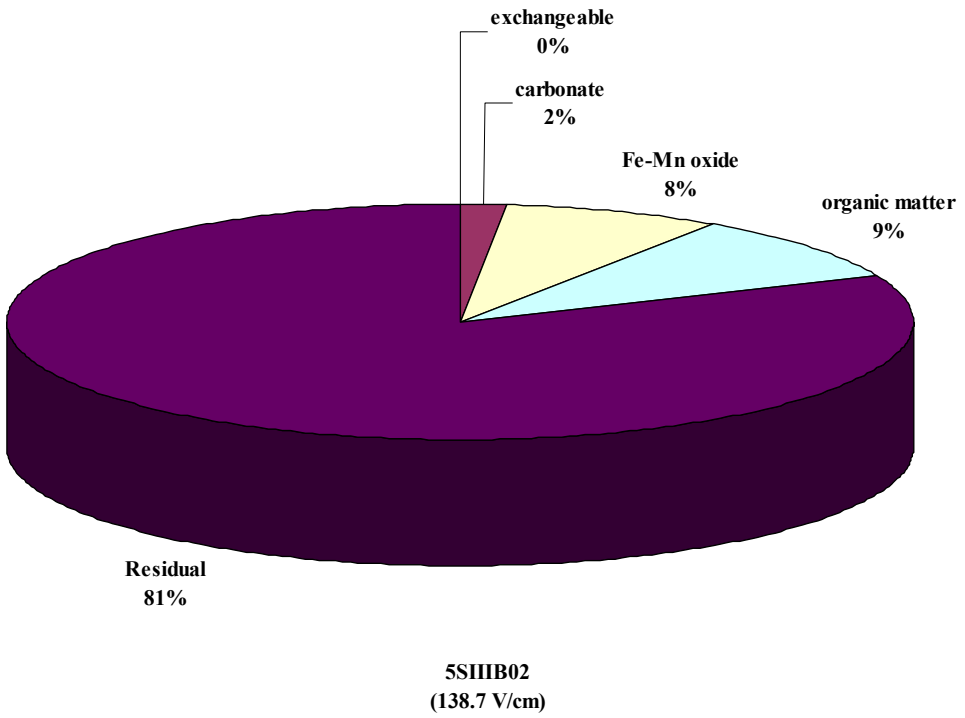

Figure A98. Distribution of lead species in particulate collected from well water sample at constant electrostatic field. Experimental condition: pH = 6.8; initial turbidity = 750 NTU; electrostatic field = 138.7 V/cm; Sample: 5SIIIB02.

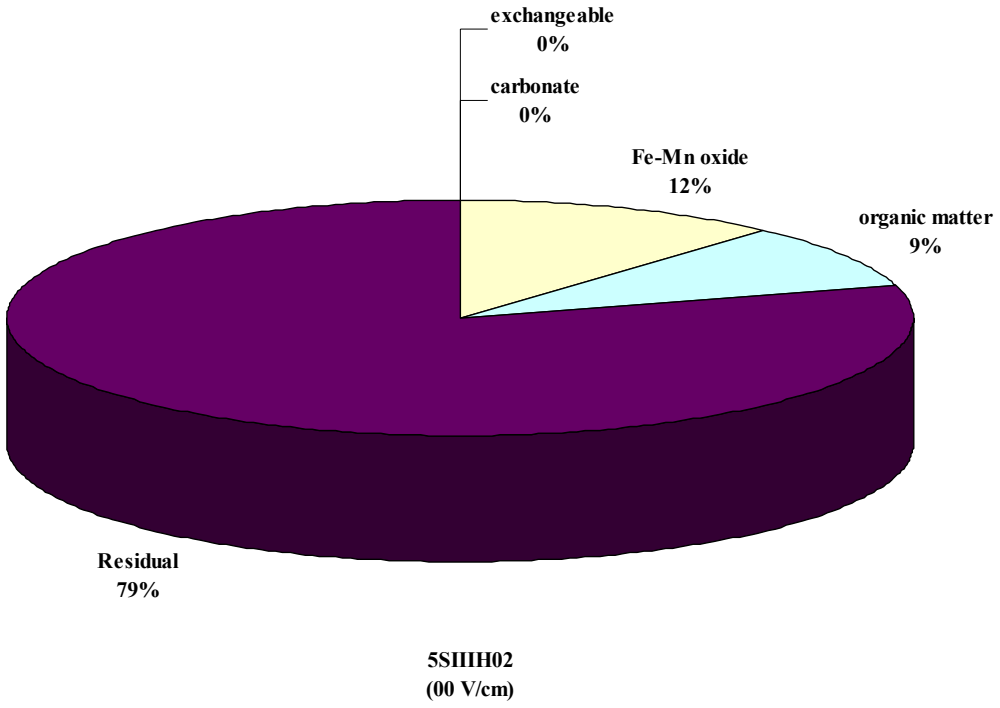

Figure A99. Distribution of lead species in particulate collected from well water sample at constant electrostatic field. Experimental condition: pH = 7.1; initial turbidity = 720 NTU; electrostatic field = 00 V/cm; Sample: 5SIIIH02.

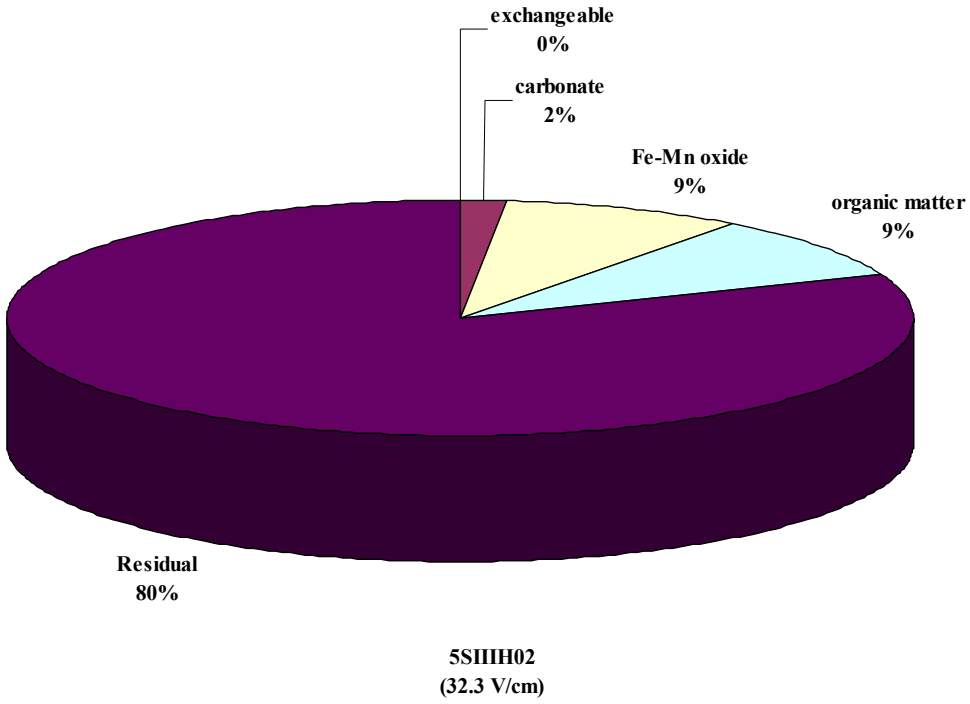

Figure A100. Distribution of lead species in particulate collected from well water sample at constant electrostatic field. Experimental condition: pH = 7.1; initial turbidity = 720 NTU; electrostatic field = 32.3 V/cm; Sample: 5SIIIH02.

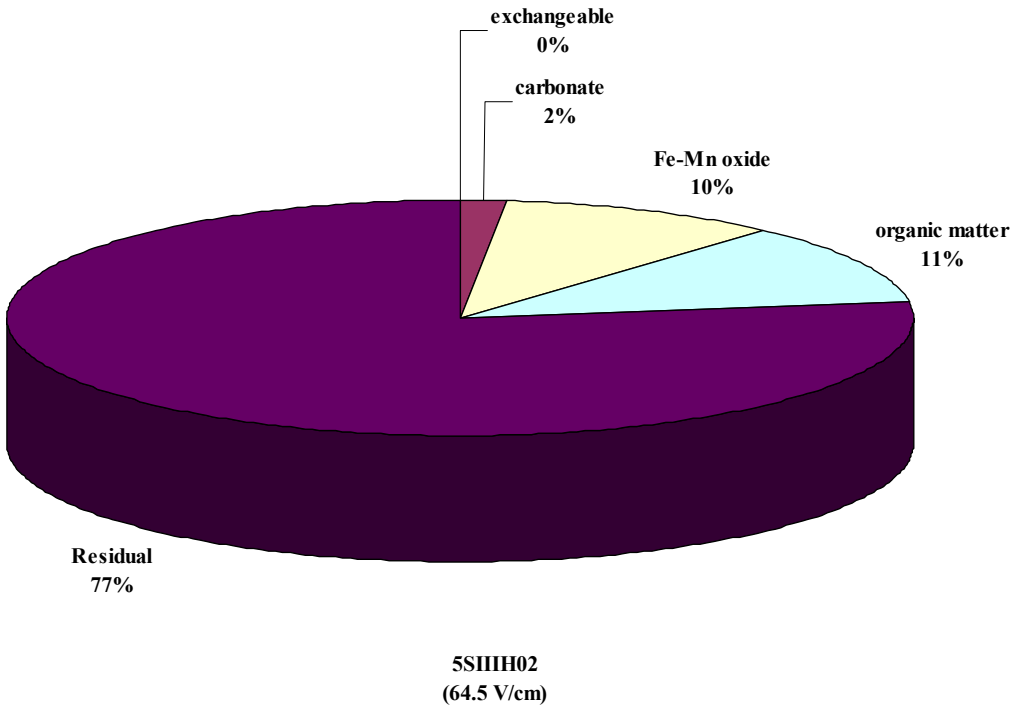

Figure A101. Distribution of lead species in particulate collected from well water sample at constant electrostatic field. Experimental condition: pH = 7.1; initial turbidity = 720 NTU; electrostatic field = 64.5 V/cm; Sample: 5SIIIH02.

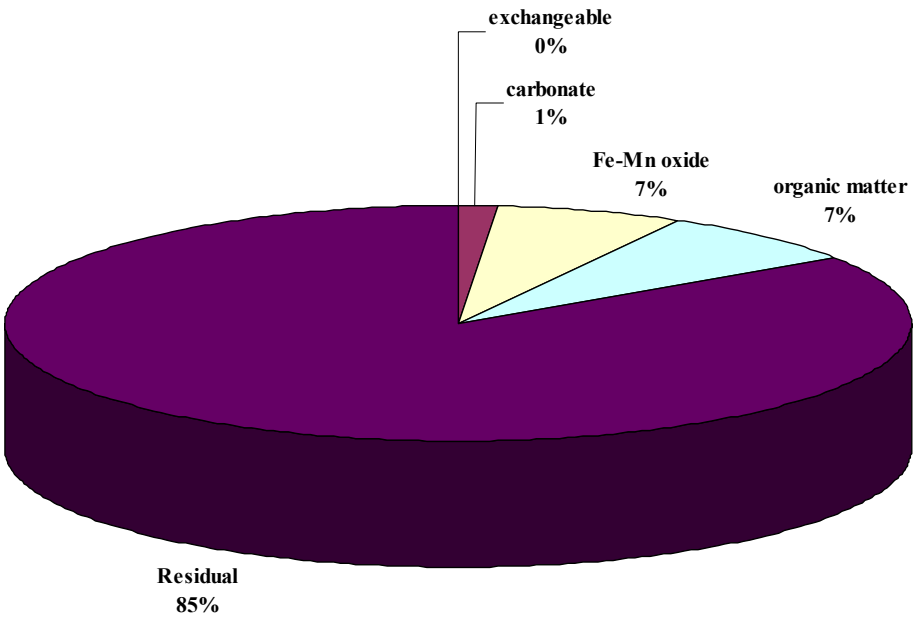

Figure A102. Distribution of lead species in particulate collected from well water sample at constant electrostatic field. Experimental condition: pH = 7.1; initial turbidity = 720 NTU; electrostatic field = 96.8 V/cm; Sample: 5SIIIH02.

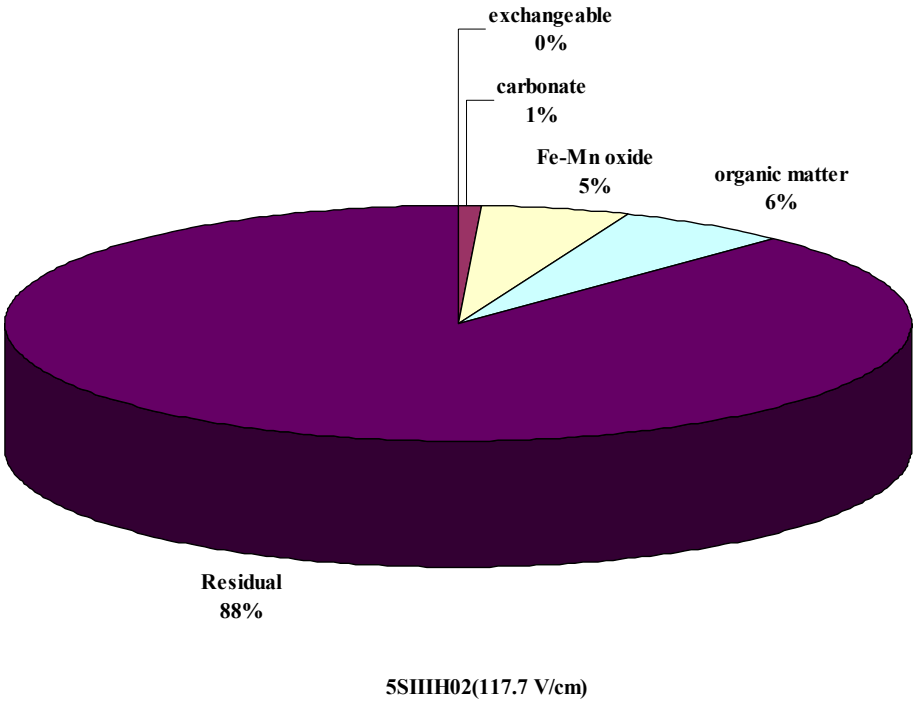

Figure A103. Distribution of lead species in particulate collected from well water sample at constant electrostatic field. Experimental condition: pH = 7.1; initial turbidity = 720 NTU; electrostatic field = 117.7 V/cm; Sample: 5SIIIH02.

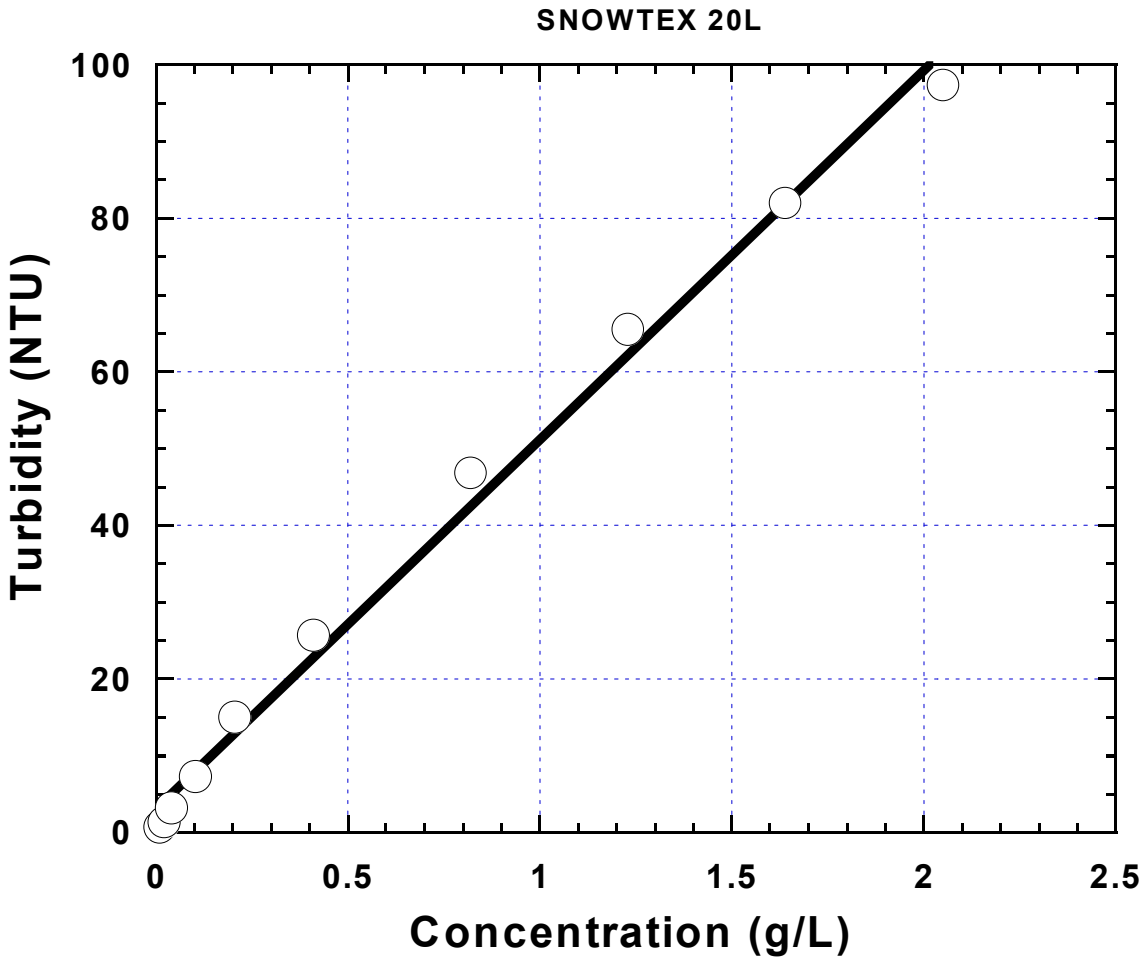

Figure A104. Calibration curve for colloidal silica as measured by turbidity (NTU). Sample: Snowtex 20L

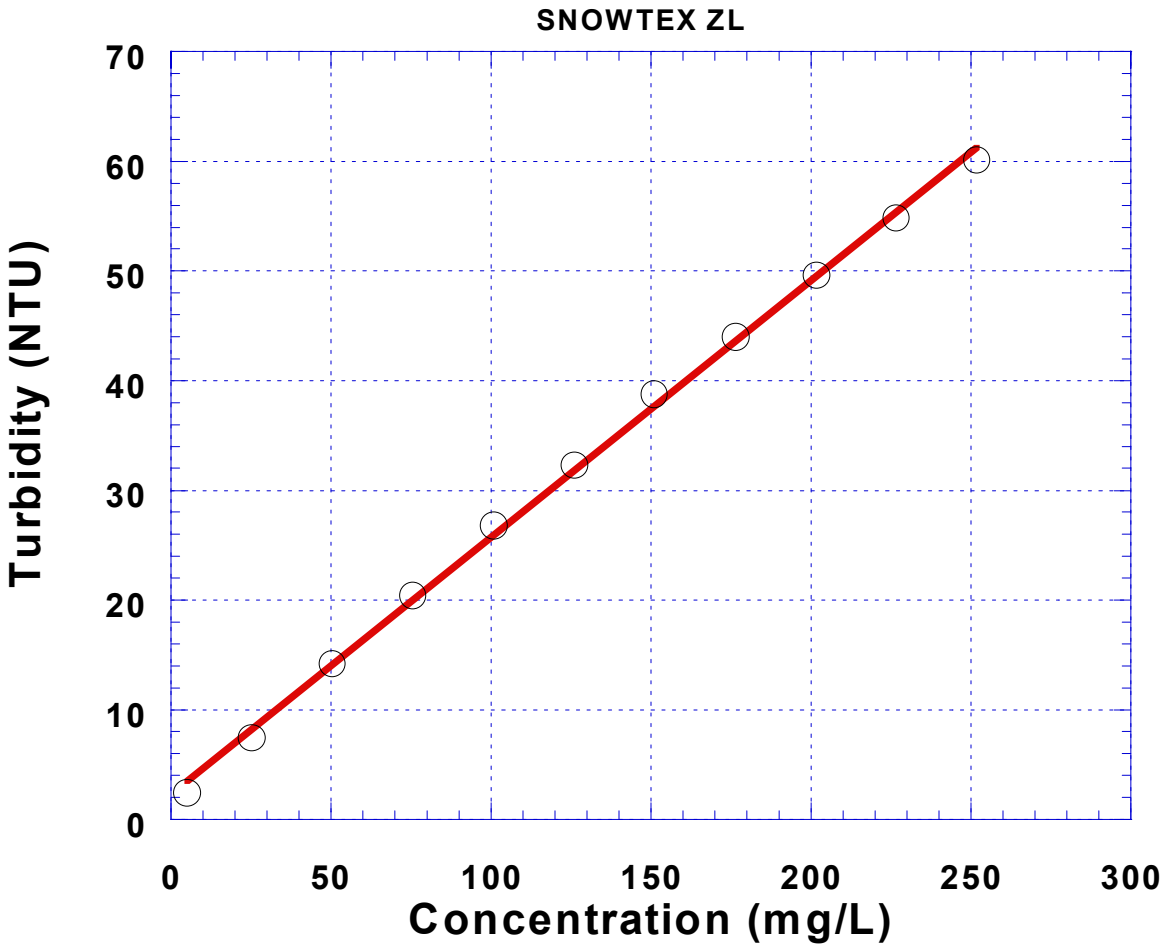

Figure A105. Calibration curve for colloidal silica as measured by turbidity (NTU). Sample: Snowtex 20L

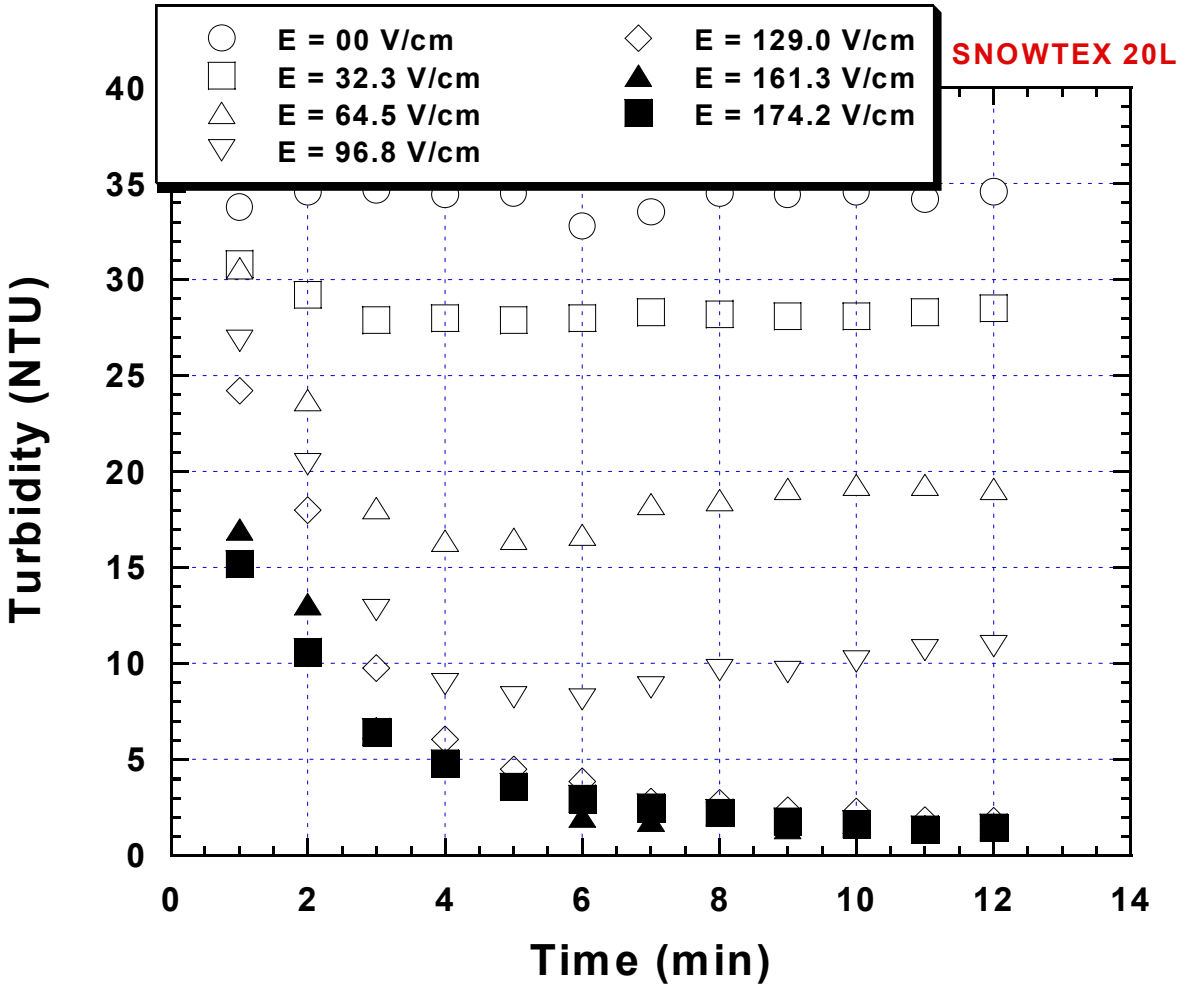

Figure A106. Effect of electrostatic fielld on change of filtrate turbidity. Experimental conditions: pH = 6.2; Sample: Snowtex 20L

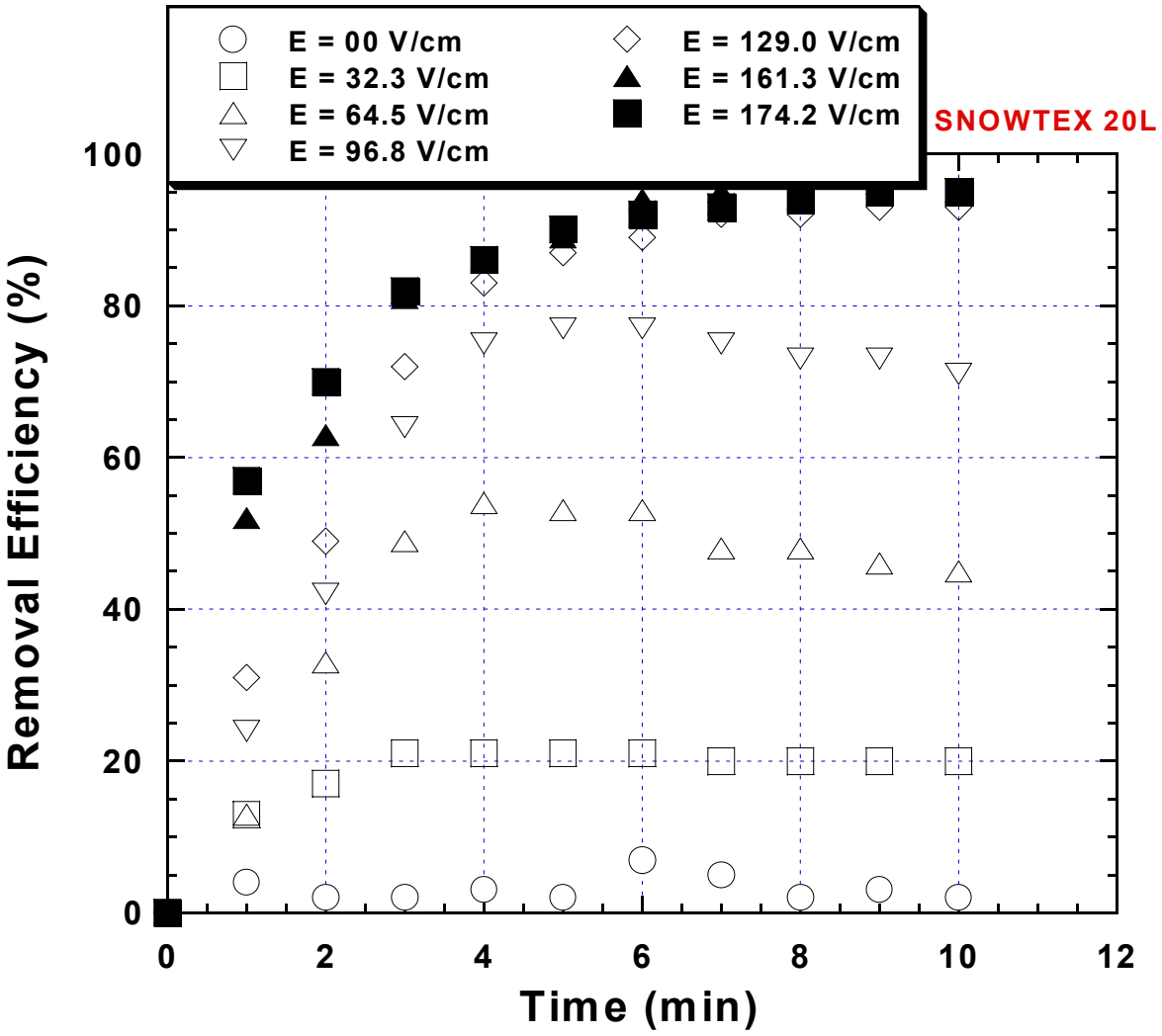

Figure A107. Effect of electrostatic field on removal of colloidal silica (I). Experimental conditions: pH = 6.2; Sample: Snowtex 20L

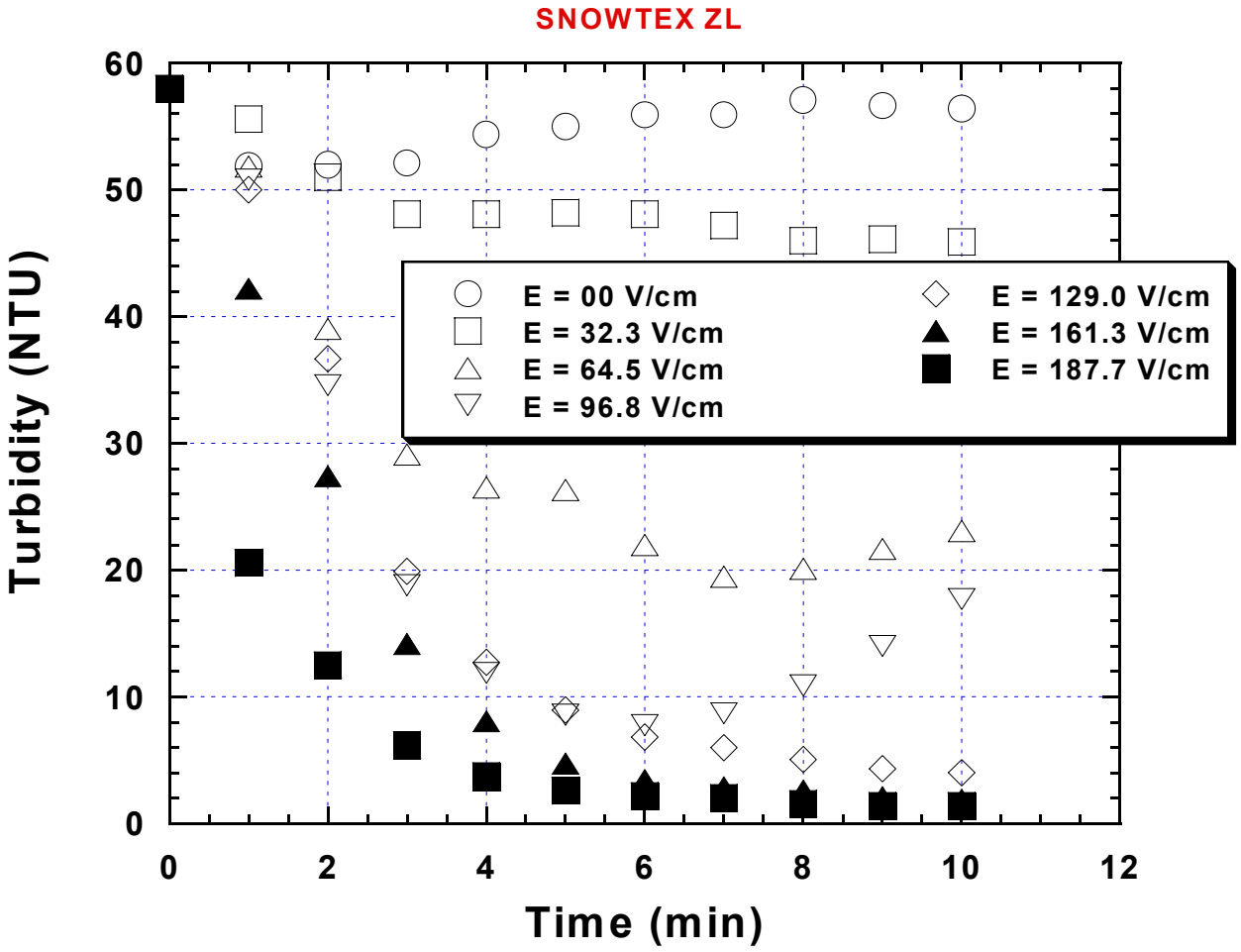

Figure A108. Effect of electrostatic field on change of filtrate turbidity. Experimental condition: pH = 5; Sample: Snowtex ZL

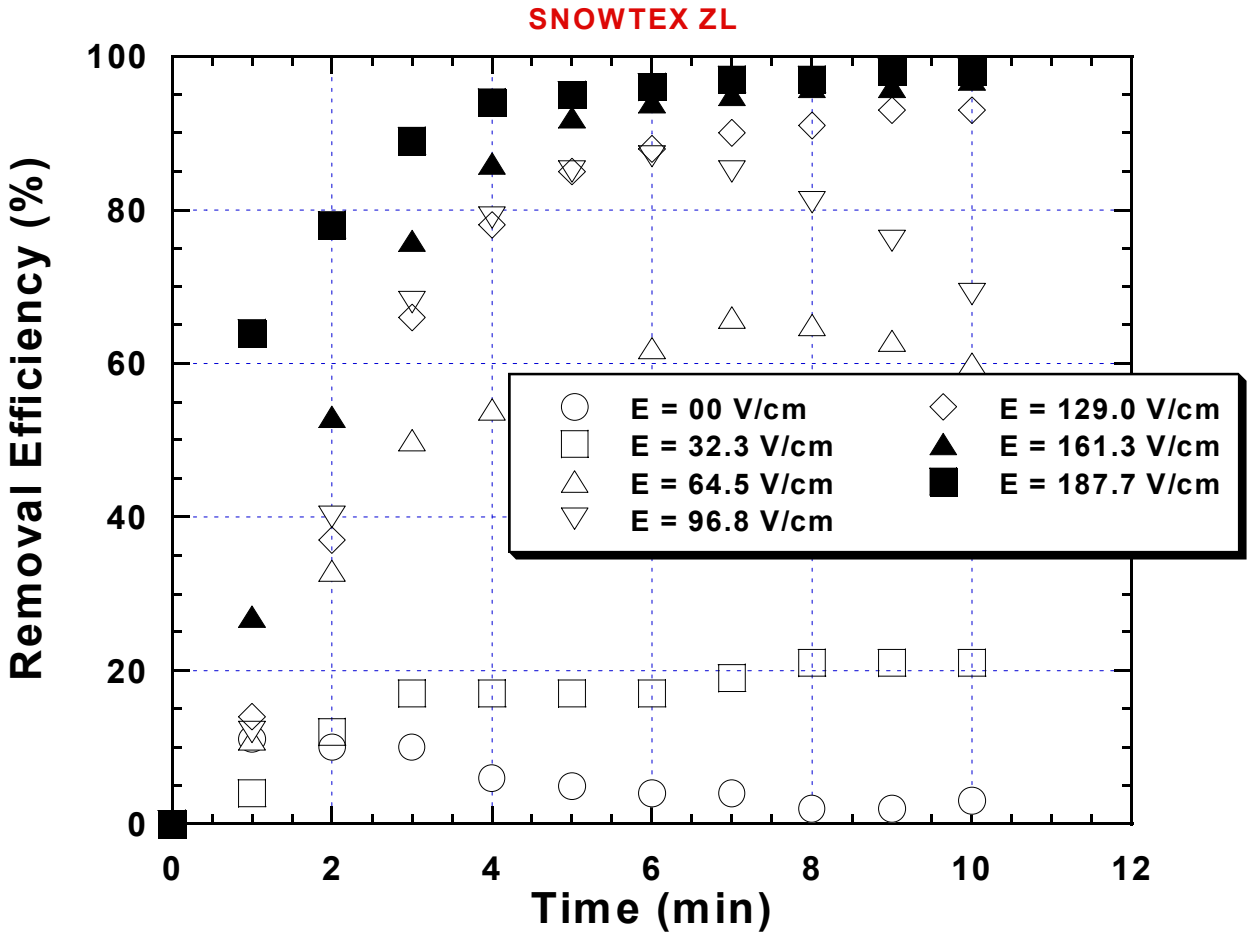

Figure A109. Effect of electrostatic field on removal of colloidal silica (I). Experimental condition: pH = 5; Sample: Snowtex ZL

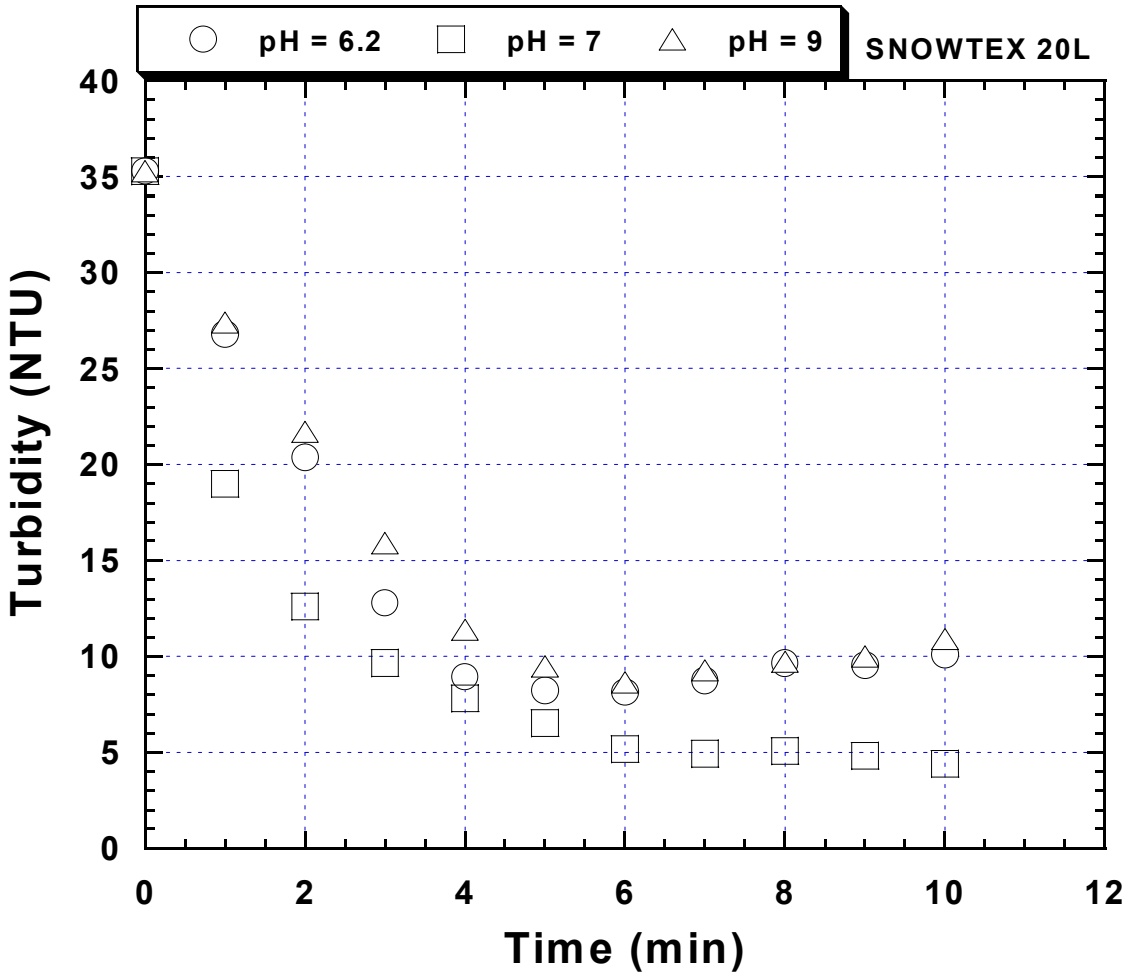

Figure A110. Change of turbidity as a function of time at various pH values. Experimental condition: electrostatic field = 96.8 V/cm; Sample: Snowtex 20L

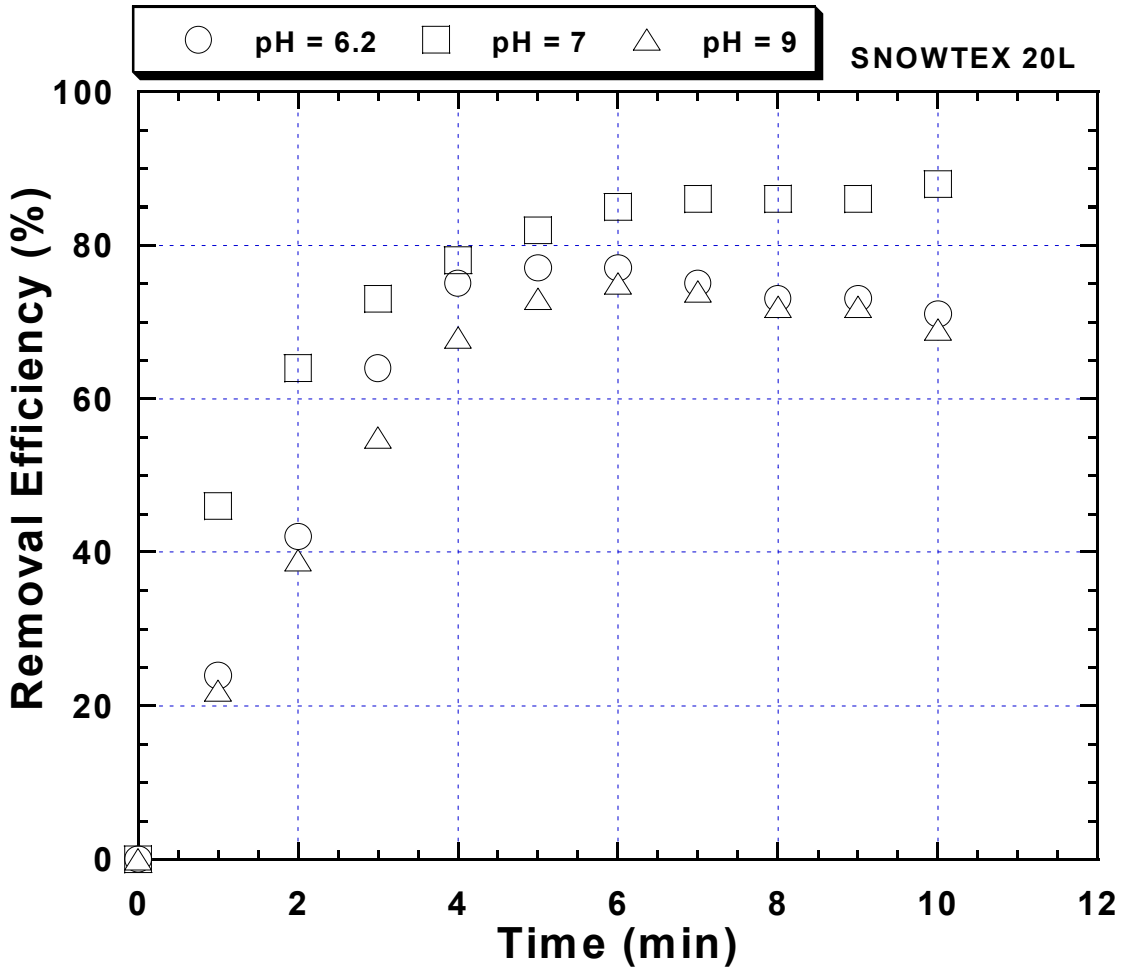

Figure A111. Removal efficiency as a function of time at various pH values. Experimental condition: electrostatic field = 96.8 V/cm; Sample: Snowtex 20L

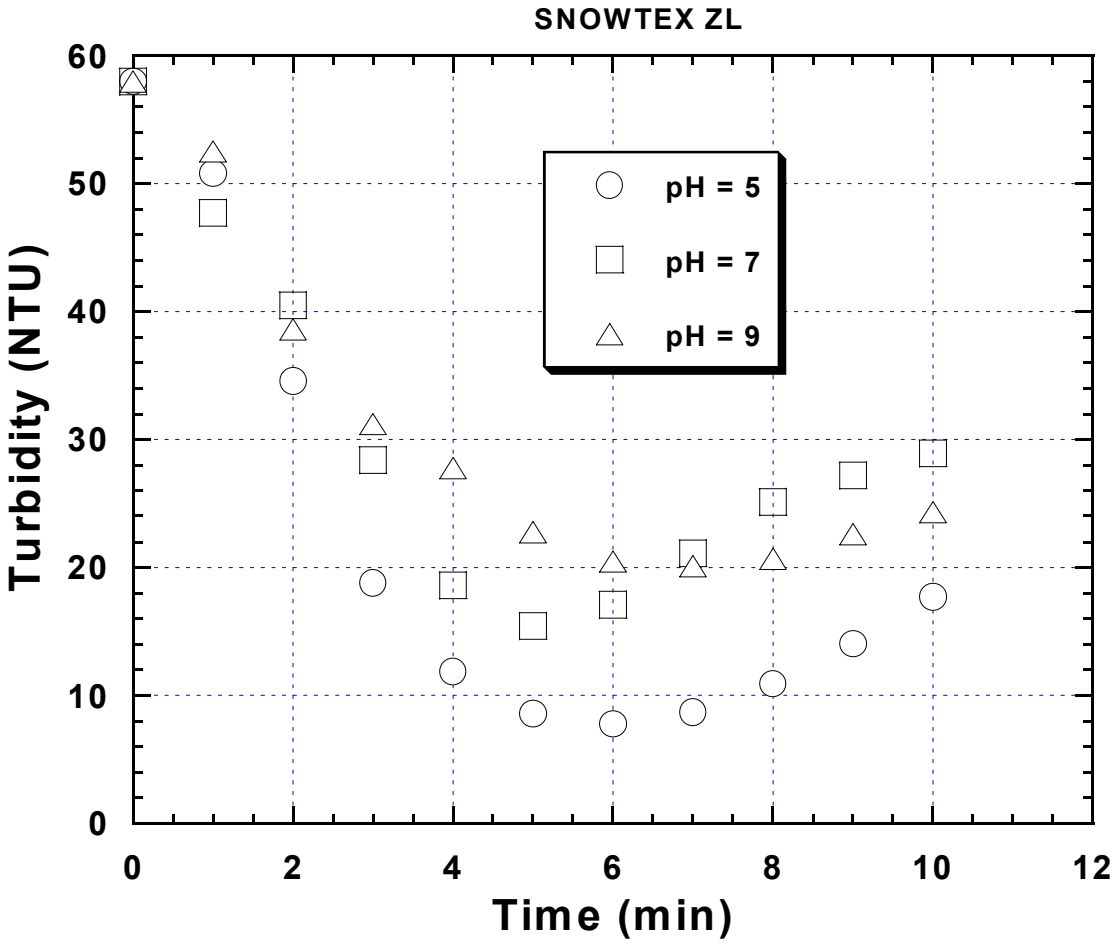

Figure A112. Change of turbidity as a function of time at various pH values. Experimental condition: electrostatic field = 96.8 V/cm; Sample: Snowtex ZL

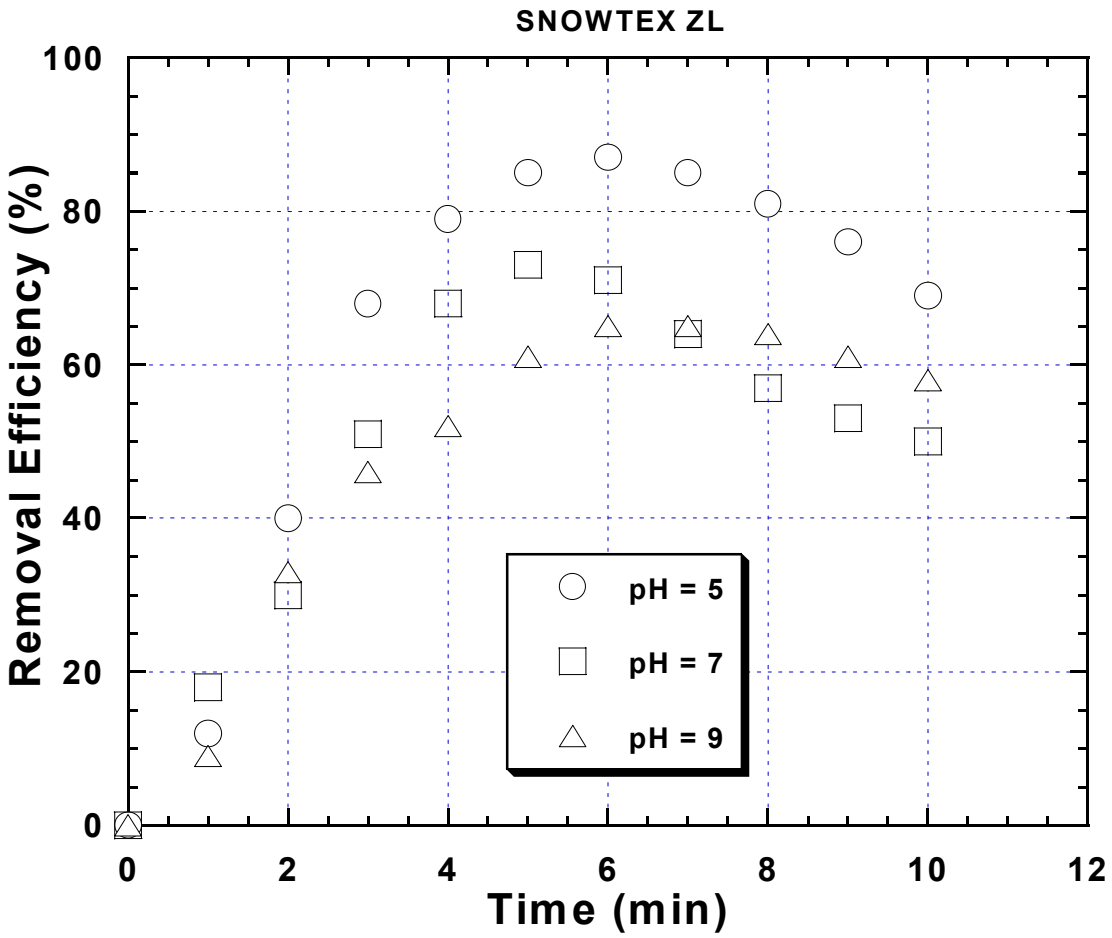

Figure A113. Removal efficiency as a function of time at various pH values. Experimental condition: electrostatic field = 96.8 V/cm; Sample: Snowtex ZL

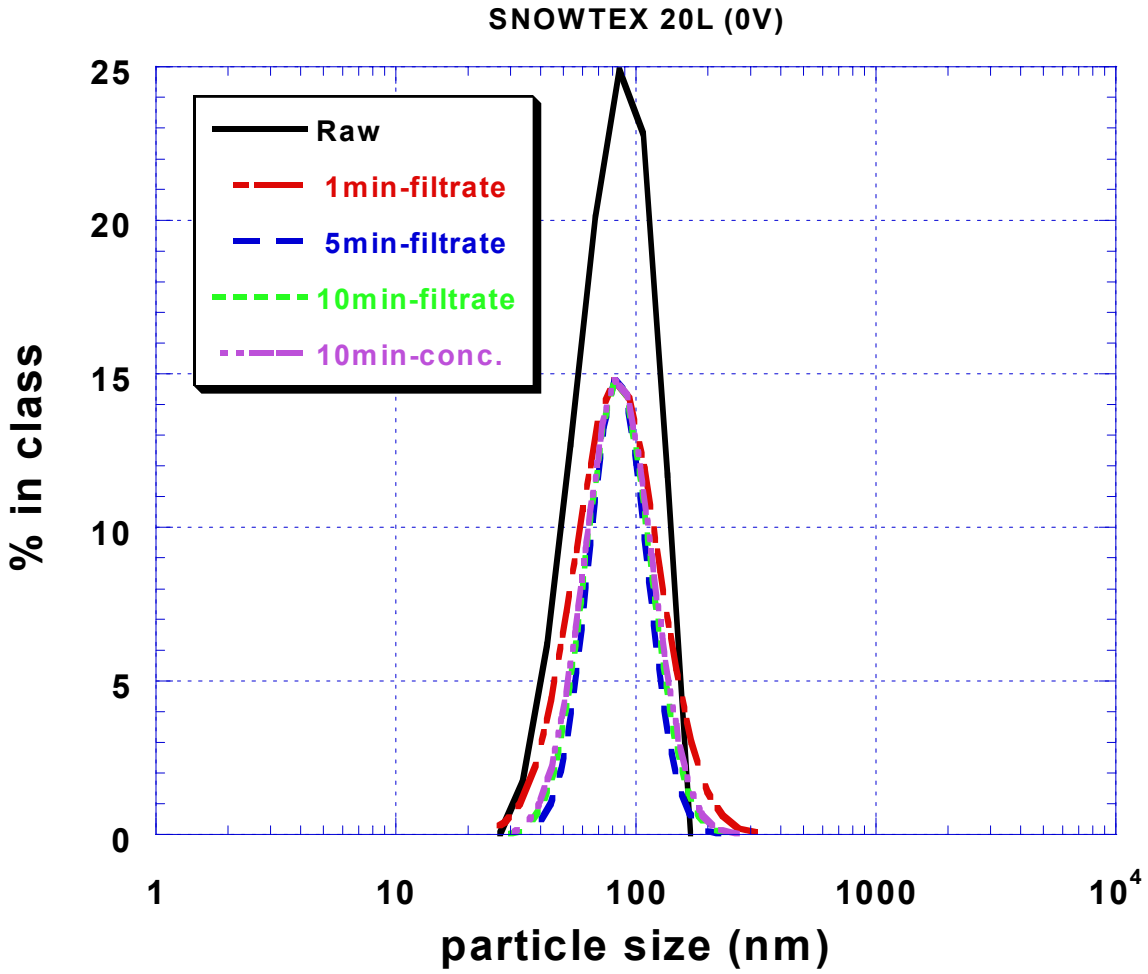

Figure A114. Change in particle size distribution during filtration operation. Experimental conditions: pH = 6.2; electrostatic field = 00V/cm; Sample: Snowtex 20L

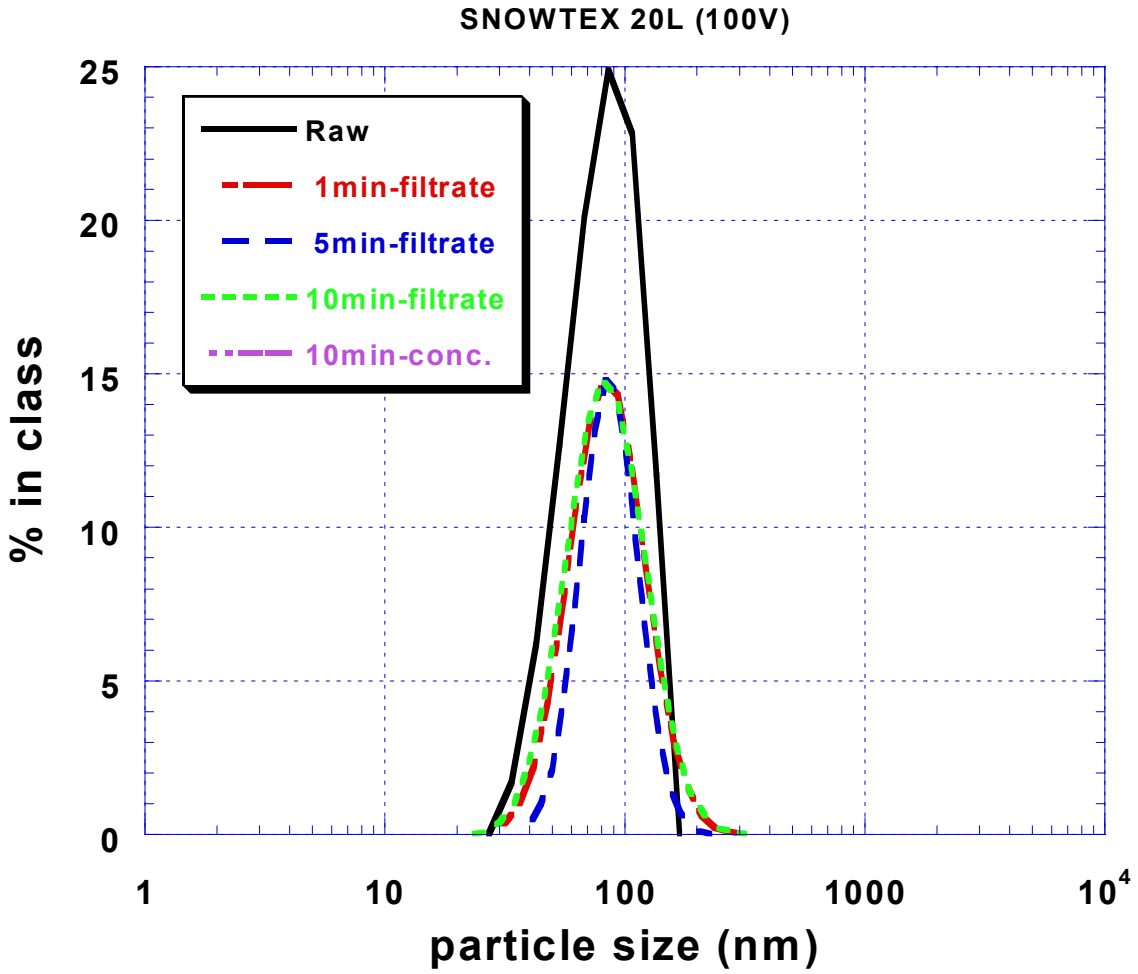

Figure A115. Change in particle size distribution during filtration operation. Experimental conditions: pH = 6.2; electrostatic field = 32.3V/cm; Sample: Snowtex 20L

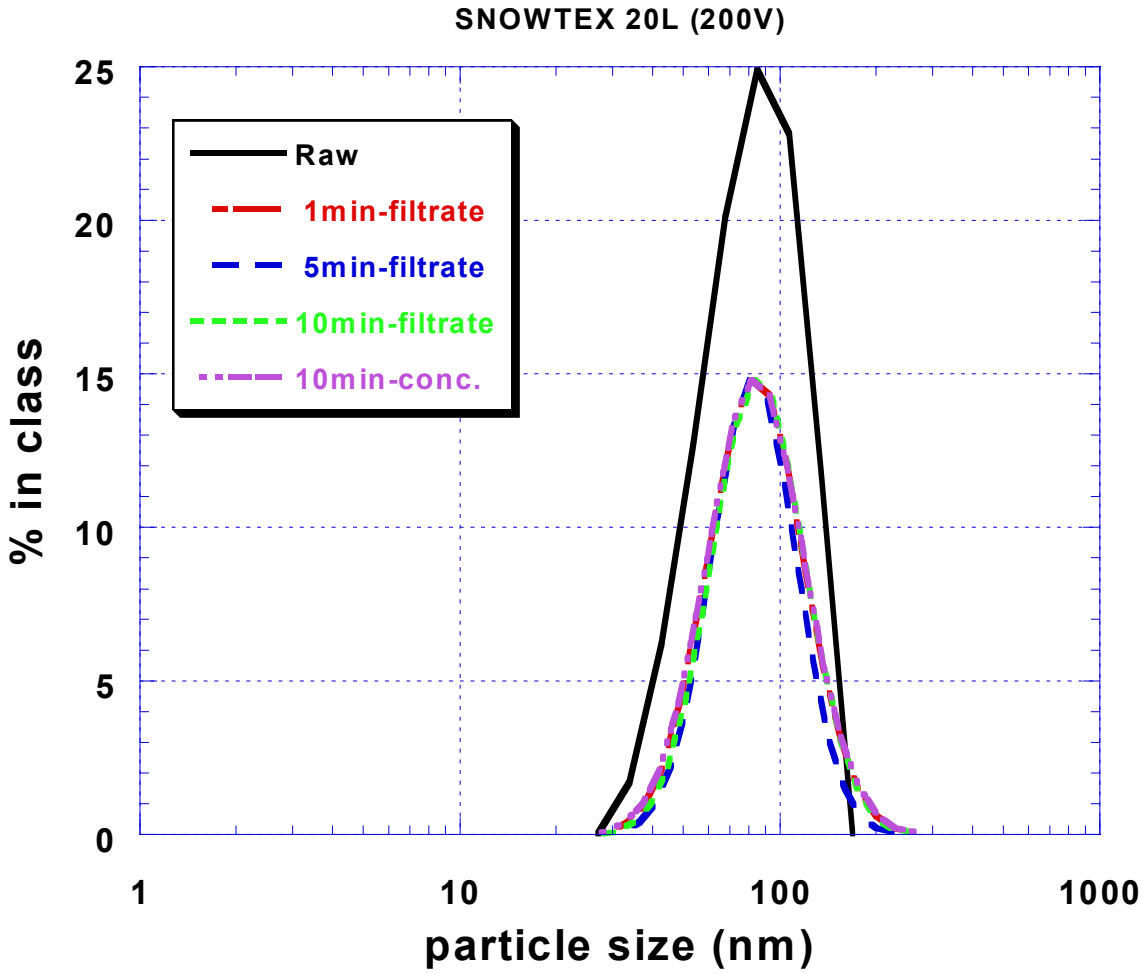

Figure A116. Change in particle size distribution during filtration operation. Experimental conditions: pH = 6.2; electrostatic field = 64.5V/cm; Sample: Snowtex 20L

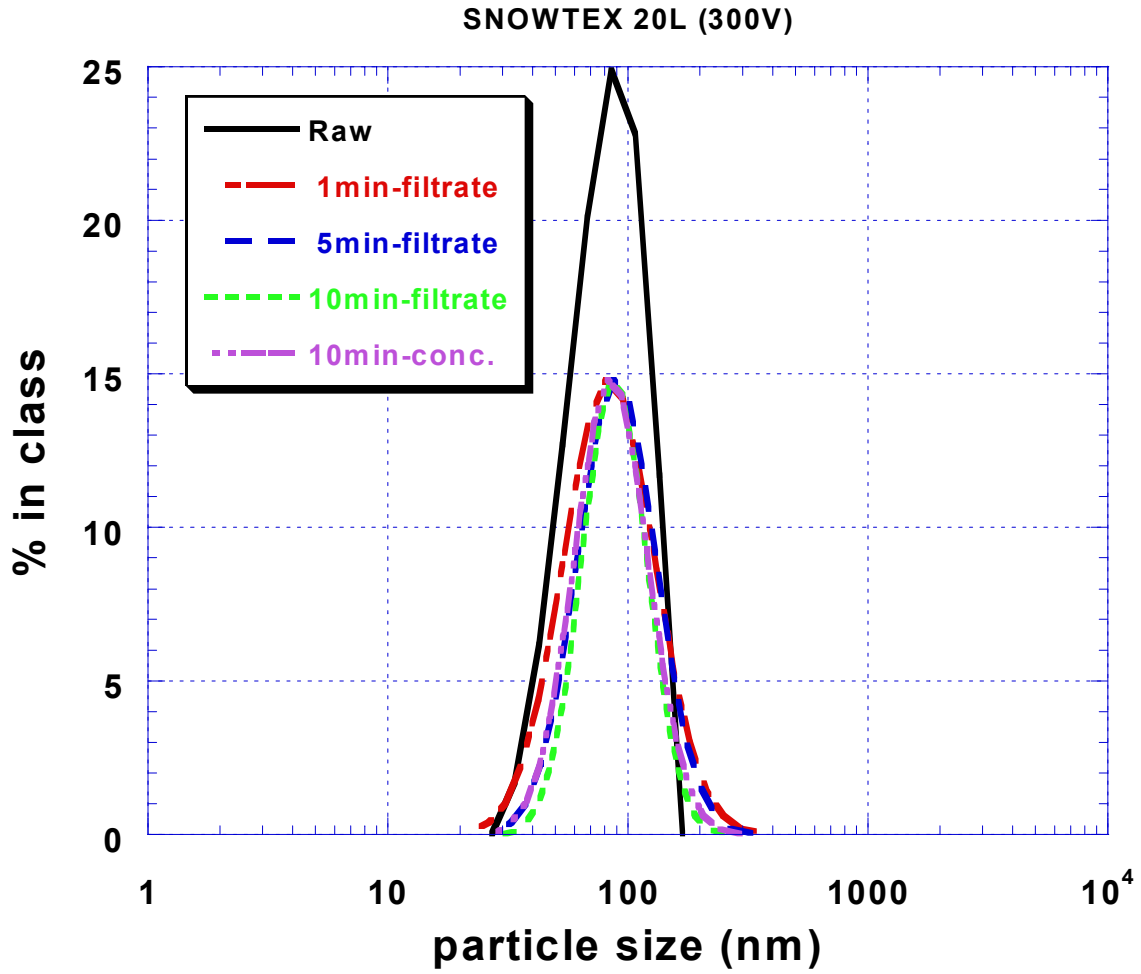

Figure A117. Change in particle size distribution during filtration operation. Experimental conditions: pH = 6.2; electrostatic field = 96.8V/cm; Sample: Snowtex 20L

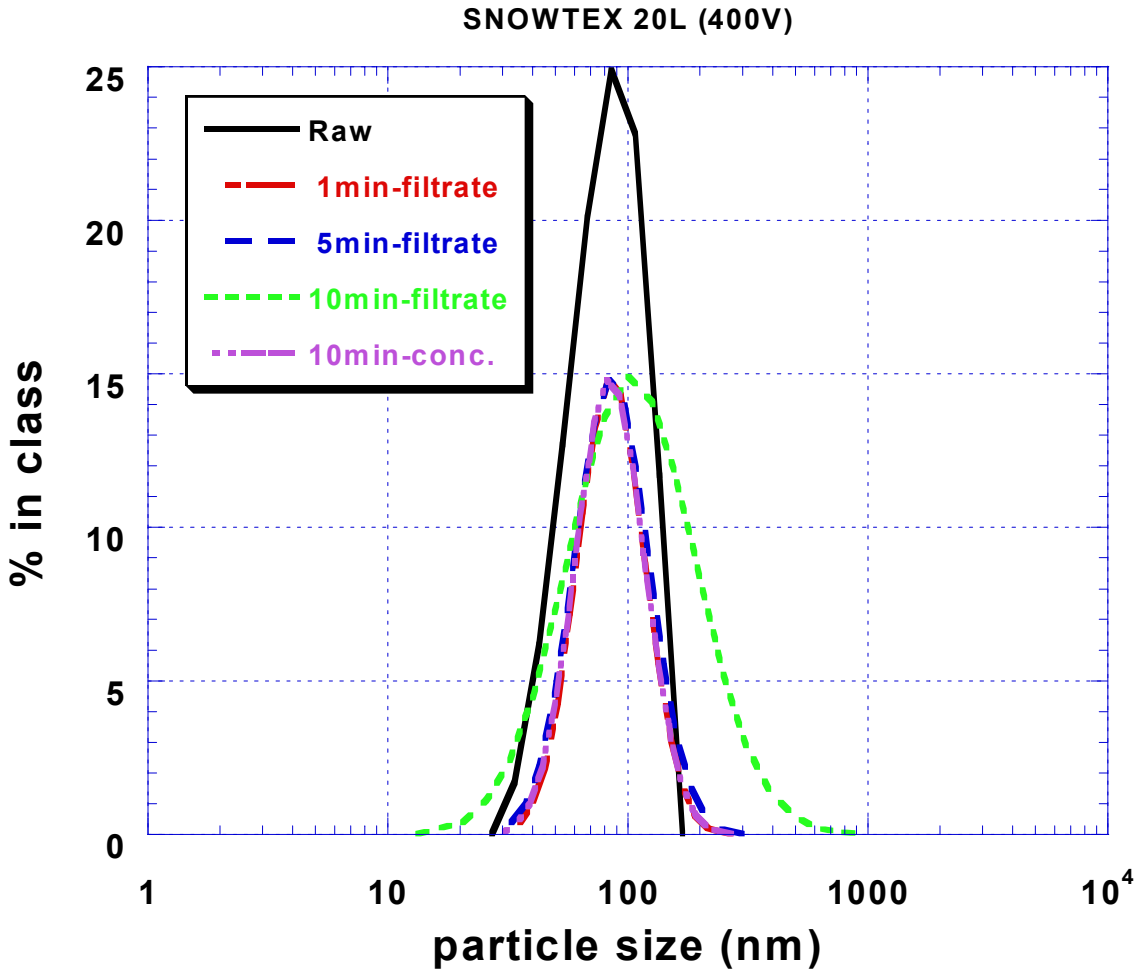

Figure A118. Change in particle size distribution during filtration operation. Experimental conditions: pH = 6.2; electrostatic field = 129V/cm; Sample: Snowtex 20L

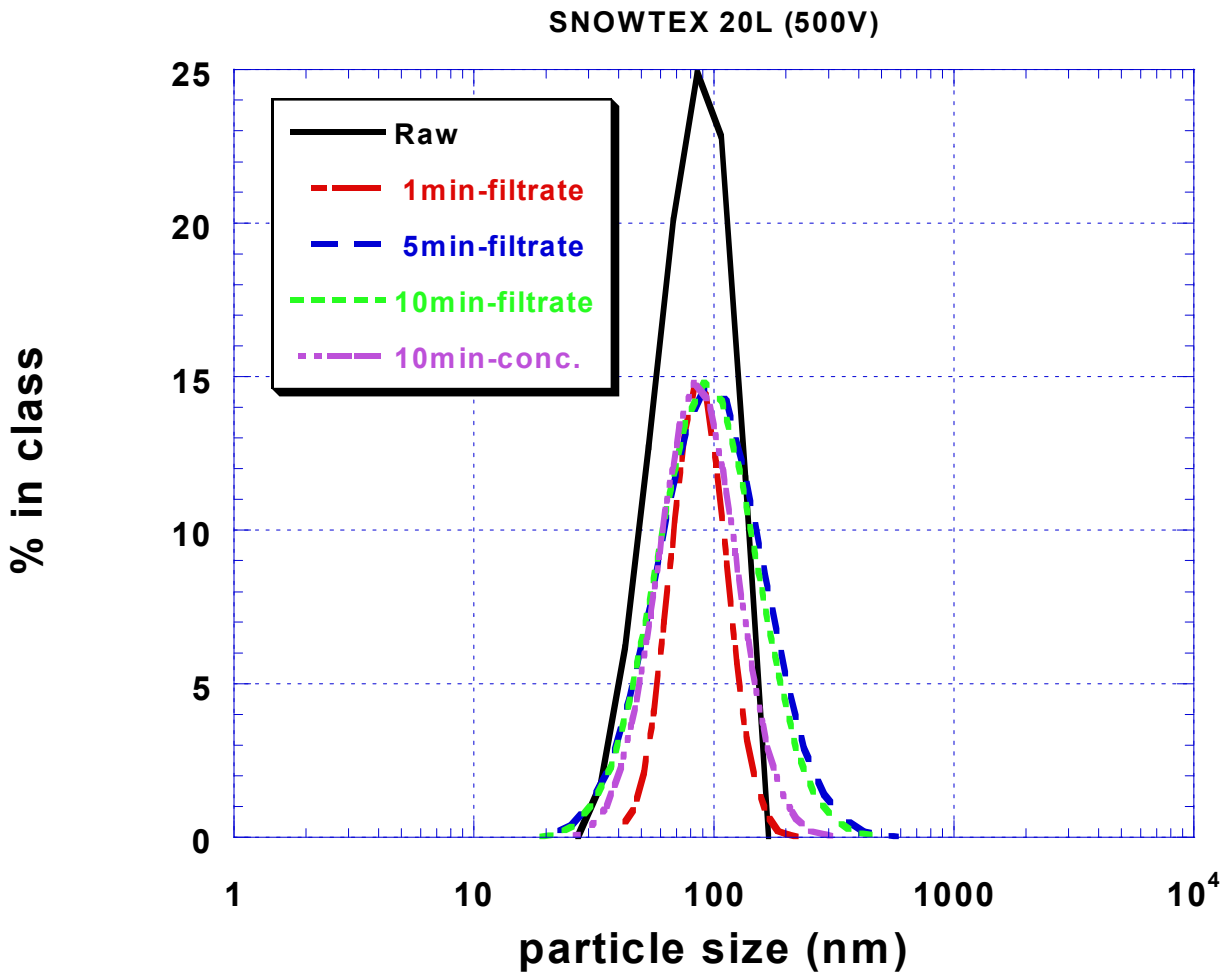

Figure A119. Change in particle size distribution during filtration operation. Experimental conditions: pH = 6.2; electrostatic field = 161.3V/cm; Sample: Snowtex 20L

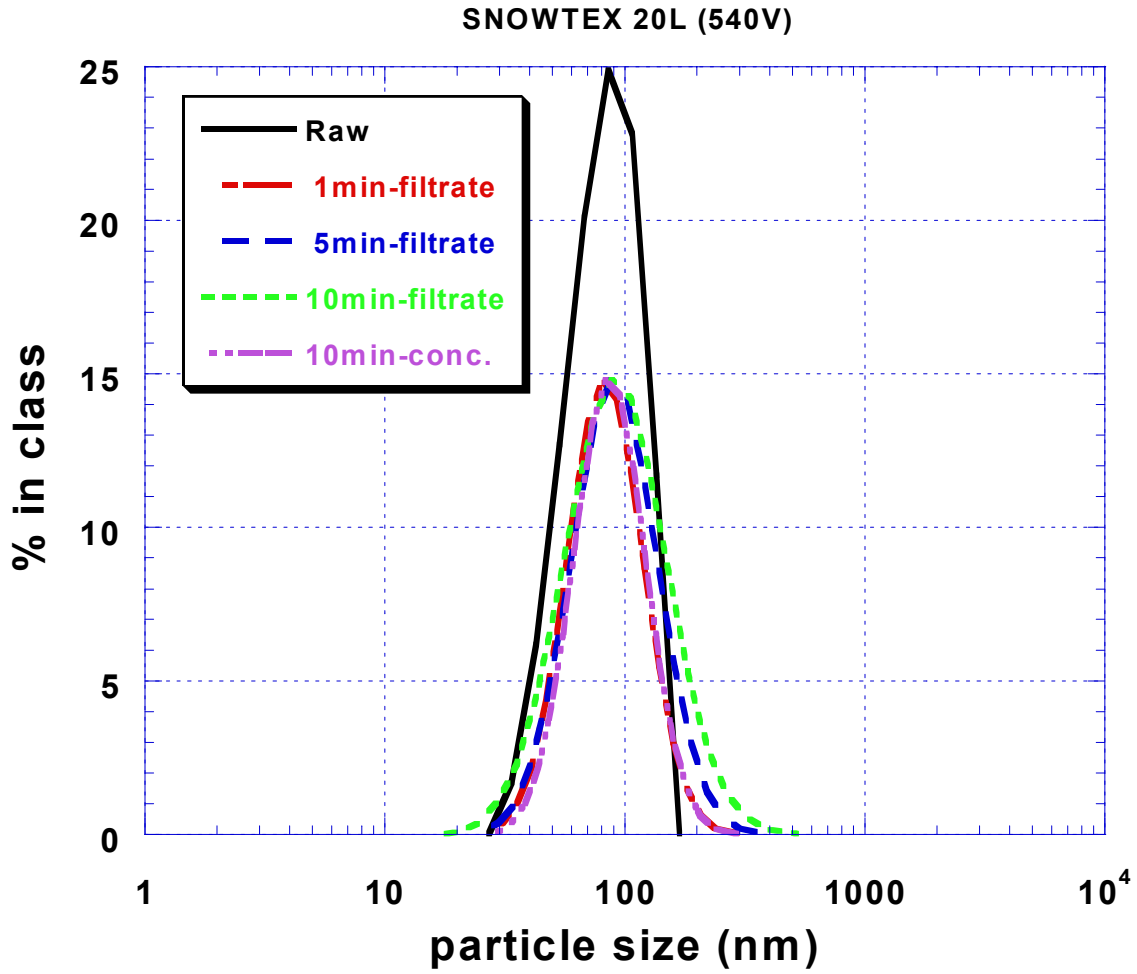

Figure A120. Change in particle size distribution during filtration operation. Experimental conditions: pH = 6.2; electrostatic field = 174.2V/cm; Sample: Snowtex 20L

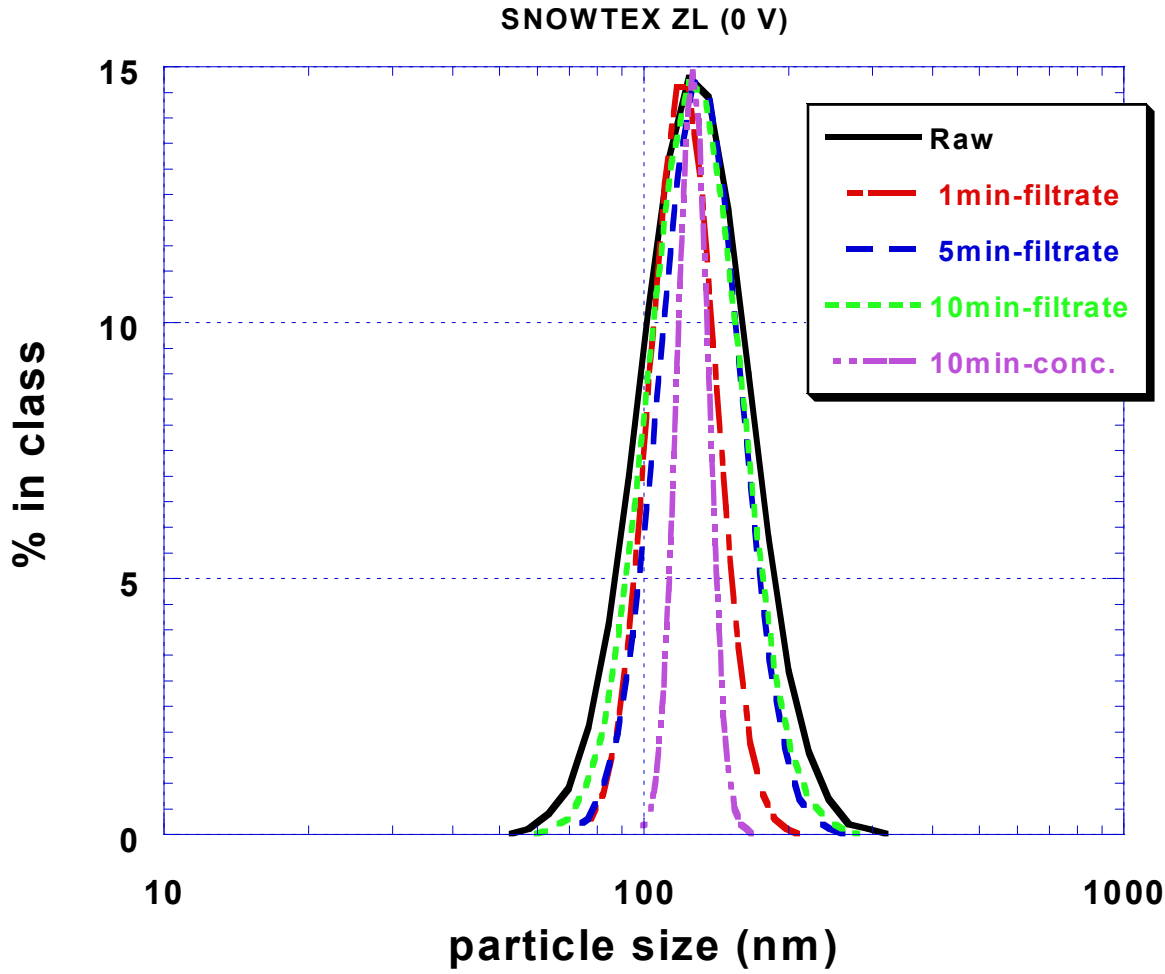

Figure A121. Changes in particle size distribution during filtration operation. Experimental conditions: pH = 5; electrostatic field = 00 V/cm; Sample: Snowtex ZL

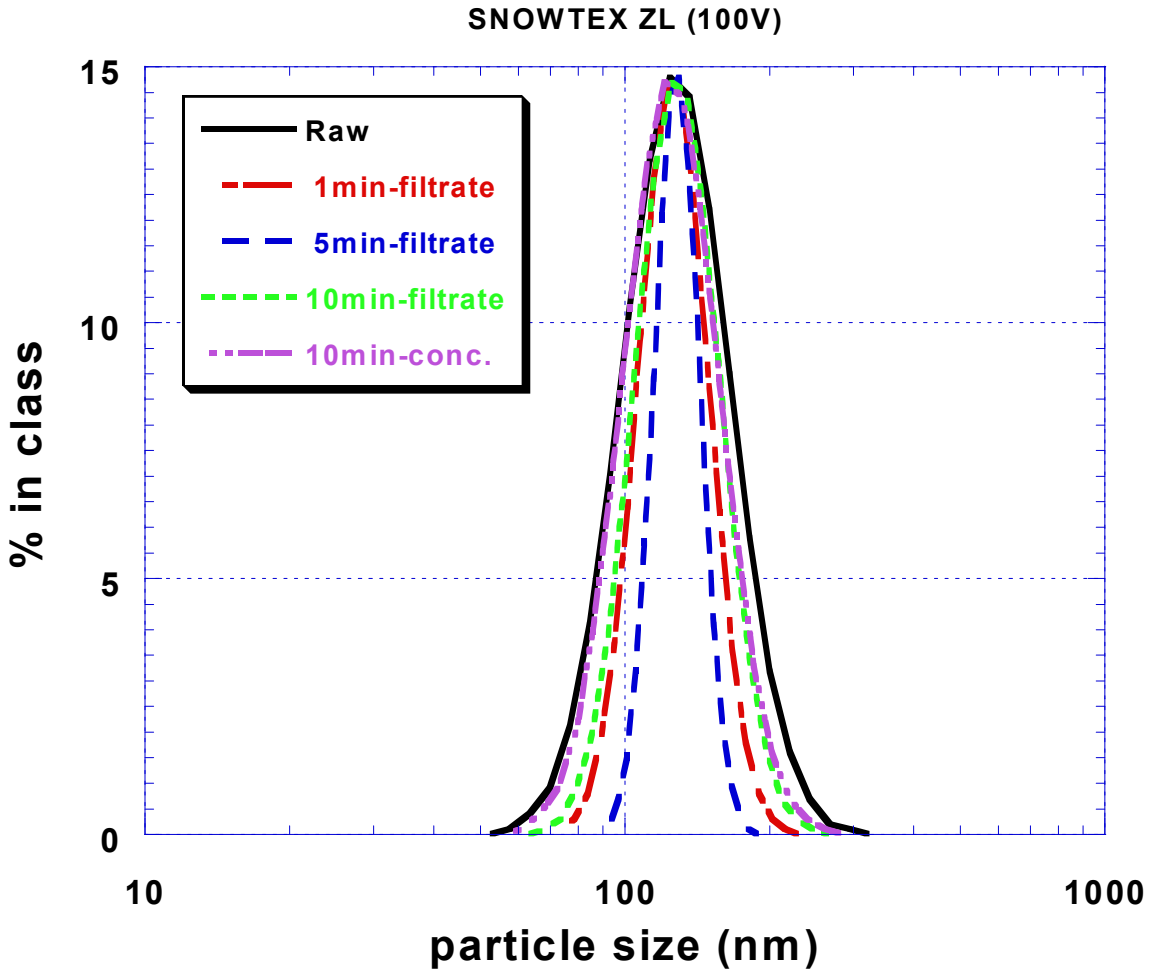

Figure A122. Changes in particle size distribution during filtration operation. Experimental conditions: pH = 5; electrostatic field = 32.3 V/cm; Sample: Snowtex ZL

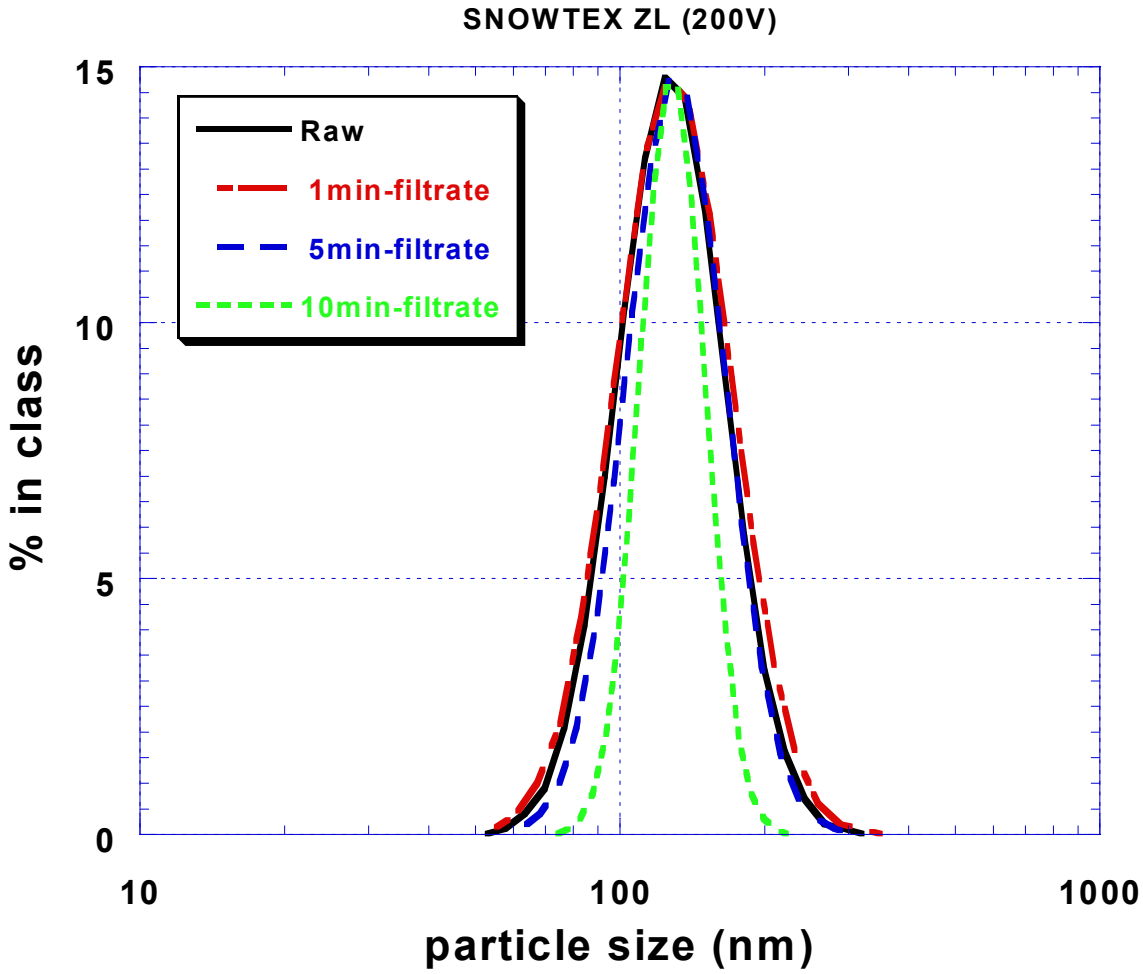

Figure A123. Changes in particle size distribution during filtration operation. Experimental conditions: pH = 5; electrostatic field = 64.5 V/cm; Sample: Snowtex ZL

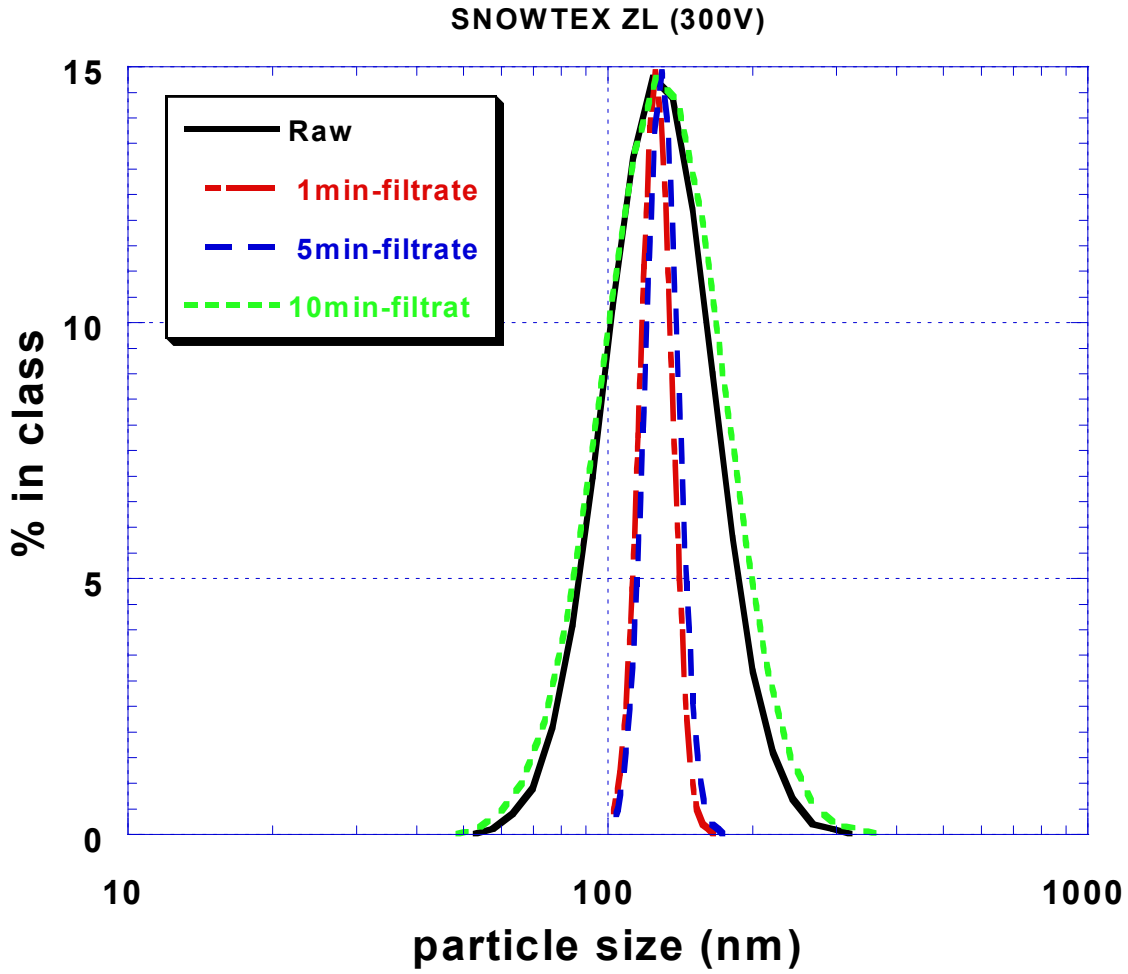

Figure 124. Changes in particle size distribution during filtration operation. Experimental conditions: pH = 5; electrostatic field = 96.8 V/cm; Sample: Snowtex ZL

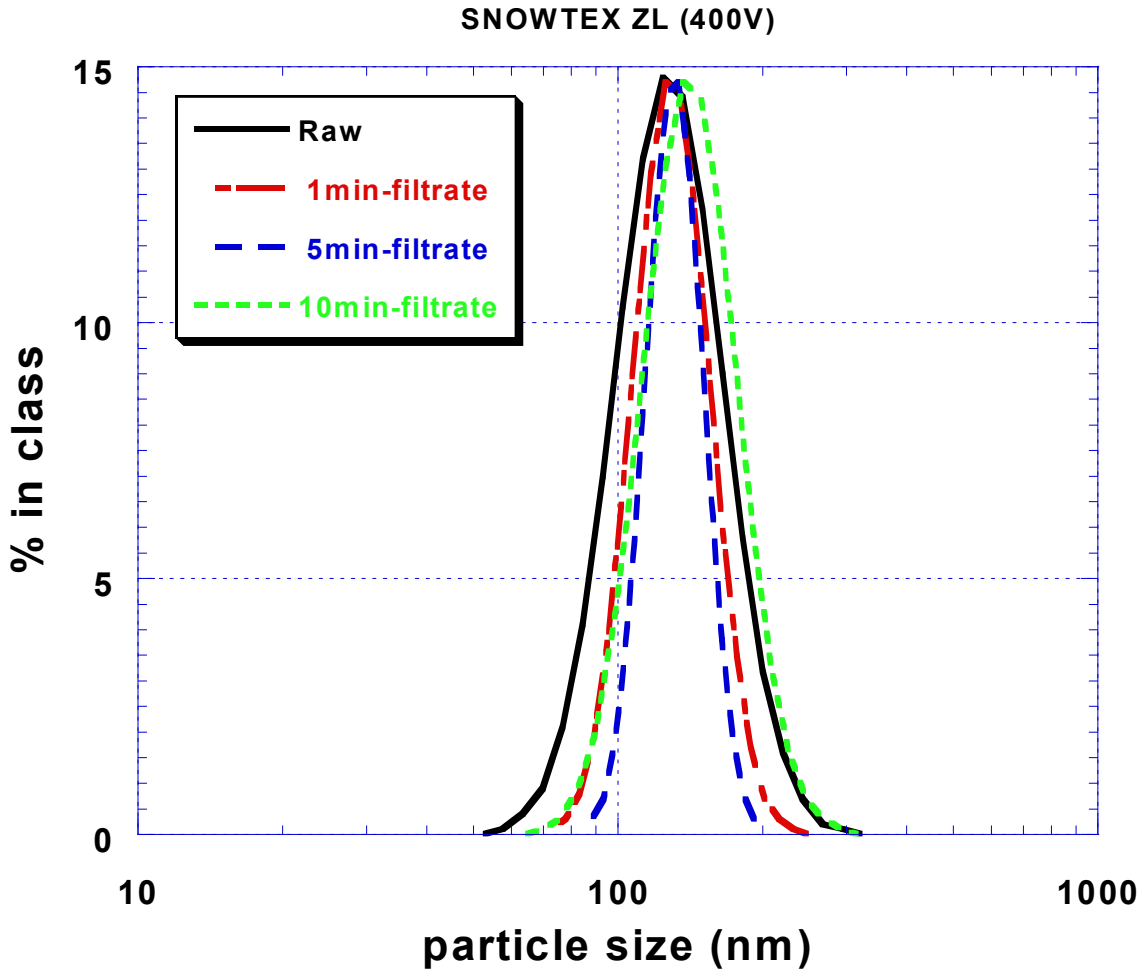

Figure A125. Changes in particle size distribution during filtration operation. Experimental conditions: pH = 5; electrostatic field = 129 V/cm; Sample: Snowtex ZL

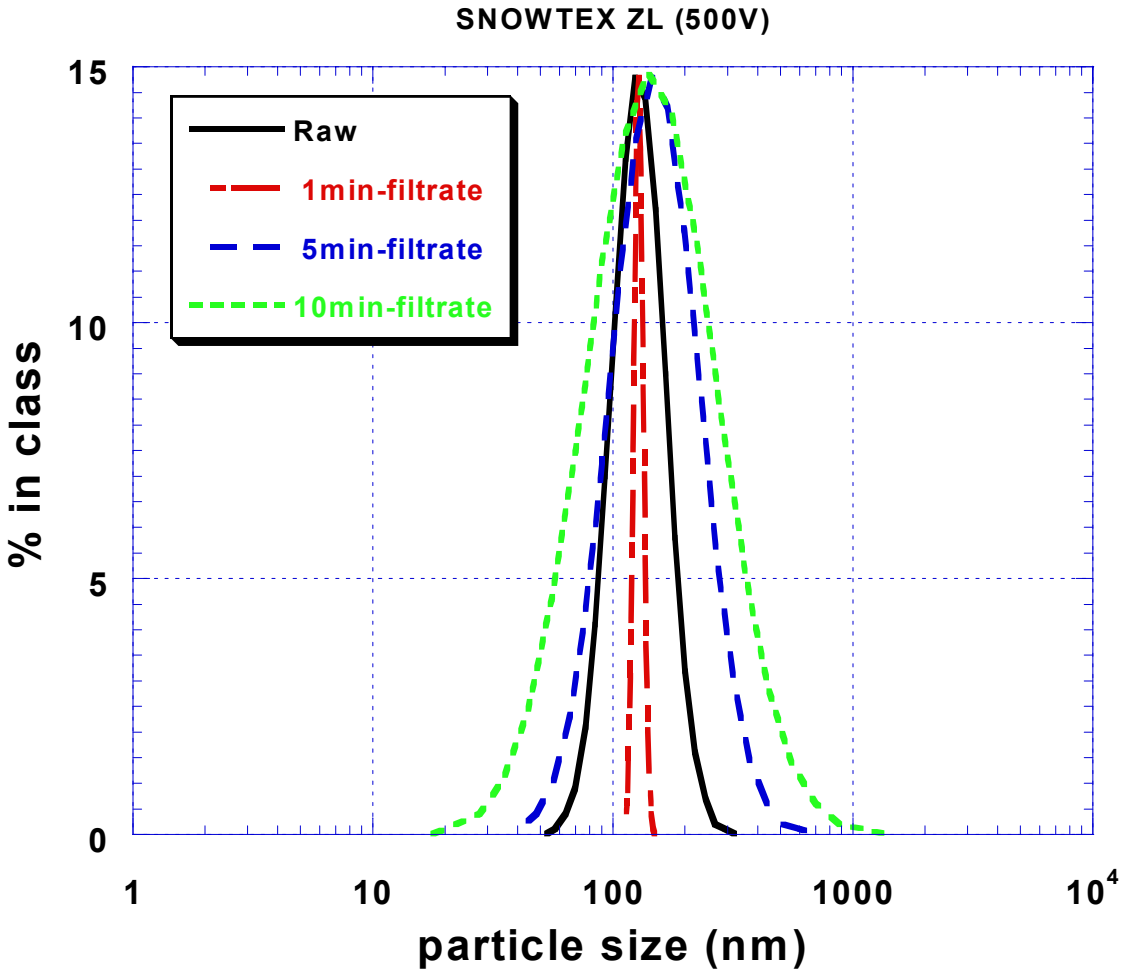

Figure A126. Changes in particle size distribution during filtration operation. Experimental conditions: pH = 5; electrostatic field = 161.3 V/cm; Sample: Snowtex ZL

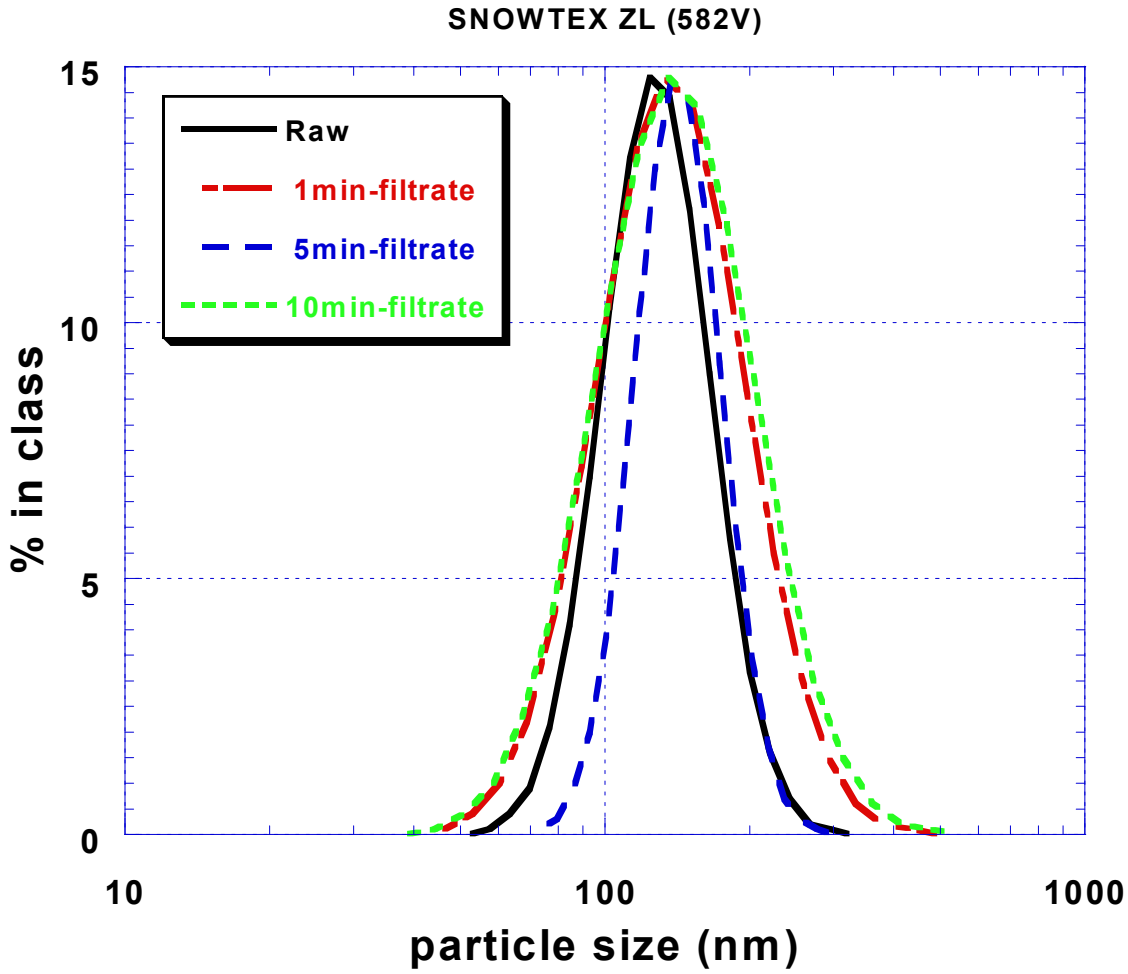

Figure 127. Changes in particle size distribution during filtration operation. Experimental conditions: pH = 5; electrostatic field = 187.7 V/cm; Sample: Snowtex ZL

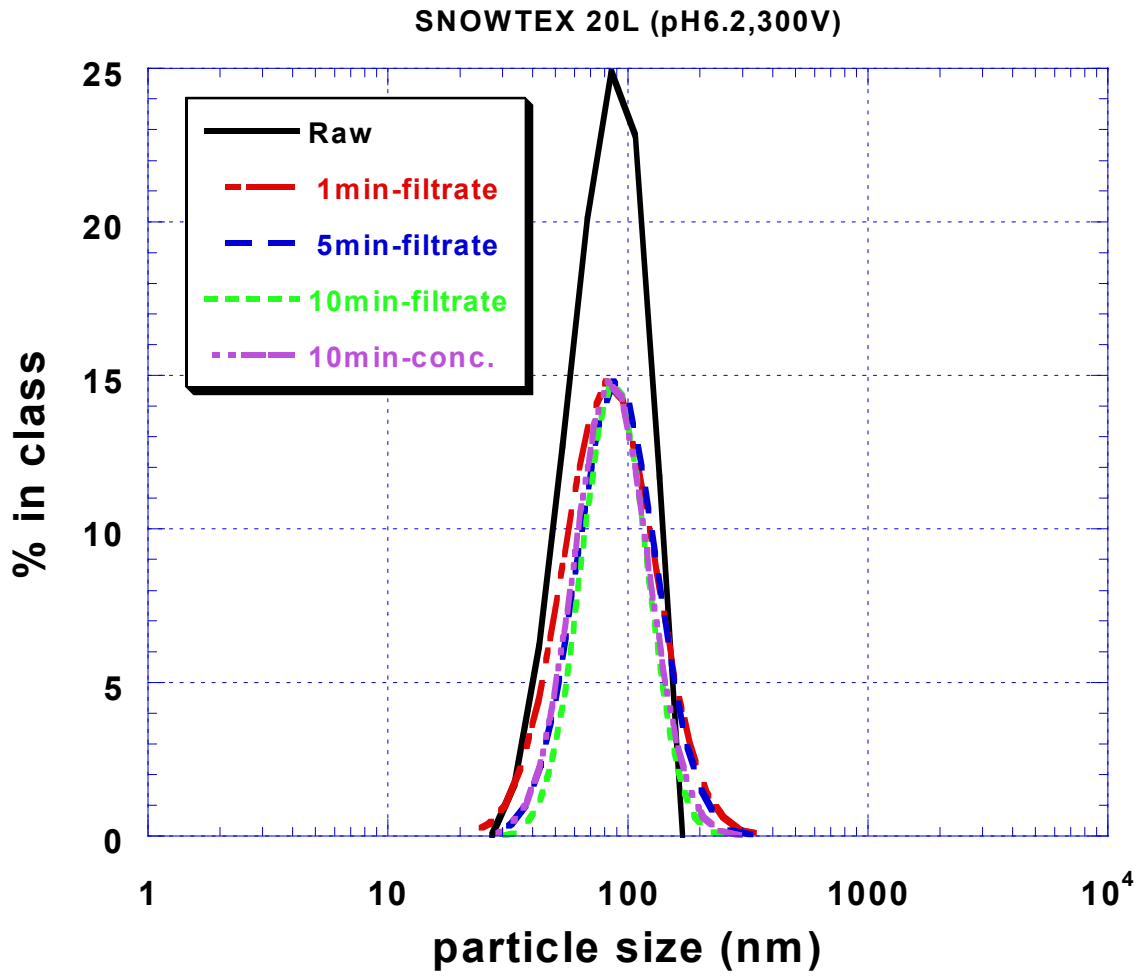

Figure A128. Changes in particle size distribution during filtration operation. Experimental conditions: pH = 6.2; electrostatic field = 96.8 V/cm; Sample: Snowtex 20L.

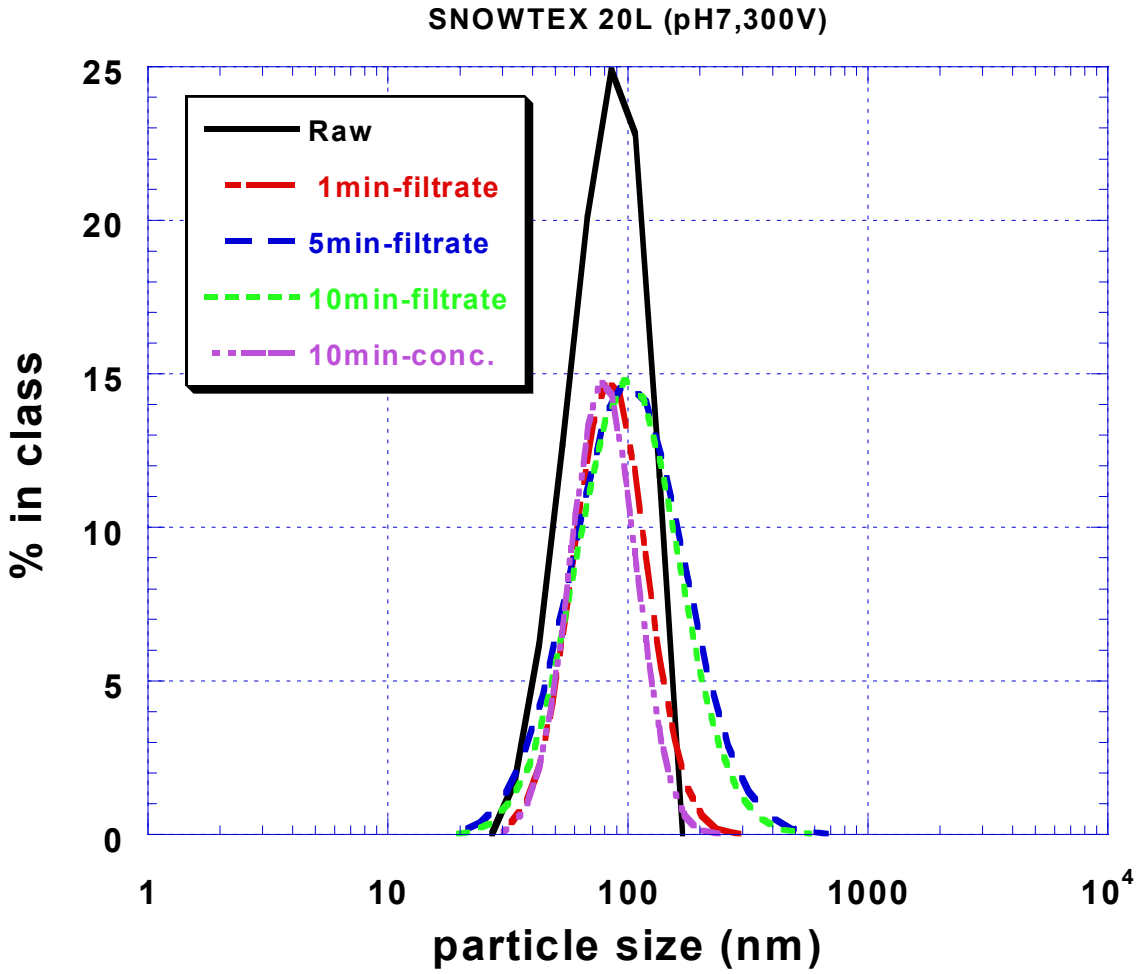

Figure A129. Changes in particle size distribution during filtration operation. Experimental conditions: pH = 7.0; electrostatic field = 96.8 V/cm; Sample: Snowtex 20L

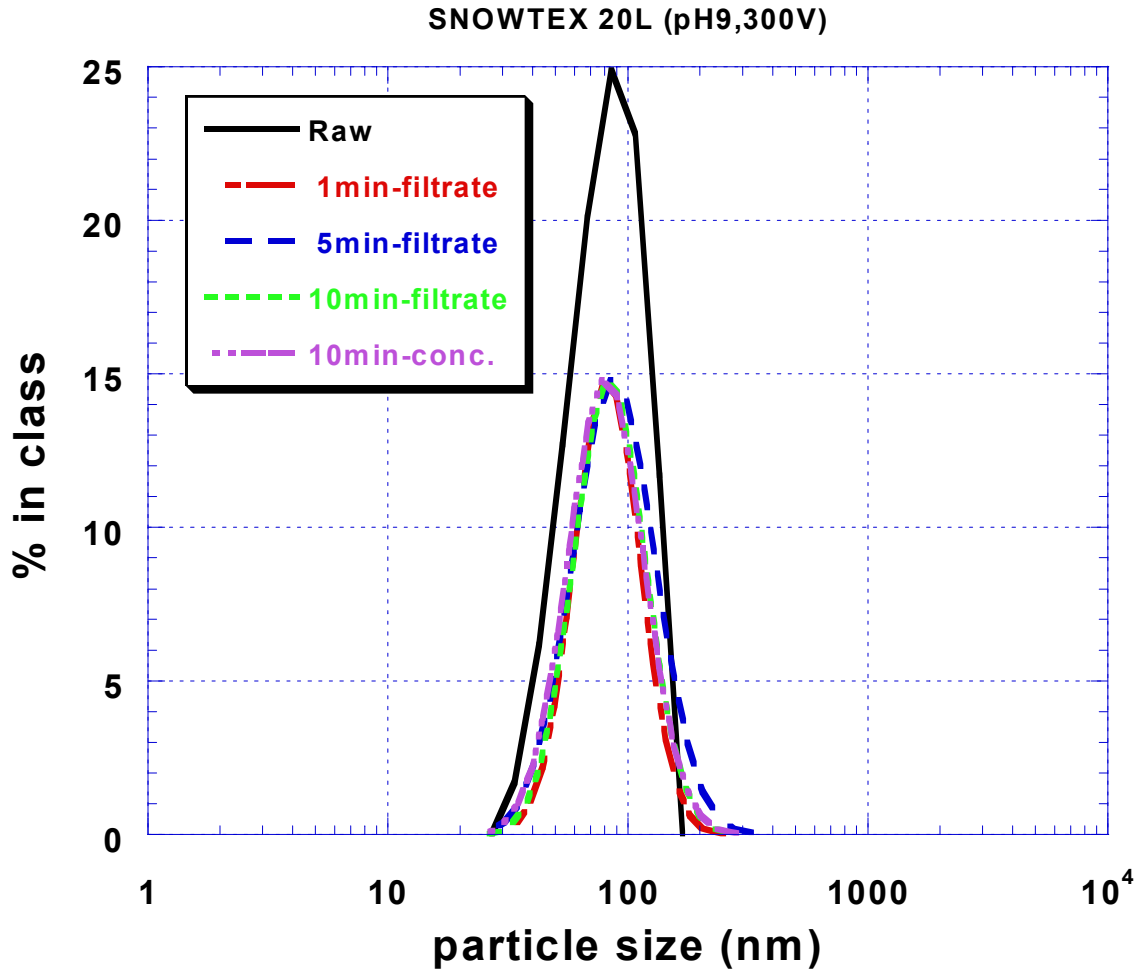

Figure A130. Changes in particle size distribution during filtration operation. Experimental conditions: pH = 9.0; electrostatic field = 96.8 V/cm; Sample: Snowtex 20L

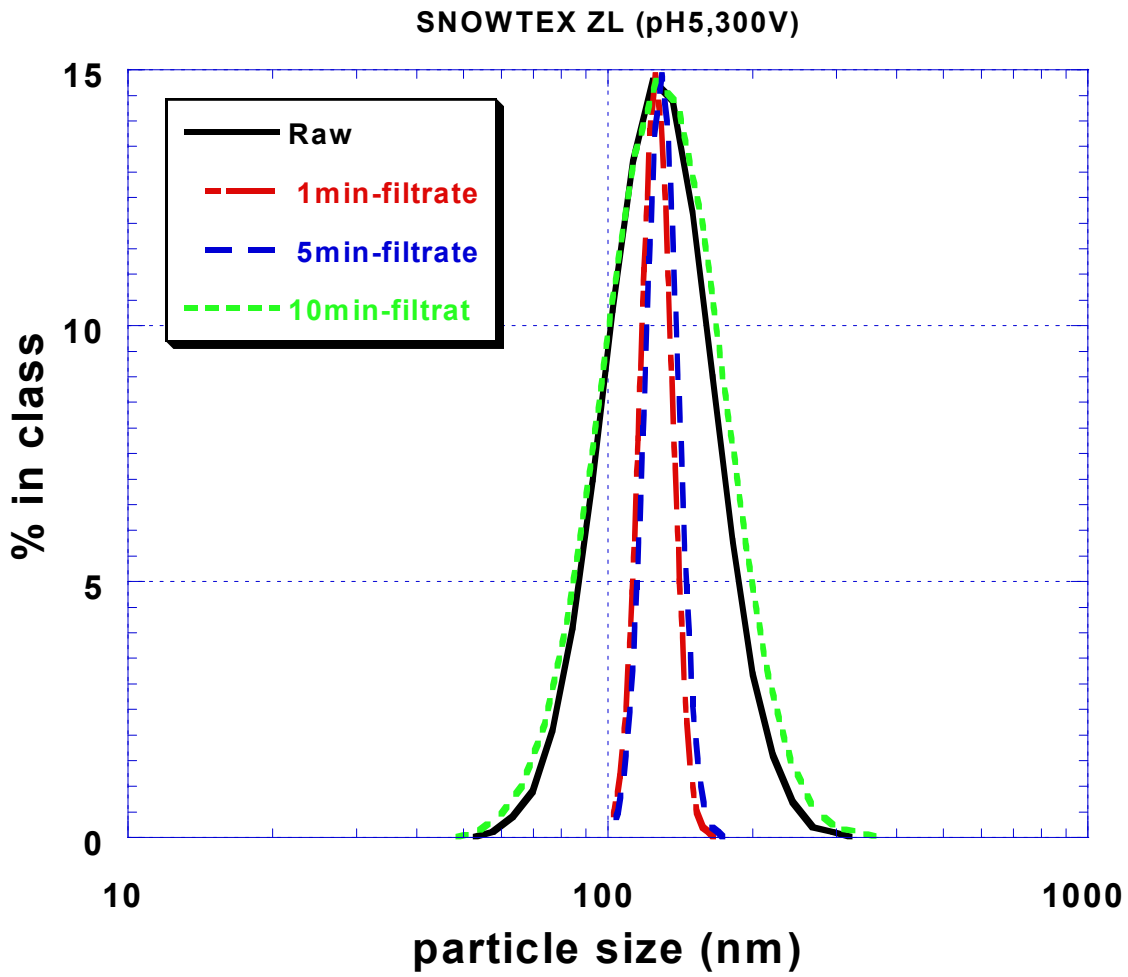

Figure A131. Changes in particle size distribution during filtration operation. Experimental conditions: pH = 5.0; electrostatic field = 96.8 V/cm; Sample: Snowtex ZL

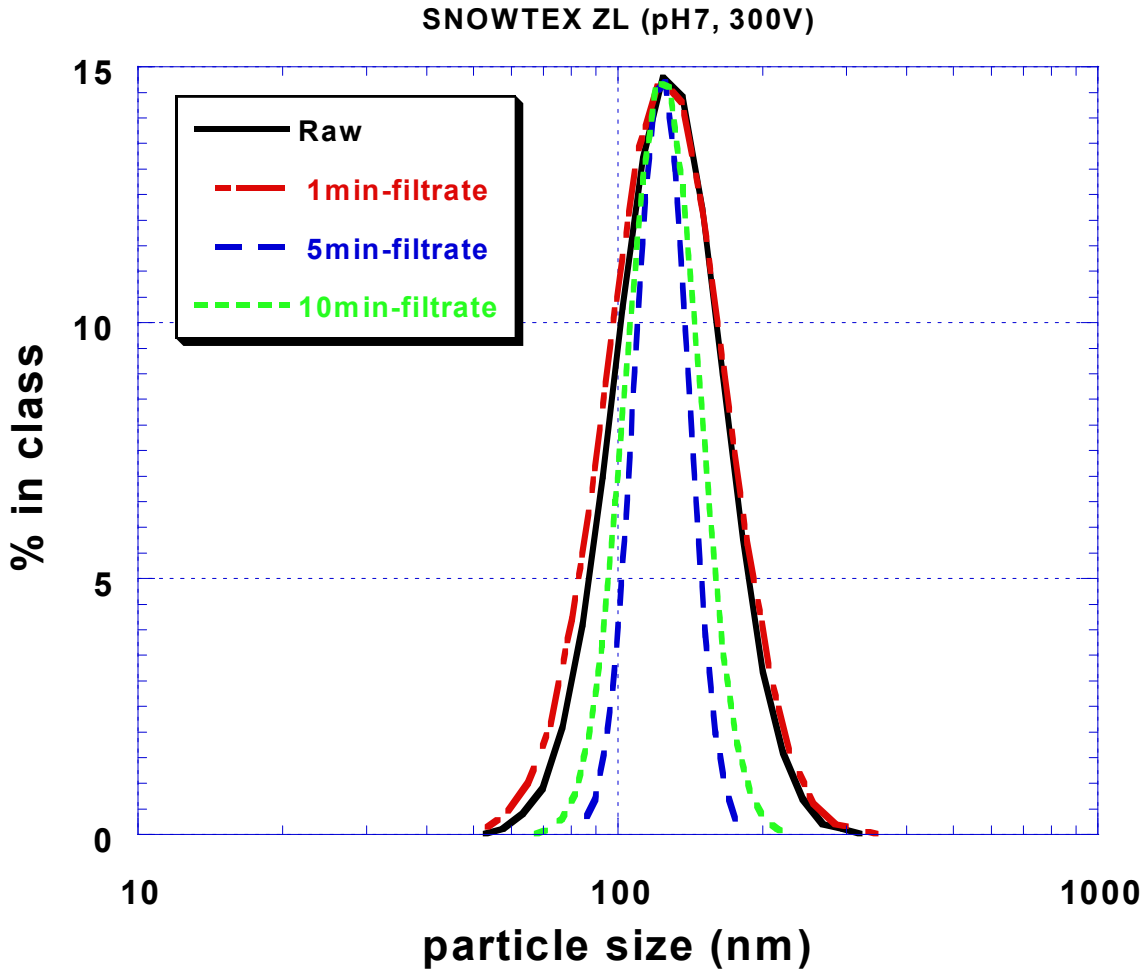

Figure A132. Changes in particle size distribution during filtration operation. Experimental conditions: pH = 7.0; electrostatic field = 96.8 V/cm; Sample: Snowtex ZL

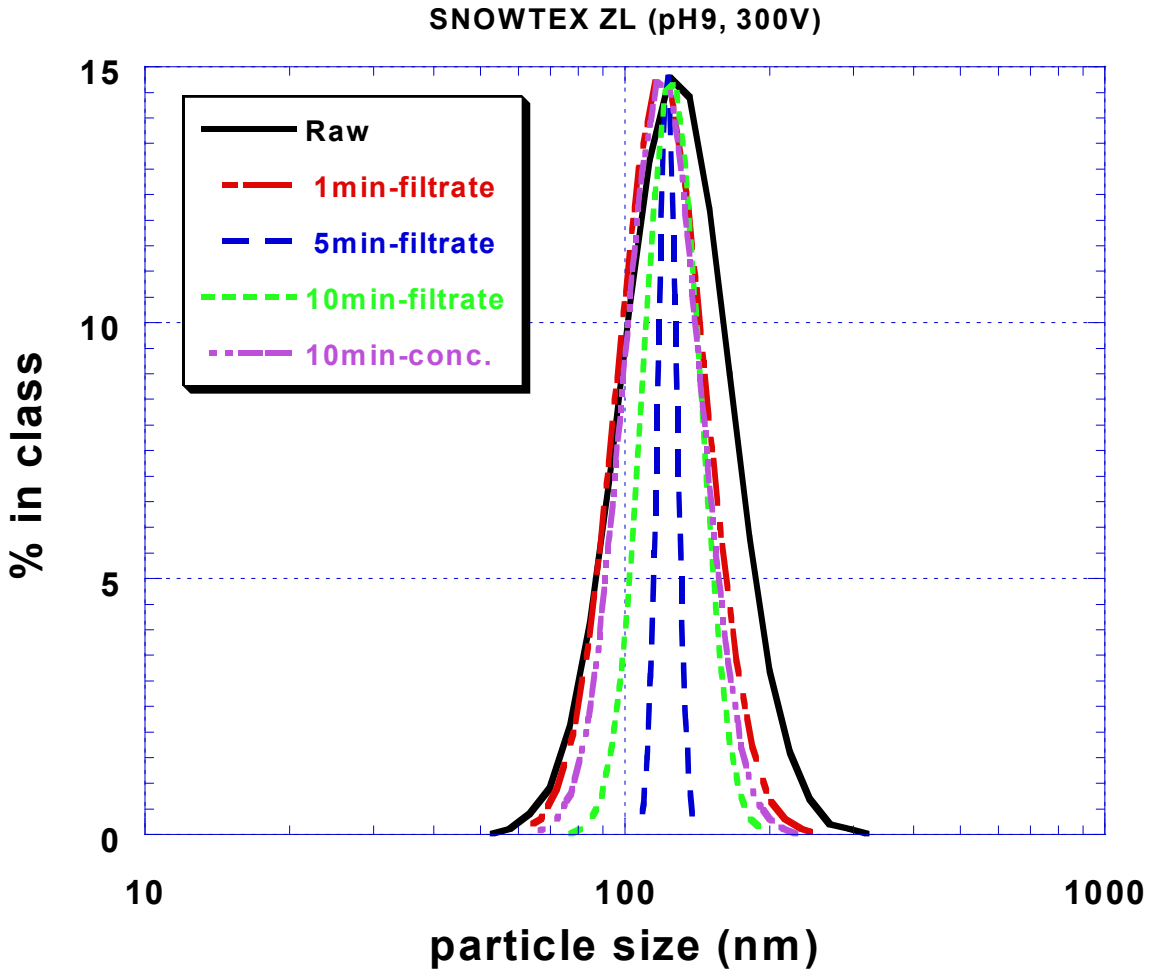

Figure A133. Changes in particle size distribution during filtration operation. Experimental conditions: pH = 9.0; electrostatic field = 96.8 V/cm; Sample: Snowtex ZL

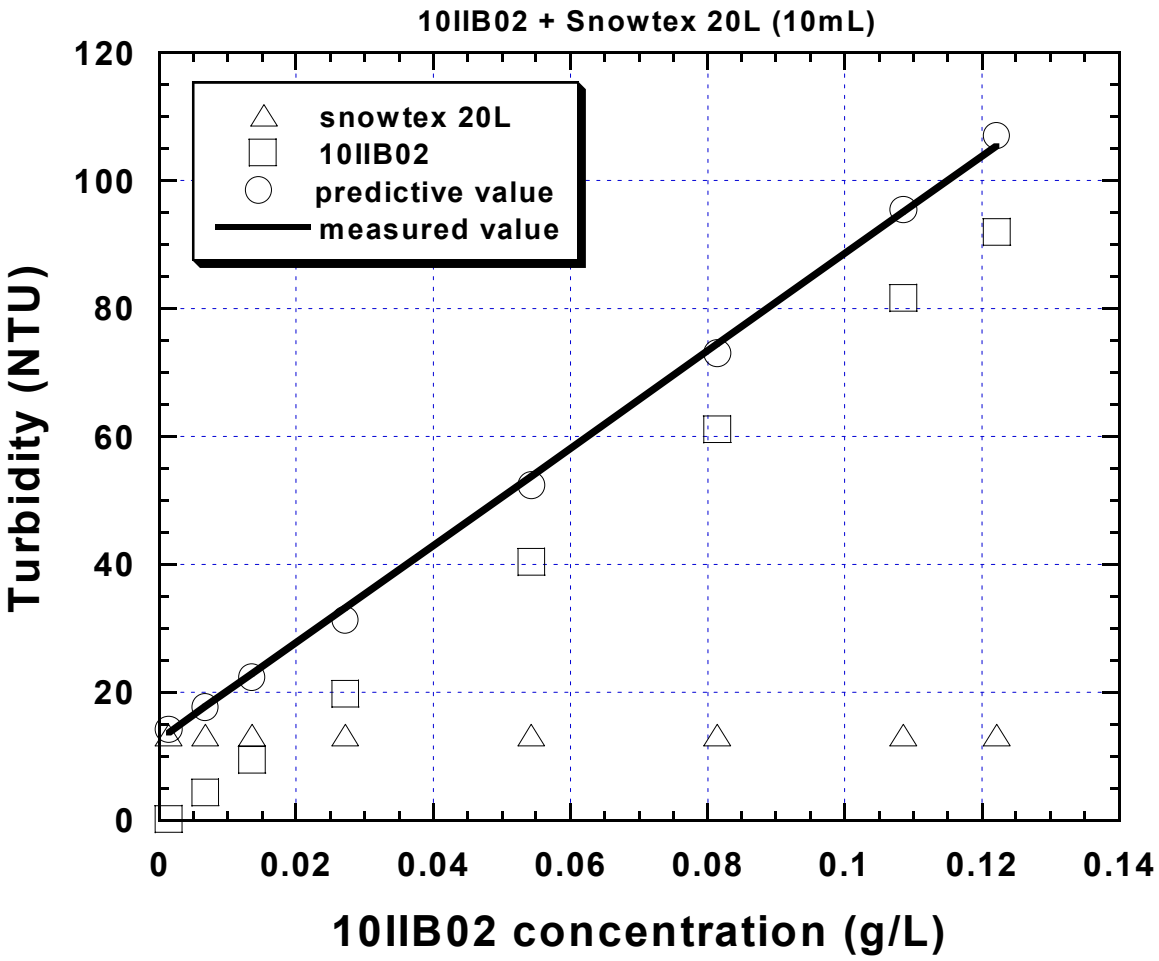

Figure A134. Calibration curve for turbidity (NTU) and particulate concentration of well water. Experimental conditions: colloidal silica = 0.205 g/L. (Well #10, bailing sample, 10IIB02)

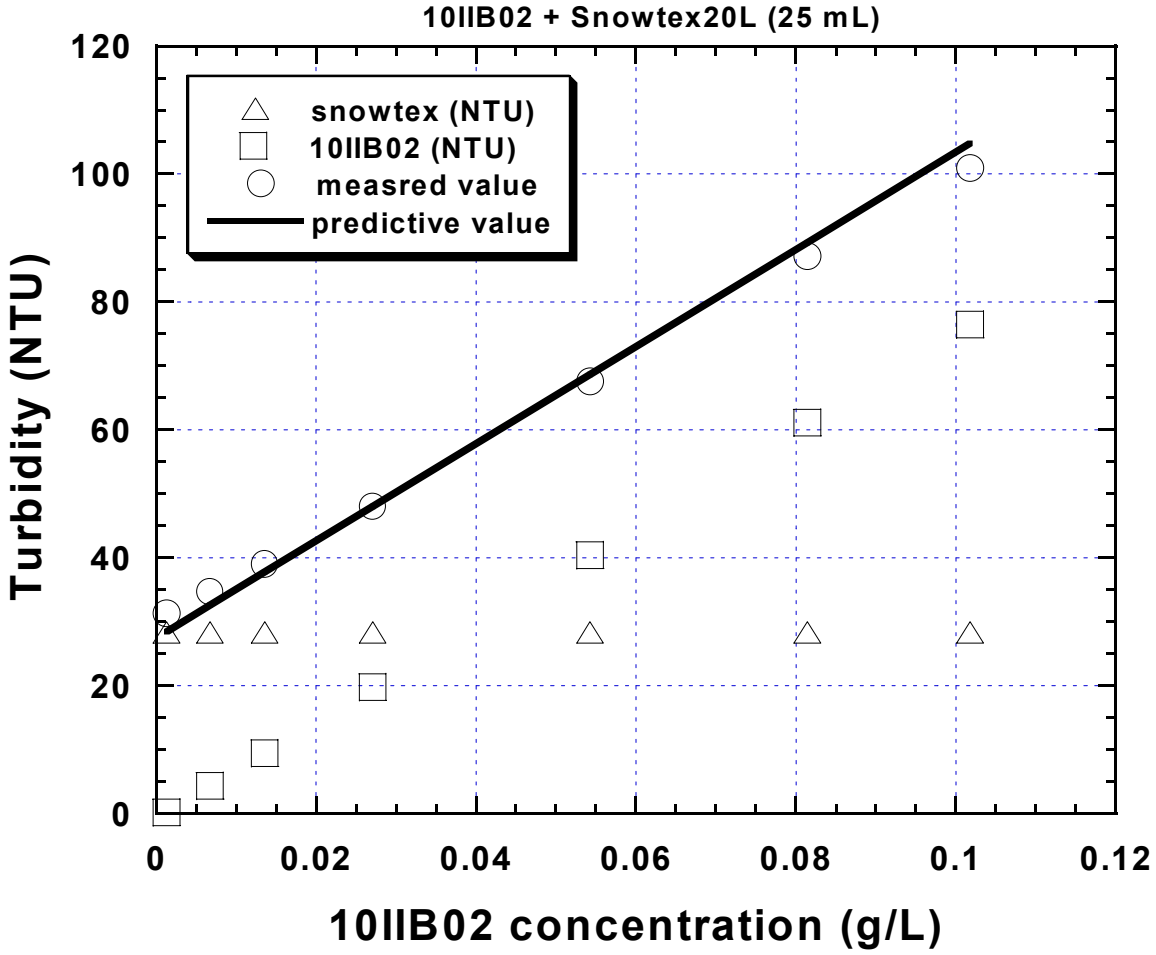

Figure A135. Calibration curve for turbidity (NTU) and particulate concentration of well water. Experimental conditions: colloidal silica = 0.513 g/L. (Well #10, bailing sample, 10IIB02)

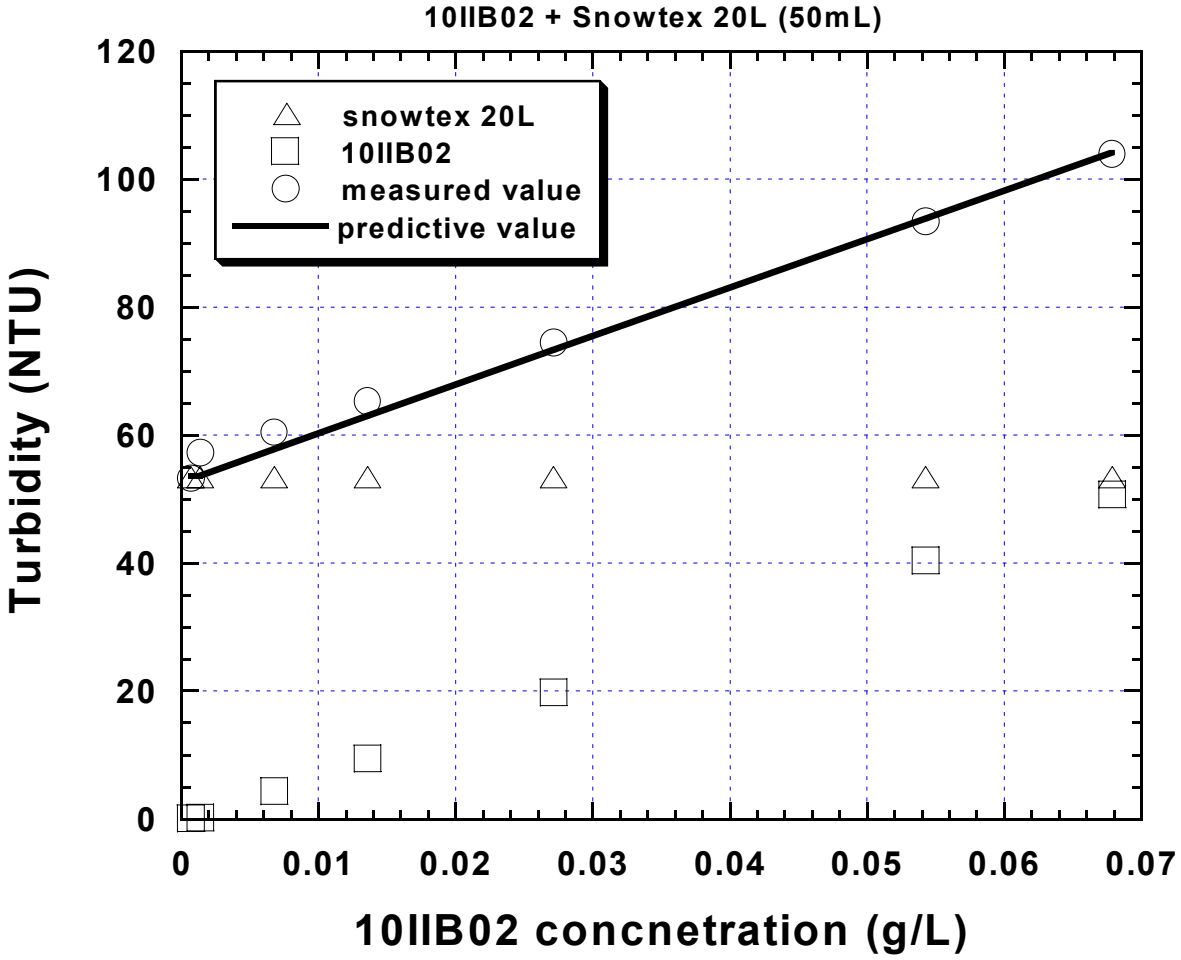

Figure A136. Calibration curve for turbidity (NTU) and particulate concentration of well water. Experimental conditions: colloidal silica = 1.025 g/L. (Well #10, bailing sample, 10IIB02)

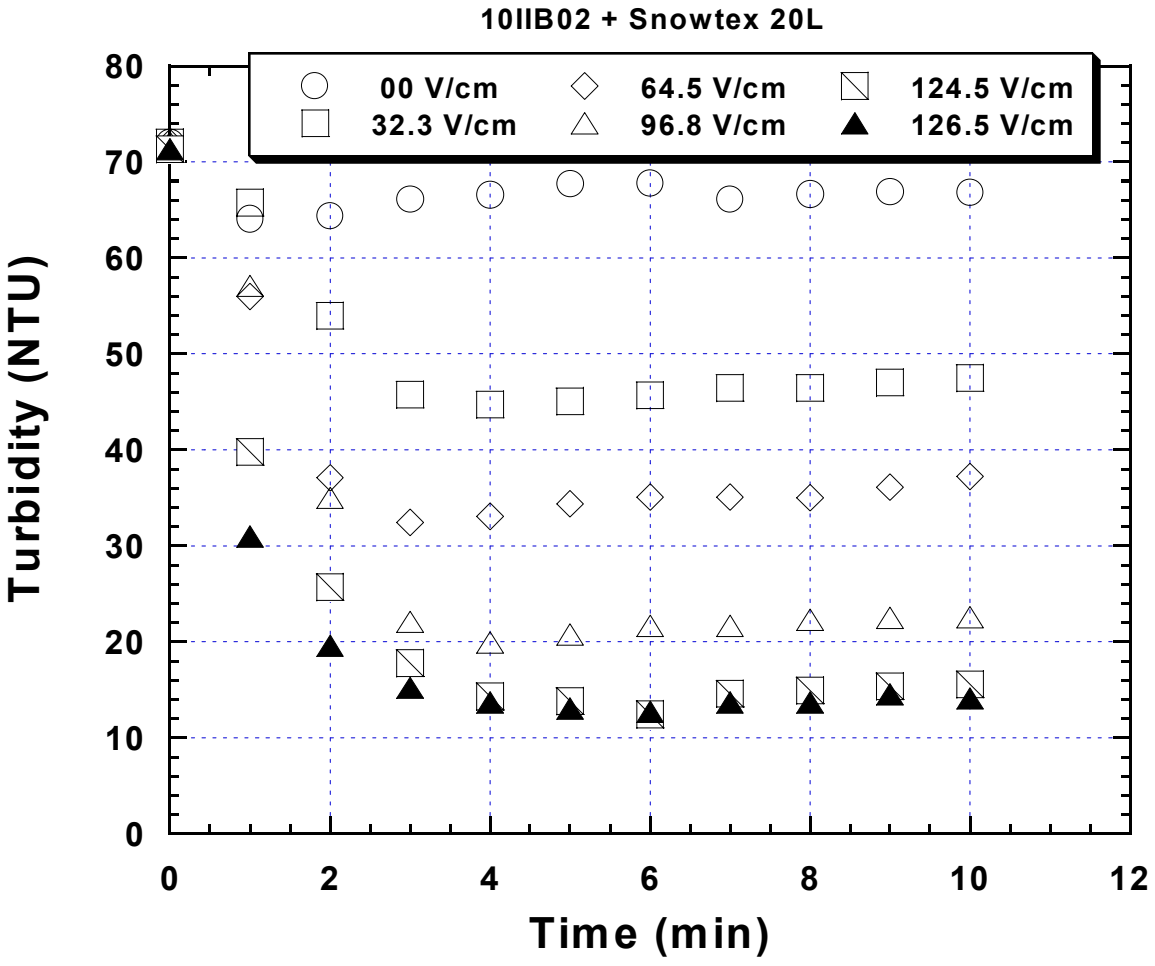

Figure A137. Change of turbidity as a function of time at various electrostatic field. Experimental condition: pH = 8.2; Sample : 10IIB02 + Snowtex 20L

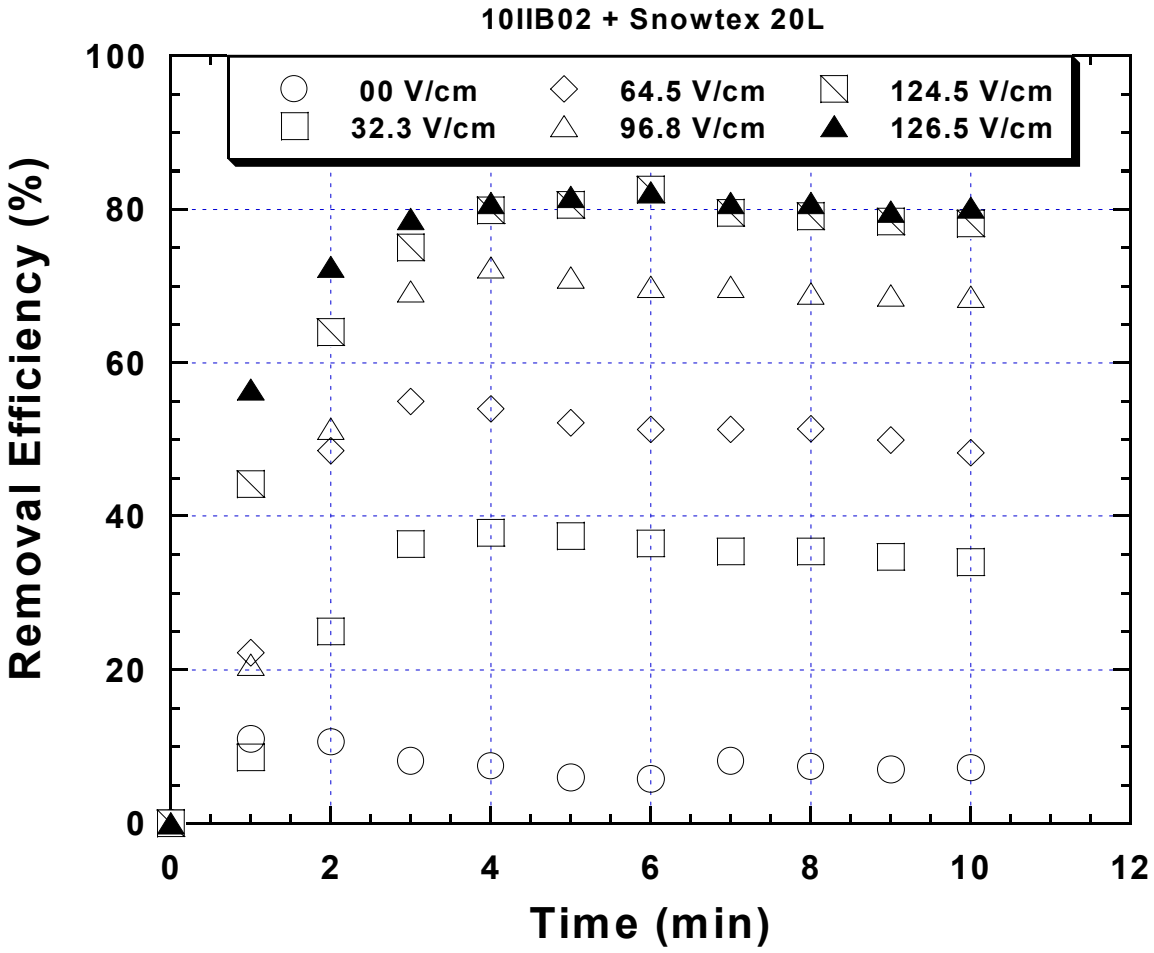

Figure A138. Removal efficiency as a function of time at various electrostatic field. Experimental condition: pH = 8.2; Sample: 10IIB02 + Snowtex 20L

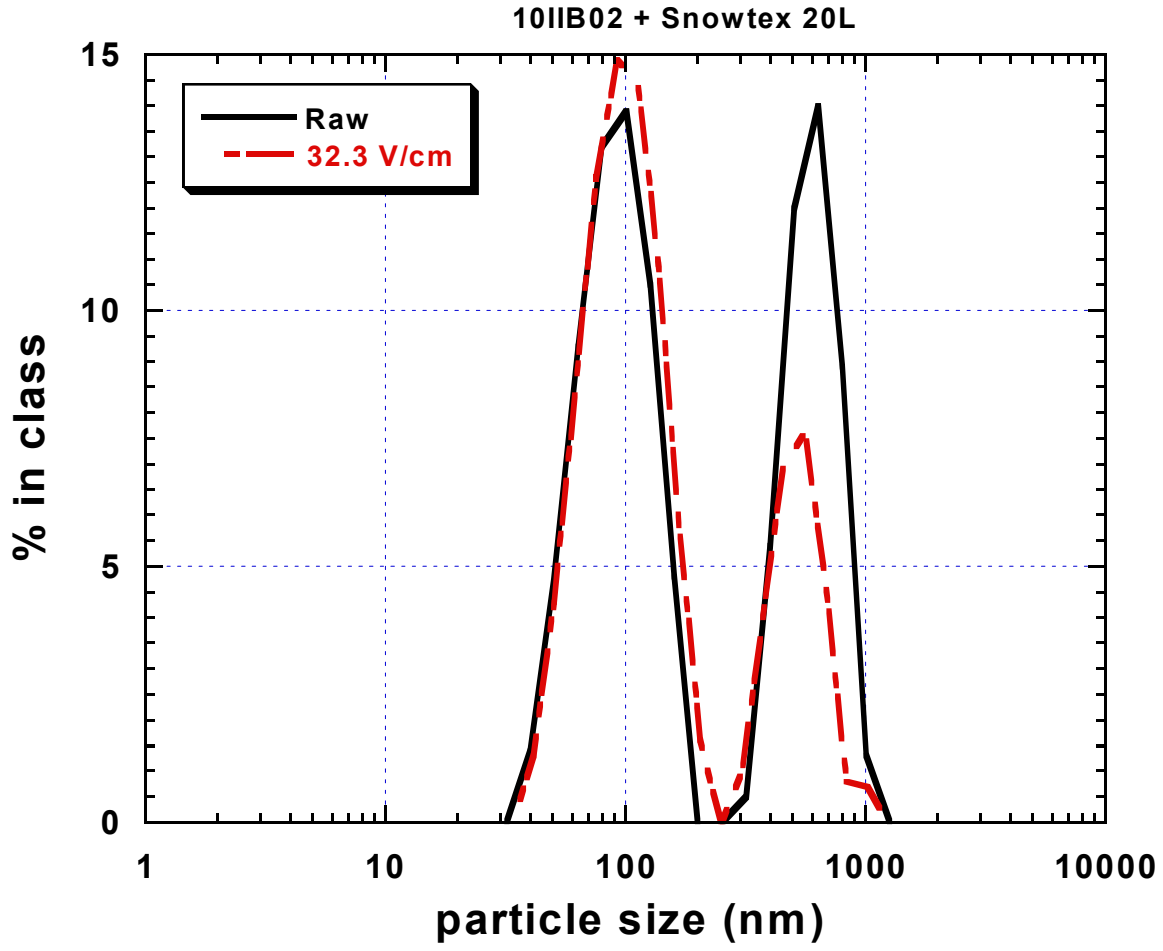

Figure A139. Distribution of particle size as affected by electrostatic field strength of 32.3 V/cm. Experimental condition: pH = 8.2; Sample: 10IIB02 + Snowtex 20L

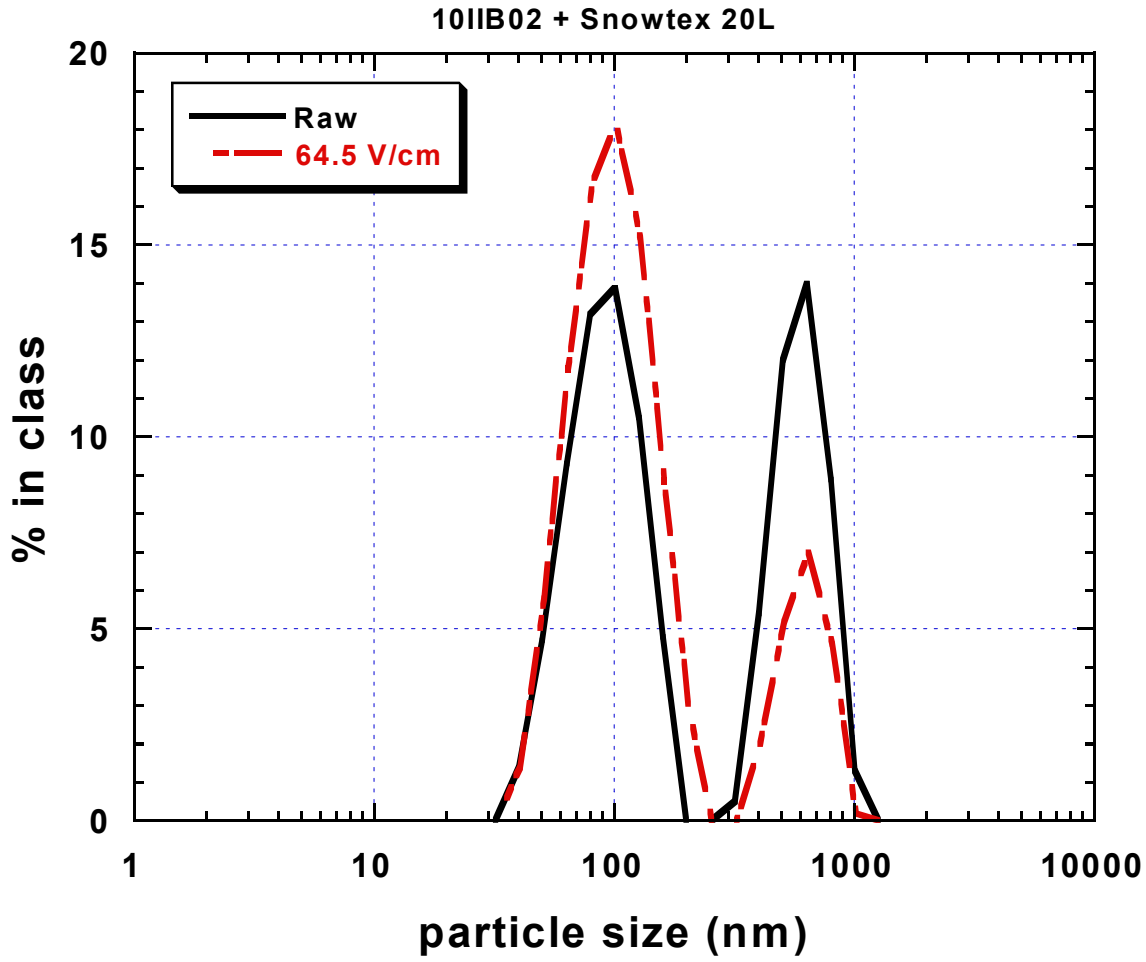

Figure A140. Distribution of particle size as affected by electrostatic field strength of 64.5 V/cm. Experimental condition: pH = 8.2; Sample: 10IIB02 + Snowtex 20L

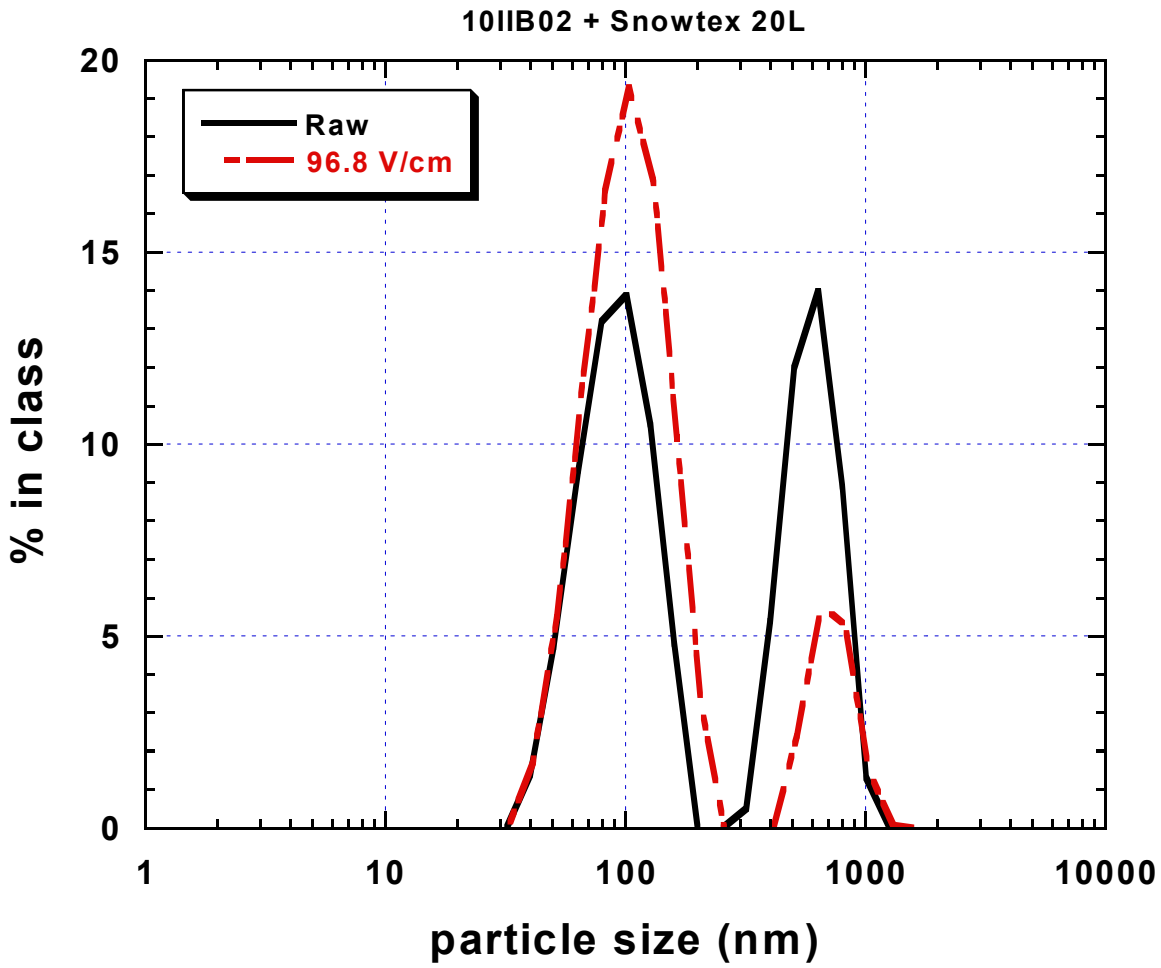

Figure A141. Distribution of particle size as affected by electrostatic field strength of of 96.8 V/cm. Experimental condition: pH = 8.2; Sample: 10IIB02 + Snowtex 20L